Dr M.Amarian

Introduction to Particle Physics

1 Special Relativity

This handout contains a brief review of the principal properties of relativistic four-vectors as derived in the course on Relativity and Electrodynamics. For the course the relativistic treatment of energy and momentum is of primary importance, and some examples illustrating the properties of four-momenta are therefore included.

1.1 4-vectors

A generic 4-vector a can be written in *contravariant* form, a^μ, with an upper index, or in *covariant* form, a_μ, with a lower index.

Examples of contravariant 4-vectors include (with $\hbar = c = 1$)

$$\begin{aligned}
\text{spacetime coordinates:} \quad & x^\mu = (x^0, x^1, x^2, x^3) = (t, x, y, z) = (t, \boldsymbol{r}) \\
\text{4-momentum:} \quad & p^\mu = (p^0, p^1, p^2, p^3) = (E, p_x, p_y, p_z) = (E, \boldsymbol{p}) \\
\text{4-vector potential:} \quad & A^\mu = (A^0, A^1, A^2, A^3) = (\phi, A_x, A_y, A_z) = (\phi, \boldsymbol{A}) \\
\text{4-vector current:} \quad & j^\mu = (j^0, j^1, j^2, j^3) = (\rho, j_x, j_y, j_z) = (\rho, \boldsymbol{j}) \, .
\end{aligned}$$

The corresponding covariant four-vectors are

$$\begin{aligned}
x_\mu &= g_{\mu\nu} x^\nu = (t, -\boldsymbol{r}) \\
p_\mu &= g_{\mu\nu} p^\nu = (E, -\boldsymbol{p}) \\
A_\mu &= g_{\mu\nu} A^\nu = (\phi, -\boldsymbol{A}) \\
j_\mu &= g_{\mu\nu} j^\nu = (\rho, -\boldsymbol{j})
\end{aligned}$$

where $g_{\mu\nu}$, the *metric tensor*, is taken to be

$$g_{\mu\nu} = g^{\mu\nu} = \begin{pmatrix} 1 & 0 & 0 & 0 \\ 0 & -1 & 0 & 0 \\ 0 & 0 & -1 & 0 \\ 0 & 0 & 0 & -1 \end{pmatrix} ,$$

and the Einstein summation convention is in use for repeated indices, namely that any Greek index appearing once as a subscript and once as a superscript should be summed over the values 0,1,2,3. Thus, for example:

$$g_{\mu\nu} x^\nu \equiv \sum_{\nu=0}^{3} g_{\mu\nu} x^\nu = g_{\mu 0} x^0 + g_{\mu 1} x^1 + g_{\mu 2} x^2 + g_{\mu 3} x^3 \, .$$

The partial derivatives $\partial/\partial x^\mu$ transform as a covariant 4-vector:

$$\partial_\mu \equiv \frac{\partial}{\partial x^\mu} = \left(\frac{\partial}{\partial t}, \frac{\partial}{\partial x}, \frac{\partial}{\partial y}, \frac{\partial}{\partial z}\right) = \left(\frac{\partial}{\partial t}, \boldsymbol{\nabla}\right) \ .$$

The corresponding contravariant 4-vector is

$$\partial^\mu \equiv \frac{\partial}{\partial x_\mu} = \left(\frac{\partial}{\partial t}, -\frac{\partial}{\partial x}, -\frac{\partial}{\partial y}, -\frac{\partial}{\partial z}\right) = \left(\frac{\partial}{\partial t}, -\boldsymbol{\nabla}\right) \ .$$

The standard quantum mechanical operator relations (with $\hbar = 1$)

$$\boldsymbol{p} = -i\boldsymbol{\nabla}; \qquad E = i\frac{\partial}{\partial t}$$

are both encompassed by the single 4-vector equation

$$p^\mu = i\partial^\mu \ .$$

1.2 Energy and Momentum

The energy, E, and momentum, $\boldsymbol{p}$, of a particle of mass m and velocity $\boldsymbol{u}$ are given by

$$E = \gamma(u)mc^2, \qquad \boldsymbol{p} = \gamma(u)m\boldsymbol{u} \tag{1}$$

where $u = |\boldsymbol{u}|$ and

$$\gamma(u) = \frac{1}{\sqrt{1-(u/c)^2}} \ .$$

The energy and momentum are connected by the relation (with $c = 1$)

$$E^2 = |\boldsymbol{p}|^2 + m^2 \ .$$

In the relativistic limit $E \gg m$, or if the particle is massless, we have simply

$$E = |\boldsymbol{p}| \ .$$

In this limit, a particle travelling in the $+z$ direction for example has a four-momentum of the form $p^\mu = (E, 0, 0, E)$. A particle of mass m at rest has 4-momentum $p^\mu = (m, 0, 0, 0)$.

Note that, from Equation (1), the speed of a particle is given in terms of its energy and momentum simply by

$$u = \frac{|\boldsymbol{p}|}{E} \ .$$

In particle interactions, such as a scattering process $a + b \to 1 + 2 + 3 + \ldots + n$, the total energy and momentum are conserved:

$$E_a + E_b = E_1 + E_2 + \ldots + E_n$$
$$\boldsymbol{p_a} + \boldsymbol{p_b} = \boldsymbol{p_1} + \boldsymbol{p_2} + \ldots + \boldsymbol{p_n} \ .$$

This can be expressed more compactly as conservation of 4-momentum:

$$p_a + p_b = p_1 + p_2 + \ldots + p_n \ .$$

The energy E of a particle is the sum of its rest mass energy mc^2 and its kinetic energy T:

$$E = mc^2 + T \ .$$

A scattering process is said to be *elastic* when the total kinetic energy of the incoming particles is the same as the total kinetic energy of the outgoing particles. Since the total energy (kinetic plus rest mass) is always conserved, the sum of the masses of the incoming particles must then be the same as the sum of the masses of the outgoing particles. In particular, this will be the case when the particle content of the initial and final states is the same. For example, the scattering process $\mathrm{e}^-\mu^- \to \mathrm{e}^-\mu^-$ is always elastic, while the process $\mathrm{e}^+\mathrm{e}^- \to \mu^+\mu^-$ is always inelastic.

1.3 Products of 4-vectors

The *scalar product* of two four-vectors a and b is defined as

$$a.b = a_\mu b^\mu = g_{\mu\nu} a^\mu b^\nu = a^\mu b_\mu \ .$$

Written out explicitly in terms of the components $a^\mu = (a^0, \boldsymbol{a})$ and $b^\mu = (b^0, \boldsymbol{b})$, the scalar product is

$$\begin{aligned} a.b &= a^0 b^0 - a^1 b^1 - a^2 b^2 - a^3 b^3 \\ &= a^0 b^0 - \boldsymbol{a.b} \\ &= a^0 b_0 + a^1 b_1 + a^2 b_2 + a^3 b_3 \ . \end{aligned}$$

Scalar products of 4-vectors are invariant under Lorentz transformations. For example, if p^μ is the 4-momentum of a particle of rest mass m then

$$p^2 = p.p = (E, \boldsymbol{p}).(E, \boldsymbol{p}) = E^2 - |\boldsymbol{p}|^2 = m^2 \ ,$$

which is a constant and therefore manifestly Lorentz invariant. Similarly, for $p_1^\mu = (E_1, \boldsymbol{p}_1)$, $p_2^\mu = (E_2, \boldsymbol{p}_2)$, we have

$$p_1.p_2 = E_1 E_2 - \boldsymbol{p}_1.\boldsymbol{p}_2 = E_1 E_2 - |\boldsymbol{p}_1||\boldsymbol{p}_2| \cos\theta$$

where θ is the opening angle between the $\boldsymbol{p}_1$ and $\boldsymbol{p}_2$ directions. The expression on the right hand side of this equation takes the same value whether it is evaluated in the laboratory, the centre of mass, or any other frame:

$$E_1 E_2 - |\boldsymbol{p}_1||\boldsymbol{p}_2| \cos\theta = E_1' E_2' - |\boldsymbol{p}_1'||\boldsymbol{p}_2'| \cos\theta' \ .$$

The scalar product of a four-momentum $p^\mu = (E, \boldsymbol{p})$ with the spacetime four-vector $x^\mu = (t, \boldsymbol{r})$ is

$$p.x = (E, \boldsymbol{p}).(t, \boldsymbol{r}) = Et - \boldsymbol{p.r} \ .$$

The phase factor $e^{i(\boldsymbol{p.r} - Et)}$ describing the propagation of a plane wave is therefore Lorentz invariant:

$$e^{i(\boldsymbol{p.r} - Et)} = e^{-ip.x} \ .$$

As another example, the scalar product $\partial_\mu j^\mu$ is

$$\partial_\mu j^\mu = g_{\mu\nu}\partial^\mu j^\nu = \left(\frac{\partial}{\partial t}, -\boldsymbol{\nabla}\right).(\rho, \boldsymbol{j}) = \frac{\partial \rho}{\partial t} + \boldsymbol{\nabla} \cdot \boldsymbol{j} \ .$$

The continuity equation, $\partial\rho/\partial t + \boldsymbol{\nabla} \cdot \boldsymbol{j} = 0$, expressing conservation of electric charge or particle number for example can therefore be expressed in the manifestly covariant form

$$\partial_\mu j^\mu = 0 \ .$$

Finally, the *d'Alembertian* operator $\Box^2$ is also a Lorentz invariant:

$$\Box^2 \equiv \partial^\mu \partial_\mu = \left(\frac{\partial}{\partial t}, \boldsymbol{\nabla}\right) . \left(\frac{\partial}{\partial t}, \boldsymbol{\nabla}\right) = \frac{\partial^2}{\partial t^2} - \nabla^2 \ .$$

1.4 Systems of Particles

Consider the decay of a particle a into a final state containing n particles:

$$a \to 1 + 2 + 3 + \ldots + n \ .$$

Working in the rest frame of particle a, conservation of energy gives

$$\begin{aligned} m_a &= E_1 + E_2 + \ldots + E_n \\ &= (m_1 + m_2 + \ldots + m_n) + (T_1 + T_2 + \ldots + T_n) \ , \end{aligned}$$

where $E_i = m_i + T_i$ is the total energy of the i'th particle. Since the kinetic energies T_i must all be positive, we immediately obtain

$$\boxed{m_a > m_1 + m_2 + \ldots + m_n} \ , \tag{2}$$

i.e. the sum of the final state masses must be less than the original mass m_a. This result involves only Lorentz invariant quantities (particle masses) and so must hold in *any* Lorentz frame, not just the rest frame. Thus, accelerating particle a to arbitrarily high energy does not allow particles heavier than a to be produced in its decay. Instead, in such a frame, the final state particles gain extra kinetic energy to maintain overall conservation of energy and momentum.

In general, the total four-momentum p of a system of n particles is simply the sum of the individual four-momenta p_i,

$$p = p_1 + p_2 + \ldots + p_n \ ,$$

and the *invariant mass* M of such a system is defined as

$$M^2 = p^2 = (p_1 + p_2 + \ldots p_n)^2 \ .$$

The same argument as used above for the decay process $a \to 1 + 2 + \ldots + n$ and which led to Equation (2) can be applied equally well to the centre of mass frame of this general n particle system to show that

$$M > m_1 + m_2 + \ldots + m_n \ .$$

In the collision of two particles with incoming four-momenta p_1 and p_2, a useful invariant is

$$\boxed{s \equiv (p_1 + p_2)^2} \, .$$

In the centre of mass frame of the two particles, with the particle motion chosen to be parallel to the z-axis, the four-momenta p_1 and p_2 are of the form

$$p_1 = (E_1^*, 0, 0, p^*), \qquad p_2 = (E_2^*, 0, 0, -p^*) \, .$$

Hence

$$s = (E_1^* + E_2^*, 0, 0, 0)^2 = (E_1^* + E_2^*)^2$$

and $\sqrt{s}$ $(= E_1^* + E_2^*)$ therefore represents the total energy of the collision in the centre of mass frame.

In the lab frame, choosing particle 2 to be at rest, we can take

$$p_1 = (E_1, 0, 0, p_1), \qquad p_2 = (m_2, 0, 0, 0)$$

which gives

$$s = (p_1 + p_2)^2 = p_1^2 + p_2^2 + 2p_1.p_2 = m_1^2 + m_2^2 + 2E_1 m_2 \, .$$

At very high energy, where the masses m_1, m_2 can be neglected, we obtain $s \approx 2E_1 m_2$.

1.5 Lorentz Transformations

Under a pure velocity transformation, with a primed frame $S'(t', x', y', z')$ moving at constant velocity v along the x axis of frame $S(t, x, y, z)$, a contravariant 4-vector a^μ transforms as

$$(a')^\mu = \Lambda^\mu{}_\nu a^\nu \qquad \text{where} \qquad \Lambda^\mu{}_\nu = \begin{pmatrix} \gamma & -\beta\gamma & 0 & 0 \\ -\beta\gamma & \gamma & 0 & 0 \\ 0 & 0 & 1 & 0 \\ 0 & 0 & 0 & 1 \end{pmatrix}$$

with $\beta = v/c$ and $\gamma = 1/\sqrt{1-\beta^2}$. For example, if a^μ is a 4-momentum $p^\mu = (E, p_x, p_y, p_z)$, then

$$E' = \gamma(E - \beta p_x) \qquad p'_y = p_y$$
$$p'_x = \gamma(p_x - \beta E) \qquad p'_z = p_z$$

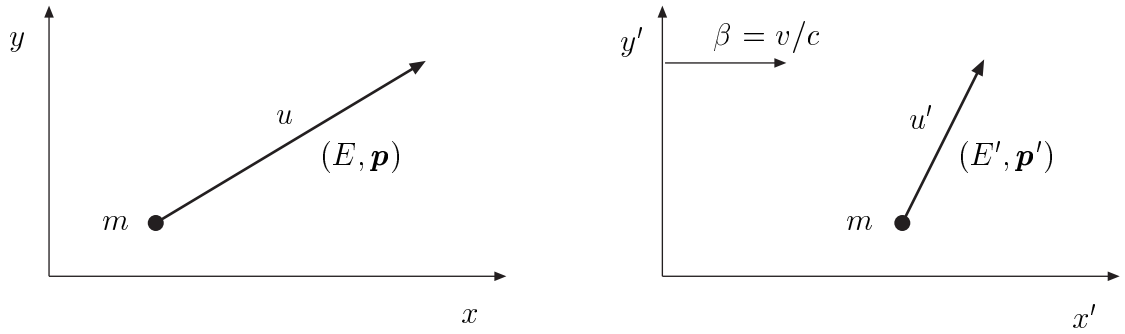

The velocity $\beta = v/c$ of the primed frame relative to the unprimed frame should not be confused with the velocities u and u' of the particle in each frame. The energies E, E' and the momenta $p = |\boldsymbol{p}|$, $p' = |\boldsymbol{p}'|$ of the particle in S and S' are

$$E = \gamma(u)mc^2 \qquad\qquad E' = \gamma(u')mc^2$$
$$p = \gamma(u)mu \qquad\qquad p' = \gamma(u')mu'$$

and the particle velocities in each frame (with $c = 1$) are

$$u = \frac{p}{E} \qquad\qquad u' = \frac{p'}{E'}$$

2 The Dirac Equation

In 1928, Paul Dirac proposed a relativistically-covariant wave equation for the electron which successfully accounted for its intrinsic angular momentum (spin) and intrinsic magnetic moment. The Dirac equation also predicted the existence of a particle with the same mass as the electron but with opposite electric charge, namely the *positron*. This prediction was soon confirmed by Anderson's observation in 1933 of the production of positrons in cosmic ray interactions.

In this handout, we consider the Dirac equation and its predictions in detail. To motivate the introduction of the Dirac equation, we first consider briefly the non-relativistic Schrödinger equation and its straightforward relativistic generalisation, the Klein-Gordon equation.

2.1 Non-Relativistic Quantum Mechanics

For a non-relativistic free particle, with $V(\boldsymbol{r}) = 0$, the operator replacements (with $\hbar = 1$)

$$\boldsymbol{p} \to -i\boldsymbol{\nabla}, \quad E \to i\frac{\partial}{\partial t} \tag{1}$$

applied to the equation

$$\frac{|\boldsymbol{p}|^2}{2m} = E$$

give the *time-dependent Schrödinger equation* for the wavefunction $\psi(\boldsymbol{r}, t)$:

$$\boxed{-\frac{1}{2m}\nabla^2\psi = i\frac{\partial\psi}{\partial t}}. \tag{2}$$

This is *not* a Lorentz-covariant equation, being first order in $\partial/\partial t$ but second order in $\partial/\partial x$. Transforming the right hand side of Equation (2) to another reference frame, for example, would introduce terms containing the first order spatial derivatives $\partial\psi/\partial x'$, $\partial\psi/\partial y'$, $\partial\psi/\partial z'$, which have no equivalent in the original (untransformed) equation.

Taking the complex conjugate of Schrödinger's equation gives

$$-\frac{1}{2m}\nabla^2\psi^* = -i\frac{\partial\psi^*}{\partial t}. \tag{3}$$

Forming the linear combination $\psi^* \times$Eqn (2)$-\psi \times$Eqn (3) then gives

$$-\frac{1}{2m}\left[\psi^*\nabla^2\psi - \psi\nabla^2\psi^*\right] = i\left[\psi^*\frac{\partial\psi}{\partial t} + \psi\frac{\partial\psi^*}{\partial t}\right] = i\frac{\partial}{\partial t}\left(\psi^*\psi\right).$$

Using the identity

$$\psi^*\nabla^2\psi - \psi\nabla^2\psi^* = \boldsymbol{\nabla}\cdot\left(\psi^*\boldsymbol{\nabla}\psi - \psi\boldsymbol{\nabla}\psi^*\right) \tag{4}$$

we obtain

$$-\frac{1}{2m}\boldsymbol{\nabla}\cdot\left(\psi^*\boldsymbol{\nabla}\psi - \psi\boldsymbol{\nabla}\psi^*\right) = i\frac{\partial}{\partial t}\left(\psi^*\psi\right).$$

A comparison with the *continuity equation*,

$$\boldsymbol{\nabla}\cdot\boldsymbol{j} + \frac{\partial\rho}{\partial t} = 0\ , \tag{5}$$

expressing conservation of particle number, leads to the following expressions for the probability density and current:

$$\rho = \psi^*\psi = |\psi|^2 \tag{6}$$

$$\boldsymbol{j} = \frac{1}{2im}\left(\psi^*\boldsymbol{\nabla}\psi - \psi\boldsymbol{\nabla}\psi^*\right)\ . \tag{7}$$

Schrödinger's equation admits plane wave solutions of the form

$$\psi = Ne^{i(\boldsymbol{p}.\boldsymbol{r}-Et)}$$

where $\boldsymbol{p}$ and E are constants, as can be checked by direct substitution into Equation (2). These plane wave solutions are easily seen to be eigenstates of the momentum and energy operators of Equation (1) with eigenvalues $\boldsymbol{p}$ and E :

$$\left(-i\boldsymbol{\nabla}\right)\psi = \boldsymbol{p}\psi, \qquad \left(i\frac{\partial}{\partial t}\right)\psi = E\psi\ ,$$

and hence correspond to free particles of definite energy, E, and momentum, $\boldsymbol{p}$. Substituting into Equations (6) and (7), the probability density ρ and current $\boldsymbol{j}$ for the plane wave ψ are found to be

$$\rho = |N|^2, \qquad \boldsymbol{j} = |N|^2\frac{\boldsymbol{p}}{m} = |N|^2\boldsymbol{v}.$$

The first of these relations shows that the number of particles per unit volume is $|N|^2$. For particles of number density $|N|^2$ travelling with velocity v, the number of particles per unit time passing through unit area (the *particle flux*) at any fixed point along the particle trajectory is $|N|^2 v$. Hence the current $\boldsymbol{j}$ is a vector pointing along the particle's direction of motion with magnitude equal to the particle flux.

2.2 The Klein-Gordon Equation

Applying the replacements $\boldsymbol{p} \to -i\boldsymbol{\nabla}, E \to i\partial/\partial t$ to the relativistic equation

$$|\boldsymbol{p}|^2 + m^2 = E^2$$

(with $\hbar = c = 1$) in place of $|\boldsymbol{p}|^2/2m = E$ gives immediately the *Klein-Gordon equation*

$$\boxed{\nabla^2\psi - m^2\psi = \frac{\partial^2\psi}{\partial t^2}}\,. \tag{8}$$

Introducing the partial derivative 4-vector

$$\partial_\mu \equiv \frac{\partial}{\partial x^\mu} = \left(\frac{\partial}{\partial t}, \frac{\partial}{\partial x}, \frac{\partial}{\partial y}, \frac{\partial}{\partial z}\right) = \left(\frac{\partial}{\partial t}, \boldsymbol{\nabla}\right)$$

with the property

$$\Box^2 \equiv \partial^\mu\partial_\mu = \left(\frac{\partial}{\partial t}, \boldsymbol{\nabla}\right) . \left(\frac{\partial}{\partial t}, \boldsymbol{\nabla}\right) = \frac{\partial^2}{\partial t^2} - \nabla^2$$

allows the Klein-Gordon equation to be written in the manifestly Lorentz-covariant form

$$\boxed{(\partial_\mu\partial^\mu + m^2)\psi = 0}\,.$$

For plane waves of the form $\psi = Ne^{i(\boldsymbol{p}.\boldsymbol{r}-Et)}$, with $\boldsymbol{p}$ and E constant, we have

$$\nabla^2\psi = -|\boldsymbol{p}|^2\psi, \qquad \frac{\partial^2\psi}{\partial t^2} = -E^2\psi\ .$$

The wave function ψ therefore satisfies the Klein-Gordon equation, Equation (8), provided that $\boldsymbol{p}$ and E are related via $|\boldsymbol{p}|^2 + m^2 = E^2$ (as expected). Unlike the non-relativistic case, where the energy $E = |\boldsymbol{p}|^2/2m$ is unambiguously positive, we now face the problem that E can be of either sign:

$$E = \pm\sqrt{|\boldsymbol{p}|^2 + m^2}\ ,$$

so that there exist negative-energy as well as positive-energy solutions to the Klein-Gordon equation for a free particle. An equivalent viewpoint is that, as well as plane wave solutions of the form

$$\psi = Ne^{i(\boldsymbol{p}.\boldsymbol{r}-Et)}\ , \tag{9}$$

the Klein-Gordon equation also accepts solutions of the form

$$\psi = Ne^{-i(\boldsymbol{p}.\boldsymbol{r}-Et)}\ , \tag{10}$$

where now, in Equations (9) and (10), it is to be understood that $E = +\sqrt{|\boldsymbol{p}|^2 + m^2}$ is always positive. Solutions of the form $Ne^{-i(\boldsymbol{p}.\boldsymbol{r}-Et)}$ have negative energy in the sense that they are eigenstates of the standard energy operator $i\partial/\partial t$ with energy eigenvalue $-E$. Such solutions do *not* exist for the Schrödinger equation, where they would result in the non-physical relation $E = -|\boldsymbol{p}|^2/2m$.

The plane wave solutions of Equations (9) and (10) are Lorentz covariant, as is easily seen by considering the four-vector scalar product $p.x = Et - \boldsymbol{p}.\boldsymbol{r}$, where $p^\mu = (E, \boldsymbol{p})$ and $x^\mu = (t, \boldsymbol{r})$. The positive and negative energy solutions can therefore be written in the manifestly covariant forms

$$\psi = Ne^{-ip.x}; \qquad \psi = Ne^{+ip.x} \ .$$

The negative energy solutions to the Klein-Gordon equation cause further problems when the probability density and current are evaluated. Taking the complex conjugate of Equation (8) gives

$$\nabla^2\psi^* - m^2\psi^* = \frac{\partial^2\psi^*}{\partial t^2} \ . \tag{11}$$

Taking $\psi^* \times$Eqn (8)$-\psi \times$Eqn (11), we then obtain

$$\psi^* \left(\nabla^2\psi - m^2\psi\right) - \psi \left(\nabla^2\psi^* - m^2\psi^*\right) = \psi^*\frac{\partial^2\psi}{\partial t^2} - \psi\frac{\partial^2\psi^*}{\partial t^2} \ .$$

Applying the identity in Equation (4) to the left-hand side of this equation then gives

$$\boldsymbol{\nabla} \cdot (\psi^*\boldsymbol{\nabla}\psi - \psi\boldsymbol{\nabla}\psi^*) = \frac{\partial}{\partial t}\left(\psi^*\frac{\partial\psi}{\partial t} - \psi\frac{\partial\psi^*}{\partial t}\right) \ .$$

Thus we again arrive at the continuity equation, Equation (5), with

$$\rho = i\left(\psi^*\frac{\partial\psi}{\partial t} - \psi\frac{\partial\psi^*}{\partial t}\right) \tag{12}$$

$$\boldsymbol{j} = i\left(\psi\boldsymbol{\nabla}\psi^* - \psi^*\boldsymbol{\nabla}\psi\right) \tag{13}$$

where the arbitrary overall normalisation factors of i are chosen to give a probability density ρ which is real, as we now see. Substituting the plane wave solution $\psi = Ne^{i(\boldsymbol{p}.\boldsymbol{r}-Et)}$ into Equations (12) and (13) gives

$$\rho = 2|N|^2E, \qquad \boldsymbol{j} = 2|N|^2\boldsymbol{p} \ . \tag{14}$$

The probability density ρ therefore has the same sign as the energy E. In particular, if the energy E is negative the probability density ρ is also negative.

The Klein-Gordon equation therefore suffers from the presence of negative energy states and negative probability densities. The presence of negative energy states is an inevitable consequence of the relativistic relation $E^2 = |\boldsymbol{p}|^2 + m^2$, and indeed such states exist also in classical (non-quantum) relativistic dynamics. In a classical context however, the negative energy states can simply be ignored, since no continuous transitions can bridge the gap between the positive energy states, with $E \geq mc^2$, and the negative energy states, with $E \leq -mc^2$. In a quantum theory, however, radiative transitions, for example, can continuously connect the two, and the negative energy states must be retained.

The negative probability densities associated with solutions to the Klein-Gordon equation led Dirac (1928) to search for an alternative relativistic wave equation. The resulting *Dirac equation* not only provided a full account of the intrinsic spin and magnetic moment of the electron, but also led Dirac to propose that the negative energy solutions be interpreted as positive energy *antiparticles*. The experimental observation by Anderson in 1933 of positrons in cosmic ray interactions was a remarkable verification of this prediction.

It was shown later by Pauli and Weisskopf (1934) that the problems with the Klein-Gordon equation could be resolved by treating $\psi(x)$ as a *field operator* rather than a single particle wavefunction. The resulting *quantum field theory* naturally described systems of spin 0 particles and antiparticles. Field-theoretic ideas were subsequently extended to particles and antiparticles of other spins, including spin-half particles and antiparticles described by the Dirac equation, and are the bedrock of the Standard Model of electromagnetic, weak and strong interactions.

Before leaving the Klein-Gordon equation, we demonstrate that the vector $\boldsymbol{j}$ of Equation (13) again represents the particle flux. The expression for ρ in Equation (14) shows that the wavefunction $\psi = Ne^{i(\boldsymbol{p}.\boldsymbol{r}-Et)}$ corresponds to a density of $2|N|^2E$ particles per unit volume. For a beam of particles of this density travelling with velocity $\boldsymbol{v}$, the number of particles per unit time passing through unit area at any point (*i.e.* the particle flux) is $2|N|^2E\boldsymbol{v}$. But the momentum and energy of a relativistic particle of velocity $\boldsymbol{v}$ are given by (with $c = 1$)

$$\boldsymbol{p} = \gamma m\boldsymbol{v}, \qquad E = \gamma m \ ,$$

where $\gamma = 1/\sqrt{1-v^2}$, so that $E\boldsymbol{v} = \boldsymbol{p}$. The particle flux is therefore $2|N|^2E\boldsymbol{v} = 2|N|^2\boldsymbol{p}$, which is indeed equal to the vector $\boldsymbol{j}$ in Equation (14).

Equations (12) and (13) can be combined into a single covariant equation by introducing the current four-vector $j^\mu = (\rho, \boldsymbol{j})$:

$$j^\mu = i\left(\psi^*\partial^\mu\psi - \psi\partial^\mu\psi^*\right).$$

(Setting $\mu = 0$ recovers Equation (12) while setting $\mu = 1, 2, 3$ recovers Equation (13)). Similarly, in covariant notation, Equation (14) is equivalent to

$$j^\mu = 2|N|^2p^\mu \ ,$$

while the continuity equation, Equation (5), can be expressed in covariant form as

$$\partial_\mu j^\mu = 0 \ .$$

2.3 The Dirac Equation

Dirac attempted to avoid the negative probability densities associated with the Klein-Gordon equation by looking for an alternative equation which was *first order* in both $\partial/\partial t$ and $\partial/\partial x$, namely the *Dirac equation*

$$\boxed{H\psi = (\boldsymbol{\alpha}.\boldsymbol{p} + \beta m)\psi = i\frac{\partial\psi}{\partial t}} \tag{15}$$

where H is the Hamiltonian operator, $\boldsymbol{p} = -i\boldsymbol{\nabla}$ is the momentum operator, and $\boldsymbol{\alpha}$ and β are constants which remain to be determined. Writing Equation (15) explicitly in terms of its components, we have

$$\left(-i\alpha_x\frac{\partial}{\partial x} - i\alpha_y\frac{\partial}{\partial y} - i\alpha_z\frac{\partial}{\partial z} + \beta m\right)\psi = \left(i\frac{\partial}{\partial t}\right)\psi \ .$$

"Squaring" this equation by operating on the left with $(-i\alpha_x\partial/\partial x - \ldots + \beta m)$ and on the right with $i\partial/\partial t$ gives

$$\left(-i\alpha_x\frac{\partial}{\partial x} - \ldots + \beta m\right)\left(-i\alpha_x\frac{\partial}{\partial x} - \ldots + \beta m\right)\psi = \left(i\frac{\partial}{\partial t}\right)\left(i\frac{\partial}{\partial t}\right)\psi\ .$$

This equation can be expanded as

$$\begin{aligned}-\alpha_x^2\frac{\partial^2\psi}{\partial x^2} - \alpha_y^2\frac{\partial^2\psi}{\partial y^2} - \alpha_z^2\frac{\partial^2\psi}{\partial z^2}& \\ - (\alpha_x\alpha_y + \alpha_y\alpha_x)\frac{\partial^2\psi}{\partial x\partial y} - (\alpha_x\alpha_z + \alpha_z\alpha_x)\frac{\partial^2\psi}{\partial x\partial z} - (\alpha_y\alpha_z + \alpha_z\alpha_y)\frac{\partial^2\psi}{\partial y\partial z}& \\ - i(\alpha_x\beta + \beta\alpha_x)m\frac{\partial\psi}{\partial x} - i(\alpha_y\beta + \beta\alpha_y)m\frac{\partial\psi}{\partial y} - i(\alpha_z\beta + \beta\alpha_z)m\frac{\partial\psi}{\partial z}& \\ + \beta^2m^2\psi = -\frac{\partial^2\psi}{\partial t^2}\ .&\quad (16)\end{aligned}$$

But a free particle (with $E^2 = p^2 + m^2$) must also satisfy the Klein-Gordon equation:

$$\frac{\partial^2\psi}{\partial x^2} + \frac{\partial^2\psi}{\partial y^2} + \frac{\partial^2\psi}{\partial z^2} - m^2\psi = \frac{\partial^2\psi}{\partial t^2}\ . \tag{17}$$

For Equations (16) and (17) to be consistent, we must have:

$$\beta^2 = \alpha_x^2 = \alpha_y^2 = \alpha_z^2 = 1 \tag{18}$$

$$\beta\alpha_j + \alpha_j\beta = 0 \tag{19}$$

$$\alpha_j\alpha_k + \alpha_k\alpha_j = 0 \quad (j \neq k) \tag{20}$$

Hence the constants α_j and β can not simply be numbers; they must be (at least) 4×4 matrices. This in turn implies that the wavefunction ψ must be a four-component object, known as a *spinor* (not to be confused with a four-vector):

$$\psi = \begin{pmatrix}\psi_1\\ \psi_2\\ \psi_3\\ \psi_4\end{pmatrix}\ .$$

We shall see below that the four spinor degrees of freedom correspond to the two spin states of a spin $\frac{1}{2}$ *particle* plus the two spin states of the associated spin $\frac{1}{2}$ *antiparticle*.

For H to be Hermitian, $\boldsymbol{\alpha}$ and β must also be Hermitian:

$$\alpha_x^\dagger = \alpha_x; \qquad \alpha_y^\dagger = \alpha_y; \qquad \alpha_z^\dagger = \alpha_z; \qquad \beta^\dagger = \beta\ . \tag{21}$$

A convenient choice for the matrices $\boldsymbol{\alpha}$ and β which satisfies Equations (18)-(20) and Equation (21) is

$$\beta = \begin{pmatrix}I & 0\\ 0 & -I\end{pmatrix}, \qquad \alpha_j = \begin{pmatrix}0 & \sigma_j\\ \sigma_j & 0\end{pmatrix}$$

where I is the 2×2 unit matrix and the σ_j are the 2×2 Pauli spin matrices:

$$I = \begin{pmatrix}1 & 0\\ 0 & 1\end{pmatrix}; \quad \sigma_x = \begin{pmatrix}0 & 1\\ 1 & 0\end{pmatrix}; \quad \sigma_y = \begin{pmatrix}0 & -i\\ i & 0\end{pmatrix}; \quad \sigma_z = \begin{pmatrix}1 & 0\\ 0 & -1\end{pmatrix}\ . \tag{22}$$

It can be shown that all physical quantities are independent of the particular representation of the matrices $\boldsymbol{\alpha}$ and β.

2.4 Probability Density and Current

Writing out each component explicitly, the Dirac equation is

$$-i\alpha_x\frac{\partial\psi}{\partial x} - i\alpha_y\frac{\partial\psi}{\partial y} - i\alpha_z\frac{\partial\psi}{\partial z} + \beta m\psi = i\frac{\partial\psi}{\partial t}\ . \tag{23}$$

Taking the Hermitian (rather than just complex) conjugate of this equation, remembering that $A^\dagger = (A^*)^T$ so $i^\dagger = -i$, and that $(AB)^\dagger = B^\dagger A^\dagger$, we obtain

$$i\frac{\partial\psi^\dagger}{\partial x}\alpha_x^\dagger + i\frac{\partial\psi^\dagger}{\partial y}\alpha_y^\dagger + i\frac{\partial\psi^\dagger}{\partial z}\alpha_z^\dagger + \psi^\dagger\beta^\dagger m = -i\frac{\partial\psi^\dagger}{\partial t}\ . \tag{24}$$

Taking the combination $\psi^\dagger \times$ Eqn (23) $-$ Eqn $(24) \times \psi$ and using the fact that $\boldsymbol{\alpha}$ and β are Hermitian then gives

$$\psi^\dagger\left(-i\alpha_x\frac{\partial\psi}{\partial x} - i\alpha_y\frac{\partial\psi}{\partial y} - i\alpha_z\frac{\partial\psi}{\partial z} + \beta m\psi\right) - \left(i\frac{\partial\psi^\dagger}{\partial x}\alpha_x + i\frac{\partial\psi^\dagger}{\partial y}\alpha_y + i\frac{\partial\psi^\dagger}{\partial z}\alpha_z + \psi^\dagger\beta m\right)\psi = i\psi^\dagger\frac{\partial\psi}{\partial t} + i\frac{\partial\psi^\dagger}{\partial t}\psi = i\frac{\partial}{\partial t}(\psi^\dagger\psi)\ .$$

Using the identity

$$\psi^\dagger\alpha_x\frac{\partial\psi}{\partial x} + \frac{\partial\psi^\dagger}{\partial x}\alpha_x\psi = \frac{\partial}{\partial x}(\psi^\dagger\alpha_x\psi)$$

(and similarly for y, z) we arrive at the continuity equation

$$\boxed{\boldsymbol{\nabla}\cdot(\psi^\dagger\boldsymbol{\alpha}\psi) + \frac{\partial}{\partial t}(\psi^\dagger\psi) = 0}\ . \tag{25}$$

The probability density ρ and current $\boldsymbol{j}$ can therefore be identified as

$$\rho = \psi^\dagger\psi \equiv |\psi_1|^2 + |\psi_2|^2 + |\psi_3|^2 + |\psi_4|^2 \tag{26}$$

$$\boldsymbol{j} = \psi^\dagger\boldsymbol{\alpha}\psi \tag{27}$$

where Equation (26) follows from the fact that $\psi^\dagger$ is the 1×4 matrix

$$\psi^\dagger = (\psi^*)^T = (\psi_1^*, \psi_2^*, \psi_3^*, \psi_4^*)\ .$$

The probability density ρ is therefore guaranteed to be positive (for both positive and negative energy solutions), in contrast to the situation for the Klein-Gordon equation alone.

2.5 Spin

Consider the commutator $[H, \boldsymbol{L}]$, where $\boldsymbol{L} = \boldsymbol{r} \wedge \boldsymbol{p}$ is the orbital angular momentum operator:

$$[H, \boldsymbol{L}] = [\boldsymbol{\alpha}.\boldsymbol{p} + \beta m, \boldsymbol{r} \wedge \boldsymbol{p}] = [\boldsymbol{\alpha}.\boldsymbol{p}, \boldsymbol{r} \wedge \boldsymbol{p}] + [\beta m, \boldsymbol{r} \wedge \boldsymbol{p}]\ .$$

Since βm is a constant matrix, independent of $\boldsymbol{r}$ and $\boldsymbol{p}$, we have $[\beta m, \boldsymbol{r} \wedge \boldsymbol{p}] = 0$. Hence

$$[H, \boldsymbol{L}] = [\boldsymbol{\alpha}.\boldsymbol{p}, \boldsymbol{r} \wedge \boldsymbol{p}] \; .$$

Consider first the x component of this equation:

$$\begin{aligned} [H, L_x] &= [\boldsymbol{\alpha}.\boldsymbol{p}, (\boldsymbol{r} \wedge \boldsymbol{p})_x] \\ &= [\alpha_x p_x + \alpha_y p_y + \alpha_z p_z \; , \; y p_z - z p_y]. \end{aligned}$$

The various operators in this expression all commute with each other except that $[x, p_x] = [y, p_y] = [z, p_z] = i$. Hence

$$\begin{aligned} [H, L_x] &= \alpha_y p_z [p_y, y] - \alpha_z p_y [p_z, z] \\ &= -i(\alpha_y p_z - \alpha_z p_y) \\ &= -i(\boldsymbol{\alpha} \wedge \boldsymbol{p})_x \; . \end{aligned}$$

Similar expressions hold for the y and z components, giving overall the vector relation

$$[H, \boldsymbol{L}] = -i\boldsymbol{\alpha} \wedge \boldsymbol{p} \; . \tag{28}$$

Hence the angular momentum operator $\boldsymbol{L} = \boldsymbol{r} \wedge \boldsymbol{p}$ does not commute with the Hamiltonian H, showing that the angular momentum $\boldsymbol{L}$ is not a constant of the motion.

Now introduce the operator $\boldsymbol{\Sigma}$ defined as

$$\boldsymbol{\Sigma} \equiv \begin{pmatrix} \boldsymbol{\sigma} & 0 \\ 0 & \boldsymbol{\sigma} \end{pmatrix}$$

where $\boldsymbol{\sigma}$ represents the three 2×2 Pauli spin matrices. Explicitly, we have

$$\Sigma_x = \begin{pmatrix} 0 & 1 & 0 & 0 \\ 1 & 0 & 0 & 0 \\ 0 & 0 & 0 & 1 \\ 0 & 0 & 1 & 0 \end{pmatrix} ; \quad \Sigma_y = \begin{pmatrix} 0 & -i & 0 & 0 \\ i & 0 & 0 & 0 \\ 0 & 0 & 0 & -i \\ 0 & 0 & i & 0 \end{pmatrix} ; \quad \Sigma_z = \begin{pmatrix} 1 & 0 & 0 & 0 \\ 0 & -1 & 0 & 0 \\ 0 & 0 & 1 & 0 \\ 0 & 0 & 0 & -1 \end{pmatrix} \; .$$

The commutator $[H, \boldsymbol{\Sigma}]$ is given by

$$[H, \boldsymbol{\Sigma}] = [\boldsymbol{\alpha}.\boldsymbol{p} + \beta m, \boldsymbol{\Sigma}] = [\boldsymbol{\alpha}.\boldsymbol{p}, \boldsymbol{\Sigma}] + [\beta m, \boldsymbol{\Sigma}] \; .$$

But

$$[\beta, \boldsymbol{\Sigma}] = \begin{pmatrix} I & 0 \\ 0 & -I \end{pmatrix} \begin{pmatrix} \boldsymbol{\sigma} & 0 \\ 0 & \boldsymbol{\sigma} \end{pmatrix} - \begin{pmatrix} \boldsymbol{\sigma} & 0 \\ 0 & \boldsymbol{\sigma} \end{pmatrix} \begin{pmatrix} I & 0 \\ 0 & -I \end{pmatrix} = 0 \; ,$$

and hence

$$[H, \boldsymbol{\Sigma}] = [\boldsymbol{\alpha}.\boldsymbol{p}, \boldsymbol{\Sigma}] \; .$$

The x component of this equation is

$$\begin{aligned} [H, \Sigma_x] &= [\alpha_x p_x + \alpha_y p_y + \alpha_z p_z, \Sigma_x] \\ &= p_x [\alpha_x, \Sigma_x] + p_y [\alpha_y, \Sigma_x] + p_z [\alpha_z, \Sigma_x] \; . \end{aligned}$$

Evaluating each of the commutators on the right-hand side in turn gives

$$\begin{aligned}
[\alpha_x, \Sigma_x] &= \begin{pmatrix} 0 & \sigma_x \\ \sigma_x & 0 \end{pmatrix}\begin{pmatrix} \sigma_x & 0 \\ 0 & \sigma_x \end{pmatrix} - \begin{pmatrix} \sigma_x & 0 \\ 0 & \sigma_x \end{pmatrix}\begin{pmatrix} 0 & \sigma_x \\ \sigma_x & 0 \end{pmatrix} = 0 \\
[\alpha_y, \Sigma_x] &= \begin{pmatrix} 0 & \sigma_y \\ \sigma_y & 0 \end{pmatrix}\begin{pmatrix} \sigma_x & 0 \\ 0 & \sigma_x \end{pmatrix} - \begin{pmatrix} \sigma_x & 0 \\ 0 & \sigma_x \end{pmatrix}\begin{pmatrix} 0 & \sigma_y \\ \sigma_y & 0 \end{pmatrix} \\
&= \begin{pmatrix} 0 & \sigma_y\sigma_x - \sigma_x\sigma_y \\ \sigma_y\sigma_x - \sigma_x\sigma_y & 0 \end{pmatrix} \\
&= \begin{pmatrix} 0 & -2i\sigma_z \\ -2i\sigma_z & 0 \end{pmatrix} \\
&= -2i\alpha_z \\
[\alpha_z, \Sigma_x] &= 2i\alpha_y
\end{aligned}$$

where the commutation relations $[\sigma_x, \sigma_y] = 2i\sigma_z$ etc. have been used. Hence

$$\begin{aligned}
[H, \Sigma_x] &= -2ip_y\alpha_z + 2ip_z\alpha_y \\
&= 2i(\boldsymbol{\alpha} \wedge \boldsymbol{p})_x.
\end{aligned}$$

A similar result holds also for the y and z components, giving altogether

$$[H, \boldsymbol{\Sigma}] = 2i\boldsymbol{\alpha} \wedge \boldsymbol{p}. \tag{29}$$

Combining Equations (28) and (29), we obtain the result

$$\boxed{[H, \boldsymbol{L} + \tfrac{1}{2}\boldsymbol{\Sigma}] = 0}.$$

Thus, the combined operator

$$\boldsymbol{J} = \boldsymbol{L} + \tfrac{1}{2}\boldsymbol{\Sigma}$$

commutes with the Hamiltonian and is therefore conserved. The operator $\frac{1}{2}\boldsymbol{\Sigma}$ can be identified as the intrinsic angular momentum or *spin* of the electron:

$$\boxed{\boldsymbol{S} = \tfrac{1}{2}\boldsymbol{\Sigma}}.$$

The components of $\boldsymbol{S}$ obey the standard angular momentum commutation relations $[S_x, S_y] = iS_z$ etc. The operators S^2 and S_z are both diagonal:

$$S^2 = \tfrac{1}{4}(\Sigma_x^2 + \Sigma_y^2 + \Sigma_z^2) = \tfrac{3}{4}\begin{pmatrix} 1 & 0 & 0 & 0 \\ 0 & 1 & 0 & 0 \\ 0 & 0 & 1 & 0 \\ 0 & 0 & 0 & 1 \end{pmatrix}; \qquad S_z = \tfrac{1}{2}\begin{pmatrix} 1 & 0 & 0 & 0 \\ 0 & -1 & 0 & 0 \\ 0 & 0 & 1 & 0 \\ 0 & 0 & 0 & -1 \end{pmatrix}.$$

Thus S^2 and S_z commute and have eigenvalues $S(S+1) = \frac{3}{4}$ and $S_z = \pm\frac{1}{2}$, respectively. The operator $\boldsymbol{S}$ therefore corresponds to a spin angular momentum $S = \frac{1}{2}$. Such an intrinsic electron angular momentum had been postulated by Goudsmit and Uhlenbeck in 1925 to account for various features of atomic spectra; the Dirac equation (1928) finally provided a proper justification from first principles for the spin of the electron.

2.6 Covariant Notation: the Dirac γ Matrices

The Dirac equation can be written more elegantly by introducing the four Dirac gamma matrices $\gamma^0, \gamma^1, \gamma^2, \gamma^3$ defined as

$$\gamma^0 \equiv \beta; \qquad \gamma^1 \equiv \beta\alpha_x; \qquad \gamma^2 \equiv \beta\alpha_y; \qquad \gamma^3 \equiv \beta\alpha_z \ . \tag{30}$$

Premultiplying Equation (23) by $-\beta$, the Dirac equation can be written

$$i\beta\alpha_x\frac{\partial\psi}{\partial x} + i\beta\alpha_y\frac{\partial\psi}{\partial y} + i\beta\alpha_z\frac{\partial\psi}{\partial z} - \beta^2 m\psi = -i\beta\frac{\partial\psi}{\partial t} \ .$$

In terms of the Dirac gamma matrices, and using $\beta^2 = I$, this is

$$i\gamma^1\frac{\partial\psi}{\partial x} + i\gamma^2\frac{\partial\psi}{\partial y} + i\gamma^3\frac{\partial\psi}{\partial z} - m\psi = -i\gamma^0\frac{\partial\psi}{\partial t} \ . \tag{31}$$

Introducing the 4-vector

$$\partial_\mu = \left(\frac{\partial}{\partial t}, \frac{\partial}{\partial x}, \frac{\partial}{\partial y}, \frac{\partial}{\partial z}\right)$$

we have

$$\gamma^\mu\partial_\mu = \gamma^0\partial_0 + \gamma^1\partial_1 + \gamma^2\partial_2 + \gamma^3\partial_3 = \gamma^0\frac{\partial}{\partial t} + \gamma^1\frac{\partial}{\partial x} + \gamma^2\frac{\partial}{\partial y} + \gamma^3\frac{\partial}{\partial z} \ .$$

Hence Equation (31), the Dirac equation, can be written compactly as

$$\boxed{(i\gamma^\mu\partial_\mu - m)\psi = 0} \ .$$

From Equations (18) and (30), we have $(\gamma^0)^2 = \beta^2 = 1$. Similarly, for $(\gamma^1)^2$, we have

$$(\gamma^1)^2 = \beta\alpha_x \cdot \beta\alpha_x = -\alpha_x\beta\beta\alpha_x = -\alpha_x^2 = -1$$

where we have used $\alpha_x\beta = -\beta\alpha_x$ from Equation (19). Continuing in this vein, it is easily seen that the anticommutation relations (18), (19), (20) for $\boldsymbol{\alpha}$ and β become

$$\begin{aligned} (\gamma^0)^2 &= 1 \\ (\gamma^1)^2 = (\gamma^2)^2 &= (\gamma^3)^2 = -1 \\ \gamma^0\gamma^j + \gamma^j\gamma^0 &= 0 \\ \gamma^j\gamma^k + \gamma^k\gamma^j &= 0 \quad (j \neq k) \ . \end{aligned}$$

The above relations are all contained within the single expression

$$\boxed{\{\gamma^\mu, \gamma^\nu\} \equiv \gamma^\mu\gamma^\nu + \gamma^\nu\gamma^\mu = 2g^{\mu\nu}} \ . \tag{32}$$

Since β is Hermitian and $\gamma^0 = \beta$, then clearly γ^0 is Hermitian. Similarly, since the $\boldsymbol{\alpha}$ matrices are Hermitian, we have

$$\gamma^{1\dagger} = (\beta\alpha_x)^\dagger = \alpha_x^\dagger\beta^\dagger = \alpha_x\beta = -\beta\alpha_x = -\gamma^1$$

and similarly $\gamma^{2\dagger} = -\gamma^2$, $\gamma^{3\dagger} = -\gamma^3$. In summary, γ^0 is Hermitian while $\gamma^1, \gamma^2, \gamma^3$ are anti-Hermitian:

$$\boxed{\gamma^{0\dagger} = \gamma^0, \quad \gamma^{1\dagger} = -\gamma^1, \quad \gamma^{2\dagger} = -\gamma^2, \quad \gamma^{3\dagger} = -\gamma^3}\,.$$

It is often convenient to work with a particular representation of the γ matrices, such as the Pauli-Dirac representation:

$$\gamma^0 = \begin{pmatrix} I & 0 \\ 0 & -I \end{pmatrix}, \qquad \gamma^k = \begin{pmatrix} 0 & \sigma_k \\ -\sigma_k & 0 \end{pmatrix}$$

where I is the 2×2 unit matrix and the σ_k are the 2×2 Pauli spin matrices of Equation (22). In full, we have

$$\gamma^0 = \begin{pmatrix} 1 & 0 & 0 & 0 \\ 0 & 1 & 0 & 0 \\ 0 & 0 & -1 & 0 \\ 0 & 0 & 0 & -1 \end{pmatrix}; \qquad \gamma^1 = \begin{pmatrix} 0 & 0 & 0 & 1 \\ 0 & 0 & 1 & 0 \\ 0 & -1 & 0 & 0 \\ -1 & 0 & 0 & 0 \end{pmatrix};$$

$$\gamma^2 = \begin{pmatrix} 0 & 0 & 0 & -i \\ 0 & 0 & i & 0 \\ 0 & i & 0 & 0 \\ -i & 0 & 0 & 0 \end{pmatrix}; \qquad \gamma^3 = \begin{pmatrix} 0 & 0 & 1 & 0 \\ 0 & 0 & 0 & -1 \\ -1 & 0 & 0 & 0 \\ 0 & 1 & 0 & 0 \end{pmatrix}.$$

As before, all physical quantities can be shown to be independent of the particular represntation of the Dirac γ-matrices.

Equations (26) and (27) for the probability density and current, $\rho = \psi^\dagger\psi$ and $\boldsymbol{j} = \psi^\dagger\boldsymbol{\alpha}\psi$, can be written in the form

$$j^\mu = \psi^\dagger\gamma^0\gamma^\mu\psi$$

where $j^\mu \equiv (\rho, \boldsymbol{j})$ is the 4-vector current, while the continuity equation, Equation (25), becomes

$$\partial_\mu j^\mu = 0.$$

It is useful to define here the *adjoint spinor*

$$\boxed{\overline{\psi} \equiv \psi^\dagger\gamma^0}\,.$$

This is a 1×4 row matrix which, in the Pauli-Dirac representation, has components

$$\overline{\psi} = \psi^\dagger\gamma^0 = (\psi^*)^T\gamma^0 = (\psi_1^*, \psi_2^*, \psi_3^*, \psi_4^*) \begin{pmatrix} 1 & 0 & 0 & 0 \\ 0 & 1 & 0 & 0 \\ 0 & 0 & -1 & 0 \\ 0 & 0 & 0 & -1 \end{pmatrix} = (\psi_1^*, \psi_2^*, -\psi_3^*, -\psi_4^*)\,.$$

In terms of the adjoint spinor $\overline{\psi}$, the current j^μ can be written

$$\boxed{j^\mu = \overline{\psi}\gamma^\mu\psi}\,.$$

We shall encounter many constructions of this form when evaluating transition matrix elements for scattering and decay processes.

Note that, despite the suggestive notation, the Dirac γ matrices by themselves do not constitute a 4-vector; they are simply constant 4×4 matrices, and so remain invariant under Lorentz transformations. However, it can be shown that, for any Lorentz transformation $x \to x'$, there exists a corresponding transformation $\psi'(x') = S\psi(x)$, with S a suitable 4×4 matrix, which keeps the form of the Dirac equation invariant. It can also be shown that the current $\overline{\psi}\gamma^\mu\psi$ does indeed transform as a four-vector. A (non-examinable) proof of these statements is provided in the Appendices, Sections 2.18 and 2.19.

2.7 Plane Wave Solutions

2.7.1 Derivation of Plane Wave Solutions

We now look for free particle (plane wave) solutions to the Dirac equation of the form

$$\boxed{\psi = u(E,\boldsymbol{p})e^{i(\boldsymbol{p}.\boldsymbol{r}-Et)}},$$

where the coefficient $u(E,\boldsymbol{p})$ is a constant 4-component spinor, and E and $\boldsymbol{p}$ are constants. The first order derivatives $\partial_\mu\psi$ are:

$$\partial_0\psi = \frac{\partial\psi}{\partial t} = -iE\psi; \qquad \partial_1\psi = \frac{\partial\psi}{\partial x} = ip_x\psi; \qquad \partial_2\psi = \frac{\partial\psi}{\partial y} = ip_y\psi; \qquad \partial_3\psi = \frac{\partial\psi}{\partial z} = ip_z\psi\ .$$

Substituting into the Dirac equation, Equation (31), and cancelling the phase factor $e^{i(\boldsymbol{p}.\boldsymbol{r}-Et)}$ then gives

$$i\gamma^1.ip_xu + i\gamma^2.ip_yu + i\gamma^3.ip_zu - mu = -i\gamma^0. - iEu\ .$$

This can be rearranged as

$$(\gamma^0E - \gamma^1p_x - \gamma^2p_y - \gamma^3p_z - m)u = 0\ ,$$

or, more compactly, as

$$\boxed{(\gamma^\mu p_\mu - m)\,u = 0}\,. \tag{33}$$

The factor in brackets is

$$\begin{aligned}\gamma^\mu p_\mu - m &= \gamma^0E - \boldsymbol{\gamma}.\boldsymbol{p} - m \\ &= \begin{pmatrix} I & 0 \\ 0 & -I \end{pmatrix} E - \begin{pmatrix} 0 & \boldsymbol{\sigma} \\ -\boldsymbol{\sigma} & 0 \end{pmatrix} \cdot \boldsymbol{p} \ - \ m \begin{pmatrix} I & 0 \\ 0 & I \end{pmatrix} \\ &= \begin{pmatrix} E-m & -\boldsymbol{\sigma}.\boldsymbol{p} \\ \boldsymbol{\sigma}.\boldsymbol{p} & -E-m \end{pmatrix}\ .\end{aligned}$$

Equation (33) can therefore be written in terms of 2×2 matrix subcomponents as

$$\begin{pmatrix} E-m & -\boldsymbol{\sigma}.\boldsymbol{p} \\ \boldsymbol{\sigma}.\boldsymbol{p} & -E-m \end{pmatrix} \begin{pmatrix} u_A \\ u_B \end{pmatrix} = \begin{pmatrix} 0 \\ 0 \end{pmatrix}$$

where u_A and u_B are two-component spinors known as *Weyl spinors*. We thus obtain two coupled equations for u_A and u_B:

$$(\boldsymbol{\sigma}.\boldsymbol{p})u_B = (E-m)u_A \tag{34}$$

$$(\boldsymbol{\sigma}.\boldsymbol{p})u_A = (E+m)u_B\ , \tag{35}$$

which can be solved to yield four linearly-independent plane-wave solutions.

Before solving Equations (34) and (35), we first check that the constants E and $\boldsymbol{p}$ appearing in the phase factor $e^{i(\boldsymbol{p}.\boldsymbol{r}-Et)}$ obey the relation $E^2 = |\boldsymbol{p}|^2 + m^2$ expected for a relativistic particle. The matrix $\boldsymbol{\sigma}.\boldsymbol{p}$ is given by

$$\begin{aligned}\boldsymbol{\sigma}.\boldsymbol{p} &= \sigma_x p_x + \sigma_y p_y + \sigma_z p_z \\ &= \begin{pmatrix} 0 & 1 \\ 1 & 0 \end{pmatrix} p_x + \begin{pmatrix} 0 & -i \\ i & 0 \end{pmatrix} p_y + \begin{pmatrix} 1 & 0 \\ 0 & -1 \end{pmatrix} p_z \\ &= \begin{pmatrix} p_z & p_x - ip_y \\ p_x + ip_y & -p_z \end{pmatrix} . \end{aligned} \tag{36}$$

Hence

$$(\boldsymbol{\sigma}.\boldsymbol{p})^2 = \begin{pmatrix} p_z & p_x - ip_y \\ p_x + ip_y & -p_z \end{pmatrix} \begin{pmatrix} p_z & p_x - ip_y \\ p_x + ip_y & -p_z \end{pmatrix} = \begin{pmatrix} |\boldsymbol{p}|^2 & 0 \\ 0 & |\boldsymbol{p}|^2 \end{pmatrix} = |\boldsymbol{p}|^2 I . \tag{37}$$

Operating on Equation (35) with $\boldsymbol{\sigma}.\boldsymbol{p}$ gives

$$(\boldsymbol{\sigma}.\boldsymbol{p})^2 u_A = (E+m)(\boldsymbol{\sigma}.\boldsymbol{p}) u_B .$$

Using Equations (34) and (37), this becomes

$$|\boldsymbol{p}|^2 u_A = (E+m)(E-m)u_A = (E^2 - m^2)u_A ,$$

so that we indeed obtain

$$E^2 = |\boldsymbol{p}|^2 + m^2 .$$

This is to be expected since ψ was required to satisfy the Klein-Gordon equation, Equation (17), as well as the Dirac equation, Equation (15). Just as for the Klein-Gordon equation, both positive energy ($E > 0$) and negative energy ($E < 0$) solutions to the Dirac equation are therefore possible.

We now obtain explicit solutions to Equations (34) and (35). Two independent solutions can be obtained with the simple (arbitrary) choices

$$u_A = \begin{pmatrix} 1 \\ 0 \end{pmatrix} \qquad \text{or} \qquad u_A = \begin{pmatrix} 0 \\ 1 \end{pmatrix} .$$

The corresponding two-component spinor u_B is then determined by Equation (35):

$$u_B = \frac{\boldsymbol{\sigma}.\boldsymbol{p}}{E+m} u_A = \frac{1}{E+m} \begin{pmatrix} p_z & p_x - ip_y \\ p_x + ip_y & -p_z \end{pmatrix} u_A .$$

Taking each choice of u_A in turn then gives

$$\boxed{u_1 = N \begin{pmatrix} 1 \\ 0 \\ p_z/(E+m) \\ (p_x + ip_y)/(E+m) \end{pmatrix} , \qquad u_2 = N \begin{pmatrix} 0 \\ 1 \\ (p_x - ip_y)/(E+m) \\ -p_z/(E+m) \end{pmatrix}} \tag{38}$$

where N is a normalisation factor, determined below.

Two further solutions can be found by choosing

$$u_B = \begin{pmatrix} 1 \\ 0 \end{pmatrix} \qquad \text{or} \qquad u_B = \begin{pmatrix} 0 \\ 1 \end{pmatrix} \ .$$

In this case, u_A is determined by Equation (34):

$$u_A = \frac{\boldsymbol{\sigma.p}}{E-m} u_B = \frac{1}{E-m} \begin{pmatrix} p_z & p_x - ip_y \\ p_x + ip_y & -p_z \end{pmatrix} u_B$$

giving

$$\boxed{u_3 = N \begin{pmatrix} p_z/(E-m) \\ (p_x + ip_y)/(E-m) \\ 1 \\ 0 \end{pmatrix}, \qquad u_4 = N \begin{pmatrix} (p_x - ip_y)/(E-m) \\ -p_z/(E-m) \\ 0 \\ 1 \end{pmatrix}}. \tag{39}$$

We have thus determined four seemingly independent solutions $\psi_i = u_i(E, \boldsymbol{p}) e^{i(\boldsymbol{p}.\boldsymbol{r} - Et)}$. In fact, as we show next, the above solutions are only independent if the energy E is chosen to be *positive* for two of the solutions (conventionally u_1 and u_2) and *negative* for the others (conventionally u_3 and u_4). First, however, we need expressions for the normalisation factors, N.

2.7.2 Normalisation of Plane Wave Solutions

For a multi-component spinor ψ, the normalisation is determined by the value of $\psi^\dagger \psi = (\psi^*)^T \psi$, the straightforward generalisation of the usual product $\psi^* \psi$ appropriate to a single-component wavefunction. For a plane wave of the form $\psi = u(p) e^{ip.x}$, we have $\psi^\dagger = u(p)^\dagger e^{-ip.x}$ and hence $\psi^\dagger \psi = u^\dagger u$.

For the basis spinor u_1 of Equation (38), we have

$$u_1^\dagger u_1 = |N|^2 \left(1 + \frac{p_z^2}{(E+m)^2} + \frac{p_x^2 + p_y^2}{(E+m)^2} \right) = |N|^2 \frac{(E+m)^2 + p^2}{(E+m)^2} \ .$$

Using the relation $E^2 = p^2 + m^2$, this can be written

$$u_1^\dagger u_1 = |N|^2 \frac{2E^2 + 2Em}{(E+m)^2} = |N|^2 \frac{2E}{E+m} \ .$$

A similar calculation for $u_2^\dagger u_2$, $u_3^\dagger u_3$, $u_4^\dagger u_4$ gives overall

$$u_1^\dagger u_1 = u_2^\dagger u_2 = |N|^2 \frac{2E}{E+m}; \qquad u_3^\dagger u_3 = u_4^\dagger u_4 = |N|^2 \frac{2E}{E-m} \ .$$

For reasons which will be explained later, it is conventional to normalise to $2|E|$ particles per unit volume and choose

$$u_1^\dagger u_1 = u_2^\dagger u_2 = u_3^\dagger u_3 = u_4^\dagger u_4 = 2|E| \ .$$

For u_1 and u_2, depending on the sign of E, we therefore have

$$\boxed{N = \sqrt{(E+m)} \quad (E > 0); \qquad N = \sqrt{(-E-m)} \quad (E < 0)},$$

while for u_3 and u_4, we have

$$\boxed{N = \sqrt{(E-m)} \quad (E > 0); \qquad N = \sqrt{(-E+m)} \quad (E < 0)}.$$

Note that, since the energy E is in fact restricted to either $E > +m$ or $E < -m$, the square root is real in all cases.

2.7.3 Negative Energy Solutions

We now consider the consequences of choosing the positive energy option, $E = +\sqrt{p^2+m^2}$, simultaneously for all four solutions u_i. We introduce spherical polar coordinates θ and ϕ and write the three-momentum $\boldsymbol{p}$ as

$$\boldsymbol{p} = (p_x, p_y, p_z) = (p\sin\theta\cos\phi, p\sin\theta\sin\phi, p\cos\theta)\ .$$

Taking $N = \sqrt{E+m}$ for u_1 and u_2, $N = \sqrt{E-m}$ for u_3 and u_4, using $p_x \pm ip_y = p\sin\theta e^{\pm i\phi}$, and noting that $p = \sqrt{E^2-m^2} = \sqrt{E-m}\sqrt{E+m}$, the u_i can then be written in the form

$$u_1 = \begin{pmatrix} \sqrt{(E+m)} \\ 0 \\ \sqrt{(E-m)}\cos\theta \\ \sqrt{(E-m)}\sin\theta e^{i\phi} \end{pmatrix}; \qquad u_2 = \begin{pmatrix} 0 \\ \sqrt{(E+m)} \\ \sqrt{(E-m)}\sin\theta e^{-i\phi} \\ -\sqrt{(E-m)}\cos\theta \end{pmatrix}$$

and

$$u_3 = \begin{pmatrix} \sqrt{(E+m)}\cos\theta \\ \sqrt{(E+m)}\sin\theta e^{i\phi} \\ \sqrt{(E-m)} \\ 0 \end{pmatrix}; \qquad u_4 = \begin{pmatrix} \sqrt{(E+m)}\sin\theta e^{-i\phi} \\ -\sqrt{(E+m)}\cos\theta \\ 0 \\ \sqrt{(E-m)} \end{pmatrix}.$$

In this form, the spinors u_3 and u_4 are easily seen to be just linear combinations of u_1 and u_2:

$$u_3 = \cos\theta u_1 + \sin\theta e^{i\phi} u_2$$
$$u_4 = \sin\theta e^{-i\phi} u_1 - \cos\theta u_2\ .$$

We conclude that it is therefore *not* possible to choose the positive energy option $E = +\sqrt{p^2+m^2}$ simultaneously for all four solutions u_i. To obtain four linearly independent solutions, we are obliged to consider both positive and negative energy solutions together. A conventional choice is to retain $E > 0$ for u_1 and u_2, and to flip the sign of E for u_3 and u_4. At this point, for the negative-energy solutions, it becomes more convenient (and standard) to work with plane waves of the form

$$\boxed{\psi = v(E,\boldsymbol{p})e^{-i(\boldsymbol{p}.\boldsymbol{r}-Et)}}, \tag{40}$$

where it is to be understood that E is now always positive: $E = +\sqrt{|\boldsymbol{p}|^2+m^2}$. Note that, although we now have $E > 0$, solutions of the form of Equation (40) are nevertheless still negative-energy solutions, in the sense that the eigenvalue of the energy operator $i\partial/\partial t$ is $-E$.

For solutions of the form $\psi = v(E, \boldsymbol{p})e^{-i(\boldsymbol{p}.\boldsymbol{r}-Et)}$, Equation (33) is replaced by

$$(\gamma^\mu p_\mu + m)\, v = 0 \ , \tag{41}$$

while Equations (34) and (35) become

$$(\boldsymbol{\sigma}.\boldsymbol{p})v_B = (E+m)v_A \tag{42}$$
$$(\boldsymbol{\sigma}.\boldsymbol{p})v_A = (E-m)v_B \ . \tag{43}$$

These equations are identical in form to Equations (34) and (35), with u_A replaced by v_B and u_B replaced by v_A. Solutions for $v(E, \boldsymbol{p})$ can therefore be written down directly from those already obtained for $u(E, \boldsymbol{p})$ simply by interchanging the upper and lower components of $u(E, \boldsymbol{p})$. Applying this transformation to the spinors u_1 and u_2 of Equation (38), for example, gives the standard solutions

$$\boxed{v_1 = \sqrt{E+m}\begin{pmatrix} (p_x - ip_y)/(E+m) \\ -p_z/(E+m) \\ 0 \\ 1 \end{pmatrix}; \qquad v_2 = \sqrt{E+m}\begin{pmatrix} p_z/(E+m) \\ (p_x + ip_y)/(E+m) \\ 1 \\ 0 \end{pmatrix}}. \tag{44}$$

The reason for labelling v_1 as the spinor with $v_B = (0, 1)$ and v_2 as the spinor with $v_B = (1, 0)$, rather than the other way round, will become clear shortly.

We note that the spinors v_1 and v_2 could also have been obtained directly from the spinors u_3 and u_4 of Equation (39) by reversing the signs of E and $\boldsymbol{p}$:

$$v_1(E, \boldsymbol{p}) = u_4(-E, -\boldsymbol{p}), \qquad v_2(E, \boldsymbol{p}) = u_3(-E, -\boldsymbol{p}) \ ,$$

provided a normalisation factor N appropriate to negative energy is used for u_3 and u_4. From now on, we shall work entirely in terms of v_1 and v_2 and make no further reference to u_3 and u_4.

2.7.4 Summary

In summary, the Dirac equation possesses four linearly independent plane wave solutions; two positive energy solutions plus two negative energy solutions. A standard choice for the positive energy solutions is

$$\psi = u_1(E, \boldsymbol{p})e^{i(\boldsymbol{p}.\boldsymbol{r}-Et)}, \qquad \psi = u_2(E, \boldsymbol{p})e^{i(\boldsymbol{p}.\boldsymbol{r}-Et)} \ ,$$

with $u_1(E, \boldsymbol{p})$ and $u_2(E, \boldsymbol{p})$ given by Equation (38), while a standard choice for the negative energy solutions is

$$\psi = v_1(E, \boldsymbol{p})e^{-i(\boldsymbol{p}.\boldsymbol{r}-Et)}, \qquad \psi = v_2(E, \boldsymbol{p})e^{-i(\boldsymbol{p}.\boldsymbol{r}-Et)} \ ,$$

with $v_1(E, \boldsymbol{p})$ and $v_2(E, \boldsymbol{p})$ given by Equation (44). For all these solutions, it is to be understood that the quantity E is always positive: $E = +\sqrt{|\boldsymbol{p}|^2 + m^2}$.

2.8 Interpretation of Plane Wave Solutions

Stückelberg (1941) and Feynman (1948) suggested that the negative energy solutions of the form $\psi = v(E,\boldsymbol{p})e^{-i(\boldsymbol{p}.\boldsymbol{r}-Et)}$ be interpreted physically as *antiparticles* with momentum $\boldsymbol{p}$ and *positive* energy $E = +\sqrt{|\boldsymbol{p}|^2+m^2}$. Schematically, these solutions can be obtained from solutions of the form $\psi = u(E,\boldsymbol{p})e^{i(\boldsymbol{p}.\boldsymbol{r}-Et)}$ by reversing the sign of the energy and three-momentum:

$$v(E,\boldsymbol{p}) \equiv u(-E,-\boldsymbol{p})\ .$$

The Stückelberg-Feynman approach therefore amounts to reinterpreting *particles* of momentum $-\boldsymbol{p}$ and *negative* energy $E = -\sqrt{|\boldsymbol{p}|^2+m^2}$ as *antiparticles* of momentum $\boldsymbol{p}$ and *positive* energy $E = +\sqrt{|\boldsymbol{p}|^2+m^2}$. [1]

Under the transformation $(E,\boldsymbol{p}) \to (-E,-\boldsymbol{p})$, the position vector $\boldsymbol{r}$ remains unchanged and hence the orbital angular momentum $\boldsymbol{L} = \boldsymbol{r}\wedge\boldsymbol{p}$ must change sign: $\boldsymbol{L}\to-\boldsymbol{L}$. Conservation of angular momentum, $[H,\boldsymbol{L}+\boldsymbol{S}]=0$, can then only be maintained if $\boldsymbol{S}\to-\boldsymbol{S}$ also. Thus we have

$$E\to -E,\quad \boldsymbol{p}\to-\boldsymbol{p},\quad \boldsymbol{S}\to-\boldsymbol{S}\ ,$$

so that, similarly to the energy and three-momentum, the *physical* spin of an antiparticle is obtained by reversing the sign of the spin given by the spin operator $\boldsymbol{S}$.

For a free particle or antiparticle travelling along the z axis, with $p_x = p_y = 0$ and $\boldsymbol{p} = (0,0,p_z)$, the spinors u_1, u_2, v_1, v_2 of Equations (38) and (44) become

$$u_1 = N\begin{pmatrix}1\\0\\\frac{p_z}{E+m}\\0\end{pmatrix};\quad u_2 = N\begin{pmatrix}0\\1\\0\\\frac{-p_z}{E+m}\end{pmatrix};\quad v_1 = N\begin{pmatrix}0\\\frac{-p_z}{E+m}\\0\\1\end{pmatrix};\quad v_2 = N\begin{pmatrix}\frac{p_z}{E+m}\\0\\1\\0\end{pmatrix}\ .$$

These spinors are easily seen to be eigenstates of the spin operator

$$S_z = \tfrac{1}{2}\Sigma_z = \tfrac{1}{2}\begin{pmatrix}\sigma_z & 0\\0&\sigma_z\end{pmatrix} = \tfrac{1}{2}\begin{pmatrix}1&0&0&0\\0&-1&0&0\\0&0&1&0\\0&0&0&-1\end{pmatrix}$$

with eigenvalues $\pm\frac{1}{2}$:

$$S_z u_1 = +\tfrac{1}{2}u_1 \qquad S_z v_1 = -\tfrac{1}{2}v_1 \tag{45}$$

$$S_z u_2 = -\tfrac{1}{2}u_2 \qquad S_z v_2 = +\tfrac{1}{2}v_2 \tag{46}$$

Thus, for the particular case of motion along the z-axis, the standard solutions u_1, u_2, v_1, v_2 become eigenstates of spin, with the spin vector aligned in the $\pm z$ direction. For antiparticles, because of the transformation $\boldsymbol{S}\to-\boldsymbol{S}$ discussed above, the *physical* spin is the *opposite* of that given by the action of the S_z operator. The physical antiparticle spin is therefore $S_z = +\frac{1}{2}$ for v_1 and $S_z = -\frac{1}{2}$ for v_2.

[1] In Feynman diagrams, a common convention (which we shall follow) is that the arrows drawn on lines representing spin-half particles or antiparticles indicate the *particle* direction. For antiparticles, the arrow therefore points in the opposite sense to the actual direction of the antiparticle.

These results can be represented schematically as

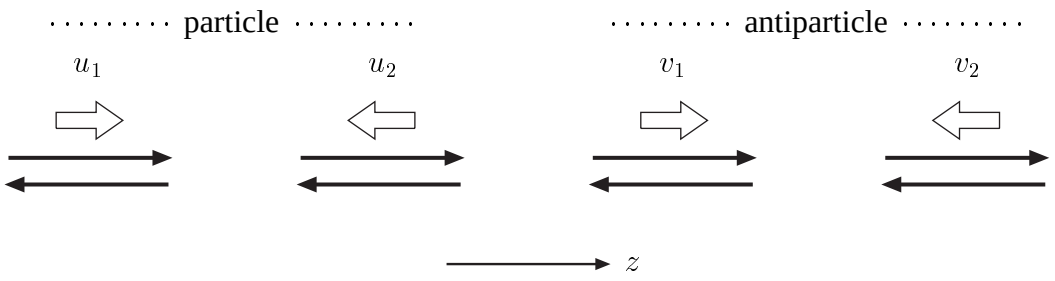

Note that the antiparticle spin $S_z = +\frac{1}{2}$ associated with the spinor v_1 is the same as the particle spin associated with the spinor u_1. Similarly, the antiparticle spinor v_2 has the same spin, $S_z = -\frac{1}{2}$, as the particle spinor u_2. This was the reason for labelling the spinors v_1 and v_2 in the order given in Equation (44), rather than the other way around.

It should be emphasised that Equations (45) and (46) hold only for motion in the $\pm z$ directions, with $p_x = p_y = 0$. For motion in any other direction, with $p_x \neq 0$ and/or $p_y \neq 0$, it is easily checked that the spinors u_i and v_i are *not* spin eigenstates. We consider this further below.

In an Appendix, Section 2.17, it is shown that an antiparticle has the same mass but opposite electric charge to its corresponding particle. This is done by considering the equation of motion of a spin-half particle in an electromagnetic field and by introducing the *charge conjugation* operator, C. As its name suggests, the operator C reverses the sign of all electric charges and hence transforms particles into antiparticles and *vice-versa*. The correspondence between u_1 and v_1, and between u_2 and v_2, emerges formally from this analysis.

2.9 Helicity

The *helicity* operator h measures the projection of the particle spin along the direction of motion. For a particle (or antiparticle) of three-momentum $\boldsymbol{p}$, the helicity is defined as

$$h \equiv 2\boldsymbol{S}.\hat{\boldsymbol{p}} = \boldsymbol{\Sigma}.\hat{\boldsymbol{p}} = \begin{pmatrix} \boldsymbol{\sigma}.\hat{\boldsymbol{p}} & 0 \\ 0 & \boldsymbol{\sigma}.\hat{\boldsymbol{p}} \end{pmatrix}$$

where $\hat{\boldsymbol{p}}$ is a constant unit vector along $\boldsymbol{p}$, and $\boldsymbol{\Sigma} = 2\boldsymbol{S}$. For a free spin $\frac{1}{2}$ particle or antiparticle there are two possible helicity eigenstates: one with spin eigenvalue $S_{z'} = +\frac{1}{2}$ with respect to an axis z' oriented along the direction of motion (helicity eigenvalue $h = +1$), and one with spin eigenvalue $S_{z'} = -\frac{1}{2}$ (helicity eigenvalue $h = -1$). Schematically, the helicity eigenstates can be pictured as:

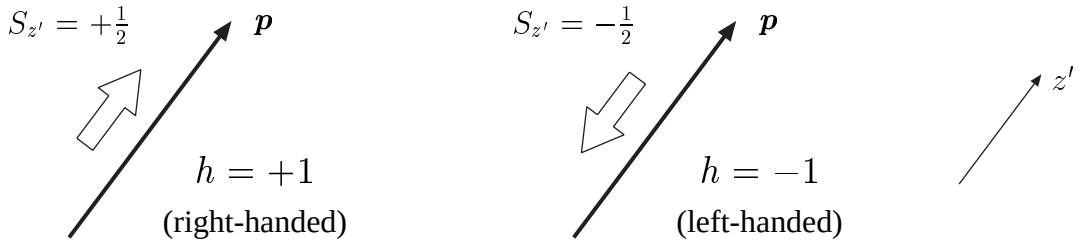

A particle or antiparticle in a helicity eigenstate with $h = +1$ is said to be *right-handed*, while one in an eigenstate with $h = -1$ is said to be *left-handed*.

For a particle or antiparticle travelling forwards or backwards along the z-axis, with $p^\mu = (E, 0, 0, p_z)$, the helicity eigenstates are given by the spinors u_i and v_i. For motion in the $+z$ direction ($p_z > 0$), the helicity eigenvalues corresponding to the spin states u_1, u_2, v_1, v_2 are $+1$, -1, $+1$, -1, respectively:

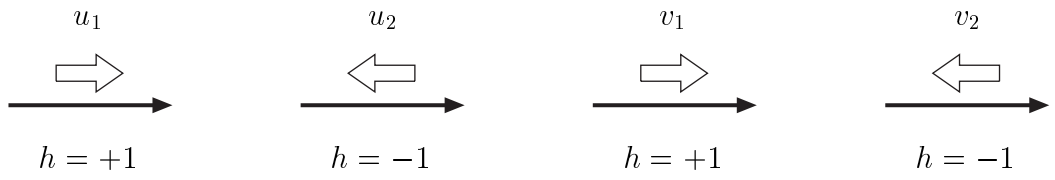

For motion in the $-z$ direction ($p_z < 0$), the spin direction remains unchanged and the helicity eigenvalues are reversed:

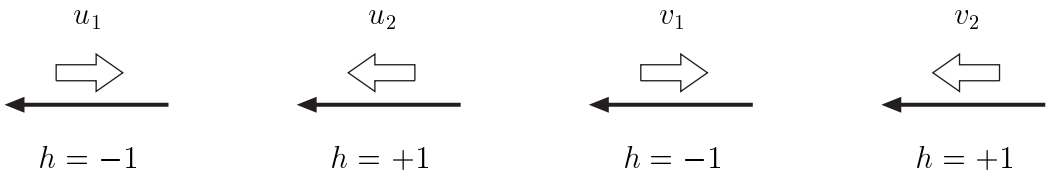

In general, *i.e.* for particle motion not directed along the z axis, the spinors u_i are *not* helicity eigenstates. In the next section, we construct the helicity eigenstates for free particles and antiparticles moving in an arbitrary direction.

2.10 Construction of Helicity Eigenstates

For a *particle* of three-momentum $\boldsymbol{p}$, the positive and negative helicity eigenstates $u_\uparrow$ and $u_\downarrow$ are defined by the equations

$$(\boldsymbol{\Sigma}.\hat{\boldsymbol{p}})u_\uparrow = +u_\uparrow \tag{47}$$
$$(\boldsymbol{\Sigma}.\hat{\boldsymbol{p}})u_\downarrow = -u_\downarrow \ . \tag{48}$$

In terms of two-component Weyl spinors u_A and u_B, this is

$$\begin{pmatrix} \boldsymbol{\sigma}.\hat{\boldsymbol{p}} & 0 \\ 0 & \boldsymbol{\sigma}.\hat{\boldsymbol{p}} \end{pmatrix} \begin{pmatrix} u_A \\ u_B \end{pmatrix} = \pm \begin{pmatrix} u_A \\ u_B \end{pmatrix} \ ,$$

which gives two identical decoupled equations

$$(\boldsymbol{\sigma}.\hat{\boldsymbol{p}})u_A = \pm u_A \tag{49}$$
$$(\boldsymbol{\sigma}.\hat{\boldsymbol{p}})u_B = \pm u_B \ . \tag{50}$$

For a particle moving at an angle θ to the z axis and with azimuthal angle ϕ, the unit vector $\hat{\boldsymbol{p}}$ is

$$\hat{\boldsymbol{p}} = (\sin\theta\cos\phi, \sin\theta\sin\phi, \cos\theta) \ .$$

Using Equation (36) and denoting the two components of the spinors u_A or u_B by a and b, Equations (49) and (50) are then both equivalent to

$$\begin{pmatrix} \cos\theta & \sin\theta e^{-i\phi} \\ \sin\theta e^{i\phi} & -\cos\theta \end{pmatrix} \begin{pmatrix} a \\ b \end{pmatrix} = \pm \begin{pmatrix} a \\ b \end{pmatrix} .$$

The first row (or equivalently the second row) of this matrix equation gives

$$\frac{b}{a} = \frac{\pm 1 - \cos\theta}{\sin\theta} e^{i\phi} .$$

For the positive helicity solution $u_\uparrow$, with $h = +1$, we have

$$\frac{b}{a} = \frac{1 - \cos\theta}{\sin\theta} e^{i\phi} = \frac{2\sin^2\theta/2}{2\sin\theta/2\cos\theta/2} e^{i\phi} = e^{i\phi}\tan\theta/2 ,$$

and we can therefore take

$$(u_\uparrow)_A \text{ or } (u_\uparrow)_B \propto \begin{pmatrix} \cos\theta/2 \\ e^{i\phi}\sin\theta/2 \end{pmatrix} . \tag{51}$$

For the negative helicity solution $u_\downarrow$, with $h = -1$, we have instead

$$\frac{b}{a} = \frac{-1 - \cos\theta}{\sin\theta} e^{i\phi} = \frac{-2\cos^2\theta/2}{2\sin\theta/2\cos\theta/2} e^{i\phi} = -e^{i\phi}\cot\theta/2 ,$$

and can take

$$(u_\downarrow)_A \text{ or } (u_\downarrow)_B \propto \begin{pmatrix} -\sin\theta/2 \\ e^{i\phi}\cos\theta/2 \end{pmatrix} . \tag{52}$$

Once u_A is chosen, u_B is given in terms of u_A by Equation (35):

$$u_B = \frac{\boldsymbol{\sigma.p}}{E+m} u_A = \frac{p}{E+m} (\boldsymbol{\sigma.\hat{p}}) u_A = \pm \frac{p}{E+m} u_A .$$

Using the two possible choices of u_A given in Equations (51) and (52) in turn then gives the helicity eigenstates as

$$\boxed{u_\uparrow(p) = N \begin{pmatrix} \cos\theta/2 \\ e^{i\phi}\sin\theta/2 \\ \frac{p}{E+m}\cos\theta/2 \\ \frac{p}{E+m} e^{i\phi}\sin\theta/2 \end{pmatrix}, \qquad u_\downarrow(p) = N \begin{pmatrix} -\sin\theta/2 \\ e^{i\phi}\cos\theta/2 \\ \frac{p}{E+m}\sin\theta/2 \\ -\frac{p}{E+m} e^{i\phi}\cos\theta/2 \end{pmatrix},}$$

where the normalisation condition $(u_\uparrow)^\dagger u_\uparrow = (u_\downarrow)^\dagger u_\downarrow = 2E$ fixes the constant N as $N = \sqrt{E+m}$.

Instead of choosing u_A and then determining u_B via Equation (35), it would be equally possible to choose u_B and then determine u_A via Equation (34). It is straightforward to verify that this results in precisely the same expressions for $u_\uparrow$ and $u_\downarrow$ as found above.

Turning now to *antiparticles*, and remembering that the spin operator changes sign ($\boldsymbol{S} \to -\boldsymbol{S}$), the positive and negative helicity eigenstates $v_\uparrow$ and $v_\downarrow$ are defined by

$$(\boldsymbol{\Sigma.\hat{p}}) v_\uparrow = -v_\uparrow$$
$$(\boldsymbol{\Sigma.\hat{p}}) v_\downarrow = +v_\downarrow .$$

This is the same as Equations (47) and (48) for particles, but with $u_\uparrow$ replaced by $v_\downarrow$ and $u_\downarrow$ replaced by $v_\uparrow$. In addition, for antiparticles, we have Equations (42) and (43) in place of Equations (34) and (35), which effectively replaces u_A by v_B and u_B by v_A. The antiparticle spinors $v_\uparrow$ and $v_\downarrow$ can therefore be written down directly by interchanging the upper and lower components of the particle spinors $u_\uparrow$ and $u_\downarrow$ and then interchanging $\uparrow$ and $\downarrow$:

$$\boxed{v_\uparrow(p) = N \begin{pmatrix} \frac{p}{E+m}\sin\theta/2 \\ -\frac{p}{E+m}e^{i\phi}\cos\theta/2 \\ -\sin\theta/2 \\ e^{i\phi}\cos\theta/2 \end{pmatrix}, \qquad v_\downarrow(p) = N \begin{pmatrix} \frac{p}{E+m}\cos\theta/2 \\ \frac{p}{E+m}e^{i\phi}\sin\theta/2 \\ \cos\theta/2 \\ e^{i\phi}\sin\theta/2 \end{pmatrix}.}$$

Here, the energy $E > 0$ is the physical energy of the antiparticle, and the normalisation factor can again be shown to be $N = \sqrt{E+m}$.

Schematically, the helicity eigenstate spinors can be pictured as:

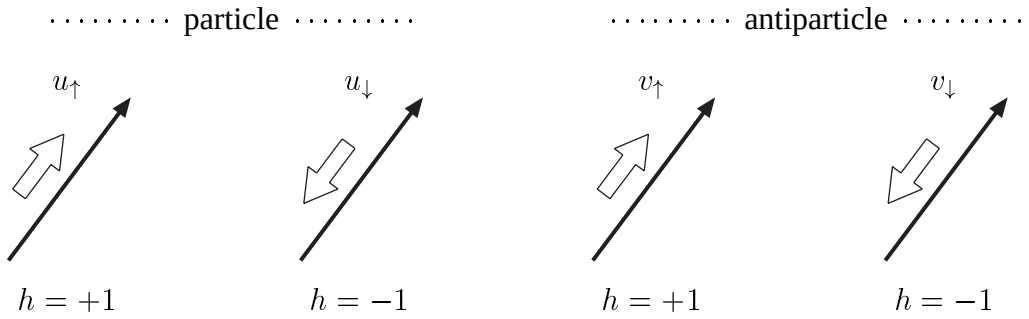

Note that when $\theta = 0$ (and hence $p_x = p_y = 0$, $p_z = p$) the spinor $u_\uparrow$ becomes equal to u_1, $u_\downarrow$ becomes equal to u_2, $v_\uparrow$ becomes equal to v_1, and $v_\downarrow$ becomes equal to v_2, as expected.

Similarly, when $\theta = \pi$ (and hence $p_x = p_y = 0$, $p_z = -p$), the spinor $u_\uparrow$ becomes equal to u_2, $u_\downarrow$ becomes equal to $-u_1$, $v_\uparrow$ becomes equal to $-v_2$, and $v_\downarrow$ becomes equal to v_1, again as expected, the arbitrary overall normalisation factors of -1 being of no physical consequence.

2.11 Summary of Plane Wave Solutions

For a free *particle*, with 4-momentum $(E, \boldsymbol{p})$, the plane wave solutions are

$$\psi = u_i(E, \boldsymbol{p}) e^{i(\boldsymbol{p}.\boldsymbol{r} - Et)}$$

$$\boxed{u_1 = \sqrt{E+m} \begin{pmatrix} 1 \\ 0 \\ p_z/(E+m) \\ (p_x + ip_y)/(E+m) \end{pmatrix}; \qquad u_2 = \sqrt{E+m} \begin{pmatrix} 0 \\ 1 \\ (p_x - ip_y)/(E+m) \\ -p_z/(E+m) \end{pmatrix}}$$

For a free *antiparticle*, with physical 4-momentum $(E > 0, \boldsymbol{p})$, the solutions are

$$\psi = v_i(E, \boldsymbol{p}) e^{-i(\boldsymbol{p}.\boldsymbol{r} - Et)}$$

$$\boxed{v_1 = \sqrt{E+m} \begin{pmatrix} (p_x - ip_y)/(E+m) \\ -p_z/(E+m) \\ 0 \\ 1 \end{pmatrix}; \qquad v_2 = \sqrt{E+m} \begin{pmatrix} p_z/(E+m) \\ (p_x + ip_y)/(E+m) \\ 1 \\ 0 \end{pmatrix}}$$

For a particle or antiparticle travelling (forwards or backwards) along the z-axis, the spinors u_i and v_i are eigenstates of the spin operator S_z, *i.e.* they are helicity eigenstates. In this case, the *physical* spin of the particle or antiparticle is $S_z = +\frac{1}{2}$ for u_1, v_1 and $S_z = -\frac{1}{2}$ for u_2, v_2.

In general, the spinors u_1, u_2, v_1, v_2 are *not* helicity eigenstates. For a particle moving at an angle θ to the z axis, with four-momentum $p^\mu = (E, p\sin\theta\cos\phi, p\sin\theta\sin\phi, p\cos\theta)$, the $h = +1$ (right-handed) and $h = -1$ (left-handed) helicity eigenstates are

$$\boxed{u_\uparrow(p) = \sqrt{E+m} \begin{pmatrix} \cos\theta/2 \\ e^{i\phi}\sin\theta/2 \\ \frac{p}{E+m}\cos\theta/2 \\ \frac{p}{E+m}e^{i\phi}\sin\theta/2 \end{pmatrix}, \qquad u_\downarrow(p) = \sqrt{E+m} \begin{pmatrix} -\sin\theta/2 \\ e^{i\phi}\cos\theta/2 \\ \frac{p}{E+m}\sin\theta/2 \\ -\frac{p}{E+m}e^{i\phi}\cos\theta/2 \end{pmatrix}} \tag{53}$$

For an antiparticle, the helicity eigenstates are (with $E > 0$)

$$\boxed{v_\uparrow(p) = \sqrt{E+m} \begin{pmatrix} \frac{p}{E+m}\sin\theta/2 \\ -\frac{p}{E+m}e^{i\phi}\cos\theta/2 \\ -\sin\theta/2 \\ e^{i\phi}\cos\theta/2 \end{pmatrix}, \qquad v_\downarrow(p) = \sqrt{E+m} \begin{pmatrix} \frac{p}{E+m}\cos\theta/2 \\ \frac{p}{E+m}e^{i\phi}\sin\theta/2 \\ \cos\theta/2 \\ e^{i\phi}\sin\theta/2 \end{pmatrix}} \tag{54}$$

Either of the two sets of basis states (u_1, u_2, v_1, v_2) or $(u_\uparrow, u_\downarrow, v_\uparrow, v_\downarrow)$ can be used equally well in matrix element calculations. In general, however, we shall tend to prefer the helicity eigenstate spinors in order to bring out more clearly the underlying spin structure of the electromagnetic, weak and strong interactions.

The spinors above are all normalised to $2E$ particles per unit volume:

$$\rho = \psi^\dagger(p)\psi(p) = \overline{\psi}(p)\gamma^0\psi(p) = 2E \ .$$

It is shown on the examples sheet that the current $j^\mu = \overline{\psi}(p)\gamma^\mu\psi(p)$ for a free (anti)particle is proportional to the physical four-momentum of the (anti)particle:

$$\boxed{j^\mu = \overline{u}(p)\gamma^\mu u(p) = \overline{v}(p)\gamma^\mu v(p) = 2p^\mu} \ ,$$

and that the (anti)particle flux is given by the three-vector current $\boldsymbol{j} = 2\boldsymbol{p}$.

2.12 Helicity and Chirality

In the extreme relativistic limit $E \gg m$, where particle masses can be neglected, the factor $p/(E+m)$ in Equations (53) and (54) tends to unity and the helicity eigenstate spinors become

$$u_\uparrow = \sqrt{E}\begin{pmatrix} c \\ e^{i\phi}s \\ c \\ e^{i\phi}s \end{pmatrix}; \quad u_\downarrow = \sqrt{E}\begin{pmatrix} -s \\ e^{i\phi}c \\ s \\ -e^{i\phi}c \end{pmatrix}; \quad v_\uparrow = \sqrt{E}\begin{pmatrix} s \\ -e^{i\phi}c \\ -s \\ e^{i\phi}c \end{pmatrix}; \quad v_\downarrow = \sqrt{E}\begin{pmatrix} c \\ e^{i\phi}s \\ c \\ e^{i\phi}s \end{pmatrix} \qquad (55)$$

where $c \equiv \cos\theta/2$ and $s \equiv \sin\theta/2$. Introducing the matrix γ^5 defined by

$$\boxed{\gamma^5 \equiv i\gamma^0\gamma^1\gamma^2\gamma^3 = \begin{pmatrix} 0 & 0 & 1 & 0 \\ 0 & 0 & 0 & 1 \\ 1 & 0 & 0 & 0 \\ 0 & 1 & 0 & 0 \end{pmatrix} = \begin{pmatrix} 0 & I \\ I & 0 \end{pmatrix}}$$

it is straightforward to check that the helicity eigenstate spinors are eigenstates of γ^5:

$$\gamma^5 u_\uparrow = u_\uparrow, \qquad \gamma^5 u_\downarrow = -u_\downarrow, \qquad \gamma^5 v_\uparrow = -v_\uparrow, \qquad \gamma^5 v_\downarrow = v_\downarrow \ . \qquad (56)$$

These equations do *not* hold for the general case where the mass m cannot be neglected, as is seen immediately by applying γ^5 to the spinors in Equations (53) and (54). Thus, in the extreme relativistic limit, and *only* in this limit, the helicity eigenstates $u_\uparrow$, $u_\downarrow$, $v_\uparrow$, $v_\downarrow$ become eigenstates of the γ^5 operator. For a *particle*, the γ^5 eigenvalue gives the helicity of the particle state while for an *antiparticle* γ^5 gives *minus* the helicity.

We now define the *left-handed* and *right-handed projection operators* P_L and P_R to be

$$P_\mathrm{L} \equiv \tfrac{1}{2}(1-\gamma^5) = \tfrac{1}{2}\begin{pmatrix} 1 & 0 & -1 & 0 \\ 0 & 1 & 0 & -1 \\ -1 & 0 & 1 & 0 \\ 0 & -1 & 0 & 1 \end{pmatrix}$$

$$P_\mathrm{R} \equiv \tfrac{1}{2}(1+\gamma^5) = \tfrac{1}{2}\begin{pmatrix} 1 & 0 & 1 & 0 \\ 0 & 1 & 0 & 1 \\ 1 & 0 & 1 & 0 \\ 0 & 1 & 0 & 1 \end{pmatrix} .$$

Any spinor ψ can trivially be decomposed as

$$\psi = \psi_{\rm L} + \psi_{\rm R} \tag{57}$$

where $\psi_{\rm L}$ and $\psi_{\rm R}$ are the *left-handed* and *right-handed chiral components* of ψ, defined as

$$\psi_{\rm L} \equiv \tfrac{1}{2}(1-\gamma^5)\psi = P_{\rm L}\psi \tag{58}$$
$$\psi_{\rm R} \equiv \tfrac{1}{2}(1+\gamma^5)\psi = P_{\rm R}\psi \tag{59}$$

Using Equation (56), we have

$$P_{\rm L}u_\uparrow = \tfrac{1}{2}(1-\gamma^5)u_\uparrow = 0 \qquad P_{\rm R}u_\uparrow = \tfrac{1}{2}(1+\gamma^5)u_\uparrow = u_\uparrow$$
$$P_{\rm L}u_\downarrow = \tfrac{1}{2}(1-\gamma^5)u_\downarrow = u_\downarrow \qquad P_{\rm R}u_\downarrow = \tfrac{1}{2}(1+\gamma^5)u_\downarrow = 0\ .$$

A general particle spinor u can always be expressed as a linear combination of the basis spinors $u_\uparrow$ and $u_\downarrow$, for example as $u = \alpha_\uparrow u_\uparrow + \alpha_\downarrow u_\downarrow$ where $\alpha_\uparrow$ and $\alpha_\downarrow$ are constants with $|\alpha_\uparrow|^2 + |\alpha_\downarrow|^2 = 1$. The chiral components of this general spinor are:

$$P_{\rm L}u = \tfrac{1}{2}(1-\gamma^5)u = \alpha_\downarrow u_\downarrow \qquad (h=-1)$$
$$P_{\rm R}u = \tfrac{1}{2}(1+\gamma^5)u = \alpha_\uparrow u_\uparrow \qquad (h=+1)\ .$$

Thus, the operators $P_{\rm L}$ and $P_{\rm R}$ project out the negative (left-handed) and positive (right-handed) helicity components, respectively, of a general particle spinor. Specifically, for any particle spinor u, the projection $P_{\rm L}u = \frac{1}{2}(1-\gamma^5)u$ is always a negative helicity (left-handed) eigenstate [2], while the projection $P_{\rm R}u = \frac{1}{2}(1+\gamma^5)u$ is always a positive helicity (right-handed) eigenstate.

For an *antiparticle*, we have

$$P_{\rm L}v_\uparrow = \tfrac{1}{2}(1-\gamma^5)v_\uparrow = v_\uparrow \qquad P_{\rm R}v_\uparrow = \tfrac{1}{2}(1+\gamma^5)v_\uparrow = 0$$
$$P_{\rm L}v_\downarrow = \tfrac{1}{2}(1-\gamma^5)v_\downarrow = 0 \qquad P_{\rm R}v_\downarrow = \tfrac{1}{2}(1+\gamma^5)v_\downarrow = v_\downarrow\ .$$

The operator $P_{\rm L}$ now projects out the *positive* (*right*-handed) helicity component while $P_{\rm R}$ projects out the *negative* (*left*-handed) component.

In summary, in the extreme relativistic limit, for any particle spinor u or antiparticle spinor v we have:

	Left-handed $(h=-1)$	Right-handed $(h=+1)$
Particle	$\frac{1}{2}(1-\gamma^5)u \ \ (=P_{\rm L}u)$	$\frac{1}{2}(1+\gamma^5)u \ \ (=P_{\rm R}u)$
Antiparticle	$\frac{1}{2}(1+\gamma^5)v \ \ (=P_{\rm R}v)$	$\frac{1}{2}(1-\gamma^5)v \ \ (=P_{\rm L}v)$

It should be emphasised that the definition of the left-handed and right-handed chiral components $\psi_{\rm L}$ and $\psi_{\rm R}$ in Equations (58) and (59) applies quite generally to any spinor ψ. In the extreme relativistic limit $E \gg m$, and only in this limit, the chiral components become states with definite helicity, *i.e.* left-handed or right-handed helicity eigenstates. Note that, for antiparticles, the *left*-handed projection operator $P_{\rm L}$ projects out the *right*-handed helicity eigenstate, while the *right*-handed projection operator $P_{\rm R}$ projects out the *left*-handed helicity eigenstate.

[2] except for the special case that u is a pure right-handed state, in which case $P_{\rm L}u = \frac{1}{2}(1-\gamma^5)u = 0$

2.13 Summary: helicity, handedness and chirality

A particle or antiparticle in an eigenstate of spin with the spin directed along (opposite to) the direction of motion has *helicity* $+1$ (-1) and is said to be *right-handed* (*left-handed*).

The *left-handed* and *right-handed chiral components* of a particle or antiparticle spinor ψ are defined as $\psi_{\rm L} \equiv \frac{1}{2}(1-\gamma^5)\psi$ and $\psi_{\rm R} \equiv \frac{1}{2}(1+\gamma^5)\psi$.

In the relativistic limit, the chiral components $\psi_{\rm L}$ and $\psi_{\rm R}$ become helicity eigenstates. For a *particle*, $\psi_{\rm L}$ becomes a left-handed helicity eigenstate and $\psi_{\rm R}$ becomes a right-handed eigenstate, while for an *antiparticle*, $\psi_{\rm L}$ becomes right-handed and $\psi_{\rm R}$ becomes left-handed.

2.14 Properties of Spin 1/2 Particles and Antiparticles

The Dirac equation makes several predictions concerning the properties of spin-half particles and antiparticles, beyond the fact, already considered above, that they possess an internal angular momentum of magnitude $S = \frac{1}{2}\hbar$:

- A pointlike spin $\frac{1}{2}$ particle or antiparticle of charge q and mass m possesses an *intrinsic magnetic moment* $\boldsymbol{\mu}$ proprtional to the spin $\boldsymbol{S}$:

$$\boxed{\boldsymbol{\mu} = g\frac{q}{2m}\boldsymbol{S}}$$

  where $S = \frac{1}{2}$ and the *gyromagnetic ratio* $g = 2$. An intrinsic magnetic moment of this magnitude had been postulated by Goudsmit and Uhlenbeck in 1925 together with the introduction of intrinsic spin. The Dirac equation successfully accounted for this hypothesis. In particular, it explained why the internal spin angular momentum gave rise to a magnetic moment which was twice as big $(g = 2)$ as would have been expected for a classical angular momentum.

- Spin-half particles and antiparticles at rest are eigenstates of the *parity operator* P which reverses the sign of the spatial coordinates (x, y, z). In this case, the eigenvalue of P is known as the *intrinsic parity* of the particle or antiparticle. The intrinsic parity of a spin $\frac{1}{2}$ antiparticle is *opposite* to that of the corresponding particle, the conventional assignment being $P = +1$ for the particle and $P = -1$ for the antiparticle;

- A spin $\frac{1}{2}$ antiparticle has the same mass as the corresponding particle but the opposite electric charge.

Formal proofs of these results, and a formal treatment of the interpretation of negative energy solutions as positive energy antiparticles, are given in the remainder of this handout. The Lorentz covariance of the Dirac equation is also formally demonstrated. This material is all non-examinable.

2.15 Magnetic Moment of a Dirac Particle (non-examinable)

In the Part II course on Relativity and Electrodynamics, it is shown that the equation of motion for a particle of charge q in an electromagnetic field $\boldsymbol{A}^\mu = (\phi, \boldsymbol{A})$ can be obtained by making the *minimal substitution*

$$\boldsymbol{p} \to \boldsymbol{p} - q\boldsymbol{A}; \qquad E \to E - q\phi.$$

Applying this prescription to Equations (34) and (35), the plane wave solutions for a spin $\frac{1}{2}$ particle in an electromagnetic field become

$$(\boldsymbol{\sigma.p} - q\boldsymbol{\sigma.A})u_B = (E - m - q\phi)u_A \tag{60}$$
$$(\boldsymbol{\sigma.p} - q\boldsymbol{\sigma.A})u_A = (E + m - q\phi)u_B. \tag{61}$$

Multiplying Equation (60) by $E + m - q\phi$ gives

$$(\boldsymbol{\sigma.p} - q\boldsymbol{\sigma.A})(E + m - q\phi)u_B = (T + 2m - q\phi)(T - q\phi)u_A$$

where $T \equiv E - m$ is the kinetic energy of the particle. Taking the non-relativistic limit $T \ll m$, and assuming that the electric potential energy is small compared to the rest mass energy, $|q\phi| \ll m$, we obtain

$$(\boldsymbol{\sigma.p} - q\boldsymbol{\sigma.A})(\boldsymbol{\sigma.p} - q\boldsymbol{\sigma.A})u_A \approx 2m(T - q\phi)u_A \ .$$

Multiplying this out gives

$$\left[(\boldsymbol{\sigma.p})^2 - q(\boldsymbol{\sigma.A})(\boldsymbol{\sigma.p}) - q(\boldsymbol{\sigma.p})(\boldsymbol{\sigma.A}) + q^2(\boldsymbol{\sigma.A})^2\right] u_A \approx 2m(T - q\phi)u_A \ . \tag{62}$$

Using Equation (36), for any two vector operators $\boldsymbol{A}$ and $\boldsymbol{B}$ we have

$$\boldsymbol{\sigma.A} = \begin{pmatrix} A_z & A_x - iA_y \\ A_x + iA_y & -A_z \end{pmatrix}; \qquad \boldsymbol{\sigma.B} = \begin{pmatrix} B_z & B_x - iB_y \\ B_x + iB_y & -B_z \end{pmatrix} \ .$$

Straightforward matrix multiplication then shows that

$$(\boldsymbol{\sigma.A})(\boldsymbol{\sigma.B}) = \boldsymbol{A.B} + i\boldsymbol{\sigma} \cdot \boldsymbol{A} \wedge \boldsymbol{B} \ .$$

This contains the special cases

$$(\boldsymbol{\sigma.p})^2 = |\boldsymbol{p}|^2, \qquad (\boldsymbol{\sigma.A})^2 = |\boldsymbol{A}|^2 \ .$$

Hence the operator on the left-hand side of Equation (62) becomes

$$\begin{aligned}
&\boldsymbol{p}^2 - q\left[\boldsymbol{A.p} + i\boldsymbol{\sigma} \cdot \boldsymbol{A} \wedge \boldsymbol{p} + \boldsymbol{p.A} + i\boldsymbol{\sigma} \cdot \boldsymbol{p} \wedge \boldsymbol{A}\right] + q^2\boldsymbol{A}^2 \\
&= (\boldsymbol{p} - q\boldsymbol{A})^2 - iq\boldsymbol{\sigma} \cdot \left[\boldsymbol{A} \wedge \boldsymbol{p} + \boldsymbol{p} \wedge \boldsymbol{A}\right] \\
&= (\boldsymbol{p} - q\boldsymbol{A})^2 - iq\boldsymbol{\sigma} \cdot -i\left[\boldsymbol{A} \wedge \boldsymbol{\nabla} + \boldsymbol{\nabla} \wedge \boldsymbol{A}\right] \\
&= (\boldsymbol{p} - q\boldsymbol{A})^2 - iq\boldsymbol{\sigma} \cdot -i\boldsymbol{\nabla} \wedge \boldsymbol{A} \\
&= (\boldsymbol{p} - q\boldsymbol{A})^2 - q\boldsymbol{\sigma.B}
\end{aligned}$$

where we have set $\boldsymbol{p} = -i\boldsymbol{\nabla}$, $\boldsymbol{B} = \boldsymbol{\nabla} \wedge \boldsymbol{A}$, and made use of the identity

$$(\boldsymbol{\nabla} \wedge \boldsymbol{A})\psi = \boldsymbol{\nabla} \wedge (\boldsymbol{A}\psi) + \boldsymbol{A} \wedge (\boldsymbol{\nabla}\psi) \ .$$

Substituting into Equation (62) gives the *Schrodinger-Pauli equation* describing the motion of a non-relativistic spin $\frac{1}{2}$ particle in an electromagnetic field:

$$\boxed{\left[\frac{1}{2m}(\boldsymbol{p}-q\boldsymbol{A})^2-\frac{q}{2m}\boldsymbol{\sigma}.\boldsymbol{B}+q\phi\right]u_A=Tu_A}\,.$$

Since the energy of a magnetic moment $\boldsymbol{\mu}$ in a magnetic field $\boldsymbol{B}$ is $-\boldsymbol{\mu}.\boldsymbol{B}$, we can associate with the Dirac particle an intrinsic (or spin) magnetic moment

$$\boldsymbol{\mu}=\frac{q}{2m}\boldsymbol{\sigma}\ .$$

In terms of the spin, $\boldsymbol{S}=\frac{1}{2}\boldsymbol{\sigma}$, this can be expressed as

$$\boxed{\boldsymbol{\mu}=g\frac{q}{2m}\boldsymbol{S}}$$

where the *gyromagnetic ratio* is $g=2$. This reflects the fact that the magnetic moment associated with the spin angular momentum is twice as large as would be expected classically.

2.16 Intrinsic Parity of a Dirac Particle (non-examinable)

The parity operation P is defined as spatial inversion through the origin:

$$x\to -x,\qquad y\to -y,\qquad z\to -z\ .$$

In terms of transformed coordinates

$$x'\equiv -x,\qquad y'\equiv -y,\qquad z'\equiv -z,\qquad t'\equiv t\ ,$$

the Dirac equation

$$i\gamma^1\frac{\partial\psi}{\partial x}+i\gamma^2\frac{\partial\psi}{\partial y}+i\gamma^3\frac{\partial\psi}{\partial z}-m\psi=-i\gamma^0\frac{\partial\psi}{\partial t}\qquad (31)'$$

becomes

$$-i\gamma^1\frac{\partial\psi}{\partial x'}-i\gamma^2\frac{\partial\psi}{\partial y'}-i\gamma^3\frac{\partial\psi}{\partial z'}-m\psi=-i\gamma^0\frac{\partial\psi'}{\partial t}\ .$$

Now define the spinor ψ' as

$$\psi'(x',t')\equiv\gamma^0\psi(x,t)\ . \qquad (63)$$

Since $(\gamma^0)^2=I_4$, this can be inverted to give

$$\psi(x,t)=\gamma^0\psi'(x',t')\ .$$

The Dirac equation then becomes

$$-i\gamma^1\gamma^0\frac{\partial\psi'}{\partial x'}-i\gamma^2\gamma^0\frac{\partial\psi'}{\partial y'}-i\gamma^3\gamma^0\frac{\partial\psi'}{\partial z'}-m\gamma^0\psi'=-i\left(\gamma^0\right)^2\frac{\partial\psi'}{\partial t'}\ .$$

Since γ^0 anticommutes with γ^1, γ^2, γ^3, we obtain

$$i\gamma^0\gamma^1\frac{\partial\psi'}{\partial x'} + i\gamma^0\gamma^2\frac{\partial\psi'}{\partial y'} + i\gamma^0\gamma^3\frac{\partial\psi'}{\partial z'} - m\gamma^0\psi' = -i\frac{\partial\psi'}{\partial t'}$$

Premultiplying both sides by γ^0 then gives

$$i\gamma^1\frac{\partial\psi'}{\partial x'} + i\gamma^2\frac{\partial\psi'}{\partial y'} + i\gamma^3\frac{\partial\psi'}{\partial z'} - m\psi' = -i\gamma^0\frac{\partial\psi'}{\partial t'} \ .$$

This is of the same form as the original equation, Equation (31), but now in terms of the primed coordinates.

In summary, under a parity transformation, the form of the Dirac equation remains unchanged provided that Dirac spinors are transformed as

$$\boxed{\psi \to \psi' = P\psi = \gamma^0\psi} \ .$$

Equivalently, if ψ is a solution of the Dirac equation in the original frame, then $\psi' = \gamma^0\psi$ is a solution of the Dirac equation in the space-inverted frame.

For a particle or antiparticle at rest, the free particle solutions to the Dirac equation in the original frame are

$$\psi = u_1 e^{-imt}; \qquad u_2 e^{-imt}; \qquad v_1 e^{+imt}; \qquad v_2 e^{+imt}$$

where

$$u_1 = N\begin{pmatrix}1\\0\\0\\0\end{pmatrix}; \quad u_2 = N\begin{pmatrix}0\\1\\0\\0\end{pmatrix}; \quad v_1 = N\begin{pmatrix}0\\0\\0\\1\end{pmatrix}; \quad v_2 = N\begin{pmatrix}0\\0\\1\\0\end{pmatrix}$$

and $N = \sqrt{2m}$. For the spinor u_1, for example, from Equation (63), the solution $\psi = u_1 e^{-imt}$ transforms under parity to $\psi' \equiv P\psi$ where

$$\psi' = \gamma^0\psi = \gamma^0 u_1 e^{-imt} = \begin{pmatrix}1&0&0&0\\0&1&0&0\\0&0&-1&0\\0&0&0&-1\end{pmatrix} \cdot N\begin{pmatrix}1\\0\\0\\0\end{pmatrix} e^{-imt} = N\begin{pmatrix}1\\0\\0\\0\end{pmatrix} e^{-imt} = \psi \ .$$

Thus $\psi' \equiv P\psi = \psi$, or equivalently $u_1' \equiv Pu_1 = +u_1$: a particle at rest in the state u_1 is an eigenstate of parity with eigenvalue $+1$.

A similar treatment of the remaining solutions $u_2 e^{-imt}$, $v_1 e^{imt}$, $v_2 e^{imt}$ gives altogether

$$u_1' = +u_1, \qquad u_2' = +u_2, \qquad v_1' = -v_1, \qquad v_2' = -v_2 \ .$$

Hence an *antiparticle* at rest (v_1, v_2) has *opposite* intrinsic parity to a *particle* at rest (u_1, u_2):

$$\begin{aligned} P\psi &= +\psi \qquad \text{for } u_1, u_2 \\ P\psi &= -\psi \qquad \text{for } v_1, v_2. \end{aligned}$$

In fact, it is only the *relative* intrinsic parities of particles and antiparticles which can unambiguously be determined; the *absolute* parities are assigned by convention to be $+1$ for particles and -1 for antiparticles. For example, we could equally well have chosen $\psi' = -\gamma^0\psi$ in place of Equation (63), which would have given parity eigenvalues -1 for u_1,u_2 and $+1$ for v_1,v_2. [3]

2.17 Charge Conjugation (non-examinable)

Since $p^\mu = (E, \boldsymbol{p}) = i\partial^\mu$ and $A^\mu = (\phi, \boldsymbol{A})$, the minimal substitution

$$\boldsymbol{p} \to \boldsymbol{p} - e\boldsymbol{A}; \qquad E \to E - e\phi$$

of Section 2.15 can be written more compactly as

$$\partial_\mu \to \partial_\mu + ieA_\mu.$$

The equation of motion for a Dirac particle in an electromagnetic field is then [4]

$$\boxed{\gamma^\mu(\partial_\mu + ieA_\mu)\psi + im\psi = 0}\,. \tag{64}$$

The complex conjugate of this equation is

$$\gamma^{\mu*}(\partial_\mu - ieA_\mu)\psi^* - im\psi^* = 0.$$

Premultiplying by $-i\gamma^2$ then gives

$$-i\gamma^2\gamma^{\mu*}(\partial_\mu - ieA_\mu)\psi^* - m\gamma^2\psi^* = 0.$$

In the Pauli-Dirac representation of the gamma matrices, only γ^2 is imaginary:

$$\gamma^{0*} = \gamma^0; \qquad \gamma^{1*} = \gamma^1; \qquad \gamma^{2*} = -\gamma^2; \qquad \gamma^{3*} = \gamma^3$$

and it can easily be checked that

$$\gamma^2\gamma^{\mu*} = -\gamma^\mu\gamma^2.$$

Hence we obtain

$$i\gamma^{\mu*}\gamma^2(\partial_\mu - ieA_\mu)\psi^* - m\gamma^2\psi^* = 0.$$

Introducing the *charge conjugation* transformation

$$\boxed{\psi' \equiv C\psi = i\gamma^2\psi^*}\,,$$

the above equation can be expressed as

$$\boxed{\gamma^\mu(\partial_\mu - ieA_\mu)\psi' + im\psi' = 0}\,.$$

[3] This is reminiscent of electric charge: particles and antiparticles have opposite electric charge but the assignment of negative charge to the electron is purely conventional.

[4] The term $ie\gamma^\mu A_\mu\psi$ in this equation contains both the electromagnetic field A_μ and the particle spinor ψ, and ultimately gives rise to the vertex factor $-ie\gamma^\mu$ in the QED Feynman rules for the interaction between a spin-half particle of charge e and a photon.

This is of the same form as the original (untransformed) Dirac equation, Equation (64), but with charge $-e$ in place of e. In other words, the spinor ψ' describes a particle with the same mass m as ψ but with opposite electric charge, namely the *antiparticle*. The charge conjugation operation transforms particles into antiparticles (and *vice versa*).

We now consider how the free particle (plane wave) solutions of the Dirac equation transform under charge conjugation. For example the *particle* plane wave solution

$$\psi = u_1 e^{i(\boldsymbol{p}.\boldsymbol{r}-Et)}$$

becomes

$$\psi' = i\gamma^2\psi^* = i\begin{pmatrix} 0 & 0 & 0 & -i \\ 0 & 0 & i & 0 \\ 0 & i & 0 & 0 \\ -i & 0 & 0 & 0 \end{pmatrix}\sqrt{E+m}\begin{pmatrix} 1 \\ 0 \\ p_z/(E+m) \\ (p_x+ip_y)/(E+m) \end{pmatrix}^* e^{-i(\boldsymbol{p}.\boldsymbol{r}-Et)}$$

$$= \sqrt{E+m}\begin{pmatrix} (p_x-ip_y)/(E+m) \\ -p_z/(E+m) \\ 0 \\ 1 \end{pmatrix} e^{-i(\boldsymbol{p}.\boldsymbol{r}-Et)} = v_1 e^{-i(\boldsymbol{p}.\boldsymbol{r}-Et)}$$

which represents a free *antiparticle*. Thus, under charge conjugation,

$$\psi = u_1 e^{i(\boldsymbol{p}.\boldsymbol{r}-Et)} \quad \xrightarrow{C} \quad \psi' = v_1 e^{-i(\boldsymbol{p}.\boldsymbol{r}-Et)} \ .$$

Similarly, it can be shown that

$$\psi = u_2 e^{i(\boldsymbol{p}.\boldsymbol{r}-Et)} \quad \xrightarrow{C} \quad \psi' = -v_2 e^{-i(\boldsymbol{p}.\boldsymbol{r}-Et)} \ .$$

Thus, under charge conjugation, the particle spinors u_1 and u_2 transform to the antiparticle spinors v_1 and v_2, respectively.

2.18 Covariance of Dirac Equation (non-examinable)

In this section, we establish that the Dirac equation,

$$i\gamma^\mu\partial_\mu\psi = m\psi \tag{65}$$

is covariant under a Lorentz transformation, *i.e.* that the form of the Dirac equation is the same in a second (primed) reference frame:

$$i\gamma^\mu\partial'_\mu\psi' = m\psi' \ . \tag{66}$$

Here,

$$\partial'_\mu \equiv \frac{\partial}{\partial x^{\mu\prime}} = \left(\frac{\partial}{\partial t'}, \frac{\partial}{\partial x'}, \frac{\partial}{\partial y'}, \frac{\partial}{\partial z'}\right)$$

is the derivative four-vector in the primed frame, and

$$\psi'(x') = S\psi(x) \tag{67}$$

is the transformed version of the spinor ψ. Covariance of the Dirac equation will be established if it can be demonstrated that a 4×4 matrix S leading to Equation (66) does indeed exist.

Choosing the Lorentz transformation such that the primed frame is moving with velocity v along the $+x$-axis, as usual, we have

$$\partial'_\mu = \Lambda^\nu{}_\mu \partial_\nu$$

where the matrix $\Lambda^\mu{}_\nu$ is given by

$$\Lambda^\mu{}_\nu = \begin{pmatrix} \gamma & -\beta\gamma & 0 & 0 \\ -\beta\gamma & \gamma & 0 & 0 \\ 0 & 0 & 1 & 0 \\ 0 & 0 & 0 & 1 \end{pmatrix} \tag{68}$$

with $\beta = v/c$ and $\gamma = 1/\sqrt{1-\beta^2}$.

Substituting Equation (67) into Equation (66) gives

$$i\gamma^\nu \partial'_\nu (S\psi) = mS\psi \ .$$

The matrix S is just a constant matrix depending only on the (fixed) parameters defining the Lorentz transformation. Further, the matrices S and Λ commute (since they act in different spaces). Therefore

$$i\gamma^\nu S\Lambda^\mu{}_\nu \partial_\mu \psi = mS\psi \ . \tag{69}$$

Operating on Equation (65) with S gives

$$iS\gamma^\mu \partial_\mu \psi = mS\psi \ .$$

Comparing with Equation (69) then gives

$$S\gamma^\mu \partial_\mu \psi = \gamma^\nu S\Lambda^\mu{}_\nu \partial_\mu \psi \ .$$

Thus the Dirac equation will be shown to be covariant provided a matrix S exists which satisfies

$$\boxed{S\gamma^\mu = \gamma^\nu S\Lambda^\mu{}_\nu}\,, \tag{70}$$

separately for each value of $\mu = 0, 1, 2, 3$.

Explicitly, taking each value of μ in turn in Equation (70) and using Equation (68), covariance requires that the matrix S satisfy

$$S\gamma^0 = \gamma\gamma^0 S - \beta\gamma\gamma^1 S \tag{71}$$
$$S\gamma^1 = -\beta\gamma\gamma^0 S + \gamma\gamma^1 S \tag{72}$$
$$S\gamma^2 = \gamma^2 S \tag{73}$$
$$S\gamma^3 = \gamma^3 S \ . \tag{74}$$

Consider (try) a matrix S of the form

$$\boxed{S = aI + b\gamma^0\gamma^1} \tag{75}$$

where a and b are constants which remain to be determined. The matrix products of the form $S\gamma^\mu$ are then

$$\begin{aligned} S\gamma^0 &= a\gamma^0 + b\gamma^0\gamma^1\gamma^0 = a\gamma^0 - b\gamma^1 \\ S\gamma^1 &= a\gamma^1 + b\gamma^0(\gamma^1)^2 = a\gamma^1 - b\gamma^0 \\ S\gamma^2 &= a\gamma^2 + b\gamma^0\gamma^1\gamma^2 \\ S\gamma^3 &= a\gamma^3 + b\gamma^0\gamma^1\gamma^3 \ , \end{aligned}$$

while those of the form $\gamma^\mu S$ are

$$\begin{aligned} \gamma^0 S &= a\gamma^0 + b(\gamma^0)^2\gamma^1 = a\gamma^0 + b\gamma^1 \\ \gamma^1 S &= a\gamma^1 + b\gamma^1\gamma^0\gamma^1 = a\gamma^1 + b\gamma^0 \\ \gamma^2 S &= a\gamma^2 + b\gamma^2\gamma^0\gamma^1 \\ \gamma^3 S &= a\gamma^3 + b\gamma^3\gamma^0\gamma^1 \ . \end{aligned}$$

Since $\gamma^0\gamma^1\gamma^2 = \gamma^2\gamma^1\gamma^0$ and $\gamma^0\gamma^1\gamma^3 = \gamma^3\gamma^1\gamma^0$, we immediately have $S\gamma^2 = \gamma^2 S$ and $S\gamma^3 = \gamma^3 S$, so that Equations (73) and (74) are indeed satisfied by a matrix S of the form of Equation (75).

Equations (71) and (72) will be satisfied if constants a and b can be found such that

$$\begin{aligned} a\gamma^0 - b\gamma^1 &= \gamma(a\gamma^0 + b\gamma^1) - \beta\gamma(a\gamma^1 + b\gamma^0) \\ a\gamma^1 - b\gamma^0 &= -\beta\gamma(a\gamma^0 + b\gamma^1) + \gamma(a\gamma^1 + b\gamma^0) \ . \end{aligned}$$

These equations can be rearranged as

$$\begin{aligned} (a - \gamma a + \beta\gamma b)\gamma^0 &= (b + \gamma b - \beta\gamma a)\gamma^1 \\ (a - \gamma a + \beta\gamma b)\gamma^1 &= (b + \gamma b - \beta\gamma a)\gamma^0 \ , \end{aligned}$$

which requires that the expressions in brackets vanish:

$$\begin{aligned} (\gamma - 1)a &= \beta\gamma b \\ (\gamma + 1)b &= \beta\gamma a \ . \end{aligned}$$

This results in two expressions for the ratio a/b,

$$\frac{a}{b} = \frac{\beta\gamma}{\gamma - 1} = \frac{\gamma + 1}{\beta\gamma} \ ,$$

which are consistent since $\gamma^2 - 1 = \beta^2\gamma^2$. We can also write

$$\frac{a}{b} = \frac{\gamma + 1}{\beta\gamma} = \frac{\gamma + 1}{\sqrt{\gamma^2 - 1}} = \frac{\sqrt{\gamma + 1}}{\sqrt{\gamma - 1}} \ .$$

In the limit $\beta \to 0$, $\gamma \to 1$, the matrix S must become the identity matrix, $S = I_4$. From Equation (75), this requires $a = 1$, $b = 0$ in this limit. This fixes

$$\boxed{a = \sqrt{\tfrac{1}{2}(\gamma + 1)}, \qquad b = \sqrt{\tfrac{1}{2}(\gamma - 1)}} \ . \tag{76}$$

Note that, for $\beta < 0$ (*i.e.* for a Lorentz transformation to a primed frame moving in the $-x$ direction), we must choose $b < 0$ (*i.e.* take the negative root).

In summary, under a Lorentz transformation to a (primed) frame moving with velocity v along the x-axis of the original frame, a spinor $\psi(x)$ transforms to the spinor $\psi'(x') = S\psi(x)$, where the 4×4 matrix S is given by Equations (75) and (76). This transformation preserves the mathematical form of the Dirac equation.

2.19 Transformation of Dirac Current (non-examinable)

In this section, we demonstrate that a current j^μ of the form $\overline{\psi}\gamma^\mu\psi$ transforms as a four-vector under a Lorentz transformation.

Under a Lorentz transformation, the spinor ψ transforms to $\psi' = S\psi$, and hence the adjoint spinor $\overline{\psi} \equiv \psi^\dagger\gamma^0$ transforms as

$$\overline{\psi} \to \overline{\psi}' = (S\psi)^\dagger\gamma^0 = \psi^\dagger S^\dagger\gamma^0 \ .$$

Consider first the product $\overline{\psi}\psi$. This transforms as

$$\overline{\psi}\psi \to (\psi^\dagger S^\dagger\gamma^0)(S\psi) \ .$$

But

$$S^\dagger = aI + b\gamma^{1\dagger}\gamma^{0\dagger} = aI - b\gamma^1\gamma^0 \ .$$

Hence

$$\begin{aligned} S^\dagger\gamma^0 S &= (aI - b\gamma^1\gamma^0)\gamma^0(aI + b\gamma^0\gamma^1) \\ &= a^2\gamma^0 - b^2\gamma^1\gamma^0\gamma^0\gamma^0\gamma^1 + ab\gamma^0\gamma^0\gamma^1 - ab\gamma^1\gamma^0\gamma^0 \\ &= a^2\gamma^0 - b^2\gamma^0 \ . \end{aligned}$$

Since $a^2 = \frac{1}{2}(\gamma + 1)$ and $b^2 = \frac{1}{2}(\gamma - 1)$, we then obtain

$$S^\dagger\gamma^0 S = \gamma^0 \ . \tag{77}$$

The product $\overline{\psi}\psi$ therefore transforms as

$$\overline{\psi}\psi \to \psi^\dagger(S^\dagger\gamma^0 S)\psi = \psi^\dagger\gamma^0\psi = \overline{\psi}\psi \ ,$$

showing that $\overline{\psi}\psi$ is invariant under Lorentz transformations.

Note that the above argument works equally well if $\overline{\psi}$ and ψ correspond to different spinors; in other words, more generally, the product $\overline{\psi}_1\psi_2$ is Lorentz covariant.

Now consider the transformation of a current j^μ of the form $\overline{\psi}\gamma^\mu\psi$:

$$\overline{\psi}\gamma^\mu\psi \to (\psi^\dagger S^\dagger\gamma^0)\gamma^\mu(S\psi) \ . \tag{78}$$

To interchange the matrices γ^μ and S on the right-hand side of this equation, we multiply both sides of Equation (70) by ${\Lambda^\rho}_\mu$ and use the relation ${\Lambda^\mu}_\nu {\Lambda^\rho}_\mu = {\delta^\rho}_\nu$:

$$S\gamma^\mu {\Lambda^\rho}_\mu = \gamma^\nu S {\Lambda^\mu}_\nu {\Lambda^\rho}_\mu = \gamma^\nu S {\delta^\rho}_\nu = \gamma^\rho S \ .$$

Relabelling the indices and rearranging gives

$$\boxed{\gamma^\mu S = {\Lambda^\mu}_\nu S \gamma^\nu} \ .$$

The right-hand side of Equation (78) can now be written as

$$\psi^\dagger S^\dagger \gamma^0 \gamma^\mu S \psi = \psi^\dagger S^\dagger \gamma^0 ({\Lambda^\mu}_\nu S \gamma^\nu)\psi = {\Lambda^\mu}_\nu \psi^\dagger (S^\dagger \gamma^0 S)\gamma^\nu \psi \ .$$

Using Equation (77), we then have

$$\boxed{\overline{\psi}\gamma^\mu \psi \rightarrow {\Lambda^\mu}_\nu \overline{\psi}\gamma^\nu \psi} \ ,$$

showing that $\overline{\psi}\gamma^\mu\psi$ indeed transforms as a four-vector.

3 Decay Rates and Cross Sections

The electromagnetic fine structure constant α, the weak coupling constants $g_{\rm W}$ and $g_{\rm Z}$, and (at sufficiently high energies) the strong coupling constant $\alpha_{\rm s}$ are all sufficiently small that it is often possible to use perturbation theory to carry out calculations of particle decay rates and scattering cross sections. The starting point for such calculations is *Fermi's Golden Rule*, a general expression giving the transition rate from an initial state $|i\rangle$ to a final state $|f\rangle$.

We begin this handout with a brief review of Fermi's Golden Rule, derived in the Part II Advanced Quantum Physics course, and then use it to obtain general expressions for decay rates and cross sections valid for relativistic incoming and outgoing particles.

3.1 Transition Rates: Fermi's Golden Rule

Time-dependent perturbation theory is based on a Hamiltonian of the form

$$H = H_0 + H'$$

where H' represents a small perturbation about an unperturbed Hamiltonian H_0. Fermi's Golden Rule states that the total transition rate (number of transitions per unit time) from an initial state $|i\rangle$ of energy $E_{\rm i}$ to the set of final states $|f\rangle$ with energies $E_{\rm f} = E_{\rm i}$ is given by (with $\hbar = 1$)

$$\boxed{\Gamma(i \to f) = 2\pi |T_{\rm fi}|^2 g(E_{\rm f})} \tag{1}$$

where the transition amplitude $T_{\rm fi}$ is given by the perturbation series

$$T_{\rm fi} = \langle f|H'|i\rangle + \sum_{k \neq i} \frac{\langle f|H'|k\rangle \langle k|H'|i\rangle}{E_{\rm i} - E_k} + \cdots$$

and

$$g(E_{\rm f}) \equiv \frac{{\rm d}n}{{\rm d}E_{\rm f}}$$

is the density of final states (number of states per unit energy interval) at energy $E_{\rm f}$. In what follows, we shall only need to work to leading order in perturbation theory, in which case we have simply

$$T_{\rm fi} = \langle f|H'|i\rangle = \int \psi_{\rm f}^* H' \psi_{\rm i} \, {\rm d}^3x.$$

Fermi's Golden Rule, Equation (1), can be reformulated as an integral over all possible final states (of any energy), with overall energy conservation ($E_{\rm f} = E_{\rm i}$) imposed by explicitly including a δ function in the integrand:

$$\begin{aligned}\Gamma(i \to f) &= 2\pi \int |T_{\rm fi}|^2 \delta(E_{\rm f} - E_{\rm i}) g(E_{\rm f})\, {\rm d}E_{\rm f} \\ &= 2\pi \int |T_{\rm fi}|^2 \delta(E_{\rm f} - E_{\rm i})\, {\rm d}n \ . \end{aligned} \tag{2}$$

This formulation of Fermi's Golden Rule simplifies the treatment of the density of final states and will be the starting point for our calculations of decay rates and cross sections.

3.2 Relativistic Phase Space

For the high energy incoming and outgoing free particles we shall be considering, it will be sufficient to work in the Born aproximation whereby particle wavefunctions are represented as plane waves of definite momentum $\boldsymbol{p} = \hbar \boldsymbol{k}$ and definite energy E :

$$\psi(\boldsymbol{r}, t) = N e^{i(\boldsymbol{k}.\boldsymbol{r} - Et)} \ .$$

To evaluate the density of final states, we employ the standard trick of normalising (to unity) the particle wavefunctions inside a cube of arbitrary volume $V = L^3$,

$$\psi = \frac{1}{\sqrt{V}}\, e^{i(\boldsymbol{k}.\boldsymbol{r} - Et)} \ ,$$

and imposing periodic boundary conditions on the walls of the cube. This restricts the allowed values of k_x, k_y, k_z to integer multiples of $2\pi/L$:

$$k_x = \frac{2\pi n_x}{L}, \qquad k_y = \frac{2\pi n_y}{L}, \qquad k_z = \frac{2\pi n_z}{L} \ .$$

The number of single-particle states per unit volume of $\boldsymbol{k}$-space is then $(L/2\pi)^3 = V/(2\pi)^3$:

$${\rm d}n = \frac{V}{(2\pi)^3} {\rm d}^3 k = \frac{V}{(2\pi)^3} {\rm d}^3 p$$

since $\boldsymbol{p} = \boldsymbol{k}$ with $\hbar = 1$. For convenience, we choose a normalisation of one particle per unit volume:

$${\rm d}n = \frac{{\rm d}^3 p}{(2\pi)^3} \qquad\qquad (V = 1) \ .$$

The arbitrary volume V would in any case cancel out in any expression for a measurable (observable) quantity such as a decay rate or cross section.

Using Fermi's Golden Rule in the form of Equation (2), the transition rate from an initial state i of energy $E_{\rm i}$ into a final state f containing n particles, $i \to 1 + 2 + 3 + \ldots + n$, is given by

$$\Gamma = 2\pi \int |T_{\rm fi}|^2 \delta \left(E_{\rm i} - \sum_{j=1}^{n} E_j \right) \frac{{\rm d}^3 p_1}{(2\pi)^3} \cdots \frac{{\rm d}^3 p_{n-1}}{(2\pi)^3} \tag{3}$$

where $E_j = \sqrt{|\boldsymbol{p}_j|^2 + m_j^2}$ is the energy of the j'th final state particle. No factor of $\mathrm{d}^3 p_n$ is needed in Equation (3) because $\boldsymbol{p}_n$ is completely constrained once the other $n-1$ final state particle momenta are specified:

$$\boldsymbol{p}_n = \boldsymbol{p}_i - \boldsymbol{p}_1 - \boldsymbol{p}_2 - \ldots - \boldsymbol{p}_{n-1}$$

where $\boldsymbol{p}_i$ is the three-momentum of the initial state. This 3-momentum constraint can be made explicit by including an additional three-dimensional δ function and integrating over $\mathrm{d}^3 p_n$:

$$\Gamma = (2\pi)^4 \int |T_{\mathrm{fi}}|^2 \delta \left(E_{\mathrm{i}} - \sum_{j=1}^{n} E_j \right) \delta^{(3)} \left(\boldsymbol{p}_i - \sum_{j=1}^{n} \boldsymbol{p}_j \right) \frac{\mathrm{d}^3 p_1}{(2\pi)^3} \cdots \frac{\mathrm{d}^3 p_{n-1}}{(2\pi)^3} \cdot \frac{\mathrm{d}^3 p_n}{(2\pi)^3} \tag{4}$$

$$= (2\pi)^4 \int |T_{\mathrm{fi}}|^2 \delta^{(4)} \left(p_{\mathrm{i}} - \sum_{j=1}^{n} p_j \right) \frac{\mathrm{d}^3 p_1}{(2\pi)^3} \cdots \frac{\mathrm{d}^3 p_n}{(2\pi)^3} \, . \tag{5}$$

It is shown in the examples sheet that the quantity $\mathrm{d}^3 p/E$ is Lorentz invariant. In relativistic quantum mechanics, it is therefore more convenient to reformulate the above expression to make manifest a Lorentz invariant factor $\mathrm{d}^3 p_j / 2E_j$ for each particle, where the factor of 2 is conventional. For example, for the decay of particle a into a final state containing n particles

$$a \to 1 + 2 + \cdots + n$$

we can achieve this by introducing the *Lorentz invariant matrix element* M_{fi} defined as

$$M_{\mathrm{fi}} \equiv (2E_a)^{1/2} (2E_1)^{1/2} \cdots (2E_n)^{1/2} \, T_{\mathrm{fi}} \, . \tag{6}$$

In terms of M_{fi}, the transition rate of Equation (5) becomes

$$\boxed{\Gamma = \frac{(2\pi)^{4-3n}}{2E_a} \int |M_{\mathrm{fi}}|^2 \delta^{(4)} \left(p_{\mathrm{i}} - \sum_{j=1}^{n} p_j \right) \frac{\mathrm{d}^3 p_1}{2E_1} \frac{\mathrm{d}^3 p_2}{2E_2} \cdots \frac{\mathrm{d}^3 p_n}{2E_n}} \, . \tag{7}$$

The advantage of this formulation is that each component of the integrand is now Lorentz invariant, as also therefore is the integral itself. To see this, we note that a time interval $\mathrm{d}t$ in the laboratory frame (in which particle a is travelling with energy E_a) is related to the corresponding time interval $d\tau$ in particle a's rest frame by

$$\mathrm{d}t = \gamma \mathrm{d}\tau$$

where the Lorentz boost $\gamma = 1/\sqrt{1-\beta^2} = E_a/m_a$. The transition rate $\Gamma = \mathrm{d}N/\mathrm{d}t$ in the lab frame is related to the transition rate $\Gamma^* = \mathrm{d}N/\mathrm{d}\tau$ in the rest frame by

$$\Gamma = \frac{\mathrm{d}N}{\mathrm{d}t} = \frac{1}{\gamma} \frac{\mathrm{d}N}{\mathrm{d}\tau} = \frac{m_a}{E_a} \Gamma^* \, .$$

But the transition rate Γ^* is just a constant, so that

$$\Gamma = \frac{1}{E_a} \times \text{constant.}$$

The $1/E_a$ dependence of the transition rate is clearly apparent in Equation (7); the integral on the right hand side of Equation (7) must therefore be Lorentz invariant. Since the factors of $\mathrm{d}^3 p/2E$ and the Dirac δ-function in the integrand are all Lorentz invariant, so too must be the matrix element M_{fi}.

Similar considerations apply to the scattering process

$$a + b \to 1 + 2 + \cdots + n \; .$$

The Lorentz-invariant matrix element $M_{\rm fi}$ is now defined as

$$M_{\rm fi} \equiv (2E_a)^{1/2}(2E_b)^{1/2}(2E_1)^{1/2}\cdots(2E_n)^{1/2}\, T_{\rm fi} \tag{8}$$

and the transition rate of Equation (5) becomes

$$\boxed{\Gamma = \frac{(2\pi)^{4-3n}}{2E_a 2E_b}\int |M_{\rm fi}|^2 \delta^{(4)}\left(p_{\rm i} - \sum_{j=1}^{n} p_j\right)\frac{{\rm d}^3p_1}{2E_1}\frac{{\rm d}^3p_2}{2E_2}\cdots\frac{{\rm d}^3p_n}{2E_n}} \; . \tag{9}$$

Again, the transition rate Γ is frame-dependent, but the integral on the right-hand side is Lorentz-invariant. In Section 3.4 below, the transition rate Γ will be converted to a Lorentz invariant quantity, the cross section σ.

The matrix elements $M_{\rm fi}$ in Equations (6) and (8) are schematically of the form

$$M_{\rm fi} = (2E_{\rm i})^{1/2}(2E_{\rm f})^{1/2}\, T_{\rm fi} = (2E_{\rm i})^{1/2}(2E_{\rm f})^{1/2}\, \langle\psi_{\rm f}|H'|\psi_{\rm i}\rangle \; .$$

The Lorentz invariance of $M_{\rm fi}$ can be exploited by introducing wavefunctions ψ' which are normalised to $2E$ particles per unit volume instead of one particle per unit volume:

$$\psi' \equiv \sqrt{2E}\cdot\psi \; .$$

Then

$$T_{\rm fi} = \langle\psi_{\rm f}|H'|\psi_{\rm i}\rangle = \frac{1}{\sqrt{2E_{\rm f}}}\frac{1}{\sqrt{2E_{\rm i}}}\left\langle\psi'_{\rm f}\middle|H'\middle|\psi'_{\rm i}\right\rangle \; ,$$

and a comparison with Equation (6) shows that

$$M_{\rm fi} = \left\langle\psi'_{\rm f}\middle|H'\middle|\psi'_{\rm i}\right\rangle .$$

Thus, calculating a matrix element using a wavefunction normalisation of $2E$ particles per unit volume gives the Lorentz invariant version, $M_{\rm fi}$, directly. This was the reason for choosing the normalisation $u_i^\dagger u_i = v_i^\dagger v_i = 2E$ for the free particle Dirac spinors u_i and v_i, for example.

In a general reference frame, the arbitrary cube in which the system is normalised appears Lorentz contracted by a factor $\gamma = E/m$. Normalising to $2E$ particles per unit volume effectively takes account of this contraction and guarantees that the result ($M_{\rm fi}$) is Lorentz invariant.

It should be emphasised that, although we shall be using wavefunctions normalised to $2E$ particles per unit volume to carry out matrix element calculations, the underlying wavefunction normalisation on which our formalism is based remains as one particle per unit volume. (This will be important shortly when we consider particle fluxes). In introducing an alternative normalisation, all we have done in effect is to rearrange various factors of $\sqrt{2E}$ in the integrands of Equations (7) and (9) in order to make each individual component of the calculation explicitly Lorentz invariant.

3.3 Two-body Decays: $a \to 1 + 2$

For a decay into a two particle final state, $a \to 1 + 2$, Equation (7) becomes

$$\Gamma = \frac{(2\pi)^{-2}}{2E_a} \int |M_{\rm fi}|^2 \delta\left(E_a - E_1 - E_2\right) \delta^{(3)}\left(\boldsymbol{p}_a - \boldsymbol{p}_1 - \boldsymbol{p}_2\right) \frac{{\rm d}^3 p_1}{2E_1} \frac{{\rm d}^3 p_2}{2E_2}$$

where it is to be understood that $E_1 = \sqrt{p_1^2 + m_1^2}$ and $E_2 = \sqrt{p_2^2 + m_2^2}$, with $p_1 \equiv |\boldsymbol{p}_1|$, $p_2 \equiv |\boldsymbol{p}_2|$. In the rest frame of particle a (the centre of mass frame), we have $E_a = m_a$, $\boldsymbol{p}_a = \boldsymbol{0}$, and the decay rate becomes

$$\Gamma = \frac{(2\pi)^{-2}}{2m_a} \int |M_{\rm fi}|^2 \delta(m_a - E_1 - E_2) \delta^{(3)}(\boldsymbol{p}_1 + \boldsymbol{p}_2) \frac{{\rm d}^3 p_1}{2E_1} \frac{{\rm d}^3 p_2}{2E_2} \,. \tag{10}$$

Carrying out the integral $\int {\rm d}^3 p_2$ (the $\delta^{(3)}$ function imposes $\boldsymbol{p}_2 = -\boldsymbol{p}_1$) gives:

$$\Gamma = \frac{1}{8\pi^2 m_a} \int |M_{\rm fi}|^2 \delta(m_a - E_1 - E_2) \frac{{\rm d}^3 p_1}{4E_1 E_2}$$

where E_2 is now to be understood as $E_2 = \sqrt{p_1^2 + m_2^2}$. Introducing the function

$$\begin{aligned} f(p_1) &\equiv m_a - E_1 - E_2 \\ &= m_a - \sqrt{p_1^2 + m_1^2} - \sqrt{p_1^2 + m_2^2} \end{aligned} \tag{11}$$

and setting ${\rm d}^3 p_1 = p_1^2 {\rm d}p_1 {\rm d}\cos\theta {\rm d}\phi$, we have

$$\Gamma = \frac{1}{8\pi^2 m_a} \int |M_{\rm fi}|^2 \delta(f(p_1)) \, \frac{p_1^2}{4E_1 E_2} \, {\rm d}p_1 {\rm d}\cos\theta {\rm d}\phi \,. \tag{12}$$

The function $f(p_1)$ has a single zero at a fixed value $p_1 = p^*$ given by the solution of the equation

$$f(p^*) = m_a - \sqrt{(p^*)^2 + m_1^2} - \sqrt{(p^*)^2 + m_2^2} = 0 \,. \tag{13}$$

This equation expresses the requirement that energy is conserved in the decay, $m_a = E_1 + E_2$. The constant p^* is simply the value of p_1 which results from the constraint of overall energy-momentum conservation; it is the physically allowed momentum of either of the final state decay particles in the centre of mass frame [1] :

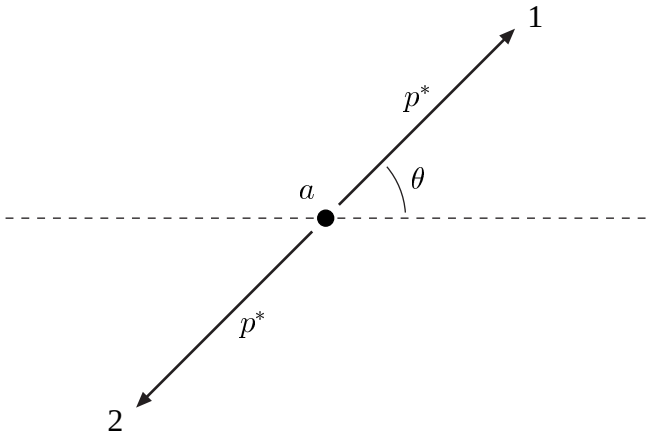

[1] In the examples sheet, it is shown that Equation (13) can be solved to give p^* in terms of the particle masses:

$$p^* = \frac{1}{2m_a} \sqrt{\left[m_a^2 - (m_1 + m_2)^2\right]\left[m_a^2 - (m_1 - m_2)^2\right]} \,.$$

We now use the general result

$$\int g(p_1)\delta(f(p_1))\mathrm{d}p_1 = \left[\frac{g(p_1)}{|\mathrm{d}f/\mathrm{d}p_1|}\right]_{f(p_1)=0}$$

to carry out the integral over p_1 in Equation (12). Differentiating Equation (11) gives

$$\frac{\mathrm{d}f}{\mathrm{d}p_1} = \frac{-p_1}{\sqrt{p_1^2+m_1^2}} - \frac{p_1}{\sqrt{p_1^2+m_2^2}} = -\frac{p_1}{E_1} - \frac{p_1}{E_2} = -p_1\frac{E_1+E_2}{E_1E_2}$$

and hence the decay rate becomes

$$\begin{aligned}\Gamma &= \frac{1}{8\pi^2 m_a}\int |M_{\mathrm{fi}}|^2 \left|\frac{1}{p_1}\frac{E_1E_2}{E_1+E_2}\frac{p_1^2}{4E_1E_2}\right|_{p_1=p^*} \mathrm{d}\cos\theta\mathrm{d}\phi \\ &= \frac{1}{32\pi^2 m_a}\int |M_{\mathrm{fi}}|^2 \left|\frac{p_1}{E_1+E_2}\right|_{p_1=p^*} \mathrm{d}\cos\theta\mathrm{d}\phi\ .\end{aligned}$$

When $p_1 = p^*$, the sum $E_1 + E_2$ is given simply by the energy conservation constraint of Equation (13): $E_1 + E_2 = m_a$. Finally, therefore, the rate for the 2-body decay $a \to 1+2$ in the rest frame of the decaying particle is obtained as

$$\boxed{\Gamma = \frac{p^*}{32\pi^2 m_a^2}\int |M_{\mathrm{fi}}|^2 \mathrm{d}\cos\theta\mathrm{d}\phi} \tag{14}$$

where $p^* = |\boldsymbol{p_1}| = |\boldsymbol{p_2}|$ is the momentum of either of the final state particles. Equation (14) can also be written in the equivalent differential form

$$\boxed{\frac{\mathrm{d}\Gamma}{\mathrm{d}\Omega} = \frac{p^*}{32\pi^2 m_a^2}|M_{\mathrm{fi}}|^2}$$

where $\mathrm{d}\Omega = \mathrm{d}\cos\theta\mathrm{d}\phi$.

For an isotropic decay, such as the decay of a spin 0 particle, there is no preferred spatial direction in the system and $|M_{\mathrm{fi}}|^2$ must be independent of θ and ϕ. Using $\int \mathrm{d}\cos\theta\mathrm{d}\phi = 4\pi$, we then obtain

$$\boxed{\Gamma = \frac{p^*}{8\pi m_a^2}|M_{\mathrm{fi}}|^2} \qquad \text{(isotropic decay)} \tag{15}$$

In general, an unstable particle will be able to decay into a variety of different final states f_i, each with its own associated partial decay rate:

$$\Gamma_i = \Gamma(a \to f_i)\ .$$

In this case, the total decay rate for a particle is the sum of the decay rates for each individual decay mode, and the *mean lifetime* τ of the particle is the inverse of the total decay rate:

$$\Gamma = \sum_i \Gamma_i = \frac{1}{\tau}\ .$$

The *branching ratio* B_i for a particular decay mode is the fraction of all decays going into that particular final state:

$$B_i \equiv \frac{\Gamma_i}{\Gamma}\ .$$

3.4 Scattering Cross Section

For a scattering process $a + b \to 1 + 2 + \cdots + n$, the transition rate Γ given by Equation (9)

$$\Gamma = \frac{(2\pi)^{4-3n}}{2E_a 2E_b} \int |M_{\rm fi}|^2 \delta^{(4)} \left(p_{\rm i} - \sum_{j=1}^{n} p_j \right) \frac{{\rm d}^3 p_1}{2E_1} \frac{{\rm d}^3 p_2}{2E_2} \cdots \frac{{\rm d}^3 p_n}{2E_n} \tag{9$'$}$$

is not Lorentz invariant due to the factor $1/E_a E_b$ outside the integral. However, we can construct a Lorentz invariant quantity, the *cross section* σ, by dividing by the incident flux. In a Lorentz frame where the two incoming particles a and b are collinear (or one of the particles is at rest), we define

$$\boxed{\sigma \equiv \frac{\Gamma}{v_a + v_b}} \tag{16}$$

where v_a and v_b are the velocities of a and b:

$$v_a = |\boldsymbol{v}_a| = \frac{|\boldsymbol{p}_a|}{E_a}, \qquad v_b = |\boldsymbol{v}_b| = \frac{|\boldsymbol{p}_b|}{E_b} \, .$$

To show that the cross section σ is Lorentz invariant, we introduce the *Lorentz invariant flux* F, defined as

$$F \equiv (v_a + v_b) \cdot 2E_a \cdot 2E_b \, . \tag{17}$$

In terms of F, the cross section σ can be written as

$$\boxed{\sigma = \frac{(2\pi)^{4-3n}}{F} \int |M_{\rm fi}|^2 \delta^{(4)} \left(p_{\rm i} - \sum_{j=1}^{n} p_j \right) \frac{{\rm d}^3 p_1}{2E_1} \frac{{\rm d}^3 p_2}{2E_2} \cdots \frac{{\rm d}^3 p_n}{2E_n}} \, . \tag{18}$$

That F is indeed Lorentz invariant can be shown by expressing F in terms of the four-vector scalar product $p_a . p_b$. To do this, we first write the flux F of Equation (17) as

$$F = \left(\frac{p_a}{E_a} + \frac{p_b}{E_b} \right) \cdot 2E_a \cdot 2E_b = 4 \left(p_a E_b + p_b E_a \right)$$

where $p_a = |\boldsymbol{p}_a|$ and $p_b = |\boldsymbol{p}_b|$. Noting that the four-vector scalar product $p_a . p_b$ is

$$p_a . p_b = E_a E_b - \boldsymbol{p_a . p_b} = E_a E_b + p_a p_b \, ,$$

we then have

$$\begin{aligned} F^2/16 - (p_a . p_b)^2 &= (p_a E_b + p_b E_a)^2 - (E_a E_b + p_a p_b)^2 \\ &= p_a^2 \left(E_b^2 - p_b^2 \right) + E_a^2 \left(p_b^2 - E_b^2 \right) \\ &= p_a^2 m_b^2 - E_a^2 m_b^2 \\ &= (p_a^2 - E_a^2) m_b^2 \\ &= -m_a^2 m_b^2 \, , \end{aligned}$$

where we have repeatedly used the relations $E_a^2 = p_a^2 + m_a^2$ and $E_b^2 = p_b^2 + m_b^2$. Hence the flux F can be expressed in the manifestly covariant form

$$\boxed{F = 4\left[(p_a.p_b)^2 - m_a^2 m_b^2\right]^{1/2}}\,. \tag{19}$$

Since F is Lorentz invariant and the integral on the right-hand side of Equation (18) is Lorentz invariant, the cross section σ must also be Lorentz invariant.

With wavefunctions normalised to one particle per unit volume, the incident flux (*i.e.* the number of particles per second passing through unit area) of particles of type a is equal to the velocity v_a, while the flux of particles of type b equals the velocity v_b. The definition of the cross section σ in Equation (16) is therefore equivalent to

$$\sigma = \frac{\text{number of scattering events per unit time per scattering centre}}{\text{incident flux}}\,.$$

This expression forms the basis of the measurement of a cross section in a scattering experiment. The cross section so determined is independent of the conditions (beam intensity, target density *etc.*) pertaining to any particular experiment. The cross section has dimensions of area, and can be interpreted as the effective "black disk" area presented by each scattering centre to an incoming particle.

We shall subsequently require explicit expressions for the flux F evaluated in the laboratory and centre of mass frames. In the laboratory frame, with particle a the beam particle and particle b the stationary target, we can take

$$p_a = (E_a, \boldsymbol{p}_a) = (E_a, 0, 0, p_a), \qquad\qquad p_b = (m_b, 0, 0, 0)\,.$$

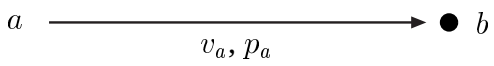

Equation (17) then gives the Lorentz invariant flux as

$$F = v_a \cdot 2E_a \cdot 2m_b = \frac{p_a}{E_a} \cdot 4E_a m_b = 4p_a m_b\,. \tag{20}$$

In the centre of mass frame, we can take the four-momenta to be

$$p_a = (E_a^*, 0, 0, p_{\rm i}^*), \qquad\qquad p_b = (E_b^*, 0, 0, -p_{\rm i}^*)\,.$$

Equation (17) then gives

$$F = (v_a^* + v_b^*) \cdot 2E_a^* \cdot 2E_b^* = \left(\frac{p_{\rm i}^*}{E_a^*} + \frac{p_{\rm i}^*}{E_b^*}\right) 4E_a^* E_b^* = 4p_{\rm i}^*(E_a^* + E_b^*)\,.$$

The sum of the incoming four-momenta is $p_a + p_b = (E_a^* + E_b^*, 0, 0, 0)$. Introducing the Lorentz invariant quantity

$$\boxed{s \equiv (p_a + p_b)^2}\,,$$

we obtain

$$\sqrt{s} = E_a^* + E_b^* \ ,$$

and the flux F can therefore be written as

$$F = 4p_{\rm i}^* \sqrt{s} \ . \tag{21}$$

The quantity $\sqrt{s}$ is just the total centre of mass energy of the collision.

Since F is Lorentz invariant, the lab and centre of mass frame evaluations of F in Equations (20) and (21) must in fact be equal. The above results can therefore be summarised as

$$\boxed{F = 4p_a m_b = 4p_{\rm i}^* \sqrt{s}} \, . \tag{22}$$

As a byproduct of the evaluation of F, we have obtained a relation between the momentum p_a of the incoming beam particle in the lab frame and its momentum $p_{\rm i}^*$ in the centre of mass.

3.5 $2 \to 2$ Body Scattering in the Centre of Mass Frame

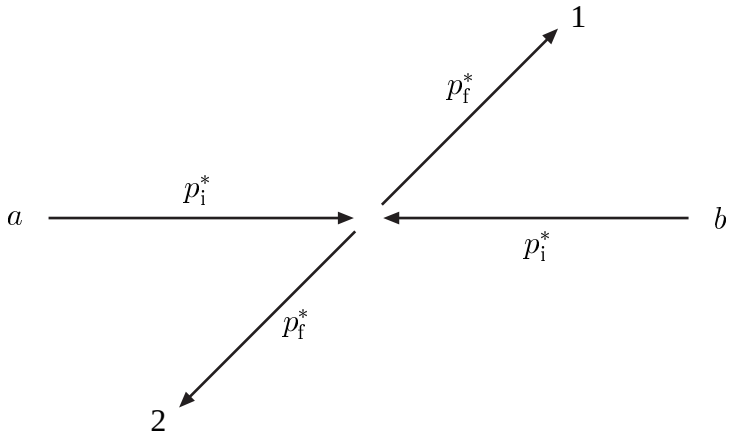

For a scattering process $a + b \to 1 + 2$ into a two particle final state, Equation (18) becomes

$$\sigma = \frac{(2\pi)^{-2}}{F} \int |M_{\rm fi}|^2 \delta(E_a + E_b - E_1 - E_2) \delta^{(3)}(\boldsymbol{p}_a + \boldsymbol{p}_b - \boldsymbol{p}_1 - \boldsymbol{p}_2) \frac{{\rm d}^3 p_1}{2E_1} \frac{{\rm d}^3 p_2}{2E_2} \tag{23}$$

In the centre of mass frame, where

$$\boldsymbol{p}_a + \boldsymbol{p}_b = 0; \qquad E_a + E_b = E_1 + E_2 = \sqrt{s}$$

this becomes

$$\sigma = \frac{(2\pi)^{-2}}{F} \int |M_{\rm fi}|^2 \delta(\sqrt{s} - E_1 - E_2) \delta^{(3)}(\boldsymbol{p}_1 + \boldsymbol{p}_2) \frac{{\rm d}^3 p_1}{2E_1} \frac{{\rm d}^3 p_2}{2E_2} \ .$$

The integral above has precisely the same form as the integral in Equation (10) for the 2-body decay $a \to 1 + 2$, with m_a replaced by $\sqrt{s}$. Hence, using the result already derived in Equation (14), we obtain immediately

$$\sigma = \frac{(2\pi)^{-2}}{F} \cdot \frac{p_{\rm f}^*}{4\sqrt{s}} \int |M_{\rm fi}|^2 {\rm d}\Omega^*$$

where $\mathrm{d}\Omega^*$ is the element of solid angle about $\boldsymbol{p}_1$, and $p_\mathrm{f}^* = |\boldsymbol{p}_1| = |\boldsymbol{p}_2|$ is the centre of mass momentum of either of the two final state particles. The differential cross section describing the scattering of particle 1 into the element of solid angle $\mathrm{d}\Omega^*$ is therefore

$$\frac{\mathrm{d}\sigma}{\mathrm{d}\Omega^*} = \frac{1}{16\pi^2\sqrt{s}}\frac{p_\mathrm{f}^*}{F}|M_\mathrm{fi}|^2 \,.$$

From Equation (22), we have $F = 4p_\mathrm{i}^*\sqrt{s}$ where $p_\mathrm{i}^* = |\boldsymbol{p}_a| = |\boldsymbol{p}_b|$ is the centre of mass momentum of either of the two initial state particles. Hence we obtain finally:

$$\boxed{\frac{\mathrm{d}\sigma}{\mathrm{d}\Omega^*} = \frac{1}{64\pi^2 s}\frac{p_\mathrm{f}^*}{p_\mathrm{i}^*}|M_\mathrm{fi}|^2} \,. \tag{24}$$

Explicit expressions for the initial and final centre of mass momenta, p_i^* and p_f^*, can be written down using the result derived in the examples sheet, with m_a again replaced by $\sqrt{s}$:

$$\begin{aligned} p_\mathrm{i}^* &= \frac{1}{2\sqrt{s}}\sqrt{[s-(m_a+m_b)^2]\,[s-(m_a-m_b)^2]} \\ p_\mathrm{f}^* &= \frac{1}{2\sqrt{s}}\sqrt{[s-(m_1+m_2)^2]\,[s-(m_1-m_2)^2]} \,. \end{aligned} \tag{25}$$

For elastic collisions (for example with $m_a = m_1$ and $m_b = m_2$), or for extreme relativistic energies where the rest masses of all initial and final state particles can be neglected, we have $p_\mathrm{i}^* = p_\mathrm{f}^*$ and hence:

$$\boxed{\frac{\mathrm{d}\sigma}{\mathrm{d}\Omega^*} = \frac{1}{64\pi^2 s}|M_\mathrm{fi}|^2} \qquad \text{(elastic)} \tag{26}$$

In the next handout, the above expression for the differential cross section $\mathrm{d}\sigma/\mathrm{d}\Omega^*$ in the centre of mass frame will be used to obtain the cross section for $\mathrm{e^+e^-} \to \mu^+\mu^-$ scattering. Experiments studying $\mathrm{e^+e^-}$ annihilation are typically carried out using counter-rotating beams of electrons and positrons of equal and opposite momentum, and therefore take place directly in the centre of mass frame.

Studies of electron-proton scattering, on the other hand, are usually carried out in the laboratory frame with the proton target at rest [2]. The underlying electron-quark scattering in these interactions takes place in a rest frame which varies from collision to collision depending on the fractional momentum of the quark within the proton. To describe these processes, we shall require general expressions for the differential cross section $\mathrm{d}\sigma/\mathrm{d}\Omega$ valid in the (laboratory) frame where one of the initial state particles is at rest, and also an explicitly Lorentz-invariant expression for the cross section valid in *any* reference frame.

[2] A notable exception is the circular high energy $\mathrm{e^\pm p}$ collider HERA currently operating at the DESY Laboratory in Hamburg. Here, 27.5 GeV beams of electrons or protons are brought into head-on collision with a proton beam of energy 820 GeV.

We proceed as follows:

1) In Section 3.6, we recast the centre of mass cross section $\mathrm{d}\sigma/\mathrm{d}\Omega^*$ of Equation (24) into a Lorentz invariant form $\mathrm{d}\sigma/\mathrm{d}t$ valid in any frame of reference;

2) In Sections 3.7 and 3.8, we evaluate this Lorentz invariant cross section in the laboratory frame, with one of the initial state particles at rest, first in the relativistic limit and then completely generally;

3) In Section 3.9, for completeness, the cross section $\mathrm{d}\sigma/\mathrm{d}\Omega$ in the laboratory frame is also derived via a direct application of Equation (18), as done above for the centre of mass frame.

Sections 3.8 and 3.9 are non-examinable.

For the remainder of this handout, we switch notation from $a + b \to 1 + 2$ to $1 + 2 \to 3 + 4$.

3.6 $2 \to 2$ Body Scattering in Any Frame

The differential cross section derived above for the centre of mass frame can be expressed in a Lorentz invariant form applicable to *any* frame of reference. To this end, and switching notation from $a+b \to 1+2$ to $1+2 \to 3+4$, we introduce the Lorentz invariant variable [3,4]

$$\boxed{t \equiv (p_1 - p_3)^2} \, .$$

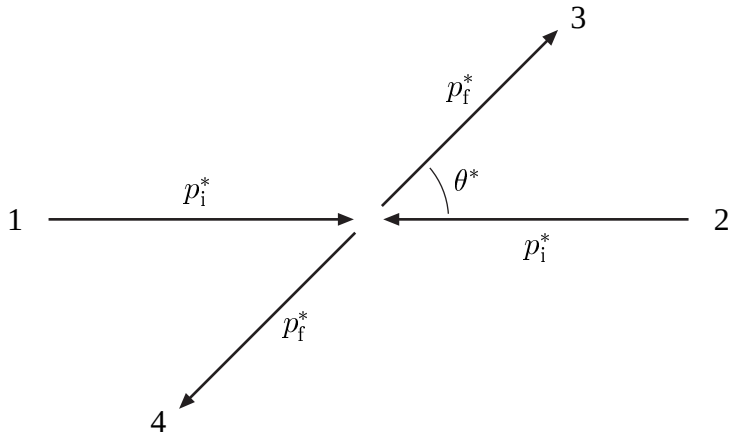

In the centre of mass frame, with $p_1 = (E_1^*, 0, 0, p_\mathrm{i}^*)$ and $p_3 = (E_3^*, p_\mathrm{f}^* \sin\theta^*, 0, p_\mathrm{f}^* \cos\theta^*)$, we have

$$t = p_1^2 + p_3^2 - 2p_1.p_3 = m_1^2 + m_3^2 - 2(E_1^* E_3^* - p_\mathrm{i}^* p_\mathrm{f}^* \cos\theta^*) \, . \tag{27}$$

In general, the element of solid angle for particle 3 is $\mathrm{d}\Omega^* = \mathrm{d}\phi^* \mathrm{d}\cos\theta^*$. Provided the matrix element is independent of azimuthal angle, which will be the case for all the processes we consider, this becomes just

$$\mathrm{d}\Omega^* = 2\pi \mathrm{d}\cos\theta^* \, .$$

[3] The three invariant quantities $s \equiv (p_1 + p_2)^2$, $t \equiv (p_1 - p_3)^2$, $u \equiv (p_1 - p_4)^2$ are known as *Mandelstam variables*. They are constrained by the relation $s + t + u = m_1^2 + m_2^2 + m_3^2 + m_4^2$.

[4] In the analysis of electron-proton scattering in Handout 5, the variable t will be equivalent to the quantity q^2, where $q = p_1 - p_3$ is the four-momentum of the virtual photon.

The differential cross section can then be expressed in terms of the Mandelstam variable t as:

$$\frac{\mathrm{d}\sigma}{\mathrm{d}t} = \frac{\mathrm{d}\Omega^*}{\mathrm{d}t}\frac{\mathrm{d}\sigma}{\mathrm{d}\Omega^*} = 2\pi\frac{\mathrm{d}\cos\theta^*}{\mathrm{d}t}\frac{\mathrm{d}\sigma}{\mathrm{d}\Omega^*} \; .$$

The quantities E_1^*, E_3^*, p_i^*, p_f^* appearing in the right-hand side of Equation (27) are constants, independent of the angle θ^*. Differentiation with respect to $\cos\theta^*$ therefore gives

$$\frac{\mathrm{d}t}{\mathrm{d}\cos\theta^*} = 2p_\mathrm{i}^* p_\mathrm{f}^* \; ,$$

and hence

$$\boxed{\frac{\mathrm{d}\sigma}{\mathrm{d}t} = \frac{\pi}{p_\mathrm{i}^* p_\mathrm{f}^*}\frac{\mathrm{d}\sigma}{\mathrm{d}\Omega^*}} \; .$$

Substituting the expression for $\mathrm{d}\sigma/\mathrm{d}\Omega^*$ from Equation (24), we then obtain

$$\frac{\mathrm{d}\sigma}{\mathrm{d}t} = \frac{\pi}{p_\mathrm{i}^* p_\mathrm{f}^*} \cdot \frac{1}{64\pi^2 s}\frac{p_\mathrm{f}^*}{p_\mathrm{i}^*}|M_\mathrm{fi}|^2$$

and hence finally

$$\boxed{\frac{\mathrm{d}\sigma}{\mathrm{d}t} = \frac{1}{64\pi s (p_\mathrm{i}^*)^2}|M_\mathrm{fi}|^2} \; . \tag{28}$$

Note that *all quantities in this equation are Lorentz invariant.* Equation (28) therefore applies to *any* frame of reference, not just the centre of mass frame. The quantity p_i^* may appear at first sight to be specific to the centre of mass frame, but is in fact just a constant:

$$p_\mathrm{i}^* = \frac{1}{2\sqrt{s}}\sqrt{\left[s-(m_1+m_2)^2\right]\left[s-(m_1-m_2)^2\right]} \; . \tag{29}$$

For the particular case where the mass of the incoming particle 1 can be neglected, for example at high beam energy $E_1 \gg m_1$ (and hence also $\sqrt{s} \gg m_1$), Equation (29) simplifies to

$$p_\mathrm{i}^* = \frac{s-m_2^2}{2\sqrt{s}} \; .$$

Thus, at high energies, the differential cross section of Equation (28) becomes

$$\boxed{\frac{\mathrm{d}\sigma}{\mathrm{d}t} = \frac{1}{16\pi(s-m_2^2)^2}|M_\mathrm{fi}|^2} \qquad (m_1 = 0) \tag{30}$$

3.7 $2 \to 2$ Body Scattering in the Lab Frame (1)

Using the Lorentz invariant cross section $\mathrm{d}\sigma/\mathrm{d}t$ derived above, we now evaluate the differential cross section $\mathrm{d}\sigma/\mathrm{d}\Omega$ for two-body scattering in the lab frame, with particle 2 at rest:

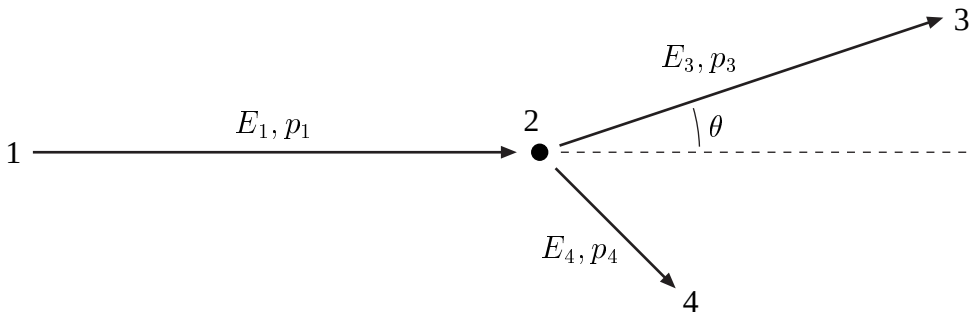

We consider first the particular case of elastic scattering at high energies where the mass of the incoming beam particle can be neglected:

$$m_1 = m_3 = 0, \qquad m_2 = m_4 = M \ ;$$

the more general case will be treated in the next section. The four-momenta can be taken to be

$$p_1 = (E_1, 0, 0, E_1), \quad p_2 = (M, 0, 0, 0), \quad p_3 = (E_3, E_3 \sin\theta, 0, E_3 \cos\theta), \quad p_4 = (E_4, \boldsymbol{p_4}) \ .$$

Since $\mathrm{d}\Omega = 2\pi \mathrm{d}\cos\theta$, the lab frame differential cross section $\mathrm{d}\sigma/\mathrm{d}\Omega$ is related to the invariant differential cross section $\mathrm{d}\sigma/\mathrm{d}t$ as

$$\frac{\mathrm{d}\sigma}{\mathrm{d}\Omega} = \frac{\mathrm{d}t}{\mathrm{d}\Omega}\frac{\mathrm{d}\sigma}{\mathrm{d}t} = \frac{1}{2\pi}\frac{\mathrm{d}t}{\mathrm{d}\cos\theta}\frac{\mathrm{d}\sigma}{\mathrm{d}t} \ . \tag{31}$$

The invariant quantity t is

$$t = (p_1 - p_3)^2 = -2p_1.p_3 = -2E_1E_3(1 - \cos\theta) \ . \tag{32}$$

Four-momentum conservation, $p_1 + p_2 = p_3 + p_4$, allows an alternative evaluation of t :

$$\begin{aligned} t = (p_2 - p_4)^2 = 2M^2 - 2p_2.p_4 &= 2M^2 - 2ME_4 \\ &= 2M^2 - 2M(E_1 + M - E_3) = -2M(E_1 - E_3) \end{aligned} \tag{33}$$

where energy conservation, $E_1 + M = E_3 + E_4$, has been used to eliminate E_4. Differentiating Equation (33) with respect to $\cos\theta$ (with the incoming beam energy E_1 considered a given constant) then gives

$$\frac{\mathrm{d}t}{\mathrm{d}\cos\theta} = 2M\frac{\mathrm{d}E_3}{\mathrm{d}\cos\theta} \ . \tag{34}$$

Equating the two expessions for t in Equations (32) and (33) gives

$$-2E_1E_3(1 - \cos\theta) = -2M(E_1 - E_3) \ ,$$

which can be rearranged to give E_3 in terms of θ:

$$E_3 = \frac{E_1 M}{M + E_1 - E_1\cos\theta} \ . \tag{35}$$

Differentiation with respect to $\cos\theta$ then gives

$$\frac{\mathrm{d}E_3}{\mathrm{d}\cos\theta} = \frac{E_1^2 M}{(M + E_1 - E_1\cos\theta)^2} = E_1^2 M \left(\frac{E_3}{E_1 M}\right)^2 = \frac{E_3^2}{M} \ .$$

Using Equation (34), the connection between the lab frame cross section $\mathrm{d}\sigma/\mathrm{d}\Omega$ and the invariant cross section $\mathrm{d}\sigma/\mathrm{d}t$ of Equation (31) then becomes

$$\boxed{\frac{\mathrm{d}\sigma}{\mathrm{d}\Omega} = \frac{1}{2\pi} 2M \frac{E_3^2}{M} \frac{\mathrm{d}\sigma}{\mathrm{d}t} = \frac{E_3^2}{\pi} \frac{\mathrm{d}\sigma}{\mathrm{d}t}} \ . \tag{36}$$

The invariant cross section, $\mathrm{d}\sigma/\mathrm{d}t$, is given by Equation (30) with $m_2 = M$:

$$\frac{\mathrm{d}\sigma}{\mathrm{d}t} = \frac{1}{16\pi(s - M^2)^2} |M_{\mathrm{fi}}|^2 \tag{37}$$

The centre of mass energy squared is

$$s = (p_1 + p_2)^2 = M^2 + 2p_1.p_2 = M^2 + 2ME_1$$

so that

$$s - M^2 = 2ME_1 \ . \tag{38}$$

Combining Equations (36), (37) and (38) then gives

$$\frac{\mathrm{d}\sigma}{\mathrm{d}\Omega} = \frac{E_3^2}{\pi} \frac{\mathrm{d}\sigma}{\mathrm{d}t} = \frac{E_3^2}{\pi} \frac{1}{16\pi(s - M^2)^2} |M_{\mathrm{fi}}|^2 = \frac{E_3^2}{16\pi^2 (2ME_1)^2} |M_{\mathrm{fi}}|^2$$

Thus we finally obtain the cross section for high energy ($E_1 \gg m$) elastic scattering in the lab frame:

$$\boxed{\frac{\mathrm{d}\sigma}{\mathrm{d}\Omega} = \frac{1}{64\pi^2} \left(\frac{E_3}{ME_1}\right)^2 |M_{\mathrm{fi}}|^2} \tag{39}$$

Note that $\mathrm{d}\Omega = 2\pi \mathrm{d}\cos\theta$ and that E_3 depends on θ via Equation (35).

3.8 $2 \to 2$ Body Scattering in the Lab Frame (2) (non-examinable)

We now extend the analysis of the previous section to derive a general expression for the differential cross section in the lab frame, valid for any energy and for arbitrary particle masses:

$$p_1 = (E_1, \boldsymbol{p}_1); \quad p_2 = (m_2, 0, 0, 0); \quad p_3 = (E_3, \boldsymbol{p}_3); \quad p_4 = (E_4, \boldsymbol{p}_4).$$

Since $\mathrm{d}\Omega = 2\pi \mathrm{d}\cos\theta$, we still have

$$\frac{\mathrm{d}\sigma}{\mathrm{d}\Omega} = \frac{\mathrm{d}t}{\mathrm{d}\Omega} \frac{\mathrm{d}\sigma}{\mathrm{d}t} = \frac{1}{2\pi} \frac{\mathrm{d}t}{\mathrm{d}\cos\theta} \frac{\mathrm{d}\sigma}{\mathrm{d}t} \ .$$

The invariant quantity t is now

$$t = (p_2 - p_4)^2 = m_2^2 + m_4^2 - 2p_2.p_4 \ .$$

In the lab frame, with $p_2 = (m_2, 0, 0, 0)$ and $p_4 = (E_4, \boldsymbol{p_4})$, this becomes

$$t = m_2^2 + m_4^2 - 2m_2 E_4 = m_2^2 + m_4^2 - 2m_2(E_1 + m_2 - E_3)$$

where we have used energy conservation, $E_1 + m_2 = E_3 + E_4$, in the last step. Differentiation with respect to $\cos\theta$ then gives

$$\frac{\mathrm{d}t}{\mathrm{d}\cos\theta} = 2m_2 \frac{\mathrm{d}E_3}{\mathrm{d}\cos\theta}$$

and hence

$$\frac{\mathrm{d}\sigma}{\mathrm{d}\Omega} = \frac{m_2}{\pi} \frac{\mathrm{d}E_3}{\mathrm{d}\cos\theta} \frac{\mathrm{d}\sigma}{\mathrm{d}t} \ . \tag{40}$$

To determine $\mathrm{d}E_3/\mathrm{d}\cos\theta$, we first differentiate $E_3^2 = m_3^2 + p_3^2$ to obtain

$$2E_3 \frac{\mathrm{d}E_3}{\mathrm{d}\cos\theta} = 2p_3 \frac{\mathrm{d}p_3}{\mathrm{d}\cos\theta} \ . \tag{41}$$

As before, four-momentum conservation, $p_1 + p_2 = p_3 + p_4$, permits two alternative expressions for t:

$$t = (p_1 - p_3)^2 = m_1^2 + m_3^2 - 2(E_1 E_3 - p_1 p_3 \cos\theta)$$
$$t = (p_4 - p_2)^2 = m_4^2 + m_2^2 - 2m_2 E_4 = m_4^2 + m_2^2 - 2m_2(E_1 + m_2 - E_3)$$

Equating these two expressions gives

$$m_1^2 + m_3^2 + m_2^2 - m_4^2 = 2(E_1 E_3 - p_1 p_3 \cos\theta - m_2 E_1 + m_2 E_3) \ . \tag{42}$$

Differentiation with respect to $\cos\theta$ then gives

$$0 = (E_1 + m_2) \frac{\mathrm{d}E_3}{\mathrm{d}\cos\theta} - p_1 \cos\theta \frac{\mathrm{d}p_3}{\mathrm{d}\cos\theta} - p_1 p_3 \ .$$

Using Equation (41) to eliminate $\mathrm{d}p_3/\mathrm{d}\cos\theta$ we obtain

$$(E_1 + m_2) \frac{\mathrm{d}E_3}{\mathrm{d}\cos\theta} = p_1 \cos\theta \cdot \frac{E_3}{p_3} \frac{\mathrm{d}E_3}{\mathrm{d}\cos\theta} + p_1 p_3 \ .$$

This can be rearranged to give

$$\left(E_1 + m_2 - \frac{E_3 p_1 \cos\theta}{p_3} \right) \frac{\mathrm{d}E_3}{\mathrm{d}\cos\theta} = p_1 p_3$$

and hence

$$\frac{\mathrm{d}E_3}{\mathrm{d}\cos\theta} = \frac{p_1 p_3^2}{E_1 p_3 + m_2 p_3 - E_3 p_1 \cos\theta} \ .$$

Substitution into Equation (40) and using the expression for $\mathrm{d}\sigma/\mathrm{d}t$ in Equation (28) then gives

$$\frac{\mathrm{d}\sigma}{\mathrm{d}\Omega} = \frac{m_2}{\pi} \frac{\mathrm{d}E_3}{\mathrm{d}\cos\theta} \frac{1}{64\pi s (p_\mathrm{i}^*)^2} |M_\mathrm{fi}|^2 \ . \tag{43}$$

The quantity $s(p_\mathrm{i}^*)^2$ appearing in Equation (43) can be expressed in terms of lab frame variables using the result already derived in Equation (22), with p_a replaced by p_1 and m_b replaced by m_2:

$$p_\mathrm{i}^* \sqrt{s} = m_2 p_1 \ .$$

The cross section then becomes

$$\begin{aligned}\frac{\mathrm{d}\sigma}{\mathrm{d}\Omega} &= \frac{\mathrm{d}E_3}{\mathrm{d}\cos\theta}\frac{m_2}{64\pi^2 s(p_1^*)^2}|M_{\mathrm{fi}}|^2 \\ &= \frac{p_1 p_3^2}{E_1 p_3 + m_2 p_3 - E_3 p_1\cos\theta}\frac{m_2}{64\pi^2 m_2^2 p_1^2}|M_{\mathrm{fi}}|^2 \ .\end{aligned}$$

Hence we finally obtain the following general expression for any $2 \to 2$ scattering process in the lab frame:

$$\boxed{\frac{\mathrm{d}\sigma}{\mathrm{d}\Omega} = \frac{1}{64\pi^2}\cdot\frac{1}{p_1 m_2}\cdot\frac{p_3^2|M_{\mathrm{fi}}|^2}{p_3(E_1+m_2) - E_3 p_1\cos\theta}} \tag{44}$$

where $p_1 = |\boldsymbol{p}_1|$ and $p_3 = |\boldsymbol{p}_3|$. Note that the variables in the above equation are not all independent. In particular, once θ is specified, the energy, E_3, and momentum, p_3, are fixed by Equation (42) in combination with the constraint $E_3 = \sqrt{p_3^2 + m_3^2}$.

Note also that we can recover the high energy result derived in the previous section by setting $m_2 = M$, $p_1 = E_1$ and $p_3 = E_3$. This gives

$$\begin{aligned}\frac{\mathrm{d}\sigma}{\mathrm{d}\Omega} &= \frac{1}{64\pi^2}\cdot\frac{1}{E_1 M}\cdot\frac{E_3^2}{E_3(E_1+M) - E_3 E_1\cos\theta}\cdot|M_{\mathrm{fi}}|^2 \\ &= \frac{1}{64\pi^2}\cdot\frac{1}{E_1 M}\cdot\frac{E_3}{E_1 + M - E_1\cos\theta}\cdot|M_{\mathrm{fi}}|^2 \\ &= \frac{1}{64\pi^2}\left(\frac{E_3}{M E_1}\right)^2|M_{\mathrm{fi}}|^2\end{aligned}$$

as in Equation (39), where we have used Equation (35) in the last step.

3.9 $2 \to 2$ Body Scattering in the Lab Frame (3) (non-examinable)

Finally, for completeness, we evaluate the cross section for two body scattering in the lab frame by a direct application of Equation (18), rather than using the invariant cross section $\mathrm{d}\sigma/\mathrm{d}t$. With 4-momenta

$$p_1 = (E_1, \boldsymbol{p}_1); \quad p_2 = (m_2, 0, 0, 0); \quad p_3 = (E_3, \boldsymbol{p}_3); \quad p_4 = (E_4, \boldsymbol{p}_4),$$

Equation (23) becomes

$$\sigma = \frac{(2\pi)^{-2}}{F}\int |M_{\mathrm{fi}}|^2\delta(E_1 + E_2 - E_3 - E_4)\delta^{(3)}(\boldsymbol{p}_1 + \boldsymbol{p}_2 - \boldsymbol{p}_3 - \boldsymbol{p}_4)\frac{\mathrm{d}^3 p_3}{2E_3}\frac{\mathrm{d}^3 p_4}{2E_4}$$

Carrying out the integral $\int \mathrm{d}^3 p_4$, and setting $F = 4p_1 m_2$, with $p_1 = |\boldsymbol{p}_1|$, gives

$$\begin{aligned}\sigma &= \frac{1}{(4\pi)^2}\frac{1}{4p_1 m_2}\int |M_{\mathrm{fi}}|^2\delta(E_1 + E_2 - E_3 - E_4)\frac{\mathrm{d}^3 p_3}{E_3 E_4} \\ &= \frac{1}{(4\pi)^2}\frac{1}{4p_1 m_2}\int |M_{\mathrm{fi}}|^2\delta\left(f(p_3)\right)\frac{p_3^2\mathrm{d}p_3\mathrm{d}\cos\theta\mathrm{d}\phi}{E_3 E_4}\end{aligned} \tag{45}$$

where $p_3 = |\boldsymbol{p}_3|$ and

$$\begin{aligned} f(p_3) &\equiv E_1 + E_2 - E_3 - E_4 \\ &= E_1 + m_2 - \sqrt{p_3^2 + m_3^2} - \sqrt{(\boldsymbol{p}_1 - \boldsymbol{p}_3)^2 + m_4^2} \\ &= E_1 + m_2 - \sqrt{p_3^2 + m_3^2} - \sqrt{p_1^2 + p_3^2 - 2p_1 p_3 \cos\theta + m_4^2} \end{aligned}$$

and θ is the angle between $\boldsymbol{p}_1$ and $\boldsymbol{p}_3$, or equivalently the angle of particle 3 with respect to the incoming beam direction.

For any given value of the scattering angle θ, the function $f(p_3)$ will have a zero at a particular value of p_3 given by

$$f(p_3) = E_1 + m_2 - \sqrt{p_3^2 + m_3^2} - \sqrt{p_1^2 + p_3^2 - 2p_1 p_3 \cos\theta + m_4^2} = 0. \tag{46}$$

Using

$$\begin{aligned} \frac{\mathrm{d}f}{\mathrm{d}p_3} &= -\frac{p_3}{\sqrt{p_3^2 + m_3^2}} - \frac{p_3 - p_1\cos\theta}{\sqrt{p_1^2 + p_3^2 - 2p_1 p_3\cos\theta + m_4^2}} \\ &= -\frac{p_3}{E_3} - \frac{p_3 - p_1\cos\theta}{E_4} \\ &= -\frac{p_3 E_4 + E_3 p_3 - E_3 p_1 \cos\theta}{E_3 E_4} \end{aligned}$$

and using

$$\int g(p_3)\delta(f(p_3))\mathrm{d}p_3 = \left[\frac{g(p_3)}{|\mathrm{d}f/\mathrm{d}p_3|}\right]_{f(p_3)=0}$$

to perform the integral over p_3 in Equation (45) gives

$$\begin{aligned} \sigma &= \frac{1}{(4\pi)^2}\frac{1}{4p_1 m_2}\int |M_{\mathrm{fi}}|^2 \left[\frac{E_3 E_4}{p_3 E_4 + E_3 p_3 - E_3 p_1\cos\theta}\frac{p_3^2}{E_3 E_4}\right]_{f(p_3)=0} \mathrm{d}\cos\theta\mathrm{d}\phi \\ &= \frac{1}{(4\pi)^2}\frac{1}{4p_1 m_2}\int \frac{p_3^2 |M_{\mathrm{fi}}|^2}{p_3(E_3 + E_4) - E_3 p_1\cos\theta}\mathrm{d}\Omega \end{aligned} \tag{47}$$

where now, in the last line, p_3, E_3 and E_4 represent the actual momenta and energies in the lab frame, as fixed by energy-momentum conservation. In differential form, Equation (47) is

$$\frac{\mathrm{d}\sigma}{\mathrm{d}\Omega} = \frac{1}{(4\pi)^2}\frac{1}{4p_1 m_2}\frac{p_3^2 |M_{\mathrm{fi}}|^2}{p_3(E_3 + E_4) - E_3 p_1\cos\theta}\ .$$

Using energy conservation, $E_1 + m_2 = E_3 + E_4$, we then arrive at the same result as derived in the previous section for the differential cross section in the laboratory frame:

$$\boxed{\frac{\mathrm{d}\sigma}{\mathrm{d}\Omega} = \frac{1}{64\pi^2}\cdot\frac{1}{p_1 m_2}\cdot\frac{p_3^2 |M_{\mathrm{fi}}|^2}{p_3(E_1 + m_2) - E_3 p_1\cos\theta}}$$

Note again that the variables in the above equation are not all independent. Once θ is specified, the momentum p_3 is fixed by Equation (46), and E_3 is then determined as $E_3 = \sqrt{p_3^2 + m_3^2}$.

3.10 Summary

For convenience, we collect together here various expressions for decay rates and cross sections which were derived above :

3.10.1 Decay rates

For a two-body decay of the form $a \to 1 + 2$, the total decay rate in the rest frame of particle a is given by

$$\boxed{\Gamma = \frac{p^*}{32\pi^2 m_a^2} \int |M_{\rm fi}|^2 {\rm d}\cos\theta {\rm d}\phi} \qquad (14)'$$

If the decay is isotropic (for example, if particle a has zero spin) this simplifies to

$$\boxed{\Gamma = \frac{p^*}{8\pi m_a^2} |M_{\rm fi}|^2} \qquad \text{(isotropic)} \qquad (15)'$$

The centre of mass momentum, p^*, in the above equations is given by

$$p^* = \frac{1}{2m_a} \sqrt{[m_a^2 - (m_1 + m_2)^2]\,[m_a^2 - (m_1 - m_2)^2]}\,.$$

3.10.2 Scattering cross sections

For a general two-body scattering process of the form $1 + 2 \to 3 + 4$, the differential cross section in the centre of mass frame is given by

$$\boxed{\frac{{\rm d}\sigma}{{\rm d}\Omega^*} = \frac{1}{64\pi^2 s} \frac{p_{\rm f}^*}{p_{\rm i}^*} |M_{\rm fi}|^2} \qquad (24)'$$

where $s \equiv (p_1 + p_2)^2$ (with $\sqrt{s} = E_1^* + E_2^*$ in the centre of mass), $p_{\rm i}^* = |\boldsymbol{p}_1| = |\boldsymbol{p}_2|$ is the centre of mass momentum of either of the initial state particles, and $p_{\rm f}^* = |\boldsymbol{p}_3| = |\boldsymbol{p}_4|$ is the centre of mass momentum of either of the final state particles.

For elastic scattering, *i.e.* for $m_1 = m_3$, $m_2 = m_4$, this expression simplifies to

$$\boxed{\frac{{\rm d}\sigma}{{\rm d}\Omega^*} = \frac{1}{64\pi^2 s} |M_{\rm fi}|^2} \qquad \text{(elastic)} \qquad (26)'$$

A general Lorentz invariant expression for the differential cross section, valid in any frame of reference, is

$$\boxed{\frac{{\rm d}\sigma}{{\rm d}t} = \frac{\pi}{p_{\rm i}^* p_{\rm f}^*} \frac{{\rm d}\sigma}{{\rm d}\Omega^*} = \frac{1}{64\pi s (p_{\rm i}^*)^2} |M_{\rm fi}|^2} \qquad (28)'$$

where $t \equiv (p_1 - p_3)^2$.

For high energy elastic scattering in the lab frame, where the mass m_1 can be neglected ($E_1 \gg m_1$) and particle 2 is at rest, the cross section is

$$\boxed{\frac{\mathrm{d}\sigma}{\mathrm{d}\Omega} = \frac{1}{64\pi^2}\left(\frac{E_3}{ME_1}\right)^2 |M_{\mathrm{fi}}|^2} \qquad (\text{elastic}, m_1 = 0) \qquad (39)'$$

The energy E_3 depends on θ via Equation (35).

A completely general expression for the cross section in the lab frame is

$$\boxed{\frac{\mathrm{d}\sigma}{\mathrm{d}\Omega} = \frac{1}{64\pi^2} \cdot \frac{1}{p_1 m_2} \cdot \frac{p_3^2 |M_{\mathrm{fi}}|^2}{p_3(E_1 + m_2) - E_3 p_1 \cos\theta}} \qquad (44)'$$

where $p_1 = |\boldsymbol{p}_1|$, $p_3 = |\boldsymbol{p}_3|$, $E_3 = \sqrt{p_3^2 + m_3^2}$, and p_3 is given in terms of θ by Equation (46).

The above expessions for decay rates and cross sections all depend on the Lorentz-invariant matrix element squared, $|M_{\mathrm{fi}}|^2$. For any particular process, such as $\pi^+ \to \mathrm{e}^+\nu_{\mathrm{e}}$ decay or $\mathrm{e}^+\mathrm{e}^- \to \mu^+\mu^-$ annihilation, the matrix element M_{fi} will be determined by writing down the Feynman diagrams appropriate to that process and applying the Feynman rules to each diagram.

3.11 Appendix: The Dirac δ Function

3.11.1 Definition

The Dirac δ function, $\delta(x-a)$, can loosely be defined as an infinitely narrow "spike" of unit area located at $x = a$:

$$\begin{aligned} \delta(x-a) &= 0 \qquad \text{for } x \neq a \\ &= \infty \qquad \text{for } x = a \end{aligned}$$

$$\int_{x_1}^{x_2} \delta(x-a)\,\mathrm{d}x = \begin{cases} 1 & \text{if } x_1 < a < x_2, \\ 0 & \text{otherwise} \end{cases} \tag{48}$$

The δ function is not strictly speaking a mathematical function at all; rather it is an example of a *distribution* or a *generalised function*.

For any function $g(x)$ we have

$$\int_{x_1}^{x_2} g(x)\delta(x-a)\,\mathrm{d}x = \begin{cases} g(a) & \text{if } x_1 < a < x_2, \\ 0 & \text{otherwise} \end{cases} \tag{49}$$

3.11.2 Change of Variable

Equation (48), with $a = 0$, gives

$$\int_{y_1}^{y_2} \delta(y)\,\mathrm{d}y = \begin{cases} 1 & \text{if } y_1 < 0 < y_2, \\ 0 & \text{otherwise} \end{cases}$$

Consider now a change of variable from y to x, where $y = f(x)$ and the function $f(x)$ has only a single zero at $x = x_0$, *i.e.* $f(x_0) = 0$. Then

$$\int_{x_1}^{x_2} \delta(f(x))\frac{\mathrm{d}y}{\mathrm{d}x}\,\mathrm{d}x = \begin{cases} 1 & \text{if } x_1 < x_0 < x_2, \\ 0 & \text{otherwise} \end{cases}$$

But $\mathrm{d}y/\mathrm{d}x = \mathrm{d}f/\mathrm{d}x$, and the δ function vanishes unless $x = x_0$. Therefore $\mathrm{d}y/\mathrm{d}x$ can be replaced by $\mathrm{d}f/\mathrm{d}x|_{x=x_0}$, giving

$$\left|\frac{\mathrm{d}f}{\mathrm{d}x}\right|_{x=x_0} \int_{x_1}^{x_2} \delta(f(x))\,\mathrm{d}x = \begin{cases} 1 & \text{if } x_1 < x_0 < x_2, \\ 0 & \text{otherwise} \end{cases}$$

A comparison with the original definition of the δ function, Equation (48), gives the final result that, for any function $f(x)$ with a single zero at x_0,

$$\boxed{\delta(f(x)) = \left|\frac{1}{\mathrm{d}f/\mathrm{d}x}\right|_{x_0} \delta(x-x_0)}$$

Inside an integral involving a second function $g(x)$, where the range of integration includes x_0, we obtain

$$\int g(x)\delta(f(x))\mathrm{d}x = \int g(x)\frac{\delta(x-x_0)}{|\mathrm{d}f/\mathrm{d}x|_{x_0}}\mathrm{d}x = \frac{g(x_0)}{|\mathrm{d}f/\mathrm{d}x|_{x_0}}$$

Hence we obtain the integral version of the above result:

$$\boxed{\int g(x)\delta(f(x))\mathrm{d}x = \left[\frac{g(x)}{|\mathrm{d}f/\mathrm{d}x|}\right]_{x_0}}.$$

3.11.3 Integral Representation

From Fourier theory, Fourier transforms $f(x)$ and $F(k)$ are related to each other via

$$f(x) = \frac{1}{2\pi}\int_{-\infty}^{+\infty} F(k)e^{ikx}\mathrm{d}k \tag{50}$$

$$F(k) = \int_{-\infty}^{+\infty} f(x)e^{-ikx}\mathrm{d}x\ . \tag{51}$$

Substituting $F(k)$ from Equation (50) into Equation (51) and inverting the order of integration gives

$$\begin{aligned} f(x) &= \frac{1}{2\pi}\int_{-\infty}^{+\infty}\left(\int_{-\infty}^{+\infty} f(y)e^{-iky}dy\right)e^{ikx}\mathrm{d}k \\ &= \int_{-\infty}^{+\infty} f(y)\left(\frac{1}{2\pi}\int_{-\infty}^{+\infty} e^{ik(x-y)}\mathrm{d}k\right)\mathrm{d}y. \end{aligned}$$

A comparison with Equation (49) shows that the Dirac δ function can be represented as

$$\boxed{\delta(x) = \frac{1}{2\pi}\int_{-\infty}^{+\infty} e^{ikx}\,\mathrm{d}k} \tag{52}$$

Since the δ function is symmetric, $\delta(x) = \delta(-x)$, we equally have

$$\delta(x) = \frac{1}{2\pi}\int_{-\infty}^{+\infty} e^{-ikx}\,\mathrm{d}k\ .$$

The δ function can easily be extended to more than one dimension, for example:

$$\begin{aligned} \delta^{(3)}(\boldsymbol{x}-\boldsymbol{a}) &= \delta(x-a_x)\delta(y-a_y)\delta(z-a_z) \\ \delta^{(4)}(x^\mu - a^\mu) &= \delta(x^0-a^0)\delta(x^1-a^1)\delta(x^2-a^2)\delta(x^3-a^3) \\ &= \delta(x^0-a^0)\delta^{(3)}(\boldsymbol{x}-\boldsymbol{a}) \end{aligned}$$

The generalisation of Equation (52) to three or four dimensions is:

$$\delta^{(3)}(\boldsymbol{x}) = \frac{1}{(2\pi)^3}\int_{-\infty}^{+\infty} e^{i\boldsymbol{k}.\boldsymbol{x}}\,\mathrm{d}^3k$$

$$\delta^{(4)}(x) = \frac{1}{(2\pi)^4}\int_{-\infty}^{+\infty} e^{ik.x}\,\mathrm{d}^4k\ .$$

4 Electron-Positron Annihilation in QED

4.1 Matrix Element for $\mathrm{e}^+\mathrm{e}^- \to \mu^+\mu^-$

At leading order in perturbation theory, the QED process $\mathrm{e}^+\mathrm{e}^- \to \mu^+\mu^-$ is governed by a single Feynman diagram mediated by a virtual photon γ^*:

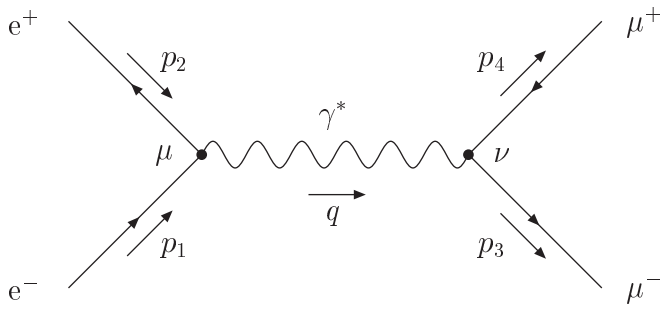

Here p_1 and p_2 are the four-momenta of the incoming e^- and e^+, p_3 and p_4 are the four-momenta of the outgoing μ^- and μ^+, and $q = p_1 + p_2 = p_3 + p_4$ is the four-momentum of the virtual photon. The arrows on the external lines in the Feynman diagram indicate *particle* direction which, for the e^+ and μ^+ antiparticles, is the opposite of the physical antiparticle direction.

The QED Feynman rules give factors of $u(p_1)$ for the incoming e^-, $\overline{v}(p_2)$ for the incoming e^+, $\overline{u}(p_3)$ for the outgoing μ^-, $v(p_4)$ for the outgoing μ^+, $-ig^{\mu\nu}/q^2$ for the photon propagator, $ie\gamma^\mu$ for the electron-photon vertex, and $ie\gamma^\nu$ for the muon-photon vertex, where $-e$ is the electric charge of the e^- and μ^-. The product of these factors determines the Lorentz-invariant matrix element M_{fi}:

$$-iM_{\mathrm{fi}} = [\overline{v}(p_2) \cdot ie\gamma^\mu \cdot u(p_1)] \cdot \frac{-ig_{\mu\nu}}{q^2} \cdot [\overline{u}(p_3) \cdot ie\gamma^\nu \cdot v(p_4)] \ .$$

Introducing the invariant scalar product $s \equiv (p_1 + p_2)^2 = q^2$, we have

$$\boxed{M_{\mathrm{fi}} = -\frac{e^2}{s} g_{\mu\nu} \left[\overline{v}(p_2)\gamma^\mu u(p_1)\right] \left[\overline{u}(p_3)\gamma^\nu v(p_4)\right]} \ . \tag{1}$$

This is just a number, which can be worked out once the initial and final spin states have been specified. With two possible spin states available to each of the four external particles involved, there are a total of 16 possible spin configurations to consider.

The various factors in Equation (1) are ordered such that factors associated purely with the $\mathrm{e}^+\mathrm{e}^-\gamma^*$ vertex are grouped together, defining the *electron current*

$$(j_e)^\mu = \overline{v}(p_2)\gamma^\mu u(p_1) \ ,$$

and similarly for factors associated purely with the $\mu^+\mu^-\gamma^*$ vertex, defining the *muon current* [1]

$$(j_\mu)^\nu = \overline{u}(p_3)\gamma^\nu v(p_4) \ .$$

The overall matrix element M_{fi} is proportional to the scalar product of the electron and muon current four-vectors:

$$M_{\mathrm{fi}} = -\frac{e^2}{s}(j_e.j_\mu) \tag{2}$$

and as such is an example of a *current-current interaction*.

We consider $\mathrm{e}^+\mathrm{e}^- \to \mu^+\mu^-$ scattering at extreme relativistic energies and work in the centre of mass frame. We choose the incoming e^- direction to be along the $+z$ axis and the outgoing μ^- to be at an angle θ to the z axis. The e^- and e^+ 4-momenta are therefore

$$p_1 = (E, 0, 0, E); \qquad p_2 = (E, 0, 0, -E) \tag{3}$$

while the μ^- and μ^+ 4-momenta can be taken to be

$$p_3 = (E, E\sin\theta, 0, E\cos\theta); \qquad p_4 = (E, -E\sin\theta, 0, -E\cos\theta) \ . \tag{4}$$

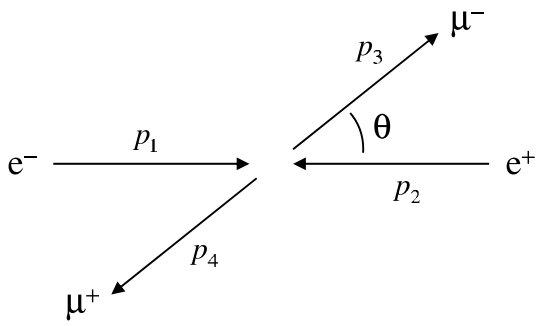

The cross section will be evaluated for each possible combination of e^+, e^-, μ^+, μ^- helicities. The spinors $u(p_1)$, $v(p_2)$, $u(p_3)$, $v(p_4)$ can be found using the general result that, for ultra-relativistic particles or antiparticles travelling at an angle θ to the z-axis, with four-momentum

$$p^\mu = (E, E\sin\theta\cos\phi, E\sin\theta\sin\phi, E\cos\theta) \ , \tag{5}$$

the helicity eigenstates are given by [2] [3]

$$u_\uparrow = \sqrt{E}\begin{pmatrix} c \\ e^{i\phi}s \\ c \\ e^{i\phi}s \end{pmatrix}; \qquad u_\downarrow = \sqrt{E}\begin{pmatrix} -s \\ e^{i\phi}c \\ s \\ -e^{i\phi}c \end{pmatrix}; \qquad v_\uparrow = \sqrt{E}\begin{pmatrix} s \\ -e^{i\phi}c \\ -s \\ e^{i\phi}c \end{pmatrix}; \qquad v_\downarrow = \sqrt{E}\begin{pmatrix} c \\ e^{i\phi}s \\ c \\ e^{i\phi}s \end{pmatrix} \tag{6}$$

[1] Note that a structure of the form $\overline{\psi}\gamma^\mu\phi$ represents the only valid ordering for the vertex factors; and other ordering, such as $\phi\gamma^\mu\overline{\psi}$ or $\gamma^\mu\overline{\psi}\phi$, would result in a nonsensical matrix multiplication structure.

[2] See Equation (55) of Handout 2.

[3] Note that the symbol s is being used to denote both $s \equiv \sin\theta/2$ and $s \equiv (p_1 + p_2)^2$. In practice these two usages remain well separated and no confusion should result.

where $c \equiv \cos\theta/2$, $s \equiv \sin\theta/2$. Once the matrix element has been evaluated using Equation (1), the differential cross section can be found from [4]

$$\frac{\mathrm{d}\sigma}{\mathrm{d}\Omega} = \frac{1}{64\pi^2 s}|M_{\mathrm{fi}}|^2 \tag{7}$$

where $s = (p_1 + p_2)^2$ is the centre of mass energy squared.

4.2 The Muon Current

We begin by evaluating the muon current $(j_\mu)^\mu = \overline{u}(p_3)\gamma^\mu v(p_4)$ for each of the four possible spin configurations for the muon pair, $\mu^+_{\mathrm{L}}\mu^-_{\mathrm{L}}$, $\mu^+_{\mathrm{L}}\mu^-_{\mathrm{R}}$, $\mu^+_{\mathrm{R}}\mu^-_{\mathrm{L}}$, $\mu^+_{\mathrm{R}}\mu^-_{\mathrm{R}}$, where the subscripts L and R refer to the helicity of the μ^+ or μ^-.

The "spin up" and "spin down" helicity eigenstates for the outgoing μ^-, with four-momentum $p_3 = (E, E\sin\theta, 0, E\cos\theta)$, can be written down directly from Equation (6) simply by setting $\phi = 0$:

$$u_\uparrow(p_3) = \sqrt{E}\begin{pmatrix} c \\ s \\ c \\ s \end{pmatrix}; \qquad u_\downarrow(p_3) = \sqrt{E}\begin{pmatrix} -s \\ c \\ s \\ -c \end{pmatrix}$$

where $c \equiv \cos\theta/2$, $s \equiv \sin\theta/2$. The μ^+ four-momentum, $p_4 = (E, -E\sin\theta, 0, -E\cos\theta)$, can be obtained from Equation (5) by setting $\theta \to \pi - \theta$ and $\phi = \pi$. Making these replacements in Equation (6) gives the "spin up" and "spin down" μ^+ spinors as

$$v_\uparrow(p_4) = \sqrt{E}\begin{pmatrix} c \\ s \\ -c \\ -s \end{pmatrix}; \qquad v_\downarrow(p_4) = \sqrt{E}\begin{pmatrix} s \\ -c \\ s \\ -c \end{pmatrix}$$

where we have used $\sin((\pi-\theta)/2) = \cos\theta/2 = c$ and $\cos((\pi-\theta)/2) = \sin\theta/2 = s$.

The muon current $\overline{u}(p_3)\gamma^\mu v(p_4)$ can now be evaluated, for each of the four possible helicity pairings in turn, using standard matrix multiplication. The adjoint spinors $\overline{u}_\uparrow(p_3)$ and $\overline{u}_\downarrow(p_3)$ are given by

$$\overline{u}_\uparrow(p_3) = \sqrt{E}\,(c, s, -c, -s); \qquad \overline{u}_\downarrow(p_3) = \sqrt{E}\,(-s, c, -s, c)\ .$$

General expressions for a matrix multiplication of the form $\overline{\psi}\gamma^\mu\phi$ are derived in the examples sheet. For arbitrary spinors ψ and ϕ, with real components ψ_i and ϕ_i, these expressions give

$$\begin{aligned}
\overline{\psi}\gamma^0\phi &= \psi_1\phi_1 + \psi_2\phi_2 + \psi_3\phi_3 + \psi_4\phi_4 \\
\overline{\psi}\gamma^1\phi &= \psi_1\phi_4 + \psi_2\phi_3 + \psi_3\phi_2 + \psi_4\phi_1 \\
\overline{\psi}\gamma^2\phi &= -i(\psi_1\phi_4 - \psi_2\phi_3 + \psi_3\phi_2 - \psi_4\phi_1) \\
\overline{\psi}\gamma^3\phi &= \psi_1\phi_3 - \psi_2\phi_4 + \psi_3\phi_1 - \psi_4\phi_2\ .
\end{aligned}$$

[4] See Equation (26) of Handout 3.

Consider first the case $\mu^+_{\rm R}\mu^-_{\rm L}$ where the μ^+ is right-handed, $\phi = v_\uparrow(p_4)$, and the μ^- is left-handed, $\psi = u_\downarrow(p_3)$. The above expressions then give

$$\begin{aligned}
\overline{u}_\downarrow(p_3)\gamma^0 v_\uparrow(p_4) &= E(-sc + cs - sc + cs) &= 0 \\
\overline{u}_\downarrow(p_3)\gamma^1 v_\uparrow(p_4) &= E(s^2 - c^2 + s^2 - c^2) &= 2E(s^2 - c^2) \\
\overline{u}_\downarrow(p_3)\gamma^2 v_\uparrow(p_4) &= -iE(s^2 + c^2 + s^2 + c^2) &= -2iE \\
\overline{u}_\downarrow(p_3)\gamma^3 v_\uparrow(p_4) &= E(sc + cs + sc + cs) &= 4Esc\,.
\end{aligned}$$

This can be written compactly as the muon current four-vector

$$\begin{aligned}
\overline{u}_\downarrow(p_3)\gamma^\mu v_\uparrow(p_4) &= 2E\left(0, s^2 - c^2, -i, 2sc\right) \\
&= 2E\left(0, -\cos\theta, -i, \sin\theta\right)
\end{aligned}$$

where we have used the identities $2sc = 2\sin\theta/2\cos\theta/2 = \sin\theta$ and $c^2 - s^2 = \cos^2\theta/2 - \sin^2\theta/2 = \cos\theta$.

The muon current for the remaining spin configurations is easily evaluated in similar fashion, giving overall (in the relativistic limit):

$\mu^+_{\rm L}\mu^-_{\rm R}$:	$\overline{u}_\uparrow(p_3)\gamma^\mu v_\downarrow(p_4)$	$=$	$2E\left(0, -\cos\theta, i, \sin\theta\right)$	(8)
$\mu^+_{\rm R}\mu^-_{\rm R}$:	$\overline{u}_\uparrow(p_3)\gamma^\mu v_\uparrow(p_4)$	$=$	$(0,0,0,0)$	(9)
$\mu^+_{\rm L}\mu^-_{\rm L}$:	$\overline{u}_\downarrow(p_3)\gamma^\mu v_\downarrow(p_4)$	$=$	$(0,0,0,0)$	(10)
$\mu^+_{\rm R}\mu^-_{\rm L}$:	$\overline{u}_\downarrow(p_3)\gamma^\mu v_\uparrow(p_4)$	$=$	$2E\left(0, -\cos\theta, -i, \sin\theta\right)$	(11)

4.3 Helicity Conservation

The results above show that the muon current (and hence the matrix element $M_{\rm fi}$) is non-zero only for the cases $\mu^+_{\rm L}\mu^-_{\rm R}$ and $\mu^+_{\rm R}\mu^-_{\rm L}$, where the μ^+ and μ^- have opposite helicity. Since the physical helicity of an *antiparticle* (μ^+ in this case) is opposite to the helicity of the corresponding negative energy *particle*, this is equivalent to the statement that the muon current is non-zero only if the *particle* helicity is the same before and after the interaction with the virtual photon. This is an example of a general property of QED known as *helicity conservation*: in the relativistic limit, the *particle* helicity is preserved in interactions with photons. Helicity conservation will be seen to apply to the weak and strong interactions also.

Helicity conservation applies equally at the electron vertex, as we shall show explicitly in the next section; the electron current is non-zero only for the cases $\mathrm{e}^+_{\rm L}\mathrm{e}^-_{\rm R}$ and $\mathrm{e}^+_{\rm R}\mathrm{e}^-_{\rm L}$. Therefore, in the massless limit, only four of the 16 possible spin configurations give a non-zero matrix element. These are illustrated overleaf; only those configurations with a total spin projection $S_z = \pm 1$ in both the initial and final states are allowed.

Helicity conservation in QED is a consequence of the following general result, the proof of which is deferred to the examples sheet:

$$\boxed{\overline{\psi}\gamma^\mu\psi = \overline{\psi_{\rm L}}\gamma^\mu\psi_{\rm L} + \overline{\psi_{\rm R}}\gamma^\mu\psi_{\rm R}}\,, \tag{12}$$

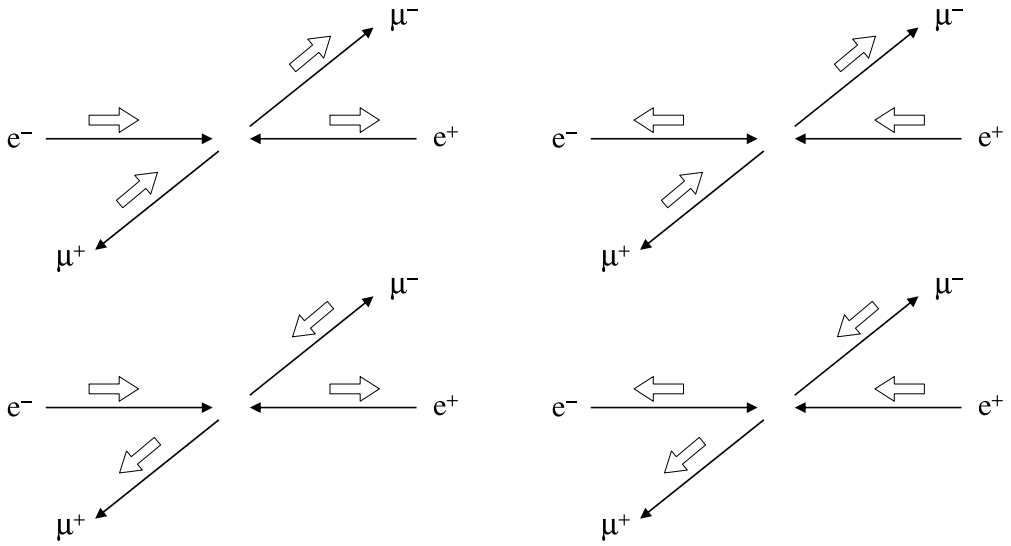

where $\psi_{\rm L} = \frac{1}{2}(1-\gamma^5)\psi$ and $\psi_{\rm R} = \frac{1}{2}(1+\gamma^5)\psi$ are the left-handed and right-handed chiral components of ψ. There is no contribution to the current $\overline{\psi}\gamma^\mu\psi$ from the mixed terms $\overline{\psi_{\rm R}}\gamma^\mu\psi_{\rm L}$ or $\overline{\psi_{\rm L}}\gamma^\mu\psi_{\rm R}$:

$$\overline{\psi_{\rm R}}\gamma^\mu\psi_{\rm L} = 0 \tag{13}$$

$$\overline{\psi_{\rm L}}\gamma^\mu\psi_{\rm R} = 0\ . \tag{14}$$

Thus, in QED, left-handed chiral components couple only to left-handed chiral components, and right-handed chiral components couple only to right-handed chiral components, *i.e.* the particle chirality is preserved in an interaction with a photon. At extreme relativistic energies, the left-handed and right-handed chiral components become helicity eigenstates, and the particle helicity is then also conserved in the interaction. Conservation of chirality, Equations (12)-(14) is a general result which holds at all particle energies whereas conservation of helicity, Equations (9) and (10), holds only in the relativistic limit [5].

4.4 The Electron Current

The electron spinors $u_\uparrow(p_1)$ and $u_\downarrow(p_1)$ can be obtained from Equation (6) by setting $\theta = 0$ and $\phi = 0$, while the positron spinors $v_\uparrow(p_2)$ and $v_\downarrow(p_2)$ can be obtained by setting $\theta = \pi$ and $\phi = 0$:

$$u_\uparrow(p_1) = \sqrt{E}\begin{pmatrix}1\\0\\1\\0\end{pmatrix};\qquad u_\downarrow(p_1) = \sqrt{E}\begin{pmatrix}0\\1\\0\\-1\end{pmatrix};\qquad v_\uparrow(p_2) = \sqrt{E}\begin{pmatrix}1\\0\\-1\\0\end{pmatrix};\qquad v_\downarrow(p_2) = \sqrt{E}\begin{pmatrix}0\\1\\0\\1\end{pmatrix}$$

The electron current $(j_e)^\mu = \overline{v}(p_2)\gamma^\mu u(p_1)$ for each possible spin configuration could clearly be evaluated using direct matrix multiplication, as was done above for the muon current. A more elegant way to proceed is to note that the electron current, of the form $\overline{v}\gamma^\mu u$, can be obtained from the

[5] In this sense, *chirality conservation* would be a better terminology for this result than *helicity conservation*.

complex conjugate of the muon current, of the form $\overline{u}\gamma^\mu v$. To demonstrate this, treat each element of the current four-vector as a 1×1 matrix, giving

$$\begin{aligned}
[\overline{u}(p_a)\gamma^\nu v(p_b)]^* &= [\overline{u}(p_a)\gamma^\nu v(p_b)]^\dagger \\
&= \left[u^\dagger(p_a)\gamma^0\gamma^\nu v(p_b)\right]^\dagger && \text{since } \overline{u} \equiv u^\dagger\gamma^0 \\
&= v^\dagger(p_b)\gamma^{\nu\dagger}\gamma^{0\dagger}u(p_a) && \text{since } (AB)^\dagger = B^\dagger A^\dagger \\
&= v^\dagger(p_b)\gamma^{\nu\dagger}\gamma^0 u(p_a) && \text{since } \gamma^{0\dagger} = \gamma^0 \\
&= v^\dagger(p_b)\gamma^0\gamma^\nu u(p_a) && \text{since } \gamma^{\nu\dagger}\gamma^0 = \gamma^0\gamma^\nu \\
&= \overline{v}(p_b)\gamma^\nu u(p_a) && \text{since } \overline{v} \equiv v^\dagger\gamma^0
\end{aligned}$$

Taking the complex conjugate of the muon currents of Equations (8)-(11) then gives

$$\overline{v}_\downarrow(p_4)\gamma^\mu u_\uparrow(p_3) = [\overline{u}_\uparrow(p_3)\gamma^\mu v_\downarrow(p_4)]^* = 2E\,(0, -\cos\theta, -i, \sin\theta) \tag{15}$$
$$\overline{v}_\uparrow(p_4)\gamma^\mu u_\uparrow(p_3) = [\overline{u}_\uparrow(p_3)\gamma^\mu v_\uparrow(p_4)]^* = (0,0,0,0) \tag{16}$$
$$\overline{v}_\downarrow(p_4)\gamma^\mu u_\downarrow(p_3) = [\overline{u}_\downarrow(p_3)\gamma^\mu v_\downarrow(p_4)]^* = (0,0,0,0) \tag{17}$$
$$\overline{v}_\uparrow(p_4)\gamma^\mu u_\downarrow(p_3) = [\overline{u}_\downarrow(p_3)\gamma^\mu v_\uparrow(p_4)]^* = 2E\,(0, -\cos\theta, i, \sin\theta)\ . \tag{18}$$

The electron four-momenta p_1 and p_2 of Equation (3) are just a special case of the muon four-momenta p_3 and p_4 of Equation (4), obtained by setting $\theta = 0$ in the latter. Hence the electron current j_e for each of the four possible combinations of e^+ and e^- helicity eigenstates can be written down directly by setting $\theta = 0$ in Equations (15)-(18):

$$\begin{aligned}
&\mathrm{e}^+_\mathrm{L}\mathrm{e}^-_\mathrm{R}\ : && \overline{v}_\downarrow(p_2)\gamma^\mu u_\uparrow(p_1) &&= && 2E(0,-1,-i,0) && (19)\\
&\mathrm{e}^+_\mathrm{R}\mathrm{e}^-_\mathrm{R}\ : && \overline{v}_\uparrow(p_2)\gamma^\mu u_\uparrow(p_1) &&= && (0,0,0,0) && (20)\\
&\mathrm{e}^+_\mathrm{L}\mathrm{e}^-_\mathrm{L}\ : && \overline{v}_\downarrow(p_2)\gamma^\mu u_\downarrow(p_1) &&= && (0,0,0,0) && (21)\\
&\mathrm{e}^+_\mathrm{R}\mathrm{e}^-_\mathrm{L}\ : && \overline{v}_\uparrow(p_2)\gamma^\mu u_\downarrow(p_1) &&= && 2E(0,-1,i,0) && (22)
\end{aligned}$$

The electron current is non-zero only if the e^+ and e^- have opposite helicity, as expected from helicity conservation.

4.5 Matrix Element Calculation

The matrix element M_fi is proportional to the scalar product of the electron current 4-vectors j_e of Equations (19)-(22) with the muon current 4-vectors j_μ of Equations (8)-(11):

$$M_\mathrm{fi} = -\frac{e^2}{s}(j_e.j_\mu)\ . \tag{2$'$}$$

This scalar product is non-zero for only four of the 16 possible helicity configurations:

$$\mathrm{e}^-_\mathrm{R}\mathrm{e}^+_\mathrm{L} \to \mu^-_\mathrm{R}\mu^+_\mathrm{L}\ :\quad M_\mathrm{RR} \propto\ 2E(0,-1,-i,0)\cdot 2E(0,-\cos\theta,i,\sin\theta) \tag{23}$$
$$\mathrm{e}^-_\mathrm{R}\mathrm{e}^+_\mathrm{L} \to \mu^-_\mathrm{L}\mu^+_\mathrm{R}\ :\quad M_\mathrm{RL} \propto\ 2E(0,-1,-i,0)\cdot 2E(0,-\cos\theta,-i,\sin\theta) \tag{24}$$
$$\mathrm{e}^-_\mathrm{L}\mathrm{e}^+_\mathrm{R} \to \mu^-_\mathrm{R}\mu^+_\mathrm{L}\ :\quad M_\mathrm{LR} \propto\ 2E(0,-1,i,0)\cdot 2E(0,-\cos\theta,i,\sin\theta) \tag{25}$$
$$\mathrm{e}^-_\mathrm{L}\mathrm{e}^+_\mathrm{R} \to \mu^-_\mathrm{L}\mu^+_\mathrm{R}\ :\quad M_\mathrm{LL} \propto\ 2E(0,-1,i,0)\cdot 2E(0,-\cos\theta,-i,\sin\theta)\ . \tag{26}$$

Here, the first suffix on the matrix elements $M_{\rm IJ}$ labels the helicity of the e^- and the second labels the helicity of the μ^-. For the process $\mathrm{e}^-_{\rm L}\mathrm{e}^+_{\rm R} \to \mu^-_{\rm L}\mu^+_{\rm R}$ of Equation (26) for example, where the e^- and μ^- are both left-handed, the matrix element is

$$\begin{aligned} M_{\rm LL} &= -\frac{e^2}{s}\left[2E(0,-1,i,0)\cdot 2E(0,-\cos\theta,-i,\sin\theta)\right] \\ &= -\frac{e^2}{s}\cdot 4E^2(-\cos\theta-1)\ . \end{aligned}$$

The sum of the initial four-momenta is $p_1+p_2=(2E,0,0,0)$, so that $s=(p_1+p_2)^2=4E^2$. Hence

$$M_{\rm LL} = e^2(1+\cos\theta)\ .$$

The matrix element squared is therefore

$$|M_{\rm LL}|^2 = (4\pi\alpha)^2(1+\cos\theta)^2$$

where $\alpha = e^2/4\pi \approx 1/137$ is the fine structure constant. The matrix elements for the remaining helicity configurations, Equations (23)-(26), can be evaluated similarly, giving

$$|M_{\rm LL}|^2 = |M_{\rm RR}|^2 = (4\pi\alpha)^2(1+\cos\theta)^2 \tag{27}$$

$$|M_{\rm LR}|^2 = |M_{\rm RL}|^2 = (4\pi\alpha)^2(1-\cos\theta)^2\ . \tag{28}$$

From Equation (7), the corresponding differential cross sections are then

$$\frac{\mathrm{d}\sigma_{\rm LL}}{\mathrm{d}\Omega} = \frac{\mathrm{d}\sigma_{\rm RR}}{\mathrm{d}\Omega} = \frac{\alpha^2}{4s}(1+\cos\theta)^2 \tag{29}$$

$$\frac{\mathrm{d}\sigma_{\rm LR}}{\mathrm{d}\Omega} = \frac{\mathrm{d}\sigma_{\rm RL}}{\mathrm{d}\Omega} = \frac{\alpha^2}{4s}(1-\cos\theta)^2\ . \tag{30}$$

The total cross sections are obtained by integrating over θ and ϕ using

$$\int(1\pm\cos\theta)^2\mathrm{d}\Omega = 2\pi\int_{-1}^{+1}(1\pm\cos\theta)^2\mathrm{d}\cos\theta = \frac{16\pi}{3}\ .$$

This gives

$$\boxed{\sigma_{\rm LL}=\sigma_{\rm RR}=\sigma_{\rm LR}=\sigma_{\rm RL}=\frac{4\pi\alpha^2}{3s}}\ .$$

Note that, in $\mathrm{e}^+\mathrm{e}^-$ annihilation, the propagator factor $1/q^2 = 1/(p_1+p_2)^2 = 1/4E^2$ in the matrix element is a finite constant, leading to a total cross section which is also finite. This is in contrast to the case of elastic scattering processes such as $\mathrm{e}^-\mu^- \to \mathrm{e}^-\mu^-$, to be considered shortly, where the propagator factor will result in a cross section which is formally infinite.

The $(1\pm\cos\theta)^2$ angular dependences found above can be understood simply in terms of $S=1$ spin wavefunctions and Part 1B Quantum Mechanics (see Section 4.8 below).

4.6 Unpolarised $\mathrm{e^+e^-} \to \mu^+\mu^-$ Cross Section

Equations (29) and (30) represent the differential cross sections for the scattering of a polarised (purely left-handed or purely right-handed) beam of electrons from a polarised beam of positrons, into a final state where the μ^+ and μ^- both have a definite polarisation. Although polarised $\mathrm{e}^\pm$ beams can indeed be produced (about 80% polarisation is achieved for the electron beam at SLAC for example), the more typical situation (as at LEP for example) is that the e^+ and e^- beams are both *unpolarised, i.e.* effectively an equal mix of left-handed and right-handed particles. Usually, also, experiments are insensitive to (*i.e.* cannot determine) the polarisation of the outgoing μ^+ and μ^-.

Typically therefore, the cross section of relevance to experiments is that where all initial state particles are unpolarised and all final state polarisations are counted without discrimination. This cross section is calculated by taking an *average* over the possible spin states of the initial-state particles and a *sum* over the possible spin states of the final-state particles. We thus need to consider the *spin-averaged matrix element squared* $\langle|M_{\mathrm{fi}}|^2\rangle$ given by

$$\langle|M_{\mathrm{fi}}|^2\rangle = \tfrac{1}{2}\cdot\tfrac{1}{2}\cdot\left(|M_{\mathrm{RR}}|^2 + |M_{\mathrm{LR}}|^2 + |M_{\mathrm{RL}}|^2 + |M_{\mathrm{LL}}|^2\right)$$

where the first factor of $\frac{1}{2}$ averages over the e^+ spins and the second averages over the e^- spins [6].

From Equations (27) and (28), we obtain

$$\begin{aligned}\langle|M_{\mathrm{fi}}|^2\rangle &= \tfrac{1}{4}(4\pi\alpha)^2\left[2(1+\cos\theta)^2 + 2(1-\cos\theta)^2\right] \\ &= (4\pi\alpha)^2(1+\cos^2\theta)\ .\end{aligned}$$

The differential cross section is then given by substituting into Equation (7):

$$\frac{\mathrm{d}\sigma}{\mathrm{d}\Omega} = \frac{1}{64\pi^2 s}(4\pi\alpha)^2(1+\cos^2\theta)\ .$$

Hence, for unpolarised high energy $\mathrm{e^+e^-} \to \mu^+\mu^-$ annihilation in the centre of mass frame, we obtain

$$\boxed{\frac{\mathrm{d}\sigma}{\mathrm{d}\Omega} = \frac{\alpha^2}{4s}(1+\cos^2\theta)} \tag{31}$$

where θ is the direction of the outgoing μ^- with respect to the incoming e^- direction.

The total unpolarised $\mathrm{e^+e^-} \to \mu^+\mu^-$ QED cross section is obtained by integrating over θ and ϕ using $\int(1+\cos^2\theta)\,\mathrm{d}\Omega = 2\pi\int(1+\cos^2\theta)\,\mathrm{d}\cos\theta = \frac{4}{3}\pi$:

$$\boxed{\sigma(\mathrm{e^+e^-} \to \mu^+\mu^-) = \frac{4\pi\alpha^2}{3s}}\ , \tag{32}$$

which is also just $\sigma = \frac{1}{2}\cdot\frac{1}{2}\cdot(\sigma_{\mathrm{LL}} + \sigma_{\mathrm{LR}} + \sigma_{\mathrm{RL}} + \sigma_{\mathrm{RR}})$.

[6] Note that the rule that matrix elements (amplitudes) should first be summed and then squared, $\sigma \propto |M_1 + M_2 + \ldots|^2$, is not appropriate here. This formalism applies when two or more amplitudes describing exactly the same overall process are to be combined. Instead, in the case being considered here, the quantity $\langle|M_{\mathrm{fi}}|^2\rangle$ should be thought of as an average over four completely separate processes distinguished by their different initial and final spin states: $\mathrm{e^-_R e^+_L} \to \mu^-_{\mathrm{R}}\mu^+_{\mathrm{L}}$, $\mathrm{e^-_R e^+_L} \to \mu^-_{\mathrm{L}}\mu^+_{\mathrm{R}}$, $\mathrm{e^-_L e^+_R} \to \mu^-_{\mathrm{R}}\mu^+_{\mathrm{L}}$, $\mathrm{e^-_L e^+_R} \to \mu^-_{\mathrm{L}}\mu^+_{\mathrm{R}}$.

In leading-order QED, the four helicity combinations RR, RL, LR, LL combine together with equal strength, resulting in the symmetric $(1 + \cos^2\theta)$ angular distribution of Equation (31). For the weak interactions, where the virtual photon is replaced by a virtual Z^0, we shall find that the left- and right-handed cross sections have different magnitudes as a consequence of parity violation, resulting in an asymmetric angular distribution [7].

4.7 $\mathrm{e}^+\mathrm{e}^- \to$ hadrons

The total and differential cross section formulae derived above for $\mathrm{e}^+\mathrm{e}^- \to \mu^+\mu^-$ apply equally well to the case $\mathrm{e}^+\mathrm{e}^- \to \mathrm{q}\overline{\mathrm{q}}$, where the final state is a quark-antiquark pair, except that an additional factor of e_q^2 is needed to account for the (fractional) electric charge e_q of the quark and an additional factor of $N_\mathrm{c} = 3$ is needed to account for the fact that each quark comes in three colours. In this case, the total spin-averaged cross section of Equation (32) becomes

$$\sigma(\mathrm{e}^+\mathrm{e}^- \to \mathrm{q}\overline{\mathrm{q}}) = 3e_q^2 \, \frac{4\pi\alpha^2}{3s} \; .$$

The quark and antiquark are not detected as free particles but instead *fragment* or *hadronise* into separate collimated *jets* of hadronic particles which are approximately back-to-back in the centre of mass frame. A quark (or antiquark) of energy 20 GeV for example produces a hadronic jet containing on average about 7-8 long-lived charged particles (mainly $\pi^\pm$ but also some $\mathrm{K}^\pm$, p, $\overline{\mathrm{p}}$, $\mathrm{e}^\pm$, $\mu^\pm$) plus a similar number of neutral particles (mainly photons from $\pi^0 \to \gamma\gamma$ decays but also some K^0, $\overline{\mathrm{K}}^0$, n, $\overline{\mathrm{n}}$). Gluon radiation from the quark or antiquark can result in additional jets.

The jets produced by the different flavours of quark (u, d, s, c, b) [8] have very similar properties, so that in practice it is difficult to measure the cross sections for each quark flavour separately [9]. Instead, what is usually measured is the combined cross section into all possible hadronic final states:

$$\sigma(\mathrm{e}^+\mathrm{e}^- \to \text{hadrons}) = \sum_q \sigma(\mathrm{e}^+\mathrm{e}^- \to \mathrm{q}\overline{\mathrm{q}}) = 3\left(\sum_q e_q^2\right)\frac{4\pi\alpha^2}{3s}$$

where the sum runs over all quark flavours which are light enough to be produced at the given centre of mass energy (*i.e.* all quark flavours for which $m_q < \frac{1}{2}\sqrt{s}$).

A very useful quantity is the ratio R of hadronic to muonic cross sections:

$$\boxed{R \equiv \frac{\sigma(\mathrm{e}^+\mathrm{e}^- \to \text{hadrons})}{\sigma(\mathrm{e}^+\mathrm{e}^- \to \mu^+\mu^-)} = 3\sum_q e_q^2} \; . \tag{33}$$

[7] It should be noted however that an asymmetric angular distribution does not necessarily imply the existence of parity violation. At higher order in perturbation theory, for example, pure QED, which is parity-conserving, also predicts a slightly asymmetric angular distribution.

[8] Due to its large mass, the top quark t has a very short lifetime and decays (dominantly via $\mathrm{t} \to \mathrm{W}^+ + \mathrm{b}$) before it can form hadrons.

[9] A noticeable exception is the b quark, where high purity samples can be obtained by resolving the short (few mm) decay path of weakly-decaying B hadrons. This requires the use of silicon detectors, which provide excellent spatial resolution of order $10\ \mu\mathrm{m}$. To a lesser extent, this works also for charm quark jets.

Experimentally, this has the advantage that the incoming e^+ and e^- fluxes, which can be difficult to determine precisely, cancel in the ratio. Equation (33) shows that the ratio R is expected to be a constant, with step increases occurring whenever an energy threshold corresponding to the production of a new flavour of quark is crossed. For example, for centre of mass energies in the range $\sqrt{s} \approx 3 - 10\,\mathrm{GeV}$ it is possible to produce $\mathrm{u\overline{u}}$, $\mathrm{d\overline{d}}$, $\mathrm{s\overline{s}}$ and $\mathrm{c\overline{c}}$ (but not $\mathrm{b\overline{b}}$ or $\mathrm{t\overline{t}}$) final states, giving the expectation

$$R = 3\left[(2/3)^2 + (1/3)^2 + (1/3)^2 + (2/3)^2\right] = 10/3 \qquad (\sqrt{s} \approx 3 - 10\,\mathrm{GeV})\,.$$

Above the $\mathrm{b\overline{b}}$ threshold at $\sqrt{s} \approx 10\,\mathrm{GeV}$ and below the top quark threshold at $\sqrt{s} \approx 350\,\mathrm{GeV}$, we expect R to increase to

$$R = 3\left[(2/3)^2 + (1/3)^2 + (1/3)^2 + (2/3)^2 + (1/3)^2\right] = 11/3 \qquad (\sqrt{s} \approx 10 - 350\,\mathrm{GeV})\,.$$

4.8 Part 1B Quantum Mechanics (non-examinable)

The angular distributions $\frac{1}{4}(1 \pm \cos\theta)^2$ found above for the individual RR, RL, LR, LL cross sections can be understood simply in terms of the quantum mechanics of $S = 1$ spin wavefunctions.

We denote the eigenstates of a general spin operator $\boldsymbol{S} = (S_x, S_y, S_z)$ by $|s, m\rangle$ where

$$S_z\,|s,m\rangle = m\hbar\,|s,m\rangle\,; \qquad S^2\,|s,m\rangle = s(s+1)\hbar^2\,|s,m\rangle\ .$$

For a system consisting of two spin $\frac{1}{2}$ particles, the total spin operator $\boldsymbol{S} = \boldsymbol{S}_1 + \boldsymbol{S}_2$ has four possible eigenstates, namely a triplet of states with $S = 1$ and a singlet with $S = 0$:

$$|S, m_S\rangle = \quad |1,1\rangle\,; \quad |1,0\rangle\,; \quad |1,-1\rangle\,; \quad |0,0\rangle\ .$$

These are eigenstates of $S_z = (S_1)_z + (S_2)_z$ such that (with $\hbar = 1$):

$$S_z\,|1,1\rangle = |1,1\rangle\,; \quad S_z\,|1,0\rangle = 0; \quad S_z\,|1,-1\rangle = -\,|1,-1\rangle\,; \quad S_z\,|0,0\rangle = 0\,.$$

In the case of $\mathrm{e^+e^-} \to \mu^+\mu^-$ scattering, helicity conservation in QED forbids the total spin states $|1,0\rangle$ and $|0,0\rangle$ in both the initial and final states. For M_{RR} for example, the total spin of the $\mathrm{e^+e^-}$ initial state was restricted to be $S_z = +1$ aligned along the e^- direction (the z-axis) while the $\mu^+\mu^-$ final state was required to have a total spin projection of $+1$ along the μ^- direction. We are therefore led to consider the probability

$$P = |\langle\psi|1,1\rangle|^2$$

that an initial state $|1,1\rangle$ with spin component $+1$ along the z-axis becomes a final state $|\psi\rangle \equiv |1,1\rangle_\theta$ with spin component $+1$ along the direction $\hat{\boldsymbol{n}} = (\sin\theta, 0, \cos\theta)$. By definition, the state $|\psi\rangle$ is an eigenstate of $\hat{\boldsymbol{n}}.\boldsymbol{S}$ with eigenvalue $+1$:

$$(\hat{\boldsymbol{n}}.\boldsymbol{S})\,|\psi\rangle = (\sin\theta\, S_x + \cos\theta\, S_z)\,|\psi\rangle = |\psi\rangle \tag{34}$$

Schematically, the states $|1,1\rangle$ and $|\psi\rangle \equiv |1,1\rangle_\theta$ can be represented as:

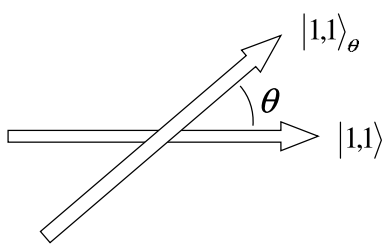

The state $|\psi\rangle = |1,1\rangle_\theta$ can be expressed as a linear combination of the $\theta = 0$ eigenstates:

$$|\psi\rangle = \alpha\,|1,1\rangle + \beta\,|1,0\rangle + \gamma\,|1,-1\rangle \tag{35}$$

where α, β and γ are unknown constants, to be determined, satisfying

$$|\alpha|^2 + |\beta|^2 + |\gamma|^2 = 1\ . \tag{36}$$

Equation (34) then becomes

$$(\sin\theta S_x + \cos\theta S_z)\left(\alpha\,|1,1\rangle + \beta\,|1,0\rangle + \gamma\,|1,-1\rangle\right) = \alpha\,|1,1\rangle + \beta\,|1,0\rangle + \gamma\,|1,-1\rangle\ . \tag{37}$$

The effect of the operator S_x on the states $|1,1\rangle$, $|1,0\rangle$, $|1,-1\rangle$ is most easily determined by introducing the ladder operators $\widehat{S}_\pm \equiv \widehat{S}_x \pm i\widehat{S}_y$ which, for spin 1, have the properties

$$\begin{array}{lll} S_+|1,1\rangle = 0 & S_+|1,0\rangle = \sqrt{2}|1,1\rangle & S_+|1,-1\rangle = \sqrt{2}|1,0\rangle \\ S_-|1,1\rangle = \sqrt{2}|1,0\rangle & S_-|1,0\rangle = \sqrt{2}|1,-1\rangle & S_-|1,-1\rangle = 0\ . \end{array}$$

Since $S_x = \frac{1}{2}(S_+ + S_-)$, we readily find

$$\begin{aligned} S_x\,|1,1\rangle = &\quad \tfrac{1}{2}(S_+ + S_-)\,|1,1\rangle &&= \frac{1}{\sqrt{2}}\,|1,0\rangle \\ S_x\,|1,0\rangle = &\quad \tfrac{1}{2}(S_+ + S_-)\,|1,0\rangle &&= \frac{1}{\sqrt{2}}\,|1,1\rangle + \frac{1}{\sqrt{2}}\,|1,-1\rangle \\ S_x\,|1,-1\rangle = &\quad \tfrac{1}{2}(S_+ + S_-)\,|1,-1\rangle &&= \frac{1}{\sqrt{2}}\,|1,0\rangle\ . \end{aligned}$$

Substitution into Equation (37) then gives

$$\begin{aligned} \sin\theta\Big[\frac{\alpha}{\sqrt{2}}\,|1,0\rangle + \frac{\beta}{\sqrt{2}}\,|1,1\rangle + \frac{\beta}{\sqrt{2}}\,|1,-1\rangle + \frac{\gamma}{\sqrt{2}}\,|1,0\rangle\Big] \\ + \cos\theta\Big[\alpha\,|1,1\rangle - \gamma\,|1,-1\rangle\Big] = \alpha\,|1,1\rangle + \beta\,|1,0\rangle + \gamma\,|1,-1\rangle\ . \end{aligned}$$

Equating the coefficients of $|1,1\rangle$, $|1,0\rangle$ and $|1,-1\rangle$ on both sides of the above equation gives

$$\begin{aligned} \frac{\sin\theta}{\sqrt{2}}\beta + \cos\theta.\alpha &= \alpha \\ \frac{\sin\theta}{\sqrt{2}}(\alpha+\gamma) &= \beta \\ \frac{\sin\theta}{\sqrt{2}}\beta - \cos\theta.\gamma &= \gamma\ . \end{aligned}$$

After some straightforward algebra, these equations, together with Equation (36), can be solved to yield

$$\alpha = \frac{1}{2}(1+\cos\theta) \qquad \beta = \frac{1}{\sqrt{2}}\sin\theta \qquad \gamma = \frac{1}{2}(1-\cos\theta)\ .$$

From Equation (35), the probability of a transition from the initial state $|1,1\rangle$ to the final state $|\psi\rangle = |1,1\rangle_\theta$ is therefore

$$\boxed{P = |\langle\psi|1,1\rangle|^2 = |\alpha|^2 = \tfrac{1}{4}(1+\cos\theta)^2}\,,$$

thereby reproducing the angular dependence found above for the $\mathrm{e}^+\mathrm{e}^- \to \mu^+\mu^-$ cross sections corresponding to M_{LL} and M_{RR}. Similar considerations apply to M_{LR} and M_{RL}, where the probability is given by $|\gamma^2| = \frac{1}{4}(1-\cos\theta)^2$.

For future reference ($\mathrm{W}^\pm$ decay), we note also that for the initial state $|1,0\rangle$, the probability of a transition to the final state $|\psi\rangle = |1,1\rangle_\theta$ is

$$\boxed{P = |\langle\psi|1,0\rangle|^2 = |\beta|^2 = \tfrac{1}{2}\sin^2\theta}\,.$$

The coefficients α, β, γ are particular examples of what are more generally known as *rotation matrices*, $d^j_{m'm}(\theta)$. In this notation, the results above correspond to

$$d^1_{11} = \frac{1}{2}(1+\cos\theta), \qquad d^1_{1,-1} = \frac{1}{2}(1-\cos\theta), \qquad d^1_{01} = \frac{1}{\sqrt{2}}\sin\theta\ .$$

5 Electron-Proton Scattering

The central theme of this handout is the investigation of the internal structure of the proton and neutron via high energy electron-nucleon (or muon-nucleon) scattering. In these processes, a high q^2 virtual photon is used to probe the structure of the nucleon down to scales of the order of the photon wavelength. Length scales of order $10^{-18}\,\mathrm{m}$ are accessible in current experiments.

We proceed via the following steps:

1) Derive the Lorentz-invariant cross section for the high energy *elastic* scattering of two non-identical, massless, *pointlike* spin-half particles ($\mathrm{e}^-\mu^- \to \mathrm{e}^-\mu^-$ scattering, for example). This cross section will subsequently be used to describe high energy electron-quark elastic scattering $\mathrm{e}^-\mathrm{q} \to \mathrm{e}^-\mathrm{q}$;

2) Derive the cross section for electron-proton elastic scattering $\mathrm{e}^-\mathrm{p} \to \mathrm{e}^-\mathrm{p}$ in the laboratory frame, with the proton target at rest, initially treating the proton as a pointlike particle and subsequently taking the *finite size* of the proton into account;

3) Combine the results from 1) and 2) to obtain the cross section for high q^2 *deep-inelastic scattering* $\mathrm{e}^-\mathrm{p} \to \mathrm{e}^-\mathrm{X}$, where the proton breaks up into a hadronic system X after the collision. Deep-inelastic scattering reveals the existence of pointlike quark constituents inside the nucleon and allows their quantum numbers and momentum fractions to be investigated.

5.1 High Energy Elastic Scattering

In leading-order QED, the elastic scattering of two non-identical, pointlike, spin $\frac{1}{2}$ particles, exemplified by the process $\mathrm{e}^-\mu^- \to \mathrm{e}^-\mu^-$, proceeds via a single Feynman diagram:

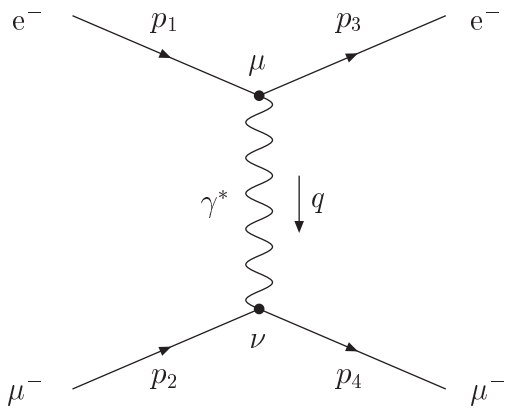

In the relativistic limit, where all particle masses can be neglected, the Lorentz invariant matrix element for this process was shown in the lectures and in the examples sheet to be given by

$$\langle |M_{\rm fi}|^2 \rangle = \frac{8e^4}{(p_1 - p_3)^4} \left[(p_1.p_2)(p_3.p_4) + (p_1.p_4)(p_2.p_3) \right] \ . \tag{1}$$

In the centre of mass frame, taking the 4-momenta to be

$$p_1 = (E, 0, 0, E) \, , \qquad p_2 = (E, 0, 0, -E) \, , \qquad p_3 = (E, E \sin\theta^*, 0, E \cos\theta^*) \ ,$$

the corresponding differential cross section was found to be

$$\frac{{\rm d}\sigma}{{\rm d}\Omega^*} = \frac{2\alpha^2}{s} \frac{\left[1 + \frac{1}{4}(1 + \cos\theta^*)^2 \right]}{(1 - \cos\theta^*)^2} \tag{2}$$

where s is the centre of mass energy squared:

$$s = (p_1 + p_2)^2 = 2p_1.p_2 = 4E^2 \ . \tag{3}$$

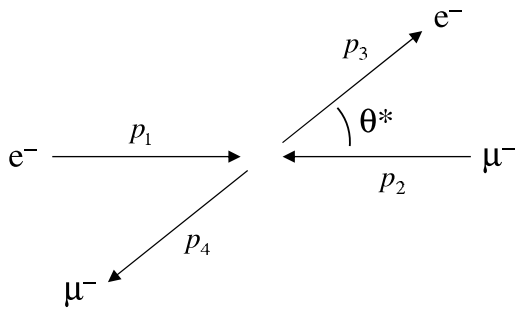

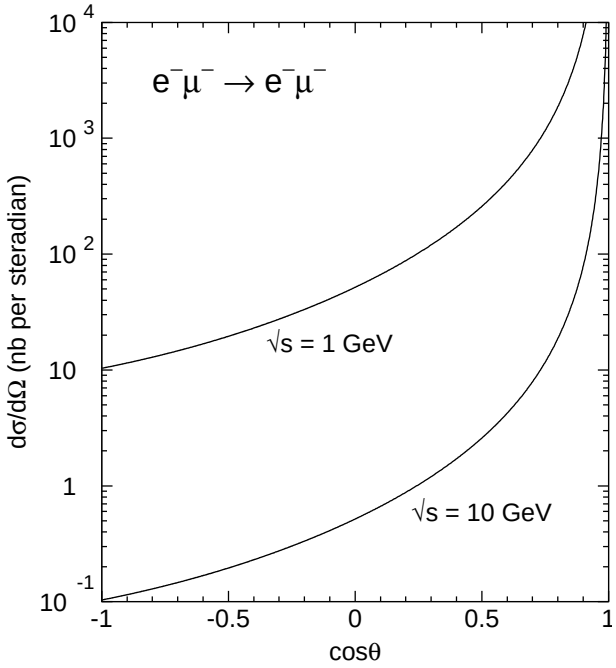

It was also shown that a Lorentz-invariant formulation of the above cross section, valid in any reference frame, is

$$\frac{{\rm d}\sigma}{{\rm d}q^2} = \frac{2\pi\alpha^2}{q^4} \left[1 + \left(1 + \frac{q^2}{s} \right)^2 \right] \ . \tag{4}$$

Here, the *four-momentum transfer* q (the four-momentum of the exchanged virtual photon) is

$$q = p_1 - p_3 = (E_1 - E_3, \boldsymbol{p}_1 - \boldsymbol{p}_3).$$

The *four-momentum transfer squared* is then given by [1]

$$q^2 = (p_1 - p_3)^2 = -2p_1.p_3 = -2E^2(1 - \cos\theta^*) \ . \tag{5}$$

[1]The quantity q^2 is identical to the Mandelstam variable t introduced in Handout 3.

A useful quantity for the description of high energy scattering is the dimensionless Lorentz invariant variable y defined as

$$\boxed{y \equiv \frac{p_2.q}{p_2.p_1}} \,. \tag{6}$$

In the centre of mass frame, the denominator in Equation (6) is

$$p_2.p_1 = 2E^2 \ ,$$

while the numerator is

$$p_2.q = p_2.p_1 - p_2.p_3 = 2E^2 - (E^2 + E^2\cos\theta^*) = E^2(1-\cos\theta^*) \ .$$

Hence y is directly related to the centre of mass scattering angle θ^*:

$$\boxed{y = \tfrac{1}{2}(1-\cos\theta^*)} \,, \tag{7}$$

and must clearly lie in the range $0 < y < 1$.

Combining Equations (3), (5) and (7), we immediately obtain, for elastic scattering,

$$q^2 = -sy \ . \tag{8}$$

In terms of y, the Lorentz invariant cross section of Equation (4) can be written as

$$\boxed{\frac{\mathrm{d}\sigma}{\mathrm{d}q^2} = \frac{1}{s}\frac{\mathrm{d}\sigma}{\mathrm{d}y} = \frac{2\pi\alpha^2}{q^4}\left[1+(1-y)^2\right]} \,. \tag{9}$$

The factor of $1/q^4$ in the above cross sections comes directly from the square of the photon propagator contribution, $-1/q^2 = 1/[2E^2(1-\cos\theta^*)]$, and gives a total cross section which is formally infinite. The scattering is dominated by virtual photon exchanges with low q^2 (*i.e.* low energy and/or low momentum transfer) and hence by small scattering angles θ^*. This is in contrast to the case of $\mathrm{e^+e^-}$ annihilation where the propagator factor $1/q^2 = 1/s$ was a finite constant ($= 1/4E^2$ in the centre of mass frame).

The factor $[1+(1-y)^2]$ appearing in the above cross section reflects the spin configurations which are allowed in the scattering. The constant term $(=1)$ arises from the isotropic component with total spin $S_z = 0$, while the $(1-y)^2 = \frac{1}{4}(1+\cos\theta^*)^2$ term arises from the component with $S_z = 1$.

In Section 5.6, the differential cross section of Eqn (9) will be applied directly to the description of electron-quark elastic scattering, $\mathrm{e^-q} \to \mathrm{e^-q}$.

5.2 Elastic Electron-Proton Scattering

When particle masses are taken into account, for example for $\mathrm{e}^-\mu^- \to \mathrm{e}^-\mu^-$ scattering with an e^- of mass m and μ^- of mass M, it is shown (optionally) in the examples sheet that the matrix element squared of Equation (1) generalises to

$$\langle |M_{\mathrm{fi}}|^2 \rangle = \frac{8e^4}{(p_1 - p_3)^4}\big[(p_1.p_2)(p_3.p_4) + (p_1.p_4)(p_2.p_3) - (p_1.p_3)M^2 - (p_2.p_4)m^2 + 2m^2M^2\big] \qquad (10)$$

where p_1 and p_3 are the initial and final 4-momenta of the particle of mass m ($m_1 = m_3 = m$) and p_2 and p_4 are the initial and final 4-momenta of the particle of mass M ($m_2 = m_4 = M$).

We now apply this result to elastic electron-proton scattering, $\mathrm{e}^-\mathrm{p} \to \mathrm{e}^-\mathrm{p}$, where the mass M of the proton can not be neglected. We work in the laboratory frame, with the proton at rest. The incoming electron, of mass m, is taken to have 4-momentum $p_1 = (E_1, \boldsymbol{p_1})$, while the target proton has 4-momentum $p_2 = (M, \mathbf{0})$.

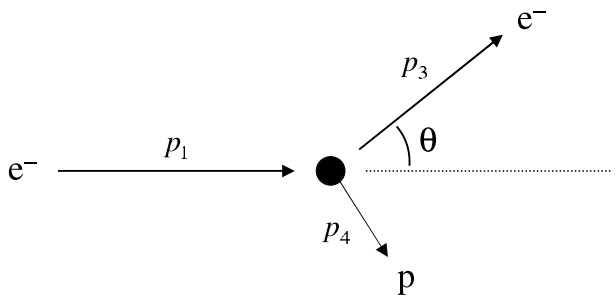

We consider two cases:

1) the low energy limit $|\boldsymbol{p}_1| \ll m$, where the recoil of the target proton can be neglected;

2) the high energy limit $E_1 \gg m$, where the electron mass can be neglected.

The proton will initially be treated as a pointlike particle, and the results subsequently extended to include the effects of proton structure.

5.2.1 Low Energy Elastic $\mathrm{e}^-\mathrm{p}$ Scattering (non-examinable)

In the lab frame, in the low energy limit where the recoil of the target proton can be neglected, the electron total momentum and energy are unchanged in the collision:

$$p = |\boldsymbol{p}_1| = |\boldsymbol{p}_3| \ll m; \qquad E = E_1 = E_3 \qquad (E^2 = p^2 + m^2)$$

and the electron and proton 4-momenta can be written:

$$p_1 = (E, \boldsymbol{p}_1); \qquad p_2 = (M, \mathbf{0}); \qquad p_3 = (E, \boldsymbol{p}_3); \qquad p_4 = (M, \mathbf{0})\ .$$

The scalar products appearing in Equation (10) are given by:

$$\begin{aligned} p_1.p_2 = p_1.p_4 = p_3.p_4 = p_2.p_3 &= ME \\ p_2.p_4 &= M^2 \\ p_1.p_3 = E^2 - |\boldsymbol{p}_1||\boldsymbol{p}_3|\cos\theta &= p^2 + m^2 - p^2\cos\theta \approx m^2 \\ (p_1 - p_3)^2 = (0, \boldsymbol{p}_1 - \boldsymbol{p}_3)^2 &= -(p^2 + p^2 - 2p^2\cos\theta) = -4p^2\sin^2\theta/2 \end{aligned}$$

Substituting into Equation (10):

$$\begin{aligned} \langle|M_{\rm fi}|^2\rangle &= \frac{8e^4}{16p^4\sin^4\theta/2}\left[ME\cdot ME + ME\cdot ME - m^2M^2 - M^2m^2 + 2m^2M^2\right] \\ &= \frac{e^4}{2p^4\sin^4\theta/2}\left[2M^2(p^2+m^2)\right] \\ &\approx \left(\frac{e^2Mm}{p^2\sin^2\theta/2}\right)^2 . \end{aligned} \tag{11}$$

In Handout 3, it was shown that the differential cross section for the scattering process $1+2\to 3+4$ is

$$\frac{{\rm d}\sigma}{{\rm d}\Omega} = \frac{1}{64\pi^2}\frac{1}{p_1M}\frac{p_3^2\,\langle|M_{\rm fi}|^2\rangle}{p_3(E_1+M) - E_3p_1\cos\theta}$$

where $p_1 = |\boldsymbol{p}_1|$ and $p_3 = |\boldsymbol{p}_3|$. In this case, we have $p_1 = p_3 = p$ and hence

$$\begin{aligned} \frac{{\rm d}\sigma}{{\rm d}\Omega} &= \frac{1}{64\pi^2}\frac{1}{pM}\frac{p^2}{p(E+M) - Ep\cos\theta}\langle|M_{\rm fi}|^2\rangle \\ &= \frac{1}{64\pi^2M}\frac{1}{E+M-E\cos\theta}\langle|M_{\rm fi}|^2\rangle . \end{aligned}$$

With $p \ll m$ we have $E = \sqrt{p^2+m^2} \approx m$. For negligible proton recoil, we must also have $m \ll M$ (which is clearly valid for the electron and proton). Hence we can also take $E \ll M$, giving

$$\frac{{\rm d}\sigma}{{\rm d}\Omega} \approx \frac{1}{64\pi^2M^2}\langle|M_{\rm fi}|^2\rangle .$$

Substituting for $\langle|M_{\rm fi}|^2\rangle$ from Equation (11) gives

$$\frac{{\rm d}\sigma}{{\rm d}\Omega} = \frac{1}{64\pi^2M^2}\left(\frac{e^2Mm}{p^2\sin^2\theta/2}\right)^2$$

At very low energy, we have $p^2 = 2mE'$ where E' is the electron kinetic energy ($p = mv, E' = \frac{1}{2}mv^2$). Also $e^2 = 4\pi\alpha$ with $\alpha \approx 1/137$ the fine structure constant, giving finally

$$\boxed{\frac{{\rm d}\sigma}{{\rm d}\Omega} = \left(\frac{\alpha}{4E'\sin^2\theta/2}\right)^2}$$

Thus, in the low energy limit, we obtain the classical *Rutherford scattering* cross section.

As is well known, the Rutherford cross section describes the scattering of two pointlike charged particles with zero spin, and thus with no intrinsic magnetic moment. The fact that, at very low energies, the Rutherford cross section is also obtained for the scattering of spin $\frac{1}{2}$ Dirac particles shows that, in this limit, the intrinsic magnetic moment of a spin $\frac{1}{2}$ particle plays no role; only the *charge* of the particle matters.

5.2.2 High Energy Elastic $e^- p$ Scattering

We now consider elastic $e^- p \to e^- p$ scattering in the lab frame in the high energy limit $p_1 \gg m$ where the electron mass can effectively be neglected:

$$p_1 = (E_1, \boldsymbol{p}_1); \qquad p_2 = (M, \mathbf{0}); \qquad p_3 = (E_3, \boldsymbol{p}_3); \qquad p_4 = (E_4, \boldsymbol{p}_4)$$

with

$$m_1 = m_3 = 0; \qquad m_2 = m_4 = M; \qquad E_1 = |\boldsymbol{p}_1|; \qquad E_3 = |\boldsymbol{p}_3|$$

In this limit, the matrix element of Equation (10) becomes

$$\langle |M_{\rm fi}|^2 \rangle = \frac{8e^4}{(p_1 - p_3)^4} \left[(p_1.p_2)(p_3.p_4) + (p_1.p_4)(p_2.p_3) - (p_1.p_3)M^2 \right] . \tag{12}$$

The 4-vector scalar products on the right-hand side of this equation which do not involve p_4 are given by:

$$\begin{aligned} p_1.p_2 &= E_1 M & p_1.p_3 &= E_1 E_3 - |\boldsymbol{p}_1||\boldsymbol{p}_3| \cos\theta \\ p_2.p_3 &= E_3 M & &= E_1 E_3 (1 - \cos\theta) . \end{aligned}$$

Using energy-momentum conservation, $p_1 + p_2 = p_3 + p_4$, the scalar products involving p_4 can then be evaluated as

$$\begin{aligned} p_3.p_4 &= p_3.(p_1 + p_2 - p_3) = p_3.p_1 + p_3.p_2 = E_1 E_3 (1 - \cos\theta) + E_3 M \\ p_1.p_4 &= p_1.(p_1 + p_2 - p_3) = p_1.p_2 - p_1.p_3 = E_1 M - E_1 E_3 (1 - \cos\theta) . \end{aligned}$$

The square bracket on the right-hand side of Equation (12) is then

$$\begin{aligned} &(p_1.p_2)(p_3.p_4) + (p_1.p_4)(p_2.p_3) - (p_1.p_3)M^2 \\ &\quad = E_1 M \cdot E_3 (E_1 + M - E_1 \cos\theta) + E_3 M \cdot E_1 (M - E_3 + E_3 \cos\theta) - E_1 E_3 (1 - \cos\theta) \cdot M^2 \\ &\quad = M E_1 E_3 \left[(E_1 + M - E_1 \cos\theta) + (M - E_3 + E_3 \cos\theta) - M(1 - \cos\theta) \right] \\ &\quad = M E_1 E_3 \left[(E_1 - E_3)(1 - \cos\theta) + M(1 + \cos\theta) \right] \\ &\quad = 2M E_1 E_3 \left[(E_1 - E_3) \sin^2\theta/2 + M \cos^2\theta/2 \right] . \end{aligned} \tag{13}$$

It remains to evaluate $q^4 = (p_1 - p_3)^4$ in Equation (12). Neglecting the electron mass, we have $p_1^2 = p_3^2 = 0$, and hence

$$q^2 = (p_1 - p_3)^2 = -2 p_1.p_3 = -2 E_1 E_3 (1 - \cos\theta) \tag{14}$$

$$= -4 E_1 E_3 \sin^2\theta/2 . \tag{15}$$

The energy transfer $E_1 - E_3$ appearing in Equation (13) can be expressed in terms of Lorentz-invariant quantities:

$$p_2.q = p_2.p_1 - p_2.p_3 = M(E_1 - E_3) . \tag{16}$$

Since $p_1 + p_2 = p_3 + p_4$, the 4-momentum transfer q can be written also as $q = p_4 - p_2$. Squaring the equation $q + p_2 = p_4$, noting that $p_2^2 = p_4^2 = M^2$, then gives

$$q^2 + 2 p_2.q = 0 . \tag{17}$$

Combining Equations (16) and (17) then gives

$$E_1 - E_3 = -\frac{q^2}{2M} \, . \tag{18}$$

Since, from Equation (15), q^2 is always negative, we must have $E_3 < E_1$, so that, as expected, the scattered electron always has lower energy than the incoming electron.

Substituting Equations (13), (15) and (18) into Equation (12), the invariant matrix element becomes

$$\begin{aligned} \langle |M_{\rm fi}|^2 \rangle &= \frac{8e^4}{16E_1^2 E_3^2 \sin^4\theta/2} \cdot 2ME_1E_3 \left(M\cos^2\theta/2 - \frac{q^2}{2M}\sin^2\theta/2 \right) \\ &= \frac{e^4M^2}{E_1E_3\sin^4\theta/2} \left(\cos^2\theta/2 - \frac{q^2}{2M^2}\sin^2\theta/2 \right) \, . \end{aligned} \tag{19}$$

In the high energy limit where the mass of the electron can be neglected ($E_1 \gg m$), the differential cross section in the lab frame is given by [2]

$$\frac{{\rm d}\sigma}{{\rm d}\Omega} = \frac{1}{64\pi^2} \left(\frac{E_3}{E_1 M} \right)^2 \langle |M_{\rm fi}|^2 \rangle \, .$$

Substituting the matrix element of Equation (19), we finally obtain, for high energy ($E_1 \gg m$) $\mathrm{e^-p} \to \mathrm{e^-p}$ scattering in the lab frame (assuming for now a pointlike Dirac proton):

$$\boxed{\frac{{\rm d}\sigma}{{\rm d}\Omega} = \frac{\alpha^2}{4E_1^2\sin^4\theta/2} \frac{E_3}{E_1} \left(\cos^2\theta/2 - \frac{q^2}{2M^2}\sin^2\theta/2 \right)} \tag{20}$$

where $\alpha = e^2/4\pi \approx 1/137$ is the fine structure constant.

It should be emphasised that the differential cross section above depends on only a single independent variable, θ say. Once θ is given, the quantities E_3 and q^2 appearing in Equation (20) are determined via a combination of Equations (14) and (18). Equating the two expressions for q^2 in these equations gives

$$-2M(E_1 - E_3) = -2E_1E_3(1 - \cos\theta)$$

which can be rearranged to give E_3 in terms of $\cos\theta$:

$$\frac{E_3}{E_1} = \frac{M}{M + E_1(1 - \cos\theta)} \, , \tag{21}$$

(a result already derived in Equation (35) of Handout 3). The dependence of q^2 on θ can then be found by substituting for E_3 in Equation (14):

$$q^2 = -\frac{2ME_1^2(1 - \cos\theta)}{M + E_1(1 - \cos\theta)} \, . \tag{22}$$

[2] See Equation (39) of Handout 3.

5.3 Interpretation of the Cross Section Result

The high energy $\mathrm{e^-p} \to \mathrm{e^-p}$ cross section, Equation (20), is seen to be the product of a Rutherford-like scattering cross section and some additional factors:

$$\frac{\mathrm{d}\sigma}{\mathrm{d}\Omega} = \frac{\alpha^2}{4E_1^2 \sin^4 \theta/2} \frac{E_3}{E_1} \left(\cos^2 \theta/2 - \frac{q^2}{2M^2} \sin^2 \theta/2 \right) \ . \qquad (20)'$$

The factor E_3/E_1 can be identified as being due to the target recoil since, in the limit where the recoil is neglected, we have $E_3 = E_1$. In general, from Equation (21), the ratio E_3/E_1 is seen to be close to unity at small scattering angles $(\theta \to 0)$ where the target recoil is small and to become smaller as θ increases, falling to $E_3/E_1 \approx M/2E_1$ at large scattering angles, $\theta \to \pi$, where the target recoil is a maximum.

The $\mathrm{e^-p} \to \mathrm{e^-p}$ cross section of Equation (20) represents scattering from a pointlike, spin $\frac{1}{2}$, Dirac proton. Such a proton would have an intrinsic magnetic moment of magnitude $e/2M = e/2m_p$, *i.e.* $\mu = 1$ in units of the nuclear magneton μ_N. If the spin $\frac{1}{2}$ target proton is replaced by a spin 0 target particle, it can be shown that the differential cross section is given by Equation (20) with the $\sin^2 \theta/2$ term omitted:

$$\left(\frac{\mathrm{d}\sigma}{\mathrm{d}\Omega} \right)_{\text{spin 0}} = \frac{\alpha^2}{4E_1^2 \sin^4 \theta/2} \frac{E_3}{E_1} \cos^2 \theta/2 \ . \qquad (23)$$

Since a spin 0 particle possesses no intrinsic magnetic dipole moment, the $\sin^2 \theta/2$ term in Equation (20) must be due to scattering from the intrinsic magnetic dipole moment of the spin $\frac{1}{2}$ target proton. The $\cos^2 \theta/2$ term, common to both Equation (20) and Equation (23), must be due to scattering from the proton's electric charge.

Examples of the cross sections $\mathrm{d}\sigma/\mathrm{d}\Omega$ and $\mathrm{d}\sigma/\mathrm{d}\Omega_{\text{spin 0}}$ predicted by Equations (20) and (23) for a pointlike Dirac target and a pointlike spin zero target are shown in Figure 1 (the curves labelled "spin 1/2, $\mu = 1$" and "spin 0", respectively). For small scattering angles θ, the spin-zero and spin-half cross sections are essentially identical. The effect of the magnetic scattering term $(-q^2/2M^2) \sin^2 \theta/2$ becomes evident at large scattering angles; the spin-zero cross section falls to zero as $\theta \to \pi$ while the spin-half cross section remains finite.

The $\cos^2 \theta/2$ factor, present both in Equation (20) and in Equation (23), is a consequence of helicity conservation in QED. In the relativistic limit, the helicity of the incoming electron is preserved in the collision. The overlap between the initial and final state electron spin wavefunctions gives a probability varying as $\cos^2 \theta/2$, which suppresses the scattering cross section at large angles.

We mention in passing that the cross section

$$\left(\frac{\mathrm{d}\sigma}{\mathrm{d}\Omega} \right)_{\text{Mott}} = \frac{\alpha^2}{4E_1^2 \sin^4 \theta/2} \cos^2 \theta/2 \qquad (24)$$

is known as the *Mott cross section*. It lacks the recoil factor E_3/E_1 and represents the cross section for the scattering of high energy electrons from a heavy, spinless, fixed potential.

Finally, we note that Equation (20), the cross section for scattering from a pointlike, spin-half, Dirac proton, can be written in the form

$$\frac{\mathrm{d}\sigma}{\mathrm{d}\Omega} = \left(\frac{\mathrm{d}\sigma}{\mathrm{d}\Omega} \right)_{\text{spin 0}} \left[1 + 2\tau \tan^2 \theta/2 \right] \qquad (25)$$

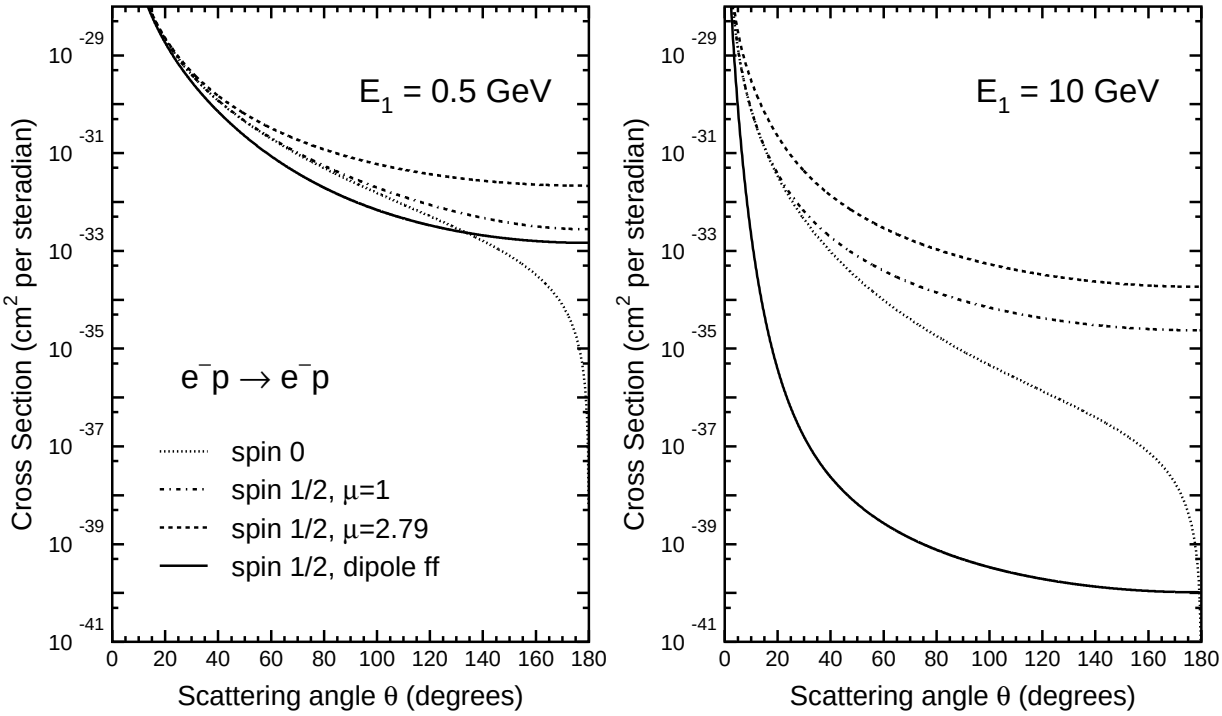

Figure 1: Differential cross section $\mathrm{d}\sigma/\mathrm{d}\Omega$ for elastic $\mathrm{e}^{-}\mathrm{p}$ scattering in the lab frame, for electron beam energies of $0.5\,\mathrm{GeV}$ and $10\,\mathrm{GeV}$, for various assumptions about the spin and structure of the target proton.

where we have introduced the dimensionless, Lorentz-invariant quantity τ defined as

$$\boxed{\tau \equiv \frac{-q^2}{4M^2} > 0}\,.$$

5.4 Scattering from a Finite Size Target

Thus far, the target proton has been assumed to be a pointlike particle. We now extend the above results to take into account the finite spatial extent of the target proton (or neutron).

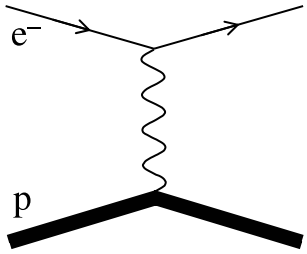

Assuming that the scattering is due to the exchange of a single virtual photon, it can be shown that the lab frame pointlike cross section of Equation (25) generalises to the *Rosenbluth Formula*

$$\boxed{\frac{\mathrm{d}\sigma}{\mathrm{d}\Omega} = \left(\frac{\mathrm{d}\sigma}{\mathrm{d}\Omega}\right)_{\text{spin 0}} \left[\frac{G_{\mathrm{E}}^2 + \tau G_{\mathrm{M}}^2}{1+\tau} + 2\tau G_{\mathrm{M}}^2 \tan^2\theta/2\right]}\,, \tag{26}$$

where the *electric and magnetic form factors* $G_{\rm E}(q^2)$ and $G_{\rm M}(q^2)$ are functions of the four-momentum transfer squared q^2. These form factors can not be predicted from first principles but must be determined from experiment. As we now demonstrate, they provide information on the spatial distribution of electric charge and magnetic moment within the proton or neutron.

The four-momentum transfer $q = (E_1 - E_3, \boldsymbol{q})$ is a combination of an energy transfer $E_1 - E_3$ and a three-momentum transfer $\boldsymbol{q}$. Using Equation (18), the four-momentum transfer squared q^2 is

$$q^2 = (E_1 - E_3)^2 - \boldsymbol{q}^2 = \left(\frac{-q^2}{2M}\right)^2 - \boldsymbol{q}^2 \ . \tag{27}$$

When $|q^2| \ll 4M^2 \sim 4\,\mathrm{GeV}^2$, or equivalently when $\tau \ll 1$, the term $(-q^2/2M)^2$ can be neglected relative to q^2. We then have $E_1 \approx E_3$ and $q^2 \approx -\boldsymbol{q}^2$, so that the four-momentum transfer $q = (E_1 - E_3, \boldsymbol{q})$ becomes approximately a pure three-momentum transfer: $q \approx (0, \boldsymbol{q})$. Also, in this low $|q^2|$ regime, the Rosenbluth formula, Equation (26), becomes

$$\frac{\mathrm{d}\sigma}{\mathrm{d}\Omega} \approx \frac{\alpha^2}{4E_1^2 \sin^2\theta/2}\frac{E_3}{E_1}\left[G_{\rm E}^2\cos^2\theta/2 + 2\tau G_{\rm M}^2 \sin^2\theta/2\right] \ , \tag{28}$$

where $G_{\rm E}(\boldsymbol{q}^2)$ and $G_{\rm M}(\boldsymbol{q}^2)$ now depend only on the *three*-momentum transfer squared. Comparing with the original pointlike cross section of Equation (20), we see that, at low $|q^2|$, the $\cos^2\theta/2$ term associated with scattering from the electric charge of the target is multiplied by a factor $G_{\rm E}(\boldsymbol{q}^2)^2$, while the $\sin^2\theta/2$ term associated with scattering from its magnetic moment is multiplied by a factor $G_{\rm M}(\boldsymbol{q}^2)^2$.

In the Part II Particle and Nuclear Physics course, it was shown that the effect of scattering from a spatial electric charge distribution $\rho(\boldsymbol{r})$ via a three-momentum transfer $\boldsymbol{q}$ could be taken into account by multiplying the differential cross section by an additional factor $|F(\boldsymbol{q}^2)|^2$:

$$\frac{\mathrm{d}\sigma}{\mathrm{d}\Omega} = \left(\frac{\mathrm{d}\sigma}{\mathrm{d}\Omega}\right)_{\text{pointlike}} |F(\boldsymbol{q}^2)|^2$$

where the *form factor*, $F(\boldsymbol{q}^2)$, is the Fourier transform of the charge distribution:

$$F(\boldsymbol{q}^2) = \int e^{i\boldsymbol{q}.\boldsymbol{r}}\rho(\boldsymbol{r})\,\mathrm{d}\boldsymbol{r} \ .$$

Equation (28) thus shows that, at low $|q^2|$, the electric and magnetic form factors $G_{\rm E}(q^2)$ and $G_{\rm M}(q^2)$ can be interpreted as Fourier transforms of the charge and magnetic moment distributions $\rho(\boldsymbol{r})$ and $\mu(\boldsymbol{r})$ within the target: [3]

$$G_{\rm E}(q^2) \approx G_{\rm E}(\boldsymbol{q}^2) = \int e^{i\boldsymbol{q}.\boldsymbol{r}}\rho(\boldsymbol{r})\,\mathrm{d}^3r \tag{29}$$

$$G_{\rm M}(q^2) \approx G_{\rm M}(\boldsymbol{q}^2) = \int e^{i\boldsymbol{q}.\boldsymbol{r}}\mu(\boldsymbol{r})\,\mathrm{d}^3r \ . \tag{30}$$

[3] More generally, this interpretation of the form factors as Fourier transforms of charge and magnetic moment spatial distributions holds in a Lorentz frame known as the *Breit frame*. This is defined as the frame in which the virtual photon carries zero energy (but non-zero three-momentum) and depends on the value of q^2. For low values of q^2, the Breit frame and the lab frame approximately coincide.

In the limit $q^2 = 0$, Equation (27) shows that $\boldsymbol{q}^2 = 0$, and hence also $\boldsymbol{q} = \mathbf{0}$. Applying this limit to Equations (29) and (30) then shows that $G_{\rm E}(0)$ is just the total charge of the target and $G_{\rm M}(0)$ is its total magnetic moment:

$$G_{\rm E}(0) = \int \rho(\boldsymbol{r})\, {\rm d}^3 r, \qquad G_{\rm M}(0) = \int \mu(\boldsymbol{r})\, {\rm d}^3 r \ .$$

With the electric charge measured in units of $+e$ and the magnetic moment measured in units of the nuclear magneton $\mu_N \equiv e\hbar/2m_{\rm p}$, we therefore expect, for proton and neutron targets,

$$\begin{aligned} G_{\rm E}^{\rm p}(0) &= 1 & \qquad G_{\rm M}^{\rm p}(0) &= \mu_{\rm p} = +2.79 \\ G_{\rm E}^{\rm n}(0) &= 0 & \qquad G_{\rm M}^{\rm n}(0) &= \mu_{\rm n} = -1.91 \end{aligned}$$

where the numbers on the right are just the experimentally measured magnetic moments of a free proton or neutron.

Equation (26) shows that $G_{\rm E}(q^2)$ and $G_{\rm M}(q^2)$ can be determined experimentally by plotting the ratio $({\rm d}\sigma/{\rm d}\Omega)/({\rm d}\sigma/{\rm d}\Omega)_{\text{spin 0}}$ as a function of $\tan^2\theta/2$, at a fixed value of q^2. This would be expected to result in a straight line with a slope and intercept (at $\theta = 0$) equal to

$$\text{slope} = 2\tau G_{\rm M}(q^2)^2 \ , \qquad \text{intercept} = \frac{G_{\rm E}(q^2)^2 + \tau G_{\rm M}(q^2)^2}{1+\tau} \ ,$$

from which the values of $G_{\rm E}(q^2)$ and $G_{\rm M}(q^2)$ can be extracted. (Note that $\tau = -q^2/4M^2$ is fixed when q^2 is fixed). When θ is varied keeping q^2 fixed, the electron beam energy E_1 must be varied at each data point according to Equation (22), and, at each point, the scattered electron should have a well defined energy E_3 given by Equation (21).

The data are consistent with the above expectations, thereby confirming that single virtual photon exchange is the dominant scattering mechanism. The measured form factors can be reasonably well fitted to a *dipole* function of the form

$$G_{\rm E}^{\rm p}(q^2) \approx \frac{G_{\rm M}^{\rm p}(q^2)}{2.79} \approx \frac{G_{\rm M}^{\rm n}(q^2)}{-1.91} \approx \frac{1}{(1+|q^2|/q_0^2)^2} \tag{31}$$

where q_0 is a constant with measured value $q_0^2 \approx 0.71\,{\rm GeV}^2$. The measured electric form factor for the neutron is consistent with zero, $G_{\rm E}^{\rm n}(q^2) \approx 0$, as expected. It is shown in the examples sheet that the dipole form above corresponds to an exponential charge distribution, $\rho(r) = \rho_0 e^{-q_0 r}$, with an r.m.s. charge radius $\sqrt{\langle r^2\rangle} = \sqrt{12}/q_0 \approx 0.81\,{\rm fm}$.

For a pointlike target, the form factors $G_{\rm E}(q^2)$ and $G_{\rm M}(q^2)$ would be constants, independent of q^2. In particular, for a pointlike Dirac proton with a magnetic moment of one nuclear magneton ($\mu = 1$), a comparison of Equations (25) and (26) shows that we would expect $G_{\rm E}^{\rm p}(q^2) = 1$ and $G_{\rm M}^{\rm p}(q^2) = 1$ for all values of q^2, in obvious disagreement with the data. More generally, a pointlike proton with an anomalous magnetic dipole moment equal to μ nuclear magnetons would give $G_{\rm M}^{\rm p}(q^2) = \mu$ for all q^2 and a differential cross section

$$\frac{{\rm d}\sigma}{{\rm d}\Omega} = \left(\frac{{\rm d}\sigma}{{\rm d}\Omega}\right)_{\text{spin 0}} \left[\frac{1+\tau\mu^2}{1+\tau} + 2\tau\mu^2 \tan^2\theta/2\right] \ . \tag{32}$$

The effect of varying the assumed magnetic moment of the proton and of taking into account the finite size of the proton is summarised in Figure 1. The curves labelled "spin 1/2, $\mu = 2.79$" show the predicted cross sections from Equation (32) for a pointlike proton with its measured magnetic dipole moment, while the solid curves labelled "spin 1/2, dipole ff" show the actual cross section including form factors with the dipole form of Equation (31). The suppression of the cross section due to the finite size of the proton (by many orders of magnitude for a beam energy of $10\,\mathrm{GeV}$ for example) is clearly evident.

5.5 Deep-Inelastic Scattering

As the energy of the incoming electron is increased, and hence the average value of $|q^2|$ increases, the elastic scattering process $\mathrm{e^-p} \to \mathrm{e^-p}$ gradually gives way to *inelastic* scattering $\mathrm{e^-p} \to \mathrm{e^-X}$ where, as a result of the collision, the proton target breaks up into a hadronic system X containing, for example, a proton plus one or more pions. When $|q^2|$ is large ($|q^2| \gg M^2$, *i.e.* the energy and/or momentum transferred to the proton target via the virtual photon is large), this is termed *deep-inelastic scattering* (DIS).

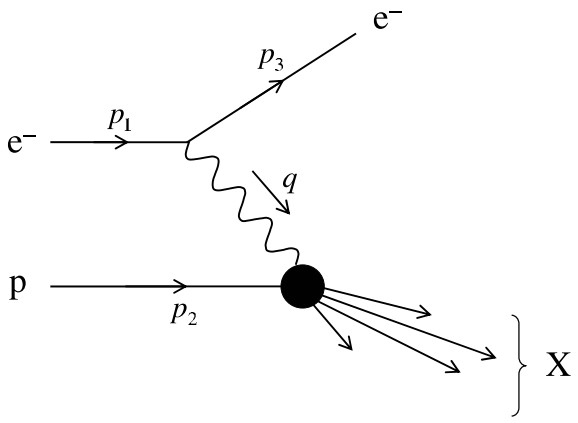

5.5.1 Kinematics of inelastic scattering

For inelastic scattering, $\mathrm{e^-p} \to \mathrm{e^-X}$, the mass of the final state hadronic system is no longer fixed to be the proton mass M, *i.e.* we lose the constraint $p_4^2 = M^2$. In fact, since the hadronic final state must contain at least one proton or neutron, we must have $M_\mathrm{X} > M$ where $M_\mathrm{X}^2 \equiv p_4^2$ and p_4 is the total four-momentum of all the particles in the system X.

At this point, it is useful to introduce the dimensionless Lorentz invariant *Bjorken scaling variable*

$$\boxed{x \equiv \frac{Q^2}{2p_2.q}},$$

where the positive quantity $Q^2 > 0$ is defined as

$$\boxed{Q^2 \equiv -q^2}.$$

Squaring the equation $p_4 = q + p_2$ gives

$$M_{\rm X}^2 = p_4^2 = (q + p_2)^2 = -Q^2 + 2p_2.q + M^2 \ .$$

Since $M_{\rm X} > M$, we must have $Q^2 < 2p_2.q$, and the variable x must therefore lie in the range

$$\boxed{0 < x < 1 \qquad \text{(inelastic)}} \ .$$

For elastic scattering, we have $M_{\rm X} = M$ and therefore simply

$$\boxed{x = 1 \qquad \text{(elastic)}} \ .$$

It is also very useful to reintroduce the Lorentz invariant variable y defined in Section 5.1 above as

$$y \equiv \frac{p_2.q}{p_2.p_1} \ . \qquad (6)'$$

In the centre of mass frame, for the elastic scattering of two massless particles, it was shown earlier, Equation (7), that $y = \frac{1}{2}(1 - \cos\theta^*)$, and hence $0 < y < 1$. In the lab frame, with proton 4-momentum $p_2 = (M, 0, 0, 0)$, we have

$$y = \frac{p_2.q}{p_2.p_1} = \frac{M(E_1 - E_3)}{ME_1} = 1 - \frac{E_3}{E_1} \ .$$

Thus, in the lab frame, y can be interpreted as the fractional energy lost by the incoming electron. Since $E_3 < E_1$ we again see that $0 < y < 1$.

The centre of mass energy squared of the electron-proton collision (still neglecting the electron mass; $p_1^2 = p_3^2 = 0$) is

$$s = (p_1 + p_2)^2 = 2p_1.p_2 + M^2 \ .$$

Therefore

$$xy = \frac{Q^2}{2p_2.q}\frac{p_2.q}{p_2.p_1} = \frac{Q^2}{2p_2.p_1} = \frac{Q^2}{s - M^2} \ ,$$

so that Q^2, x and y are not independent variables but are related via

$$Q^2 = (s - M^2)xy \ .$$

Finally, we mention that it is common to introduce a further Lorentz-invariant quantity ν, defined as

$$\boxed{\nu \equiv \frac{p_2.q}{M}} \ .$$

In the lab frame, we have $p_2.q = M(E_1 - E_3)$, and hence ν is just the energy transfer:

$$\nu = E_1 - E_3 \ .$$

In terms of ν, the scaling variables x and y are (in any frame)

$$x = \frac{Q^2}{2M\nu}, \qquad y = \frac{2M}{s - M^2}\nu \ ,$$

so that y and ν are related simply by a constant scale factor $2M/(s - M^2)$.

5.5.2 Inelastic scattering cross section

To motivate the general form of the deep-inelastic scattering cross section, we return briefly to the lab frame Rosenbluth cross section for $\mathrm{e^-p} \to \mathrm{e^-p}$ *elastic* scattering:

$$\frac{\mathrm{d}\sigma}{\mathrm{d}\Omega} = \frac{\alpha^2}{4E_1^2 \sin^4\theta/2}\frac{E_3}{E_1}\left[\frac{G_{\mathrm{E}}^2 + \tau G_{\mathrm{M}}^2}{1+\tau}\cos^2\theta/2 + 2\tau G_{\mathrm{M}}^2 \sin^2\theta/2\right] . \tag{33}$$

It is shown on the examples sheet that this cross section can be written in the Lorentz invariant form [4]

$$\boxed{\frac{\mathrm{d}\sigma}{\mathrm{d}Q^2} = \frac{4\pi\alpha^2}{Q^4}\left[\frac{G_{\mathrm{E}}^2 + \tau G_{\mathrm{M}}^2}{1+\tau}\left(1 - y - \frac{M^2y^2}{Q^2}\right) + \frac{1}{2}y^2 G_{\mathrm{M}}^2\right]} . \tag{34}$$

For *inelastic* scattering, $\mathrm{e^-p} \to \mathrm{e^-X}$, it can be shown that the differential cross section is a straightforward extension of Equation (34):

$$\boxed{\frac{\mathrm{d}^2\sigma}{\mathrm{d}x\mathrm{d}Q^2} = \frac{4\pi\alpha^2}{Q^4}\left[\left(1 - y - \frac{M^2x^2y^2}{Q^2}\right)\frac{F_2(x,Q^2)}{x} + \frac{1}{2}y^2\frac{2xF_1(x,Q^2)}{x}\right]} , \tag{35}$$

where $F_1(x,Q^2)$ and $F_2(x,Q^2)$ are dimensionless functions known as *structure functions*. Equation (35) is the most general possible form for the inelastic cross section assuming only Lorentz invariance, single virtual photon exchange, and conservation of parity. The reason for writing the F_1 contribution as $(2xF_1)/x$ rather than simply as $2F_1$ will become clear shortly.

The loss of the constraint $x = 1$ implies that, instead of depending on only a single independent Lorentz invariant (*e.g.* Q^2 or y), the inelastic cross section depends on *two* independent Lorentz invariants (*e.g.* x and Q^2 or x and y). Inelastic scattering is therefore described by a *double*-differential cross section $\mathrm{d}^2\sigma/\mathrm{d}x\mathrm{d}Q^2$ or $\mathrm{d}^2\sigma/\mathrm{d}x\mathrm{d}y$. Since F_1 and F_2 depend on x as well as Q^2, they can no longer be interpreted as Fourier transforms of spatial charge or magnetic moment distributions. Instead, we shall see that they give information about the fractional momentum distributions of the quarks and gluons making up the nucleon.

The structure functions F_1 and F_2 can not (yet) be predicted from first principles but must be determined experimentally. All the relevant kinematic quantities (x, y, Q^2) can be measured by detecting the scattered electron alone; the final state hadronic system does not have to be measured [5]. In the

[4] Note that for high energy ($Q^2 \gg M^2$) elastic scattering from a pointlike spin-half Dirac target, for which $G_{\mathrm{E}}(q^2) = G_{\mathrm{M}}(q^2) = 1$, we recover Equation (9):

$$\frac{\mathrm{d}\sigma}{\mathrm{d}Q^2} = \frac{4\pi\alpha^2}{Q^4}\left[(1-y) + \frac{1}{2}y^2\right] = \frac{2\pi\alpha^2}{Q^4}\left[1 + (1-y)^2\right] .$$

Note also that at high Q^2, the dipole form for the form factors gives $G_{\mathrm{E}}(Q^2) \sim 1/Q^4$, $G_{\mathrm{M}}(Q^2) \sim 1/Q^4$, and hence

$$\frac{\mathrm{d}\sigma}{\mathrm{d}Q^2} \sim \frac{1}{Q^{12}} ,$$

making clear that the elastic cross section falls off very rapidly as Q^2 increases.

[5] In practice, the hadronic system *is* often also detected. This provides a second, independent determination of the kinematic variables, which can be very helpful in reducing experimental uncertainties, for example.

laboratory frame, for example, the quantities Q^2, x and y can be computed from the scattered electron energy E_3 and angle θ using

$$Q^2 = 4E_1E_3\sin^2\theta/2\,, \qquad x = \frac{Q^2}{2M(E_1-E_3)}\,, \qquad y = 1-\frac{E_3}{E_1}\,.$$

It is shown in the examples sheet that, in the lab frame, the deep-inelastic cross section takes the form

$$\frac{\mathrm{d}^2\sigma}{\mathrm{d}E_3\mathrm{d}\Omega} = \frac{\alpha^2}{4E_1^2\sin^4\theta/2}\left[\frac{F_2}{\nu}\cos^2\frac{\theta}{2} + \frac{2F_1}{M}\sin^2\frac{\theta}{2}\right] \tag{36}$$

where $\nu = E_1 - E_3$ is the energy carried by the virtual photon. To measure $F_1(x,Q^2)$ and $F_2(x,Q^2)$ for given values of x and Q^2 requires the cross section to be measured at several different scattering angles θ, for several incoming beam energies E_1. This is considered further on the examples sheet.

The formalism above applies equally to electron-proton and electron-neutron scattering, with each process having its own structure functions, F_1^{ep}, F_2^{ep}, F_1^{en}, F_2^{en}. In the deep-inelastic regime, $Q^2 \gg M^2$, Equation (35) becomes

$$\frac{\mathrm{d}^2\sigma^{\mathrm{ep}}}{\mathrm{d}x\mathrm{d}Q^2} = \frac{4\pi\alpha^2}{Q^4}\left[(1-y)\frac{F_2^{\mathrm{ep}}}{x} + \frac{1}{2}y^2\frac{2xF_1^{\mathrm{ep}}}{x}\right] \tag{37}$$

$$\frac{\mathrm{d}^2\sigma^{\mathrm{en}}}{\mathrm{d}x\mathrm{d}Q^2} = \frac{4\pi\alpha^2}{Q^4}\left[(1-y)\frac{F_2^{\mathrm{en}}}{x} + \frac{1}{2}y^2\frac{2xF_1^{\mathrm{en}}}{x}\right] \tag{38}$$

5.5.3 Bjorken scaling and the Callan-Gross relation

The first deep-inelastic scattering experiments were carried out at the SLAC laboratory in California beginning in the late 1960's, using a $20\,\mathrm{GeV}$ electron beam from a two mile long linear accelerator. A striking and surprising feature of the structure functions measured in these experiments was that F_1 and F_2 were found to be approximately independent of Q^2 at a fixed value of x:

$$\boxed{F_1(x,Q^2) \longrightarrow F_1(x), \qquad F_2(x,Q^2) \longrightarrow F_2(x)}\,.$$

This is known as *Bjorken scaling*, and strongly suggests that the scattering is taking place from *point-like constituents* within the proton. If the proton contained some internal structure whose Fourier transform was characterised by a constant, Q_0^2, then the (dimensionless) structure functions would be expected to depend on Q^2 through the dimensionless combination Q^2/Q_0^2, just as for the elastic scattering dipole form factors G_{E} and G_{M} of Equation (31). For pointlike constituents on the other hand, such terms can not arise and no Q^2-dependence of the structure functions is possible. Bjorken scaling is analagous to the constant elastic form factors which would be expected for scattering from a pointlike proton.

Bjorken scaling can also be understood through a consideration of the wavelength $\lambda \sim h/|\boldsymbol{q}| = 2\pi/|\boldsymbol{q}|$ of the virtual photon exchanged in the scattering, though it should be said at the outset that the concept of wavelength for virtual particles is a somewhat delicate concept. In the lab frame, the four-momentum of the virtual photon is $q = (\nu, \boldsymbol{q})$ where $\nu = E_1 - E_3 = Q^2/2Mx$. The relation $q^2 = \nu^2 - |\boldsymbol{q}|^2$ then gives

$$-Q^2 = \left(\frac{Q^2}{2Mx}\right)^2 - |\boldsymbol{q}|^2\,.$$

For $Q^2 \gg M^2$, we then obtain a wavelength

$$\lambda \sim \frac{2\pi}{|\boldsymbol{q}|} \approx \frac{4\pi M x}{Q^2} \, .$$

The fact that the cross section is independent of Q^2 at fixed x then implies that the scattering is independent of the photon wavelength. This is exactly what would be expected if the photon were scattering from a pointlike object: a point looks like a point at any wavelength.

Besides the observation of Bjorken scaling, another important feature of the data was that the structure functions F_1 and F_2 were found not to be independent functions but to be related to each other by the *Callan-Gross relation*

$$\boxed{F_2(x) = 2xF_1(x)} \, .$$

We shall see below that the Callan-Gross relation arises naturally if the pointlike constituents within the proton are spin-half particles.

5.6 The Quark-Parton Model

The deep-inelastic cross section expressions in the previous section are completely general in form; they assume only Lorentz invariance, the dominance of single-photon exchange, and parity conservation. We now derive specific predictions for the form of these cross sections based on a model of elastic scattering from pointlike spin-half constituents, known as the *parton model* [6].

The key assumptions of the parton model are that the virtual photon scatters elastically from pointlike constituents (*partons*) within the nucleon, and that these constituents can be considered to be "quasi-free" particles. Given that no free quark has ever been seen and that quarks are believed to be permanently confined within hadrons, the assumption that quarks can be treated as effectively free particles within the nucleon seems somewhat questionable. The justification for this assumption came after the introduction of the parton model, and relies on a property of QCD known as *asymptotic freedom*. This refers to the fact that the strong coupling "constant" $\alpha_{\rm s}(Q^2)$ actually *falls* with increasing Q^2. At large Q^2, binding effects due to the strong interaction are effectively much reduced and the struck quark can be treated as a free particle.

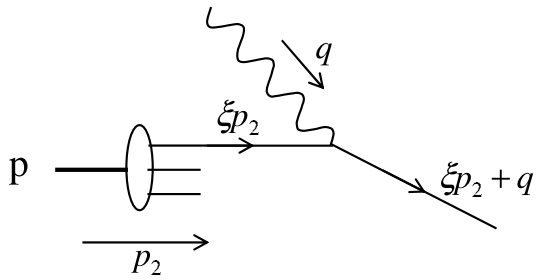

[6] The term *parton* was introduced by Feynman to refer to putative pointlike constituents within the nucleon, at a time before the existence of quarks as real particles was generally accepted.

The parton model is most easily formulated in the *infinite-momentum frame* [7] where the proton (or neutron) is moving with very high energy: $p_2 = (E_2, 0, 0, E_2)$ with $E_2 \gg M$. In this frame, the parton mass and transverse momentum can be neglected; the parton can be assumed to be moving parallel to the proton direction with a four-momentum $\hat{p}_2$ which is a fraction ξ of the proton's four-momentum p_2:

$$\hat{p}_2 = \xi p_2 \ .$$

After the interaction with the virtual photon, the scattered parton has four-momentum $\xi p_2 + q$. Since the parton can be taken to be massless, we then have

$$0 = (\xi p_2 + q)^2 = 2\xi p_2.q - Q^2 \ .$$

Recalling that Bjorken x is defined as $x = Q^2/2p_2.q$, we then obtain

$$\boxed{\xi = x} \ .$$

Thus, in the parton model, Bjorken x can be interpreted as the fractional parton momentum in a frame where the proton has very high energy.

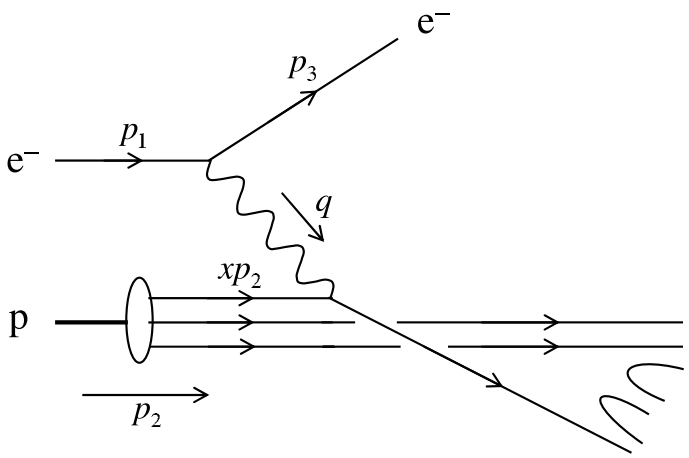

The centre of mass energy squared, $\hat{s}$, for the underlying scattering of an electron of 4-momentum p_1 from a quark of 4-momentum $\hat{p}_2 = xp_2$ is given by

$$\hat{s} \equiv (p_1 + \hat{p}_2)^2 = (p_1 + xp_2)^2 = 2xp_1.p_2 = xs \ .$$

Similarly, the quantity $\hat{y}$ appropriate to the electron-quark collision is

$$\hat{y} \equiv \frac{\hat{p}_2.q}{\hat{p}_2.p_1} = \frac{xp_2.q}{xp_2.p_1} = \frac{p_2.q}{p_2.p_1} = y \ ,$$

i.e. the value of y for the electron-quark scattering is the same as that for the electron-nucleon scattering.

[7] This formulation is usually referred to as the *naive* parton model. The parton model can also be formulated in a fully relativistically covariant manner.

The differential cross section for the underlying electron-quark scattering can be taken directly from Equation (9) of Section 5.1:

$$\frac{\mathrm{d}\sigma}{\mathrm{d}Q^2} = \frac{2\pi\alpha^2}{Q^4} e_q^2 \left[1 + (1-\hat{y})^2\right] = \frac{2\pi\alpha^2}{Q^4} e_q^2 \left[1 + (1-y)^2\right]$$

where we have included a factor of e_q^2 to take into account the quark charge e_q (in units of $+e$).

The momentum fraction x carried by a particular parton within the nucleon (the d quark within the proton, for example) is not fixed, but varies as partons exchange momentum with each other. In QCD, this is due to the exchange of gluons between different quarks. To take this into account, we introduce *parton distribution functions* $u^{\mathrm{p}}(x)$, $d^{\mathrm{p}}(x)$ *etc.* where, for example, $u^{\mathrm{p}}(x)\mathrm{d}x$ is defined as the number of u quarks in the proton with a momentum fraction lying between x and $x + \mathrm{d}x$. The contribution to the overall cross section due to scattering from quarks of flavour q in this momentum range is then

$$\frac{\mathrm{d}\sigma}{\mathrm{d}Q^2} = \frac{2\pi\alpha^2}{Q^4} \left[1 + (1-y)^2\right] \cdot e_q^2 \, q^{\mathrm{p}}(x)\mathrm{d}x \; .$$

Summing over all possible flavours of quark and dividing by $\mathrm{d}x$ gives the overall electron-proton differential cross section

$$\frac{\mathrm{d}^2\sigma^{\mathrm{ep}}}{\mathrm{d}x\mathrm{d}Q^2} = \frac{2\pi\alpha^2}{Q^4} \left[1 + (1-y)^2\right] \cdot \sum_q e_q^2 \, q^{\mathrm{p}}(x) \; .$$

The summation over quark flavours must take into account not only the *valence* quarks (uud) or (ddu) in the proton or neutron, but also the *quark-antiquark sea* that can be produced by higher order processes such as $\mathrm{g} \to \mathrm{u}\overline{\mathrm{u}}$, $\mathrm{g} \to \mathrm{d}\overline{\mathrm{d}}$ *etc.*. Including scattering from sea quarks and antiquarks, the electron-proton scattering cross section becomes

$$\frac{\mathrm{d}^2\sigma^{\mathrm{ep}}}{\mathrm{d}x\mathrm{d}Q^2} = \frac{2\pi\alpha^2}{Q^4} \left[1 + (1-y)^2\right] \left[\frac{4}{9}u^{\mathrm{p}}(x) + \frac{1}{9}d^{\mathrm{p}}(x) + \frac{4}{9}\overline{u}^{\mathrm{p}}(x) + \frac{1}{9}\overline{d}^{\mathrm{p}}(x)\right] \; , \tag{39}$$

where possible contributions from the heavier sea quarks $\mathrm{s}\overline{\mathrm{s}}$, $\mathrm{c}\overline{\mathrm{c}}$, $\mathrm{b}\overline{\mathrm{b}}$ have been neglected. The functions $u^{\mathrm{p}}(x)$ and $d^{\mathrm{p}}(x)$ contain contributions from both valence and sea quarks, while the functions $\overline{u}^{\mathrm{p}}(x)$ and $\overline{d}^{\mathrm{p}}(x)$ receive only sea contributions.

Noting that

$$1 + (1-y)^2 = 2\left[(1-y) + \frac{1}{2}y^2\right] \; ,$$

we see that the cross section predicted by the parton model, Equation (39), has the same structure as the general deep-inelastic cross section of Equation (37). Comparing the coefficients of $(1-y)$ and $\frac{1}{2}y^2$ in these two equations immediately gives the parton model predictions

$$F_2^{\mathrm{ep}}(x,Q^2) = 2xF_1^{\mathrm{ep}}(x,Q^2) = x\left[\frac{4}{9}u^{\mathrm{p}}(x) + \frac{1}{9}d^{\mathrm{p}}(x) + \frac{4}{9}\overline{u}^{\mathrm{p}}(x) + \frac{1}{9}\overline{d}^{\mathrm{p}}(x)\right] \; .$$

Hence the quark-parton model naturally predicts the Callan-Gross relation $F_2 = 2xF_1$. This relation is a consequence of quarks being pointlike spin-half Dirac particles, and hence there being a relation between the electric charge of the quark and its magnetic moment. For spin-zero quarks, which

have no intrinsic magnetic moment and hence no magnetic scattering $\sin^2\theta/2$ term, we would instead expect $F_1 = 0$.

For electron scattering from neutrons, rather than protons, the parton model cross section has the same form as Equation (39) but with the suffix 'p' replaced by 'n':

$$\frac{\mathrm{d}^2\sigma^{\mathrm{en}}}{\mathrm{d}x\mathrm{d}Q^2} = \frac{2\pi\alpha^2}{Q^4}\left[1+(1-y)^2\right]\left[\frac{4}{9}u^{\mathrm{n}}(x) + \frac{1}{9}d^{\mathrm{n}}(x) + \frac{4}{9}\overline{u}^{\mathrm{n}}(x) + \frac{1}{9}\overline{d}^{\mathrm{n}}(x)\right] \ . \tag{40}$$

Comparison with Equation (38) then gives

$$F_2^{\mathrm{en}}(x,Q^2) = 2xF_1^{\mathrm{en}}(x,Q^2) = x\left[\frac{4}{9}u^{\mathrm{n}}(x) + \frac{1}{9}d^{\mathrm{n}}(x) + \frac{4}{9}\overline{u}^{\mathrm{n}}(x) + \frac{1}{9}\overline{d}^{\mathrm{n}}(x)\right] \ .$$

Since the quark content of the proton is (uud) and of the neutron is (ddu), we expect the roles of the u and d quarks to be symmetric between the proton and the neutron: [8]

$$u^{\mathrm{n}}(x) = d^{\mathrm{p}}(x), \qquad d^{\mathrm{n}}(x) = u^{\mathrm{p}}(x) \ ,$$

and similarly for antiquarks. We can therefore define distribution functions $u(x)$, $d(x)$, $\overline{u}(x)$, $\overline{d}(x)$ as

$$\begin{aligned} u(x) \equiv u^{\mathrm{p}}(x) = d^{\mathrm{n}}(x), \qquad & d(x) \equiv d^{\mathrm{p}}(x) = u^{\mathrm{n}}(x) \ , \\ \overline{u}(x) \equiv \overline{u}^{\mathrm{p}}(x) = \overline{d}^{\mathrm{n}}(x), \qquad & \overline{d}(x) \equiv \overline{d}^{\mathrm{p}}(x) = \overline{u}^{\mathrm{n}}(x) \ , \end{aligned}$$

and hence obtain parton model expressions for the structure functions which avoid the need for "p" and "n" suffices:

$$\boxed{F_2^{\mathrm{ep}} = 2xF_1^{\mathrm{ep}} = x\left[\frac{4}{9}u(x) + \frac{1}{9}d(x) + \frac{4}{9}\overline{u}(x) + \frac{1}{9}\overline{d}(x)\right]} \tag{41}$$

$$\boxed{F_2^{\mathrm{en}} = 2xF_1^{\mathrm{en}} = x\left[\frac{4}{9}d(x) + \frac{1}{9}u(x) + \frac{4}{9}\overline{d}(x) + \frac{1}{9}\overline{u}(x)\right]} \tag{42}$$

Hence, by measuring both $F_2^{\mathrm{ep}}(x)$ and $F_2^{\mathrm{en}}(x)$, the parton distribution function combinations $u(x) + \overline{u}(x)$ and $d(x) + \overline{d}(x)$ can be extracted from the data.

5.6.1 Structure function integrals

Integrating the parton model predictions of Equations (41) and (42) over the range $0 < x < 1$ gives the total areas under the structure functions $F_2^{\mathrm{ep}}(x)$ and $F_2^{\mathrm{en}}(x)$:

$$\begin{aligned} \int_0^1 F_2^{\mathrm{ep}}(x)\mathrm{d}x &= \int_0^1 x\left[\frac{4}{9}u(x) + \frac{1}{9}d(x) + \frac{4}{9}\overline{u}(x) + \frac{1}{9}\overline{d}(x)\right]\mathrm{d}x = \frac{4}{9}f_u + \frac{1}{9}f_d \\ \int_0^1 F_2^{\mathrm{en}}(x)\mathrm{d}x &= \int_0^1 x\left[\frac{4}{9}d(x) + \frac{1}{9}u(x) + \frac{4}{9}\overline{d}(x) + \frac{1}{9}\overline{u}(x)\right]\mathrm{d}x = \frac{4}{9}f_d + \frac{1}{9}f_u \end{aligned}$$

[8] This symmetry between u (d) quarks in the proton and d (u) quarks in the neutron is known formally as *isospin symmetry* and will be considered in detail later.

where we have introduced the quantities f_u and f_d defined as

$$f_u \equiv \int_0^1 x\left[u(x) + \overline{u}(x)\right] \mathrm{d}x, \qquad f_d \equiv \int_0^1 x\left[d(x) + \overline{d}(x)\right] \mathrm{d}x \; .$$

Since $u(x)\mathrm{d}x$ is the number of u quarks in the proton with fractional momentum x to $x + \mathrm{d}x$, and similarly for $\overline{u}(x)\mathrm{d}x$, we can interpret f_u as the overall fraction of the proton's momentum carried by u quarks plus $\overline{\mathrm{u}}$ antiquarks. Similarly, f_d is the overall fraction of the proton's momentum carried by d quarks plus $\overline{\mathrm{d}}$ antiquarks.

Experimental measurements of these integrals give $\int_0^1 F_2^{\mathrm{ep}}(x)\mathrm{d}x \approx 0.18$ and $\int_0^1 F_2^{\mathrm{en}}(x)\mathrm{d}x \approx 0.12$, which can be used to infer

$$f_u \approx 0.36, \qquad f_d \approx 0.18 \; .$$

Hence the average total momentum carried by u quarks plus $\overline{\mathrm{u}}$ antiquarks in the proton is about twice as large as that carried by d quarks plus $\overline{\mathrm{d}}$ antiquarks, which seems reasonable, but the overall total $f_u + f_d$ accounts for only around 50% of the proton's momentum. The remaining $\sim 50\%$ must be carried by constituents which can *not* interact with virtual photons, and are therefore electrically neutral. In QCD, these constituents are the *gluons*.

5.6.2 Valence and sea quarks

The functions $u(x)$ and $d(x)$ can be resolved into *valence* and *sea* components:

$$u(x) = u_{\mathrm{V}}(x) + u_{\mathrm{S}}(x), \qquad d(x) = d_{\mathrm{V}}(x) + d_{\mathrm{S}}(x)$$

where the valence quarks (uud for the proton and udd for the neutron) are the quark model constituents of the proton or neutron and the sea quarks are produced in higher order QCD processes such as $\mathrm{g} \to \mathrm{u}\overline{\mathrm{u}}$ and $\mathrm{g} \to \mathrm{d}\overline{\mathrm{d}}$. Since the proton contains two valence u quarks and one valence d quark, the integrals over all x of the distribution functions $u_{\mathrm{V}}(x)$ and $d_{\mathrm{V}}(x)$ are expected to be

$$\int_0^1 u_{\mathrm{V}}(x)\mathrm{d}x = 2, \qquad \int_0^1 d_{\mathrm{V}}(x)\mathrm{d}x = 1 \; .$$

The total number of sea quarks and antiquarks is not known *a priori* and there is therefore no corresponding constraint on the integrals of $u_{\mathrm{S}}(x)$, $d_{\mathrm{S}}(x)$, $\overline{u}(x)$ and $\overline{d}(x)$.

A reasonable expectation would be that all quark and antiquark sea components have the same momentum distribution, characterised by a common distribution function $S(x)$ say:

$$u(x) = u_{\mathrm{V}}(x) + S(x), \qquad d(x) = d_{\mathrm{V}}(x) + S(x), \qquad \overline{u}(x) = \overline{d}(x) = S(x) \; .$$

In this picture, the parton model predictions for the structure functions of Equations (41) and (42) become

$$F_2^{\mathrm{ep}}(x) = x\left[\frac{4}{9}u_{\mathrm{V}}(x) + \frac{1}{9}d_{\mathrm{V}}(x) + \frac{10}{9}S(x)\right]$$
$$F_2^{\mathrm{en}}(x) = x\left[\frac{4}{9}d_{\mathrm{V}}(x) + \frac{1}{9}u_{\mathrm{V}}(x) + \frac{10}{9}S(x)\right] \; .$$

Information on the valence components alone can then be obtained by taking the difference of these two expressions:

$$F_2^{\rm ep}(x) - F_2^{\rm en}(x) = x\left[\frac{1}{3}u_{\rm V}(x) - \frac{1}{3}d_{\rm V}(x)\right] \ .$$

The effect of the sea can be demonstrated by forming the ratio

$$\frac{F_2^{\rm en}(x)}{F_2^{\rm ep}(x)} = \frac{4d_{\rm V}(x) + u_{\rm V}(x) + 10S(x)}{4u_{\rm V}(x) + d_{\rm V}(x) + 10S(x)} \ .$$

Higher order processes such as $\rm g \to u\overline{u}$, $\rm g \to d\overline{d}$ would be expected to involve mainly low energy gluons, because of the $1/q^2$ gluon propagator. We therefore expect the sea to consist mainly of low energy quarks and antiquarks, and for the sea distribution $S(x)$ to dominate completely as $x \to 0$. In this limit we therefore expect

$$\frac{F_2^{\rm en}(x)}{F_2^{\rm ep}(x)} \to 1 \qquad \text{as} \quad x \to 0 \ ,$$

and this prediction is borne out by the data. By contrast, at large values of x, we would expect the sea contribution to be negligible:

$$\frac{F_2^{\rm en}(x)}{F_2^{\rm ep}(x)} \to \frac{4d_{\rm V}(x) + u_{\rm V}(x)}{4u_{\rm V}(x) + d_{\rm V}(x)} \qquad \text{as} \quad x \to 1 \ .$$

A reasonable guess would be that the momentum distribution functions of $\rm u$ and $\rm d$ valence quarks within the proton have the same shape. In this case, we would expect $u_{\rm V}(x) = 2d_{\rm V}(x)$, reflecting the fact that there are twice as many valence $\rm u$ quarks as $\rm d$ quarks in the proton. This would give $F_2^{\rm en}(x)/F_2^{\rm ep}(x) \to (2/3)$ as $x \to 1$. In fact, the data show rather that $F_2^{\rm en}(x)/F_2^{\rm ep}(x) \to (1/4)$ as $x \to 1$, giving $d_{\rm V}(x) \ll u_{\rm V}(x)$ in this limit. The relation $u_{\rm V}(x) \approx 2d_{\rm V}(x)$ thus holds only rather approximately, for reasons that are not well understood.

The figure below shows parton distribution functions resulting from a recent fit to all available deep-inelastic scattering data, including data from *neutrino*-nucleon scattering experiments, to be considered later.

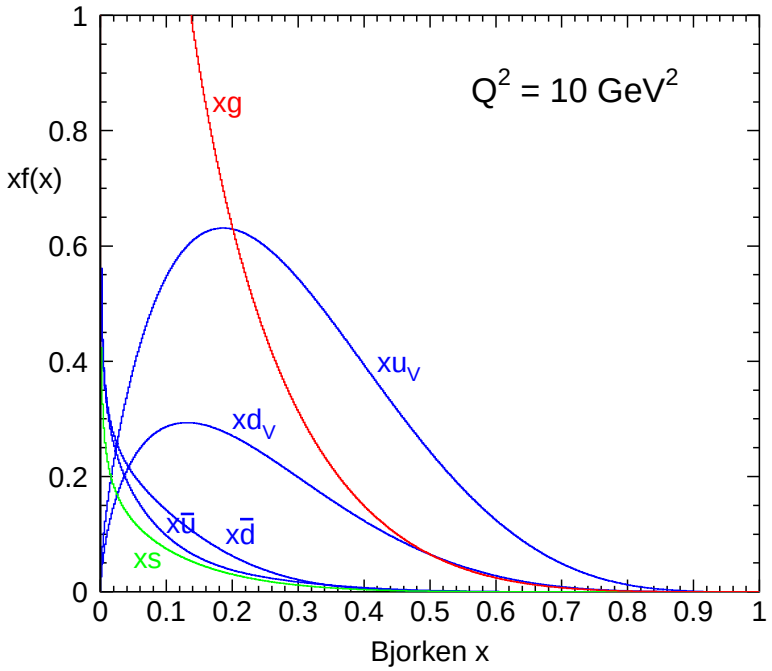

The u and d valence quark distributions peak at about $x \approx 0.2$ and approximately satisfy $u_{\mathrm{V}}(x) \approx 2d_{\mathrm{V}}(x)$, but there are visible differences in the shapes of these two distributions. The sea quark distributions all rise rapidly towards small values of x. For $x < 0.2$, the overwhelmingly dominant constituent of the nucleon is the gluon.

5.7 Summary

For convenience, we summarise below the Lorentz-invariant kinematic variables used to describe elastic ($\mathrm{e^-N} \to \mathrm{e^-N}$) and inelastic ($\mathrm{e^-N} \to \mathrm{e^-X}$) electron-nucleon scattering, and collect together the main cross section formulae for these processes.

5.7.1 Kinematic variables

The square of the centre of mass energy of the electron-nucleon collision is

$$s = (p_1 + p_2)^2 = 2p_1.p_2 + M^2 \ .$$

The four-momentum transfer squared of the virtual photon is

$$Q^2 = -q^2 = -(p_1 - p_3)^2 > 0 \ .$$

The scaling variables x and y are defined as

$$x \equiv \frac{Q^2}{2p_2.q} \ , \qquad y \equiv \frac{p_2.q}{p_2.p_1} \ ,$$

and cover the ranges $0 < x < 1$, $0 < y < 1$, with $x = 1$ for elastic scattering. The variable ν is defined as

$$\nu \equiv \frac{p_2.q}{M} \ .$$

The quantities s, Q^2, x, y, and ν above are all Lorentz-invariant. They are related via

$$Q^2 = (s - M^2)xy \ , \qquad x = \frac{Q^2}{2M\nu} \ , \qquad y = \frac{2M}{s - M^2}\nu \ .$$

In the laboratory frame, with incoming electron beam energy E_1, we have

$$s = 2ME_1 + M^2, \qquad Q^2 = 2E_1E_3(1 - \cos\theta), \qquad y = 1 - \frac{E_3}{E_1}, \qquad \nu = E_1 - E_3 \ ,$$

where E_3 and θ are the energy and angle of the scattered electron.

In the centre of mass frame, for the elastic scattering of two massless particles (electron-quark scattering for example), we have

$$y = \tfrac{1}{2}(1 - \cos\theta^*) \ .$$

5.7.2 Cross section formulae

For the elastic scattering of two pointlike particles, neglecting all masses, the Lorentz-invariant cross section is

$$\frac{\mathrm{d}\sigma}{\mathrm{d}q^2} = \frac{1}{s}\frac{\mathrm{d}\sigma}{\mathrm{d}y} = \frac{2\pi\alpha^2}{q^4}\left[1+(1-y)^2\right] \ . \qquad (9)'$$

For elastic electron-nucleon scattering, treating the nucleon as pointlike, and neglecting the electron mass, the differential cross section in the lab frame is

$$\frac{\mathrm{d}\sigma}{\mathrm{d}\Omega} = \frac{\alpha^2}{4E_1^2\sin^4\theta/2}\frac{E_3}{E_1}\left(\cos^2\theta/2 - \frac{q^2}{2M^2}\sin^2\theta/2\right) \ . \qquad (20)'$$

For elastic electron-nucleon scattering, taking the finite size of the nucleon into account via elastic form factors $G_{\mathrm{E}}(q^2)$ and $G_{\mathrm{M}}(q^2)$, the covariant and lab frame (Rosenbluth formula) cross sections are

$$\frac{\mathrm{d}\sigma}{\mathrm{d}Q^2} = \frac{1}{s}\frac{\mathrm{d}\sigma}{\mathrm{d}y} = \frac{4\pi\alpha^2}{Q^4}\left[\frac{G_{\mathrm{E}}^2+\tau G_{\mathrm{M}}^2}{1+\tau}(1-y) + \frac{1}{2}y^2 G_{\mathrm{M}}^2\right] \ . \qquad (34)'$$

$$\frac{\mathrm{d}\sigma}{\mathrm{d}\Omega} = \frac{\alpha^2}{4E_1^2\sin^4\theta/2}\frac{E_3}{E_1}\left[\frac{G_{\mathrm{E}}^2+\tau G_{\mathrm{M}}^2}{1+\tau}\cos^2\theta/2 + 2\tau G_{\mathrm{M}}^2\sin^2\theta/2\right] \ . \qquad (26)'$$

For deep-inelastic scattering, the covariant and lab frame cross sections are

$$\frac{\mathrm{d}^2\sigma}{\mathrm{d}x\mathrm{d}Q^2} = \frac{4\pi\alpha^2}{Q^4}\left[(1-y)\frac{F_2(x,Q^2)}{x} + \frac{1}{2}y^2\frac{2xF_1(x,Q^2)}{x}\right] \ . \qquad (35)'$$

$$\frac{\mathrm{d}^2\sigma}{\mathrm{d}E_3\mathrm{d}\Omega} = \frac{\alpha^2}{4E_1^2\sin^4\theta/2}\left[\frac{F_2}{\nu}\cos^2\frac{\theta}{2} + \frac{2F_1}{M}\sin^2\frac{\theta}{2}\right] \ . \qquad (36)'$$

The parton model predictions for the electron-proton and electron-neutron deep-inelastic scattering cross sections and structure functions are

$$\frac{\mathrm{d}^2\sigma^{\mathrm{ep}}}{\mathrm{d}x\mathrm{d}Q^2} = \frac{2\pi\alpha^2}{Q^4}\left[1+(1-y)^2\right]\left[\frac{4}{9}u(x) + \frac{1}{9}d(x) + \frac{4}{9}\overline{u}(x) + \frac{1}{9}\overline{d}(x)\right] \ . \qquad (39)'$$

$$\frac{\mathrm{d}^2\sigma^{\mathrm{en}}}{\mathrm{d}x\mathrm{d}Q^2} = \frac{2\pi\alpha^2}{Q^4}\left[1+(1-y)^2\right]\left[\frac{4}{9}d(x) + \frac{1}{9}u(x) + \frac{4}{9}\overline{d}(x) + \frac{1}{9}\overline{u}(x)\right] \ . \qquad (40)'$$

$$F_2^{\mathrm{ep}} = 2xF_1^{\mathrm{ep}} = x\left[\frac{4}{9}u(x) + \frac{1}{9}d(x) + \frac{4}{9}\overline{u}(x) + \frac{1}{9}\overline{d}(x)\right] \ . \qquad (41)'$$

$$F_2^{\mathrm{en}} = 2xF_1^{\mathrm{en}} = x\left[\frac{4}{9}d(x) + \frac{1}{9}u(x) + \frac{4}{9}\overline{d}(x) + \frac{1}{9}\overline{u}(x)\right] \ . \qquad (42)'$$

6 Colour Forces

6.1 Matrix Element for Quark-Quark Scattering

At leading order in perturbative QCD, the elastic scattering of two distinct quark flavours, $\mathrm{u} + \mathrm{d} \to \mathrm{u} + \mathrm{d}$ for example, is governed by a single Feynman diagram:

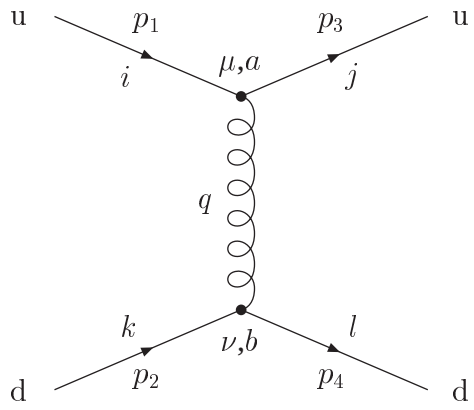

Here, p_1 and p_3 are the 4-momenta of the incoming and outgoing u quark, p_2 and p_4 are the 4-momenta of the incoming and outgoing d quark, and $q = p_1 - p_3 = p_4 - p_2$ is the 4-momentum of the virtual gluon. The labels $i, j, k, l = 1, 2, 3$ (or r,g,b) specify the colour state of the incoming and outgoing quarks; in colour terms the scattering is $ik \to jl$. The labels $\mu, \nu = 0, 1, 2, 3$ at each vertex are spacetime indices, while $a, b = 1, 2, \ldots, 8$ are colour indices.

Applying the QCD Feynman rules to the diagram above gives the following expression for the invariant matrix element:

$$-iM_{\mathrm{fi}} = \left[\overline{u}(p_3) \cdot -\tfrac{1}{2} i g_{\mathrm{s}} \lambda^a_{ij} \gamma^\mu \cdot u(p_1)\right] \cdot \frac{-i g_{\mu\nu}}{q^2} \delta^{ab} \cdot \left[\overline{u}(p_4) \cdot -\tfrac{1}{2} i g_{\mathrm{s}} \lambda^b_{kl} \gamma^\nu \cdot u(p_2)\right] \tag{1}$$

where summation over a and b (and μ and ν) is implied. Hence

$$\boxed{M_{\mathrm{fi}} = -\frac{g_{\mathrm{s}}^2}{4} \lambda^a_{ij} \lambda^a_{kl} \frac{1}{(p_1 - p_3)^2} g_{\mu\nu} \left[\overline{u}(p_3) \gamma^\mu u(p_1)\right] \left[\overline{u}(p_4) \gamma^\nu u(p_2)\right]}, \tag{2}$$

which is just a number which can be worked out once the initial and final spin states and the initial and final colour states have been specified.

The factor λ^a_{ij} in Equation (2) is the element appearing in row i and column j of the SU(3) matrix λ^a, and similarly for the factor λ^b_{kl}. The standard representation of the λ matrices is

$$\lambda^1 = \begin{pmatrix} 0 & 1 & 0 \\ 1 & 0 & 0 \\ 0 & 0 & 0 \end{pmatrix} \qquad \lambda^2 = \begin{pmatrix} 0 & -i & 0 \\ i & 0 & 0 \\ 0 & 0 & 0 \end{pmatrix} \qquad \lambda^3 = \begin{pmatrix} 1 & 0 & 0 \\ 0 & -1 & 0 \\ 0 & 0 & 0 \end{pmatrix}$$

$$\lambda^4 = \begin{pmatrix} 0 & 0 & 1 \\ 0 & 0 & 0 \\ 1 & 0 & 0 \end{pmatrix} \qquad \lambda^5 = \begin{pmatrix} 0 & 0 & -i \\ 0 & 0 & 0 \\ i & 0 & 0 \end{pmatrix} \qquad \lambda^6 = \begin{pmatrix} 0 & 0 & 0 \\ 0 & 0 & 1 \\ 0 & 1 & 0 \end{pmatrix}$$

$$\lambda^7 = \begin{pmatrix} 0 & 0 & 0 \\ 0 & 0 & -i \\ 0 & i & 0 \end{pmatrix} \qquad \lambda^8 = \frac{1}{\sqrt{3}} \begin{pmatrix} 1 & 0 & 0 \\ 0 & 1 & 0 \\ 0 & 0 & -2 \end{pmatrix} .$$

The colour indices i and j, or k and l, appearing in the vertex factors λ^a_{ij} and λ^b_{kl} are ordered such that they follow the colour flow through the vertex, *i.e.* such that the *in*coming colour index (i or k) appears first.

The QCD process $\mathrm{ud} \to \mathrm{ud}$ can be compared with the analagous QED process $\mathrm{e}^-\mu^- \to \mathrm{e}^-\mu^-$, already considered in Handout 5:

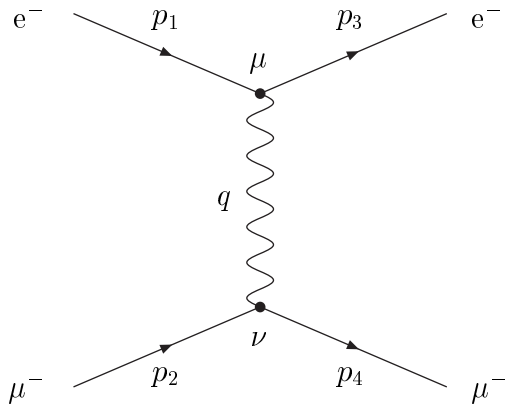

The QED Feynman rules give

$$-iM_{\mathrm{fi}} = [\overline{u}(p_3) \cdot ie\gamma^\mu \cdot u(p_1)] \cdot \frac{-ig_{\mu\nu}}{q^2} \cdot [\overline{u}(p_4) \cdot ie\gamma^\nu \cdot u(p_2)]$$

where p_1 and p_2 are the 4-momenta of the incoming e^- and μ^-, p_3 and p_4 are the 4-momenta of the outgoing e^- and μ^-, and $q = p_1 - p_3 = p_4 - p_2$ is the 4-momentum of the virtual photon. Hence

$$M_{\mathrm{fi}}(\mathrm{e}^-\mu^- \to \mathrm{e}^-\mu^-) = -\frac{e^2}{(p_1 - p_3)^2} g_{\mu\nu} \, [\overline{u}(p_3)\gamma^\mu u(p_1)] \, [\overline{u}(p_4)\gamma^\nu u(p_2)] \ . \tag{3}$$

A comparison of Equations (2) and (3) shows that the QCD matrix element is the same as that from QED, except that the electromagnetic coupling constant e is replaced by the strong coupling constant g_{s} (or equivalently, the fine structure constant $\alpha = e^2/4\pi$ is replaced by the strong coupling constant $\alpha_{\mathrm{s}} = g_{\mathrm{s}}^2/4\pi$), and the QCD matrix element contains an additional *colour factor*

$$\boxed{C(ik \to jl) \equiv \frac{1}{4} \sum_{a=1}^{8} \lambda^a_{ij} \lambda^a_{kl}} \tag{4}$$

where the summation over the eight SU(3) λ matrices has now been made explicit.

6.2 Evaluation of Colour Factors

The colour factor of Equation (4) has to be evaluated for all possible colour configurations of the initial and final states, a total of $3^4 = 81$ possibilities. However, most of these configurations violate conservation of colour charge, and will be seen below to have a colour factor $C = 0$.

6.2.1 Configurations involving a single colour

We consider first those configurations where all incoming and outgoing quarks have the same colour, namely $rr \to rr$, $gg \to gg$ and $bb \to bb$. For $rr \to rr$ for example, we have $i = j = k = l = 1$, and Equation (4) becomes

$$C(rr \to rr) = \frac{1}{4} \sum_{a=1}^{8} (\lambda^a_{11})^2 \ .$$

Inspection of the λ matrices shows that only two of them, λ^3 and λ^8, have non-zero entries in the 11-position: $\lambda^3_{11} = 1$, $\lambda^8_{11} = 1/\sqrt{3}$. Hence

$$C(rr \to rr) = \frac{1}{4} \left[(\lambda^3_{11})^2 + (\lambda^8_{11})^2 \right] = \frac{1}{4} \left(1 + \frac{1}{3} \right) = \frac{1}{3} \ .$$

For $gg \to gg$, we have $i = j = k = l = 2$, and again only λ^3 and λ^8 give a non-zero contribution: $\lambda^3_{22} = -1$, $\lambda^8_{11} = 1/\sqrt{3}$. Hence

$$C(gg \to gg) = \frac{1}{4} \left[(\lambda^3_{22})^2 + (\lambda^8_{22})^2 \right] = \frac{1}{4} \left(1 + \frac{1}{3} \right) = \frac{1}{3} \ .$$

Finally, for $bb \to bb$, we have $i = j = k = l = 3$, and only λ^8 contributes:

$$C(bb \to bb) = \frac{1}{4} (\lambda^8_{33})^2 = \frac{1}{4} \left(\frac{-2}{\sqrt{3}} \right)^2 = \frac{1}{3} \ .$$

In summary, all three such colour configurations produce the same colour factor, reflecting the underlying invariance of QCD under colour rotations:

$$\boxed{C(rr \to rr) = C(gg \to gg) = C(bb \to bb) = \frac{1}{3}} \tag{5}$$

6.2.2 Configurations involving two colours

We now consider colour configurations of the form $rg \to rg$ where the u quark and d quark have different colours and each retains its colour after the scattering. For $rg \to rg$, we have $i = j = 1$ and $k = l = 2$, so

$$C(rg \to rg) = \frac{1}{4} \sum_{a=1}^{8} \lambda^a_{11} \lambda^a_{22} \ .$$

Again, only the matrices λ^3 and λ^8 contribute:

$$C(rg \to rg) = \frac{1}{4}\left(\lambda^3_{11}\lambda^3_{22} + \lambda^8_{11}\lambda^8_{22}\right) = \frac{1}{4}\left(1 \cdot -1 + \frac{1}{\sqrt{3}} \cdot \frac{1}{\sqrt{3}}\right) = -\frac{1}{6}\,.$$

It is straightforward to check that all colour configurations of this type give rise to the same colour factor:

$$\boxed{C(rg \to rg) = C(rb \to rb) = C(gr \to gr) = C(gb \to gb) = C(br \to br) = C(bg \to bg) = -\frac{1}{6}} \tag{6}$$

Another possibility is that the u quark and d quark exchange colours during the scattering, for example $rg \to gr$. In this case we have $i = 1, j = 2$ for the u quark, and $k = 2, l = 1$ for the d quark. The colour factor is then

$$C(rg \to gr) = \frac{1}{4}\sum_{a=1}^{8} \lambda^a_{12}\lambda^a_{21}\,.$$

In this case, only the matrices λ^1 and λ^2 have non-zero entries in the 12 and 21 positions:

$$C(rg \to gr) = \frac{1}{4}\left(\lambda^1_{12}\lambda^1_{21} + \lambda^2_{12}\lambda^2_{21}\right) = \frac{1}{4}\left(1 \cdot 1 + i \cdot -i\right) = \frac{1}{2}\,.$$

Again, it is straightforward to check that all colour configurations of this type give the same colour factor:

$$\boxed{C(rg \to gr) = C(rb \to br) = C(gr \to rg) = C(gb \to bg) = C(br \to rb) = C(bg \to gb) = \frac{1}{2}} \tag{7}$$

6.2.3 Configurations involving all three colours

It remains to consider configurations for which all three colours r,g,b are involved in the scattering, such as $rg \to gb$. For this example we have $i = 1, j = 2$ for the u quark and $k = 2, l = 3$ for the d quark, so that the colour factor is

$$C(rg \to gb) = \frac{1}{4}\sum_{a=1}^{8} \lambda^a_{12}\lambda^a_{23}\,.$$

However, none of the eight λ-matrices has a non-zero entry in both the 12-position and the 23-position, and we therefore obtain immediately that

$$C(rg \to gb) = 0\,.$$

It can easily be checked that the same result holds for all other colour configurations of this type. This is a reflection of *colour conservation* in QCD, namely that the three colour charges (red, green, blue) are *separately* conserved in all processes. To be precise, for a process to be allowed, the net amount of red charge must be the same for the initial and final states, and similarly for the net green charge and the net blue charge.

In summary, for the scattering of two quarks of different flavour, the allowed colour configurations and their associated colour factors are:

$$C(rr \to rr) = C(gg \to gg) = C(bb \to bb) = \frac{1}{3}$$

$$C(rg \to rg) = C(rb \to rb) = C(gr \to gr) = C(gb \to gb) = C(br \to br) = C(bg \to bg) = -\frac{1}{6}$$

$$C(rg \to gr) = C(rb \to br) = C(gr \to rg) = C(gb \to bg) = C(br \to rb) = C(bg \to gb) = \frac{1}{2}$$

6.3 Quark-Antiquark Scattering

For the scattering of a quark and an antiquark of different flavour, such as $\mathrm{u} + \overline{\mathrm{d}} \to \mathrm{u} + \overline{\mathrm{d}}$, the leading-order Feynman diagram becomes

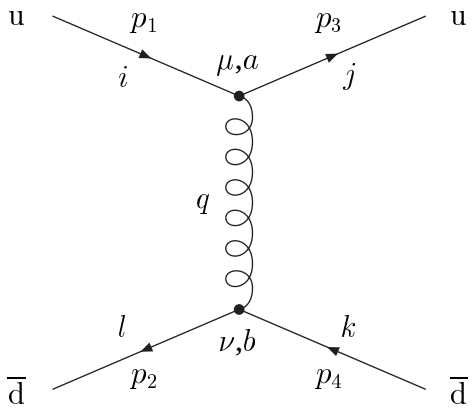

Compared to the quark-quark scattering case just considered, the direction of *particle* flow (the arrows) for the d quark is now reversed. It is convenient also to interchange the colour indices k and l, so that k still labels *particle* colour flowing *into* the lower vertex. Thus, we choose the index k to label the colour state of the outgoing $\overline{\mathrm{d}}$ antiquark, giving a scattering process which in colour terms is of the form $i\overline{l} \to j\overline{k}$. The ordering of the colour indices k and l in the vertex factor then remains unchanged, *i.e.* the matrix element M_{fi} contains a factor λ^b_{kl}, as before.

The QCD Feynman rules give

$$-iM_{\mathrm{fi}} = \left[\overline{u}(p_3) \cdot -\tfrac{1}{2} i g_{\mathrm{s}} \lambda^a_{ij} \gamma^\mu \cdot u(p_1)\right] \cdot \frac{-i g_{\mu\nu}}{q^2} \delta^{ab} \cdot \left[\overline{v}(p_2) \cdot -\tfrac{1}{2} i g_{\mathrm{s}} \lambda^b_{kl} \gamma^\nu \cdot v(p_4)\right]$$

which, apart from the introduction of the antiparticle spinors $\overline{v}(p_2)$ and $v(p_4)$, is the same as the quark-quark scattering matrix element of Equation (1). The colour factor $C(i\overline{l} \to j\overline{k})$ for quark-antiquark scattering is therefore given by the same expression, Equation (4), as for quark-quark scattering:

$$\boxed{C(i\overline{l} \to j\overline{k}) = \frac{1}{4} \sum_{a=1}^{8} \lambda^a_{ij} \lambda^a_{kl} = C(ik \to jl)}. \tag{8}$$

The various non-zero colour factors for $\mathrm{u} + \overline{\mathrm{d}} \to \mathrm{u} + \overline{\mathrm{d}}$ scattering can therefore be written down directly from Equations (5), (6) and (7):

$$C(r\overline{r} \to r\overline{r}) = C(g\overline{g} \to g\overline{g}) = C(b\overline{b} \to b\overline{b}) = \frac{1}{3}$$

$$C(r\overline{g} \to r\overline{g}) = C(r\overline{b} \to r\overline{b}) = C(g\overline{r} \to g\overline{r}) = C(g\overline{b} \to g\overline{b}) = C(b\overline{r} \to b\overline{r}) = C(b\overline{g} \to b\overline{g}) = -\frac{1}{6}$$

$$C(r\overline{r} \to g\overline{g}) = C(r\overline{r} \to b\overline{b}) = C(g\overline{g} \to r\overline{r}) = C(g\overline{g} \to b\overline{b}) = C(b\overline{b} \to r\overline{r}) = C(b\overline{b} \to g\overline{g}) = \frac{1}{2}$$

All other colour configurations have a colour factor of zero and are therefore forbidden.

Quarks and antiquarks of different flavour can also interact through annihilation processes such as $\mathrm{u} + \overline{\mathrm{u}} \to \mathrm{d} + \overline{\mathrm{d}}$:

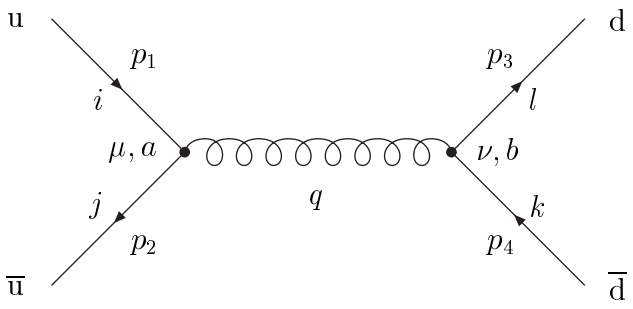

Choosing i and j to label the colours of the incoming u and $\overline{\mathrm{u}}$, and k and l to label the colours of the outgoing $\overline{\mathrm{d}}$ and d, the colour structure is of the form $i\overline{j} \to l\overline{k}$, and the colour factor is again the same as for the quark-quark scattering case:

$$\boxed{C(i\overline{j} \to l\overline{k}) = \frac{1}{4}\sum_{a=1}^{8} \lambda^a_{ij}\lambda^a_{kl} = C(ik \to jl)}. \tag{9}$$

Hence we can write immediately

$$C(r\overline{r} \to r\overline{r}) = C(g\overline{g} \to g\overline{g}) = C(b\overline{b} \to b\overline{b}) = \frac{1}{3}$$

$$C(r\overline{g} \to r\overline{g}) = C(r\overline{b} \to r\overline{b}) = C(g\overline{r} \to g\overline{r}) = C(g\overline{b} \to g\overline{b}) = C(b\overline{r} \to b\overline{r}) = C(b\overline{g} \to b\overline{g}) = \frac{1}{2}$$

$$C(r\overline{r} \to g\overline{g}) = C(r\overline{r} \to b\overline{b}) = C(g\overline{g} \to r\overline{r}) = C(g\overline{g} \to b\overline{b}) = C(b\overline{b} \to r\overline{r}) = C(b\overline{b} \to g\overline{g}) = -\frac{1}{6}$$

In summary, the colour factors found earlier for quark-quark scattering apply equally well to quark-antiquark scattering (for either Feynman diagram), with an appropriate reinterpretation of the colour configuration for the scattering.

6.4 Scattering Involving a Single Quark Flavour (non-examinable)

For completeness, we mention briefly quark-quark and quark-antiquark scattering where only a single quark flavour is involved, for example $\mathrm{u} + \mathrm{u} \to \mathrm{u} + \mathrm{u}$ or $\mathrm{u} + \overline{\mathrm{u}} \to \mathrm{u} + \overline{\mathrm{u}}$. In each case, the scattering is now described by *two* leading-order Feynman diagrams, rather than just one.

For quark-quark scattering, $\mathrm{u} + \mathrm{u} \to \mathrm{u} + \mathrm{u}$, the two leading-order Feynman diagrams are

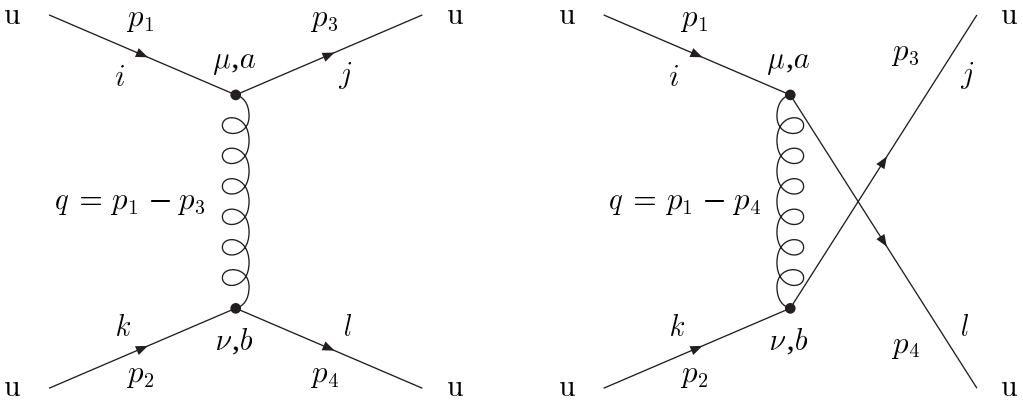

The two diagrams differ by the interchange of the two final-state u quarks, so that the four-momentum carried by the gluon ($q = p_1 - p_3$ or $q = p_1 - p_4$) is different in the two cases. The labelling of the colour structure (taken to be $ik \to jl$) must be the same for both diagrams. The matrix element $M_{\mathrm{fi}}^{(1)}$ for the first diagram then contains the colour factor $\frac{1}{4}\lambda_{ij}^a \lambda_{kl}^a$, while the matrix element $M_{\mathrm{fi}}^{(2)}$ for the second diagram contains instead the colour factor $\frac{1}{4}\lambda_{il}^a \lambda_{kj}^a$ [1]. The overall matrix element for the process $\mathrm{u} + \mathrm{u} \to \mathrm{u} + \mathrm{u}$ is obtained by summing the matrix elements for each diagram: $M_{\mathrm{fi}} = M_{\mathrm{fi}}^{(1)} + M_{\mathrm{fi}}^{(2)}$.

For quark-antiquark scattering, $\mathrm{u} + \overline{\mathrm{u}} \to \mathrm{u} + \overline{\mathrm{u}}$ for example, the two leading-order Feynman diagrams are

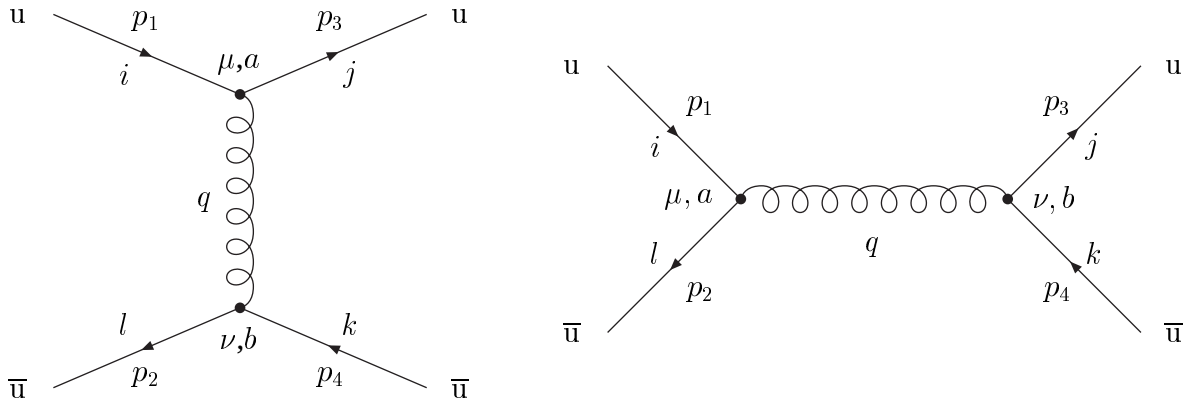

The colour configuration for both diagrams is $i\overline{l} \to j\overline{k}$. As above, the matrix element $M_{\mathrm{fi}}^{(1)}$ for the first diagram contains the colour factor $\frac{1}{4}\lambda_{ij}^a \lambda_{kl}^a$, while the matrix element $M_{\mathrm{fi}}^{(2)}$ for the second diagram contains the colour factor $\frac{1}{4}\lambda_{il}^a \lambda_{kj}^a$.

[1] The matrix elements $M_{\mathrm{fi}}^{(1)}$ and $M_{\mathrm{fi}}^{(2)}$ also have a relative minus sign because of the effect of Fermi statistics due to the interchange of the two final state u quarks.

6.5 Hadron-hadron Scattering

High energy hadron-hadron collisions, as studied at proton-antiproton or proton-proton colliders, for example, involve a mixture of parton-level suprocesses, such as (anti)quark-(anti)quark, (anti)quark-gluon and gluon-gluon scattering.

For the quark-quark scattering subprocess, for example, the incoming quarks are in general not in a well defined colour state, but instead each quark "beam" can be considered to consist of an equal mix of all three colours (r,g,b). Similarly, the colour state of the two final state quarks is in general not fixed. To calculate the contribution to the overall cross section from quark-quark scattering, we must therefore sum over all possible colour configurations and average over all possible colours of each of the incoming quarks [2]:

$$\langle |M_{\rm fi}^2| \rangle = \frac{1}{3} \cdot \frac{1}{3} \cdot \sum_{i,j,k,l=1}^{3} |M_{\rm fi}(ij \to kl)|^2 \ .$$

The colour-averaged matrix element squared then contains the colour factor

$$\langle |C|^2 \rangle = \frac{1}{9} \sum_{i,j,k,l=1}^{3} |C(ij \to kl)|^2 \ .$$

For $\mathrm{u}+\mathrm{d} \to \mathrm{u}+\mathrm{d}$ scattering, for example, summing over the non-zero colour factors in Equations (5), (6) and (7) gives

$$\langle |C(\mathrm{ud} \to \mathrm{ud})|^2 \rangle = \frac{1}{9} \left[3 \times \left(\frac{1}{3} \right)^2 + 6 \times \left(-\frac{1}{6} \right)^2 + 6 \times \left(\frac{1}{2} \right)^2 \right] = \frac{2}{9} \ .$$

The cross section for $\mathrm{u} + \mathrm{d} \to \mathrm{u} + \mathrm{d}$ scattering can be written down directly from the corresponding electromagnetic cross section for $\mathrm{e}^-\mu^- \to \mathrm{e}^-\mu^-$ scattering by replacing α by $\alpha_{\rm s}$ and including an extra colour factor of $2/9$. Thus, the QED Lorentz-invariant cross section [3]

$$\left. \frac{\mathrm{d}\sigma}{\mathrm{d}q^2} \right|_{(\mathrm{e}^-\mu^- \to \mathrm{e}^-\mu^-)} = \frac{2\pi\alpha^2}{q^4} \left[1 + \left(1 + \frac{q^2}{s} \right)^2 \right]$$

becomes the QCD cross section

$$\left. \frac{\mathrm{d}\sigma}{\mathrm{d}q^2} \right|_{(\mathrm{ud} \to \mathrm{ud})} = \frac{4\pi\alpha_{\rm s}^2}{9q^4} \left[1 + \left(1 + \frac{q^2}{\hat{s}} \right)^2 \right] \ ,$$

where $\hat{s}$ is the centre of mass energy squared of the quark-quark collision. This can be expressed as $\hat{s} = (x_1 p_1 + x_2 p_2)^2$, where p_1, p_2 are the four-momenta of the incoming hadrons and x_1, x_2 are the fractional momenta of the incoming partons (the u and d quarks in this case). An integration over $0 < x_1 < 1$ and $0 < x_2 < 1$ is required to obtain the overall cross section, taking into account the parton distribution functions $u(x_1)$ and $d(x_2)$.

Similar considerations apply to quark-antiquark scattering involving two distinct quark flavours, such as $\mathrm{u} + \overline{\mathrm{d}} \to \mathrm{u} + \overline{\mathrm{d}}$ or $\mathrm{u} + \overline{\mathrm{u}} \to \mathrm{d} + \overline{\mathrm{d}}$. The quark-antiquark cross section again contains a colour factor of $2/9$.

[2] This is analagous to the calculation of the spin-averaged matrix element squared for the scattering of unpolarised particles. Such a spin-averaging will also in general be needed for quark-quark scattering, in addition to colour-averaging.

[3] See Equation (4) of Handout 5.

7 Neutrino and Antineutrino Scattering

In Handout 5, deep-inelastic electromagnetic electron-nucleon scattering, $\mathrm{e}^{\pm}\mathrm{N} \to \mathrm{e}^{\pm}\mathrm{X}$, was considered, and parton model predictions were obtained for the electromagnetic structure functions F_1 and F_2. We now consider weak interaction equivalents of this process, namely deep-inelastic (anti)neutrino-nucleon scattering, $\nu_\mu\mathrm{N} \to \mu^-\mathrm{X}$ and $\overline{\nu}_\mu\mathrm{N} \to \mu^+\mathrm{X}$, in which a virtual charged weak boson $\mathrm{W}^{\pm}$ acts as a probe of nucleon structure in place of the virtual photon of electromagnetic scattering.

Neutrino beams from particle accelerators are derived by selecting positively charged hadrons (mainly pions π^+ and kaons K^+) produced by the interactions of a primary proton beam in a target, and allowing these hadrons to decay. The dominant decay modes are $\pi^+ \to \mu^+\nu_\mu$ (BR $\approx 100\%$) and $\mathrm{K}^+ \to \mu^+\nu_\mu$ (BR $\approx 64\%$). The dominant neutrino type (flavour) in a neutrino beam is therefore ν_μ, with only a small (few percent) contamination of ν_e, $\overline{\nu}_\mathrm{e}$ and $\overline{\nu}_\mu$. Similarly, antineutrino beams are obtained by letting negative hadrons decay and are overwhelmingly composed of $\overline{\nu}_\mu$ antineutrinos.

Neglecting contributions from the heavier quark flavours s, c, b, and t, the leading-order quark-level subprocesses contributing to deep-inelastic (anti)neutrino scattering are $\nu_\mu\mathrm{d} \to \mu^-\mathrm{u}$ and $\nu_\mu\overline{\mathrm{u}} \to \mu^-\overline{\mathrm{d}}$ for neutrinos, and $\overline{\nu}_\mu\mathrm{u} \to \mu^+\mathrm{d}$ and $\overline{\nu}_\mu\overline{\mathrm{d}} \to \mu^+\overline{\mathrm{u}}$ for antineutrinos. We begin by obtaining the cross sections for each of these processes in turn, and then use these cross sections to obtain parton model predictions for the (anti)neutrino structure functions F_1, F_2 and F_3. Compared to electromagnetic scattering, an extra structure function F_3 appears because the weak interactions do not conserve parity.

7.1 Neutrino-Quark Scattering

At leading order in perturbation theory, the scattering process $\nu_\mu\mathrm{d} \to \mu^-\mathrm{u}$ is governed by a single Feynman diagram involving the exchange of a virtual $\mathrm{W}^{\pm}$ boson:

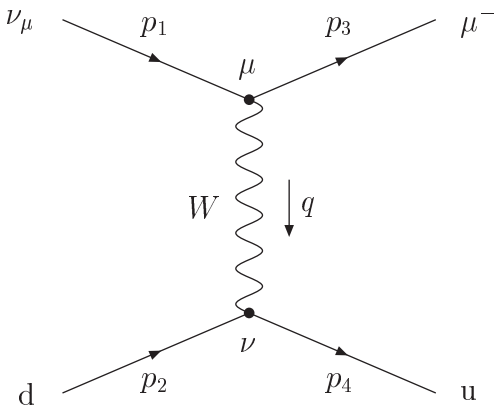

The Feynman rules give

$$-iM_{\rm fi} = \overline{u}(p_3)\cdot -i\frac{g_{\rm W}}{\sqrt{2}}\gamma^\mu \tfrac{1}{2}(1-\gamma^5)\cdot u(p_1)\cdot \frac{-ig_{\mu\nu}}{q^2-m_{\rm W}^2}\cdot \overline{u}(p_4)\cdot -i\frac{g_{\rm W}}{\sqrt{2}}\gamma^\nu \tfrac{1}{2}(1-\gamma^5)\cdot u(p_2)$$

where p_1 and p_2 are the 4-momenta of the incoming ν_μ and d quark, p_3 and p_4 are the 4-momenta of the outgoing μ^- and u quark, and $q = p_1 - p_3 = p_4 - p_2$ is the 4-momentum of the virtual $\mathrm{W}^\pm$.

For current neutrino experiments, with neutrino beam energies ranging up to several hundred GeV, it is shown in the examples sheet that the maximum 4-momentum transfer is small in relation to the W boson mass: $|q^2| \ll m_{\rm W}^2$. The $\mathrm{W}^\pm$ propagator term can therefore be taken to be approximately constant ($\approx ig_{\mu\nu}/m_{\rm W}^2$), in which case the matrix element becomes

$$\boxed{M_{\rm fi} = \frac{g_{\rm W}^2}{2m_{\rm W}^2} g_{\mu\nu}\left[\overline{u}(p_3)\gamma^\mu \tfrac{1}{2}(1-\gamma^5)u(p_1)\right]\left[\overline{u}(p_4)\gamma^\nu \tfrac{1}{2}(1-\gamma^5)u(p_2)\right]}\,. \qquad (1)$$

The matrix element $M_{\rm fi}$ will be evaluated in the extreme relativistic limit where the quark and lepton masses can be neglected.

7.1.1 Helicity considerations

It was shown in Handout 2 that, for a highly relativistic particle, the helicity eigenstates $u_\uparrow(p)$ and $u_\downarrow(p)$ are eigenstates of the operator γ^5: $\gamma^5 u_\uparrow = +u_\uparrow$, $\gamma^5 u_\downarrow = -u_\downarrow$. For these eigenstates, the factors $\frac{1}{2}(1-\gamma^5)u(p_1)$ and $\frac{1}{2}(1-\gamma^5)u(p_2)$ appearing in Equation (1) become

$$\tfrac{1}{2}(1-\gamma^5)u_\uparrow(p_1) = 0 \qquad \tfrac{1}{2}(1-\gamma^5)u_\uparrow(p_2) = 0 \qquad (2)$$
$$\tfrac{1}{2}(1-\gamma^5)u_\downarrow(p_1) = u_\downarrow(p_1) \qquad \tfrac{1}{2}(1-\gamma^5)u_\downarrow(p_2) = u_\downarrow(p_2)\,. \qquad (3)$$

The factors $\frac{1}{2}(1-\gamma^5)u(p_1)$ and $\frac{1}{2}(1-\gamma^5)u(p_2)$ are therefore non-zero only if the incoming ν_μ and the incoming d quark are both in a left-handed (negative helicity) eigenstate, *i.e.* we must take:

$$u(p_1) = u_\downarrow(p_1) \qquad u(p_2) = u_\downarrow(p_2)\,.$$

Similarly, for the outgoing μ^- and u quark, we have

$$\tfrac{1}{2}(1-\gamma^5)u_\uparrow(p_3) = 0 \qquad \tfrac{1}{2}(1-\gamma^5)u_\uparrow(p_4) = 0 \qquad (4)$$
$$\tfrac{1}{2}(1-\gamma^5)u_\downarrow(p_3) = u_\downarrow(p_3) \qquad \tfrac{1}{2}(1-\gamma^5)u_\downarrow(p_4) = u_\downarrow(p_4)\,. \qquad (5)$$

Since the spinors $u(p_3)$ and $u(p_4)$ actually appear in Equation (1) as *adjoint* spinors $\overline{u}(p_3)$ and $\overline{u}(p_4)$, we need to take the adjoints of the above expressions. For a general spinor $u(p)$, with adjoint spinor $\overline{u}(p) \equiv u^\dagger(p)\gamma^0$, we have

$$\overline{\tfrac{1}{2}(1-\gamma^5)u} = \left[\tfrac{1}{2}(1-\gamma^5)u\right]^\dagger \gamma^0 = u^\dagger \tfrac{1}{2}(1-\gamma^5)\gamma^0 = u^\dagger\gamma^0\tfrac{1}{2}(1+\gamma^5) = \overline{u}\tfrac{1}{2}(1+\gamma^5)\,,$$

where we have used the fact that the matrix γ^5 is hermitian: $(\gamma^5)^\dagger = \gamma^5$. Taking the adjoint of Equations (4) and (5) therefore gives

$$\overline{u}_\uparrow(p_3)\tfrac{1}{2}(1+\gamma^5) = 0 \qquad \overline{u}_\uparrow(p_4)\tfrac{1}{2}(1+\gamma^5) = 0 \qquad (6)$$
$$\overline{u}_\downarrow(p_3)\tfrac{1}{2}(1+\gamma^5) = \overline{u}_\downarrow(p_3) \qquad \overline{u}_\downarrow(p_4)\tfrac{1}{2}(1+\gamma^5) = \overline{u}_\downarrow(p_4)\,. \qquad (7)$$

Since γ^μ and γ^5 anticommute, the matrix element of Equation (1) can equally well be written as

$$M_{\rm fi} = \frac{g_{\rm W}^2}{2m_{\rm W}^2} g_{\mu\nu} \left[\overline{u}(p_3)\tfrac{1}{2}(1+\gamma^5)\gamma^\mu u(p_1)\right] \left[\overline{u}(p_4)\tfrac{1}{2}(1+\gamma^5)\gamma^\nu u(p_2)\right] \ .$$

Equations (6) and (7) then show that the matrix element $M_{\rm fi}$ is non-zero only if the outgoing μ^- and the outgoing $\rm u$ quark are both in a left-handed (negative helicity) eigenstate, *i.e.* we must take:

$$u(p_3) = u_\downarrow(p_3) \qquad\qquad u(p_4) = u_\downarrow(p_4) \ .$$

In summary, in the relativistic limit, the matrix element of Equation (1) is non-zero only if *all* the particles involved in the scattering have negative helicity:

$$u(p_1) = u_\downarrow(p_1) \qquad u(p_2) = u_\downarrow(p_2) \qquad u(p_3) = u_\downarrow(p_3) \qquad u(p_4) = u_\downarrow(p_4) \ . \tag{8}$$

In this case, the matrix element simplifies to

$$\boxed{M_{\rm fi} = \frac{g_{\rm W}^2}{2m_{\rm W}^2} g_{\mu\nu} \left[\overline{u}_\downarrow(p_3)\gamma^\mu u_\downarrow(p_1)\right] \left[\overline{u}_\downarrow(p_4)\gamma^\nu u_\downarrow(p_2)\right]} \ . \tag{9}$$

In the centre of mass frame, for example, the scattering can be represented as:

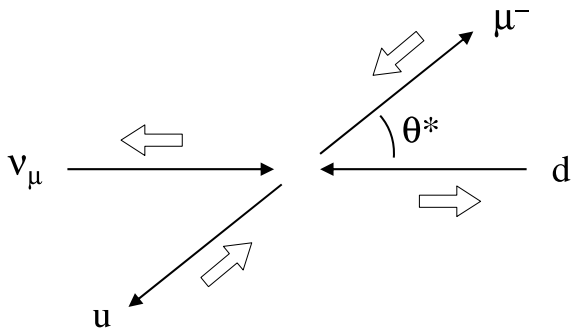

The allowed particle helicities of Equation (8) could also have been deduced using a general result derived in the examples sheet for any two spinors ϕ and ψ:

$$\overline{\phi_{\rm L}}\gamma^\mu\tfrac{1}{2}(1-\gamma^5)\psi_{\rm R} = \overline{\phi_{\rm R}}\gamma^\mu\tfrac{1}{2}(1-\gamma^5)\psi_{\rm L} = \overline{\phi_{\rm R}}\gamma^\mu\tfrac{1}{2}(1-\gamma^5)\psi_{\rm R} = 0 \tag{10}$$

$$\overline{\phi_{\rm L}}\gamma^\mu\tfrac{1}{2}(1-\gamma^5)\psi_{\rm L} = \overline{\phi}\gamma^\mu\tfrac{1}{2}(1-\gamma^5)\psi \ . \tag{11}$$

Thus a current of the form $\overline{\phi}\gamma^\mu\frac{1}{2}(1-\gamma^5)\psi$ is non-zero only for the left-handed chiral components $\phi_{\rm L} = \frac{1}{2}(1-\gamma^5)\phi$ and $\psi_{\rm L} = \frac{1}{2}(1-\gamma^5)\psi$ of the spinors ϕ and ψ. In the relativistic limit, the left-handed chiral component for a particle is identical to the left-handed (negative) helicity eigenstate. Hence, in this limit, all the particles involved in the scattering must have negative helicity.

Equations (10) and (11) show that, in the relativistic limit, *helicity conservation* applies to the weak interactions just as it does in QED and QCD, namely that *particle* helicity is conserved at each weak interaction vertex. For the case of $\nu_\mu {\rm d} \to \mu^- {\rm u}$ scattering considered above, this is illustrated by the fact that the incoming ν_μ and outgoing μ^- have the same helicity, as do the incoming $\rm d$ quark and outgoing $\rm u$ quark.

7.1.2 Evaluation of $M_{\rm fi}$

To evaluate the matrix element of Equation (9), we work in the centre of mass frame and take the 4-momenta to be

$$\begin{aligned} p_1 &= (E,0,0,E), & p_3 &= (E, E\sin\theta^*, 0, E\cos\theta^*) \\ p_2 &= (E,0,0,-E), & p_4 &= (E, -E\sin\theta^*, 0, -E\cos\theta^*)\ . \end{aligned}$$

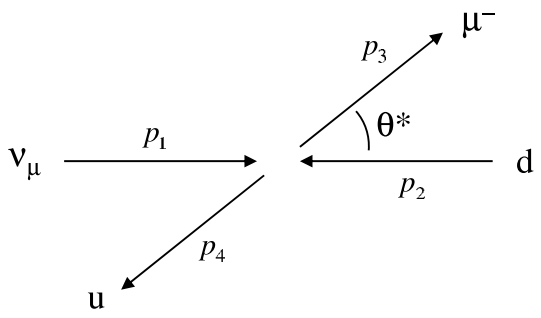

For a highly-relativistic particle with four-momentum $p^\mu = (E, E\sin\theta\cos\phi, E\sin\theta\sin\phi, E\cos\theta)$, the left-handed helicity eigenstate $u_\downarrow(p)$ is [1]

$$u_\downarrow(p) = \sqrt{E}\begin{pmatrix} -s \\ e^{i\phi}c \\ s \\ -e^{i\phi}c \end{pmatrix}$$

where $c \equiv \cos\theta/2$ and $s \equiv \sin\theta/2$. Taking $(\theta,\phi) = (0,0), (\pi,0), (\theta^*,0)$ and $(\pi-\theta^*,\pi)$ for the ν_μ, d, μ^- and u respectively, the left-handed spinors for each particle are

$$u_\downarrow(p_1) = \sqrt{E}\begin{pmatrix} 0 \\ 1 \\ 0 \\ -1 \end{pmatrix};\quad u_\downarrow(p_2) = \sqrt{E}\begin{pmatrix} -1 \\ 0 \\ 1 \\ 0 \end{pmatrix};\quad u_\downarrow(p_3) = \sqrt{E}\begin{pmatrix} -s \\ c \\ s \\ -c \end{pmatrix};\quad u_\downarrow(p_4) = \sqrt{E}\begin{pmatrix} -c \\ -s \\ c \\ s \end{pmatrix}$$

where $c \equiv \cos\theta^*/2$, $s \equiv \sin\theta^*/2$, and we have used the identities $\sin((\pi-\theta^*)/2) = \cos\theta^*/2 = c$ and $\cos((\pi-\theta^*)/2) = \sin\theta^*/2 = s$.

With the replacement

$$\frac{e^2}{(p_1-p_3)^2} \quad\longrightarrow\quad \frac{g_{\rm W}^2}{2m_{\rm W}^2}\ , \tag{12}$$

the matrix element of Equation (9), and the spinors above, are the same as those used in the evaluation of the matrix element

$$(M_{\rm LL})_{(e\mu\to e\mu)} = \frac{e^2}{(p_1-p_3)^2} g_{\mu\nu}\left[\overline{u}_\downarrow(p_3)\gamma^\mu u_\downarrow(p_1)\right]\left[\overline{u}_\downarrow(p_4)\gamma^\nu u_\downarrow(p_2)\right]$$

[1] See Equation (55) of Handout 2.

for $\mathrm{e}^-\mu^- \to \mathrm{e}^-\mu^-$ scattering in Question 10 on the examples sheet. It was found there that

$$|M_{\mathrm{LL}}|^2_{(\mathrm{e}\mu\to\mathrm{e}\mu)} = \frac{e^4}{(p_1-p_3)^4}\cdot 4s^2$$

where $s = (p_1+p_2)^2$ is the centre of mass energy squared. Applying the transformation of Equation (12) to this result, we obtain directly, for neutrino-quark scattering,

$$|M_{\mathrm{LL}}|^2 = \left(\frac{g_{\mathrm{W}}^2}{2m_{\mathrm{W}}^2}\right)^2 \cdot 4\hat{s}^2 = \left(\frac{g_{\mathrm{W}}^2\hat{s}}{m_{\mathrm{W}}^2}\right)^2 \tag{13}$$

where $\hat{s} \equiv (p_1+p_2)^2$ is the neutrino-quark centre of mass energy squared. (The variable s will be reserved for the neutrino-*nucleon* cms energy squared.)

In the case of $\mathrm{e}^-\mu^- \to \mathrm{e}^-\mu^-$ scattering, the spin-averaged matrix element squared appropriate to unpolarised scattering was evaluated as

$$\langle|M_{\mathrm{fi}}|^2\rangle_{(\mathrm{e}\mu\to\mathrm{e}\mu)} = \tfrac{1}{2}\cdot\tfrac{1}{2}\cdot\left(|M_{\mathrm{LL}}|^2+|M_{\mathrm{RR}}|^2+|M_{\mathrm{LR}}|^2+|M_{\mathrm{RL}}|^2\right)$$

where the first factor of $\frac{1}{2}$ represents an average over the incoming e^- spin states and the second an average over the incoming μ^- spins. For neutrino-quark scattering, only left-handed particles contribute, so that $M_{\mathrm{RR}} = M_{\mathrm{LR}} = M_{\mathrm{RL}} = 0$. In addition, no averaging over the incoming *neutrino* spin states is necessary because neutrinos are *always* produced with negative helicity, and a neutrino beam is therefore always purely left-handed (at least to the extent that neutrinos are exactly massless). For neutrino-quark scattering, we therefore have just

$$\langle|M_{\mathrm{fi}}|^2\rangle = \tfrac{1}{2}\cdot|M_{\mathrm{LL}}|^2 \tag{14}$$

where the single factor of $\frac{1}{2}$ averages over the possible spin states of the incoming d quark.

Combining Equations (13) and (14), we obtain, for neutrino-quark scattering,

$$\langle|M_{\mathrm{fi}}|^2\rangle = \left(\frac{g_{\mathrm{W}}^2\hat{s}}{\sqrt{2}m_{\mathrm{W}}^2}\right)^2 . \tag{15}$$

In the extreme relativistic limit, the differential cross section for any $2\to 2$ body scattering process in the centre of mass frame is given by [2]

$$\frac{\mathrm{d}\sigma}{\mathrm{d}\Omega} = \frac{1}{64\pi^2\hat{s}}\langle|M_{\mathrm{fi}}|^2\rangle .$$

Hence:

$$\frac{\mathrm{d}\sigma}{\mathrm{d}\Omega} = \frac{1}{64\pi^2\hat{s}}\left(\frac{g_{\mathrm{W}}^2\hat{s}}{\sqrt{2}m_{\mathrm{W}}^2}\right)^2 = \left(\frac{g_{\mathrm{W}}^2}{8\sqrt{2}\pi m_{\mathrm{W}}^2}\right)^2\hat{s} .$$

Using the relation

$$\frac{G_{\mathrm{F}}}{\sqrt{2}} = \frac{g_{\mathrm{W}}^2}{8m_{\mathrm{W}}^2}$$

[2] See Equation (26) of Handout 3.

between the weak coupling constant g_{W} and the Fermi constant G_{F} (see Section 7.7 below), the neutrino-quark differential cross section can be written as

$$\boxed{\frac{\mathrm{d}\sigma^{\nu q}}{\mathrm{d}\Omega} = \frac{G_{\mathrm{F}}^2}{4\pi^2}\hat{s}}\,. \tag{16}$$

The neutrino-quark cross section is therefore proportional to the centre of mass energy squared $\hat{s}$ and independent of the scattering angle θ^*, *i.e.* neutrino-quark scattering in the centre of mass frame is isotropic. This can be understood because the incoming ν_μ neutrino and the incoming d quark both have negative helicity; hence the total spin of the initial state is zero. Since the total 3-momentum is also zero in the centre of mass frame, there is no preferred spatial direction involved in the scattering.

Integrating the differential cross section of Equation (16) over all possible angles θ^* and ϕ^* results in an extra factor of 4π and hence a total cross section

$$\boxed{\sigma_{\nu q} = \frac{G_{\mathrm{F}}^2\hat{s}}{\pi}}\,. \tag{17}$$

Note that this expression is Lorentz invariant and hence valid in any frame of reference.

7.2 Antineutrino-Quark Scattering

The leading-order Feynman diagram for the antineutrino-quark scattering process $\overline{\nu}_\mu \mathrm{u} \to \mu^+ \mathrm{d}$ is

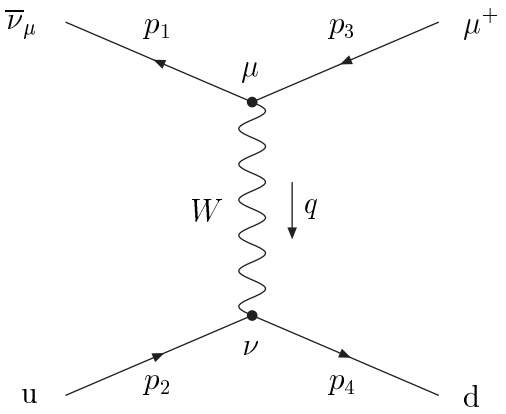

The matrix element for this process is the same as that for neutrino-quark scattering, Equation (1), except that the lepton current now contains the *antiparticle* spinors $v(p_1)$ and $v(p_3)$ in place of the particle spinors $u(p_1)$ and $u(p_3)$:

$$M_{\mathrm{fi}} = \frac{g_{\mathrm{W}}^2}{2m_{\mathrm{W}}^2} g_{\mu\nu} \left[\overline{v}(p_1)\gamma^\mu \tfrac{1}{2}(1-\gamma^5)v(p_3)\right]\left[\overline{u}(p_4)\gamma^\nu \tfrac{1}{2}(1-\gamma^5)u(p_2)\right]\,. \tag{18}$$

As before, this matrix element is non-zero only for the left-handed chiral components of all the particles and antiparticles involved in the scattering. In the relativistic limit, the left-handed chiral component of a *particle* corresponds to the left-handed helicity eigenstate $u_\downarrow$ while the left-handed chiral

component of an *antiparticle* corresponds to the right-handed helicity eigenstate $v_\uparrow$. This requires that we take the u and d quarks to be left-handed and the $\overline{\nu}_\mu$ and μ^+ antiparticles to be right-handed:

$$v(p_1) = v_\uparrow(p_1); \qquad u(p_2) = u_\downarrow(p_2); \qquad v(p_3) = v_\uparrow(p_3); \qquad u(p_4) = u_\downarrow(p_4)\ .$$

The matrix element then becomes

$$M_{\rm fi} = \frac{g_{\rm W}^2}{2m_{\rm W}^2} g_{\mu\nu} \left[\overline{v}_\uparrow(p_1)\gamma^\mu \tfrac{1}{2}(1-\gamma^5)v_\uparrow(p_3)\right]\left[\overline{u}_\downarrow(p_4)\gamma^\nu \tfrac{1}{2}(1-\gamma^5)u_\downarrow(p_2)\right]\ . \tag{19}$$

In the centre of mass frame, the spin states can be represented schematically as:

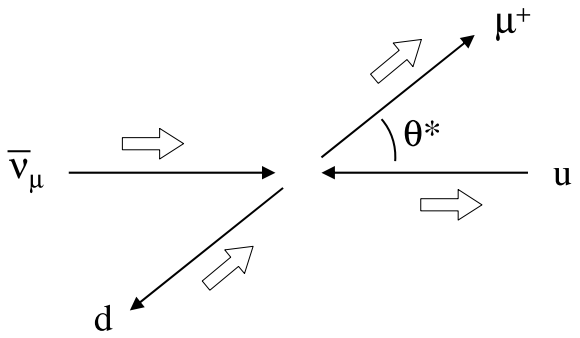

The quark current $\overline{u}_\downarrow(p_4)\gamma^\nu \frac{1}{2}(1-\gamma^5)u_\downarrow(p_2)$ appearing in Equation (19) is the same as that already considered above for neutrino-quark scattering, but the lepton current $\overline{v}_\uparrow(p_1)\gamma^\mu \frac{1}{2}(1-\gamma^5)v_\uparrow(p_3)$ is of a form not so far encountered. This current could clearly be evaluated in the standard way using explicit forms for the spinors $v_\uparrow(p_1)$ and $v_\uparrow(p_3)$, but we can instead anticipate the result simply by considering the overall spin configuration for the scattering. Taking the incoming antineutrino to be travelling in the $+z$ direction, the initial state has a total spin $S_z = +1$ directed along the z-axis, while the final state has a total spin projection of $+1$ directed at an angle θ^* to the z-axis. Just as was found earlier for $\mathrm{e}^-\mu^- \to \mathrm{e}^-\mu^-$ scattering, the matrix element squared therefore picks up an extra factor of $\frac{1}{4}(1+\cos\theta^*)^2$ compared to isotropic scattering, Equation (15), and we can immediately write

$$\langle |M_{\rm fi}|^2 \rangle = \left(\frac{g_{\rm W}^2 \hat{s}}{\sqrt{2}m_{\rm W}^2}\right)^2 \cdot \tfrac{1}{4}(1+\cos\theta^*)^2\ .$$

The differential cross section for antineutrino-quark scattering in the centre of mass frame is therefore

$$\boxed{\frac{{\rm d}\sigma^{\overline{\nu}q}}{{\rm d}\Omega} = \frac{G_{\rm F}^2}{16\pi^2}\hat{s}(1+\cos\theta^*)^2\ .} \tag{20}$$

with ${\rm d}\Omega = 2\pi {\rm d}\cos\theta^*$. Integrating over all solid angles using

$$\int (1+\cos\theta^*)^2 {\rm d}\Omega = 2\pi \int_{-1}^{+1} (1+\cos\theta^*)^2 {\rm d}\cos\theta^* = \frac{16\pi}{3}$$

gives the total cross section

$$\boxed{\sigma^{\overline{\nu}q} = \frac{G_{\rm F}^2}{3\pi}\hat{s}}\ .$$

This is a factor of three smaller than the corresponding neutrino total cross section of Equation (17):

$$\boxed{\frac{\sigma^{\overline{\nu}q}}{\sigma^{\nu q}} = \frac{1}{3}}\ .$$

7.3 Neutrino-Antiquark and Antineutrino-Antiquark Scattering

The cross sections for neutrino and antineutrino scattering from an antiquark rather than a quark can be written down directly from the results above; explicit calculation of the currents appearing in the matrix element expressions can again be avoided by appealing to a consideration of the spin states involved in the scattering.

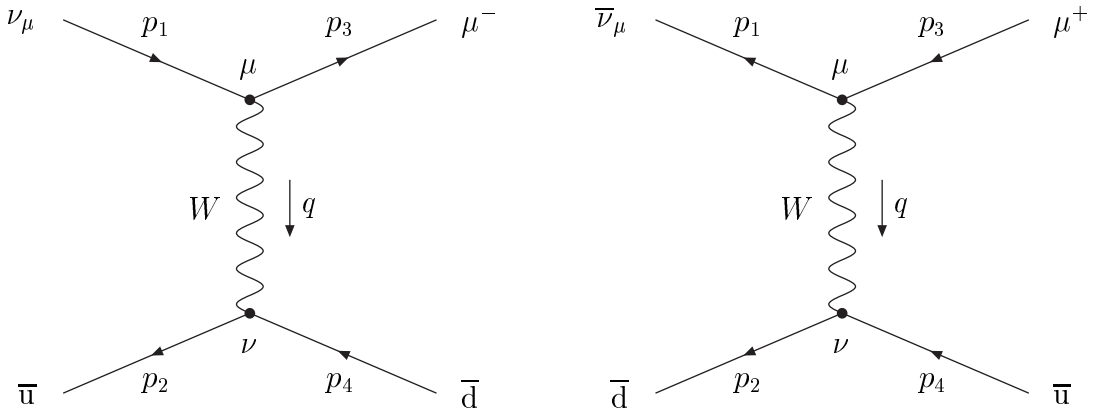

For neutrino-antiquark scattering, $\nu_\mu \overline{\mathrm{u}} \to \mu^- \overline{\mathrm{d}}$, the ν_μ and μ^- particles must be left-handed while the $\overline{\mathrm{u}}$ and $\overline{\mathrm{d}}$ antiquarks must be right-handed. The matrix element is therefore

$$M_{\mathrm{fi}} = \frac{g_{\mathrm{W}}^2}{2m_{\mathrm{W}}^2} g_{\mu\nu} \left[\overline{u}_\downarrow(p_3)\gamma^\mu \tfrac{1}{2}(1-\gamma^5)u_\downarrow(p_1)\right]\left[\overline{v}_\uparrow(p_2)\gamma^\nu \tfrac{1}{2}(1-\gamma^5)v_\uparrow(p_4)\right] \ . \tag{21}$$

In the centre of mass frame, the initial state has a total spin $S_z = -1$ directed along the z-axis while the final state has a total spin projection of -1 directed at an angle θ^* to the z-axis. The matrix element squared therefore has an angular dependence of the form $\frac{1}{4}(1+\cos\theta^*)^2$ and the resulting differential cross section is the same as for antineutrino-quark scattering:

$$\boxed{\frac{\mathrm{d}\sigma^{\nu\overline{\mathrm{q}}}}{\mathrm{d}\Omega} = \frac{G_{\mathrm{F}}^2}{16\pi^2}\hat{s}(1+\cos\theta^*)^2} \ . \tag{22}$$

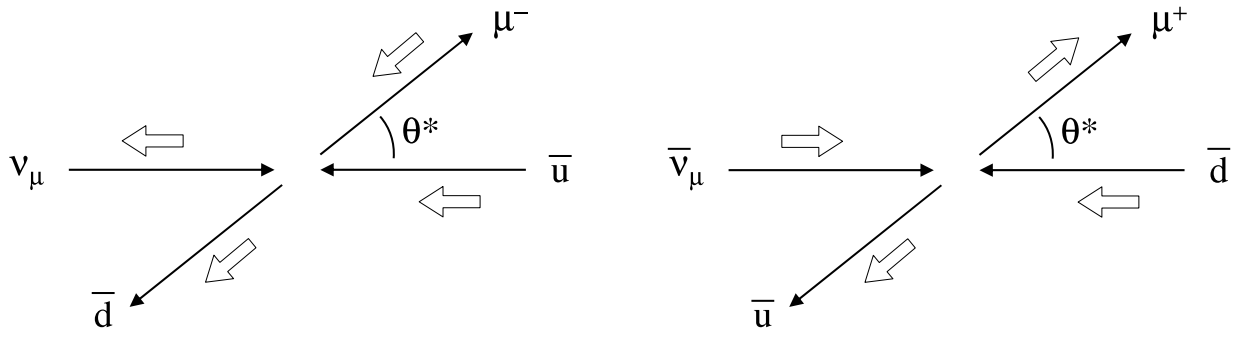

For antineutrino-antiquark scattering, $\overline{\nu}_\mu \overline{\mathrm{d}} \to \mu^+ \overline{\mathrm{u}}$, all antiparticles involved must be right-handed and the matrix element is

$$M_{\mathrm{fi}} = \frac{g_{\mathrm{W}}^2}{2m_{\mathrm{W}}^2} g_{\mu\nu} \left[\overline{v}_\uparrow(p_1)\gamma^\mu \tfrac{1}{2}(1-\gamma^5)v_\uparrow(p_3)\right]\left[\overline{v}_\uparrow(p_2)\gamma^\nu \tfrac{1}{2}(1-\gamma^5)v_\uparrow(p_4)\right] \ . \tag{23}$$

The initial and final states in the centre of mass frame both have zero total spin, and the scattering is therefore isotropic:

$$\boxed{\frac{\mathrm{d}\sigma^{\overline{\nu}\mathrm{q}}}{\mathrm{d}\Omega} = \frac{G_{\mathrm{F}}^2}{4\pi^2}\hat{s}} \,. \tag{24}$$

7.4 The Differential Cross Section $\mathrm{d}\sigma/\mathrm{d}y$

The differential cross sections derived above, Equations (16), (20), (22) and (24), are valid only in the (anti)neutrino-(anti)quark centre of mass frame. To obtain parton model predictions for the overall (anti)neutrino-nucleon differential cross sections, we require Lorentz-invariant forms of the quark-level cross sections valid in any reference frame.

A useful Lorentz-invariant variable for the description of high energy scattering is

$$y \equiv \frac{p_2.q}{p_2.p_1} \,.$$

In the relativistic limit, the variable y is related to the centre of mass scattering angle θ^* as [3]

$$y = \tfrac{1}{2}(1 - \cos\theta^*) \,. \tag{25}$$

The variable y therefore covers the range

$$0 < y < 1 \,.$$

Using Equation (25), we can convert a differential cross section $\mathrm{d}\sigma/\mathrm{d}\Omega$ evaluated in the centre of mass frame ($\mathrm{d}\Omega = 2\pi \mathrm{d}\cos\theta^*$) to a Lorentz-invariant differential cross section of the form $\mathrm{d}\sigma/\mathrm{d}y$:

$$\frac{\mathrm{d}\sigma}{\mathrm{d}y} = \left|\frac{\mathrm{d}\cos\theta^*}{\mathrm{d}y}\right| \frac{\mathrm{d}\sigma}{\mathrm{d}\cos\theta^*} = \left|\frac{\mathrm{d}\cos\theta^*}{\mathrm{d}y}\right| 2\pi\frac{\mathrm{d}\sigma}{\mathrm{d}\Omega} = 4\pi\frac{\mathrm{d}\sigma}{\mathrm{d}\Omega} \,.$$

The neutrino-quark and antineutrino-antiquark scattering cross sections of Equations (16) and (24) can then be expressed in invariant form as

$$\boxed{\frac{\mathrm{d}\sigma^{\nu q}}{\mathrm{d}y} = \frac{\mathrm{d}\sigma^{\overline{\nu}\mathrm{q}}}{\mathrm{d}y} = \frac{G_{\mathrm{F}}^2}{\pi}\hat{s}} \,. \tag{26}$$

Similarly, the $\overline{\nu}q$ and $\nu\overline{\mathrm{q}}$ cross sections of Equations (20) and (22) become

$$\frac{\mathrm{d}\sigma^{\overline{\nu}q}}{\mathrm{d}y} = \frac{\mathrm{d}\sigma^{\nu\overline{\mathrm{q}}}}{\mathrm{d}y} = 4\pi \cdot \frac{G_{\mathrm{F}}^2}{16\pi^2}\hat{s}(1 + \cos\theta^*)^2 \,.$$

Since $1 - y = \frac{1}{2}(1 + \cos\theta^*)$, we obtain

$$\boxed{\frac{\mathrm{d}\sigma^{\overline{\nu}q}}{\mathrm{d}y} = \frac{\mathrm{d}\sigma^{\nu\overline{\mathrm{q}}}}{\mathrm{d}y} = \frac{G_{\mathrm{F}}^2}{\pi}\hat{s}(1-y)^2} \,. \tag{27}$$

[3] See Equation (7) of Handout 5.

The invariant cross sections of Equations (26) and (27) will be used below to obtain parton model predictions for the neutrino and antineutrino deep-inelastic cross sections.

For comparison, we note that the corresponding electromagnetic cross sections for $\mathrm{e}^{\pm}\mathrm{q} \to \mathrm{e}^{\pm}\mathrm{q}$ or $\mathrm{e}^{\pm}\overline{\mathrm{q}} \to \mathrm{e}^{\pm}\overline{\mathrm{q}}$ elastic scattering take the form [4]

$$\frac{\mathrm{d}\sigma^{\mathrm{eq}}}{\mathrm{d}y} = \frac{2\pi\alpha^2}{q^4} e_q^2 \hat{s}\left[1 + (1-y)^2\right] \ .$$

7.5 Deep-inelastic Neutrino Scattering

We now consider deep-inelastic neutrino-nucleon and antineutrino-nucleon scattering, $\nu_\mu \mathrm{N} \to \mu^- \mathrm{X}$ and $\overline{\nu}_\mu \mathrm{N} \to \mu^+ \mathrm{X}$:

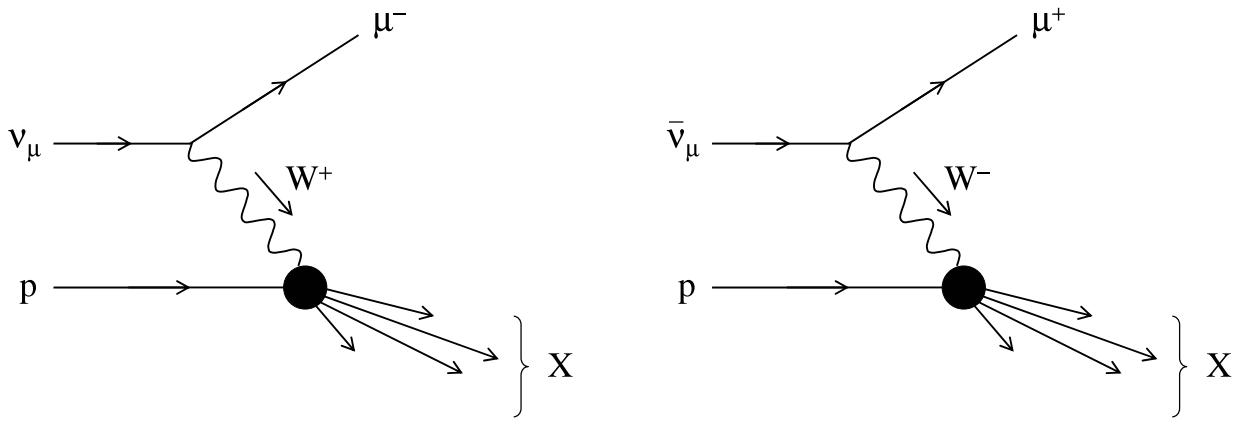

In this section, general model-independent expressions for the inelastic cross sections are presented which assume only that the scattering is dominated by the exchange of a single, virtual $\mathrm{W}^{\pm}$ boson. In the next section, these general expressions are compared with the cross sections predicted by the quark-parton model.

7.5.1 Electromagnetic scattering revisited

The most general possible form for the high energy ($s \gg M^2$) electromagnetic deep-inelastic cross section consistent with single photon exchange and parity conservation was presented in Handout 5 in the form [5]

$$\frac{\mathrm{d}^2\sigma^{\mathrm{em}}}{\mathrm{d}x\mathrm{d}Q^2} = \frac{4\pi\alpha^2}{Q^4}\left[(1-y)\frac{F_2(x,Q^2)}{x} + \frac{1}{2}y^2\frac{2xF_1(x,Q^2)}{x}\right] \ . \tag{28}$$

Instead of using x and Q^2 as the independent variables, we could equally well use the variables x and y, and this is in fact a more usual choice for the neutrino case. At high energy, $s \gg M^2$, we have

[4] See Equation (9) of Handout 5.

[5] See Equations (37) and (38) of Handout 5.

$Q^2 = (s - M^2)xy \approx sxy$ and hence

$$\frac{\mathrm{d}^2\sigma}{\mathrm{d}x\mathrm{d}y} = \left|\frac{\mathrm{d}Q^2}{\mathrm{d}y}\right| \frac{\mathrm{d}^2\sigma}{\mathrm{d}x\mathrm{d}Q^2} = sx\frac{\mathrm{d}^2\sigma}{\mathrm{d}x\mathrm{d}Q^2} \ .$$

Hence, in terms of x and y, the electromagnetic cross section becomes

$$\boxed{\frac{\mathrm{d}^2\sigma^{\mathrm{em}}}{\mathrm{d}x\mathrm{d}y} = \frac{4\pi\alpha^2 s}{Q^4}\left[(1-y)\,F_2(x,y) + \frac{y^2}{2}2xF_1(x,y)\right]}.$$

7.5.2 General form of the neutrino cross section

In the case of (anti)neutrino deep-inelastic scattering, the general, model-independent cross section expressions are similar in form to the electromagnetic cross section given above except that now *three* structure functions F_1, F_2, F_3 are involved. The extra structure function F_3 is permitted because the weak interactions are not invariant under parity.

It can be shown that, for $s \gg M^2$, the most general form of the neutrino-proton cross section is

$$\nu_\mu \mathrm{p} \to \mu^- \mathrm{X}: \qquad \frac{\mathrm{d}^2\sigma^{\nu\mathrm{p}}}{\mathrm{d}x\mathrm{d}y} = \frac{G_{\mathrm{F}}^2 s}{2\pi}\left[(1-y)\,F_2^{\nu\mathrm{p}} + \frac{y^2}{2}2xF_1^{\nu\mathrm{p}} + y\left(1-\frac{y}{2}\right)xF_3^{\nu\mathrm{p}}\right] \ , \qquad (29)$$

and that the antineutrino cross section is similar except that the parity-violating F_3 term changes sign:

$$\overline{\nu}_\mu \mathrm{p} \to \mu^+ \mathrm{X}: \qquad \frac{\mathrm{d}^2\sigma^{\overline{\nu}\mathrm{p}}}{\mathrm{d}x\mathrm{d}y} = \frac{G_{\mathrm{F}}^2 s}{2\pi}\left[(1-y)\,F_2^{\overline{\nu}\mathrm{p}} + \frac{y^2}{2}2xF_1^{\overline{\nu}\mathrm{p}} - y\left(1-\frac{y}{2}\right)xF_3^{\overline{\nu}\mathrm{p}}\right] \ . \qquad (30)$$

Exactly similar expressions hold for scattering from a neutron target, with the proton structure functions $F_i^{\nu\mathrm{p}}$ and $F_i^{\overline{\nu}\mathrm{p}}$ replaced by the neutron structure functions $F_i^{\nu\mathrm{n}}$ and $F_i^{\overline{\nu}\mathrm{n}}$:

$$\nu_\mu \mathrm{n} \to \mu^- \mathrm{X}: \qquad \frac{\mathrm{d}^2\sigma^{\nu\mathrm{n}}}{\mathrm{d}x\mathrm{d}y} = \frac{G_{\mathrm{F}}^2 s}{2\pi}\left[(1-y)\,F_2^{\nu\mathrm{n}} + \frac{y^2}{2}2xF_1^{\nu\mathrm{n}} + y\left(1-\frac{y}{2}\right)xF_3^{\nu\mathrm{n}}\right] \ , \qquad (31)$$

$$\overline{\nu}_\mu \mathrm{n} \to \mu^+ \mathrm{X}: \qquad \frac{\mathrm{d}^2\sigma^{\overline{\nu}\mathrm{n}}}{\mathrm{d}x\mathrm{d}y} = \frac{G_{\mathrm{F}}^2 s}{2\pi}\left[(1-y)\,F_2^{\overline{\nu}\mathrm{n}} + \frac{y^2}{2}2xF_1^{\overline{\nu}\mathrm{n}} - y\left(1-\frac{y}{2}\right)xF_3^{\overline{\nu}\mathrm{n}}\right] \ . \qquad (32)$$

Note that, compared to the electromagnetic case, the replacement

$$\frac{4\pi\alpha^2}{Q^4} \to \frac{G_{\mathrm{F}}^2}{2\pi}$$

has been made for the overall factor on the right-hand side. The absence of the $1/Q^4$ factor in the neutrino case reflects the fact that the $\mathrm{W}^\pm$ propagator factor $-ig_{\mu\nu}/(q^2 - m_{\mathrm{W}}^2) = ig_{\mu\nu}/(Q^2 + m_{\mathrm{W}}^2)$ is approximately constant for $Q^2 \ll m_{\mathrm{W}}^2$.

Just as in the electromagnetic case, the structure functions F_i cannot (yet) be predicted from first principles and have to be determined experimentally. In general, they are two-dimensional functions of the form $F_i(x,y)$ or $F_i(x,Q^2)$, but in practice show approximate Bjorken scaling $F_i = F_i(x)$.

7.6 The Parton Model for Neutrino Scattering

7.6.1 Parton model cross sections

At the quark level, neglecting contributions from the heavier quark flavours s, c, b and t, neutrino-proton scattering can take place via scattering from (valence or sea) d quarks, $\nu_\mu \mathrm{d} \to \mu^- \mathrm{u}$, or via scattering from $\overline{\mathrm{u}}$ antiquarks in the sea, $\nu_\mu \overline{\mathrm{u}} \to \mu^- \overline{\mathrm{d}}$:

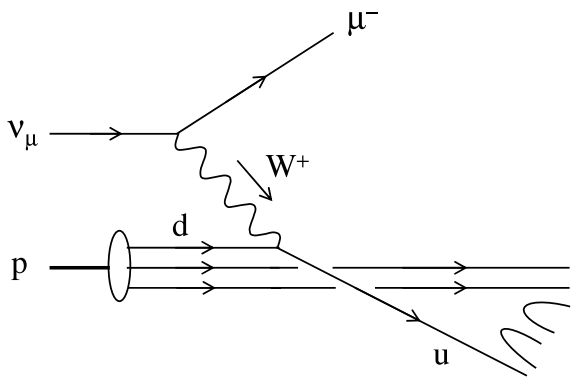

In the parton model, the contribution to the neutrino-proton cross section from d quarks with momentum fraction in the range x to $x + \mathrm{d}x$ is obtained by multiplying the $\nu_\mu \mathrm{d} \to \mu^- \mathrm{u}$ cross section of Equation (26) by a factor $d^{\mathrm{p}}(x)\mathrm{d}x$ representing the number of d quarks in this interval of x:

$$\frac{\mathrm{d}\sigma^{\nu \mathrm{p}}}{\mathrm{d}y} = \frac{G_{\mathrm{F}}^2}{\pi} \hat{s} \cdot d^{\mathrm{p}}(x)\mathrm{d}x \ .$$

Similarly, the contribution from $\overline{\mathrm{u}}$ antiquarks in this momentum range is obtained from Equation (27):

$$\frac{\mathrm{d}\sigma^{\nu \mathrm{p}}}{\mathrm{d}y} = \frac{G_{\mathrm{F}}^2}{\pi} \hat{s}(1-y)^2 \cdot \overline{u}^{\mathrm{p}}(x)\mathrm{d}x \ .$$

The overall neutrino-proton cross section is obtained by summing these two contributions and dividing by $\mathrm{d}x$:

$$\frac{\mathrm{d}^2\sigma^{\nu \mathrm{p}}}{\mathrm{d}x\mathrm{d}y} = \frac{G_{\mathrm{F}}^2}{\pi} sx \left[d^{\mathrm{p}}(x) + (1-y)^2 \overline{u}^{\mathrm{p}}(x) \right] \ ,$$

where we have also used the connection $\hat{s} = sx$ between the neutrino-quark and neutrino-proton centre of mass energies squared.

For antineutrino-proton scattering, the possible parton level scattering processes are $\overline{\nu}_\mu \mathrm{u} \to \mu^+ \mathrm{d}$ and $\overline{\nu}_\mu \overline{\mathrm{d}} \to \mu^+ \overline{\mathrm{u}}$. These combine to give an overall cross section

$$\frac{\mathrm{d}^2\sigma^{\overline{\nu} \mathrm{p}}}{\mathrm{d}x\mathrm{d}y} = \frac{G_{\mathrm{F}}^2}{\pi} sx \left[(1-y)^2 u^{\mathrm{p}}(x) + \overline{d}^{\mathrm{p}}(x) \right] \ .$$

Similarly, for scattering from a neutron target instead of a proton target, the parton model cross sections are

$$\frac{\mathrm{d}^2\sigma^{\nu \mathrm{n}}}{\mathrm{d}x\mathrm{d}y} = \frac{G_{\mathrm{F}}^2}{\pi} sx \left[d^{\mathrm{n}}(x) + (1-y)^2 \overline{u}^{\mathrm{n}}(x) \right]$$

$$\frac{\mathrm{d}^2\sigma^{\overline{\nu}\mathrm{n}}}{\mathrm{d}x\mathrm{d}y} = \frac{G_\mathrm{F}^2}{\pi} sx\left[(1-y)^2 u^\mathrm{n}(x) + \overline{d}^\mathrm{n}(x)\right] \ .$$

The parton distribution functions for the proton and neutron can be related via isospin invariance as

$$\begin{aligned} u(x) \equiv u^\mathrm{p}(x) = d^\mathrm{n}(x), \qquad & d(x) \equiv d^\mathrm{p}(x) = u^\mathrm{n}(x) \ , \\ \overline{u}(x) \equiv \overline{u}^\mathrm{p}(x) = \overline{d}^\mathrm{n}(x), \qquad & \overline{d}(x) \equiv \overline{d}^\mathrm{p}(x) = \overline{u}^\mathrm{n}(x) \ . \end{aligned}$$

The parton model predictions for the various differential cross sections can then all be written in terms of the functions $u(x)$, $d(x)$, $\overline{u}(x)$ and $\overline{d}(x)$:

$$\nu_\mu\mathrm{p} \to \mu^-\mathrm{X}: \qquad \frac{\mathrm{d}^2\sigma^{\nu\mathrm{p}}}{\mathrm{d}x\mathrm{d}y} = \frac{G_\mathrm{F}^2}{\pi} sx\left[d(x) + (1-y)^2\overline{u}(x)\right] \tag{33}$$

$$\overline{\nu}_\mu\mathrm{p} \to \mu^+\mathrm{X}: \qquad \frac{\mathrm{d}^2\sigma^{\overline{\nu}\mathrm{p}}}{\mathrm{d}x\mathrm{d}y} = \frac{G_\mathrm{F}^2}{\pi} sx\left[(1-y)^2 u(x) + \overline{d}(x)\right] \tag{34}$$

$$\nu_\mu\mathrm{n} \to \mu^-\mathrm{X}: \qquad \frac{\mathrm{d}^2\sigma^{\nu\mathrm{n}}}{\mathrm{d}x\mathrm{d}y} = \frac{G_\mathrm{F}^2}{\pi} sx\left[u(x) + (1-y)^2\overline{d}(x)\right] \tag{35}$$

$$\overline{\nu}_\mu\mathrm{n} \to \mu^+\mathrm{X}: \qquad \frac{\mathrm{d}^2\sigma^{\overline{\nu}\mathrm{n}}}{\mathrm{d}x\mathrm{d}y} = \frac{G_\mathrm{F}^2}{\pi} sx\left[(1-y)^2 d(x) + \overline{u}(x)\right] \tag{36}$$

Parton model predictions for the total $\nu\mathrm{p}$, $\overline{\nu}\mathrm{p}$, $\nu\mathrm{n}$ and $\overline{\nu}\mathrm{n}$ cross sections can be obtained by integrating the differential cross sections of Equations (33)-(36) over all values of x and y. The details are deferred to the examples sheet. Neutrino experiments are often performed using an *isoscalar target* containing an approximately equal number of protons and neutrons. In this case, the total neutrino and antineutrino cross sections are found to be

$$\begin{aligned} \sigma^{\nu\mathrm{N}} &= \frac{G_\mathrm{F}^2 s}{2\pi}\left[f_\mathrm{q} + \frac{1}{3} f_{\overline{\mathrm{q}}}\right] \\ \sigma^{\overline{\nu}\mathrm{N}} &= \frac{G_\mathrm{F}^2 s}{2\pi}\left[\frac{1}{3} f_\mathrm{q} + f_{\overline{\mathrm{q}}}\right] \end{aligned}$$

where f_q and $f_{\overline{\mathrm{q}}}$ are the total momentum fractions carried by quarks and antiquarks inside the proton:

$$f_\mathrm{q} \equiv f_\mathrm{u} + f_\mathrm{d} = \int_0^1 x\left[u(x) + d(x)\right]\mathrm{d}x, \qquad f_{\overline{\mathrm{q}}} \equiv f_{\overline{u}} + f_{\overline{d}} = \int_0^1 x\left[\overline{u}(x) + \overline{d}(x)\right]\mathrm{d}x \ .$$

Measurements of the total cross sections show that only about half of the proton's momentum can be accounted for by quarks and antiquarks. The remaining $\sim 50\%$ must be carried by partons which do not interact with $\mathrm{W}^\pm$ bosons, and is attributed to gluons within the nucleon.

7.6.2 Structure function predictions

For neutrino-proton scattering, a comparison of the general expression for the cross section given in Equation (29) with the parton model cross section of Equation (33) immediately gives the following predictions for the proton structure functions:

$$F_2^{\nu\mathrm{p}} = 2xF_1^{\nu\mathrm{p}} = 2x\left[d(x) + \overline{u}(x)\right] \tag{37}$$

$$xF_3^{\nu\mathrm{p}} = 2x\left[d(x) - \overline{u}(x)\right] \ . \tag{38}$$

Hence, as in the electromagnetic case, we naturally obtain the Callan-Gross relation $F_2 = 2xF_1$ between the structure functions F_1 and F_2, reflecting the fact that the underlying scattering is from pointlike spin-half partons. In addition, by measuring both $F_2^{\nu\mathrm{p}}$ and $F_3^{\nu\mathrm{p}}$, the parton distribution functions $d(x)$ and $\overline{u}(x)$ can be separately determined by solving Equations (37) and (38).

Similar predictions are easily obtained for neutrino-neutron scattering:

$$\begin{aligned} F_2^{\nu\mathrm{n}} = 2xF_1^{\nu\mathrm{n}} &= 2x\left[u(x) + \overline{d}(x)\right] \\ xF_3^{\nu\mathrm{n}} &= 2x\left[u(x) - \overline{d}(x)\right] \ . \end{aligned}$$

In this case, the distribution functions $u(x)$ and $\overline{d}(x)$ can be separately extracted from measurements of $F_2^{\nu\mathrm{n}}$ and $F_3^{\nu\mathrm{n}}$.

Finally, the structure functions for antineutrino scattering depend on the same combinations of quark distribution functions, $d(x) \pm \overline{u}(x)$ and $u(x) \pm \overline{d}(x)$, as in neutrino scattering, and we obtain

$$F_2^{\overline{\nu}\mathrm{p}} = F_2^{\nu\mathrm{n}}, \qquad F_3^{\overline{\nu}\mathrm{p}} = F_3^{\nu\mathrm{n}}, \qquad F_2^{\overline{\nu}\mathrm{n}} = F_2^{\nu\mathrm{p}}, \qquad F_3^{\overline{\nu}\mathrm{n}} = F_3^{\nu\mathrm{p}} \ .$$

Studies of neutrino and antineutrino deep-inelastic scattering therefore allow each of the distribution functions $d(x)$, $u(x)$, $\overline{d}(x)$ and $\overline{u}(x)$ to be determined separately. This possibility arises because neutrinos and antineutrinos couple to different quark flavours (d and $\overline{\mathrm{u}}$ for neutrinos, u and $\overline{\mathrm{d}}$ for antineutrinos) and produce angular distributions which depend on the underlying scattering process (isotropic for $\nu\mathrm{q}$ and $\overline{\nu\mathrm{q}}$ scattering, $(1-y)^2$ for $\nu\overline{\mathrm{q}}$ and $\overline{\nu}\mathrm{q}$ scattering). By contrast, in electromagnetic scattering, the virtual photon couples to all quark flavours, and the resulting angular distribution, $1 + (1-y)^2$, is the same for each flavour.

Notice that since the sea contribution is small at large values of x, we expect to find $F_2 \approx xF_3$ in all cases as $x \to 1$.

For an isoscalar target (containing an equal number of protons and neutrons), the structure functions are given by

$$F_2^{\nu\mathrm{N}} \equiv \frac{1}{2}\left(F_2^{\nu\mathrm{p}} + F_2^{\nu\mathrm{n}}\right) = x\left[u(x) + d(x) + \overline{u}(x) + \overline{d}(x)\right] \tag{39}$$

$$xF_3^{\nu\mathrm{N}} \equiv \frac{1}{2}\left(xF_3^{\nu\mathrm{p}} + xF_3^{\nu\mathrm{n}}\right) = x\left[u(x) + d(x) - \overline{u}(x) - \overline{d}(x)\right] \tag{40}$$

In the case of electromagnetic scattering, the electron-proton and electron-neutron structure functions were found to be given by

$$\begin{aligned} F_2^{\mathrm{ep}} = 2xF_1^{\mathrm{ep}} &= x\left[\frac{4}{9}u(x) + \frac{1}{9}d(x) + \frac{4}{9}\overline{u}(x) + \frac{1}{9}\overline{d}(x)\right] \\ F_2^{\mathrm{en}} = 2xF_1^{\mathrm{en}} &= x\left[\frac{4}{9}d(x) + \frac{1}{9}u(x) + \frac{4}{9}\overline{d}(x) + \frac{1}{9}\overline{u}(x)\right] \ . \end{aligned}$$

Hence the electromagnetic structure function for an isoscalar target is

$$F_2^{\mathrm{eN}} \equiv \frac{1}{2}\left(F_2^{\mathrm{ep}} + F_2^{\mathrm{en}}\right) = \frac{5}{18}x\left[u(x) + d(x) + \overline{u}(x) + \overline{d}(x)\right] \ . \tag{41}$$

A comparison of Equations (39) and (41) then gives the prediction

$$\boxed{F_2^{\mathrm{eN}} = \frac{5}{18} F_2^{\nu\mathrm{N}}} .$$

The numerical factor of 5/18 arises as the average of the squares of the quark charges:

$$\frac{5}{18} = \frac{1}{2}\left[\left(\frac{1}{3}\right)^2 + \left(\frac{2}{3}\right)^2\right] .$$

Hence, by measuring both the electromagnetic structure function (which depends on the quark charges squared) and the weak structure function (which does not), the average of the quark charges squared can be measured.

Each parton distribution function can be expressed as the sum of a valence and a sea contribution:

$$u(x) = u_{\mathrm{V}}(x) + S(x), \qquad d(x) = d_{\mathrm{V}}(x) + S(x), \qquad \overline{u}(x) = \overline{d}(x) = S(x) ,$$

where the valence distributions are normalised as

$$\int_0^1 u_{\mathrm{V}}(x)\mathrm{d}x = 2, \qquad \int_0^1 d_{\mathrm{V}}(x)\mathrm{d}x = 1 .$$

Substitution into Equation (40) then gives the following prediction for $F_3^{\nu\mathrm{N}}$:

$$F_3^{\nu\mathrm{N}} = u_{\mathrm{V}}(x) + d_{\mathrm{V}}(x) .$$

Integrating this equation over the full range of Bjorken x gives the *Gross-Llewellyn-Smith sum rule* for $F_3^{\nu\mathrm{N}}$:

$$\boxed{\int_0^1 F_3^{\nu\mathrm{N}}(x)\mathrm{d}x = \int_0^1 \left[u_{\mathrm{V}}(x) + d_{\mathrm{V}}(x)\right]\mathrm{d}x = 3} .$$

Thus the area under the structure function F_3 determines the number of valence quarks inside the nucleon.

7.7 Appendix: Connection with Fermi Theory of β-decay

In 1934, well before parity violation was observed for the weak interactions, and before it was realised that the weak interactions were mediated by the exchange of massive vector bosons, Fermi proposed, in analogy with QED, that the invariant amplitude for β-decay be of the parity conserving form

$$M_{\rm fi} = G_{\rm F}\, g_{\mu\nu} \left[\overline{\psi}\gamma^{\mu}\psi\right] \left[\overline{\psi}\gamma^{\nu}\psi\right]$$

where $G_{\rm F}$ is the *Fermi constant*: $G_{\rm F} = 1.166 \times 10^{-5}$ GeV^{-2}. (Note the absence of a propagator term).

After the observation of parity violation in 1957, this was modified to the V$-$A form

$$M_{\rm fi} = \frac{G_{\rm F}}{\sqrt{2}}\, g_{\mu\nu} \left[\overline{\psi}\gamma^{\mu}(1-\gamma^5)\psi\right] \left[\overline{\psi}\gamma^{\nu}(1-\gamma^5)\psi\right] \tag{42}$$

where the factor of $1/\sqrt{2}$ is needed to preserve the original numerical value of $G_{\rm F}$.

The Feynman rules applied to a leading order diagram involving the exchange of a virtual W$^{\pm}$ boson of mass $m_{\rm W}$ give a matrix element of the form

$$M_{\rm fi} = -\frac{g_{\rm W}^2}{2(q^2 - m_{\rm W}^2)}\, g_{\mu\nu} \left[\overline{\psi}\gamma^{\mu}\tfrac{1}{2}(1-\gamma^5)\psi\right] \left[\overline{\psi}\gamma^{\nu}\tfrac{1}{2}(1-\gamma^5)\psi\right]$$

In the low energy limit $q^2 \ll m_{\rm W}^2$ appropriate to β-decay, this agrees with the original Fermi theory of Equation (42) provided we identify

$$\boxed{\frac{G_{\rm F}}{\sqrt{2}} = \frac{g_{\rm W}^2}{8m_{\rm W}^2}}\,.$$

8 CP Violation

8.1 Introduction

Following the initial observation, in 1957, that the weak interactions are not invariant under the parity transformation, P, it was soon established that parity non-conservation arises because the weak charged current has a $V-A$ structure. An immediate consequence of this result is that, as well as parity violation, the weak interactions are also not invariant under the charge conjugation operation, C, which transforms particles into antiparticles and *vice versa*. In particular, charge conjugation would transform a left-handed neutrino into a left-handed antineutrino, and the latter is not permitted for a $V-A$ current. It was initially believed that invariance could be restored by the application of both P *and* C *together*. A combined CP operation transforms a left-handed (right-handed) particle into a right-handed (left-handed) antiparticle, and *vice versa*. In particular, a left-handed neutrino would become a right-handed antineutrino, which *is* permitted for a $V-A$ current.

In 1964, however, even CP was found not to be a symmetry of the weak interactions. This observation was made in an experiment studying the decay of the long-lived neutral kaon state, $\mathrm{K_L}$, a linear combination of the strange meson states K^0 ($\mathrm{d\overline{s}}$) and $\overline{\mathrm{K}}^0$ ($\mathrm{\overline{d}s}$). For the next 35 years, observations of CP violation were confined to the neutral kaon system. Not until 2000 was CP violation finally observed elsewhere, in the $\mathrm{B}^0-\overline{\mathrm{B}}^0$ system of neutral mesons containing the heavier b quark in place of the strange quark.

In this handout, the formalism needed to describe the neutral kaon and neutral B meson systems is developed and various manifestations of CP violation in these systems are considered.

8.2 The Neutral Kaon System

The neutral kaon system consists of the two strong interaction eigenstates K^0 and $\overline{\mathrm{K}}^0$, with flavour content

$$\left|\mathrm{K}^0\right\rangle = \left|\mathrm{d\overline{s}}\right\rangle, \qquad \left|\overline{\mathrm{K}}^0\right\rangle = \left|\mathrm{\overline{d}s}\right\rangle \ .$$

The K^0 and $\overline{\mathrm{K}}^0$ are *strangeness eigenstates* with strangeness quantum number $S=+1$ and $S=-1$ respectively. They belong to the $J^{PC}=0^{-+}$ SU(3) multiplet which also contains the π^+, π^- and π^0 mesons. Thus the K^0 and $\overline{\mathrm{K}}^0$ are eigenstates of parity with intrinsic parity -1:

$$P\left|\mathrm{K}^0\right\rangle = -\left|\mathrm{K}^0\right\rangle, \qquad P\left|\overline{\mathrm{K}}^0\right\rangle = -\left|\overline{\mathrm{K}}^0\right\rangle \ , \tag{1}$$

but, since they are a distinct particle and antiparticle, they are *not* eigenstates of the charge conjugation operator C. Instead, the effect of the operator C can be taken to be

$$C\left|\mathrm{K}^0\right\rangle = \left|\overline{\mathrm{K}}^0\right\rangle, \qquad C\left|\overline{\mathrm{K}}^0\right\rangle = \left|\mathrm{K}^0\right\rangle \ , \tag{2}$$

where the choice of sign here is purely conventional. We could equally well choose $C\left|\mathrm{K}^0\right\rangle = -\left|\overline{\mathrm{K}}^0\right\rangle$, $C\left|\overline{\mathrm{K}}^0\right\rangle = -\left|\mathrm{K}^0\right\rangle$, with no observable physical consequences.

When the weak interactions are taken into account, strangeness is no longer a conserved quantity and it is possible to have $\Delta S = 2$ transitions, $\mathrm{K}^0 \leftrightarrow \overline{\mathrm{K}}^0$, between the K^0 and $\overline{\mathrm{K}}^0$ states, which change the strangeness by two units. In the Standard Model, these transitions take place via "box diagrams" containing two virtual W bosons and two virtual u, c or t quarks:

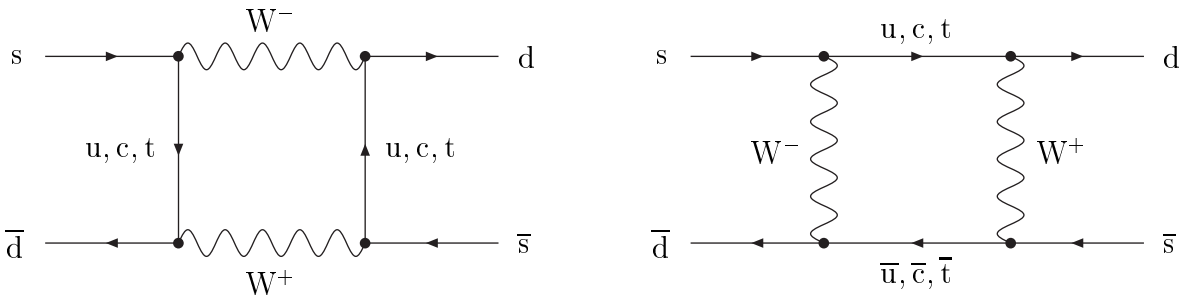

As shown formally in the Appendix (Section 8.12), the eigenstates of the overall (strong plus weak) Hamiltonian are quantum mechanical mixtures (linear combinations) of the basis states K^0 and $\overline{\mathrm{K}}^0$. These overall eigenstates are known as the "K-short" ($\mathrm{K_S}$) and "K-long" ($\mathrm{K_L}$) states, and are closely related to the CP eigenstates of the system, K_1 and K_2.

Combining Equations (1) and (2), the effect of the combined operation CP is

$$CP\left|\mathrm{K}^0\right\rangle = -\left|\overline{\mathrm{K}}^0\right\rangle, \qquad CP\left|\overline{\mathrm{K}}^0\right\rangle = -\left|\mathrm{K}^0\right\rangle \ .$$

Thus K^0 and $\overline{\mathrm{K}}^0$ are not themselves CP-eigenstates, but it is straightforward to form states K_1 and K_2 which *are* CP eigenstates:

$$\left|\mathrm{K}_1\right\rangle \equiv \frac{1}{\sqrt{2}}\left(\left|\mathrm{K}^0\right\rangle - \left|\overline{\mathrm{K}}^0\right\rangle\right); \qquad CP\left|\mathrm{K}_1\right\rangle = +\left|\mathrm{K}_1\right\rangle \tag{3}$$

$$\left|\mathrm{K}_2\right\rangle \equiv \frac{1}{\sqrt{2}}\left(\left|\mathrm{K}^0\right\rangle + \left|\overline{\mathrm{K}}^0\right\rangle\right); \qquad CP\left|\mathrm{K}_2\right\rangle = -\left|\mathrm{K}_2\right\rangle \tag{4}$$

The K^0 and $\overline{\mathrm{K}}^0$ mesons are unstable particles which decay via the weak interactions [1]. The states which propagate as free particles and have definite mass and lifetime are the "K-short" ($\mathrm{K_S}$) and "K-long" ($\mathrm{K_L}$). These states have approximately equal masses, $m_{\mathrm{S}} \approx m_{\mathrm{L}} \approx 498\,\mathrm{MeV}$, but very different lifetimes: $\tau_{\mathrm{S}} = 0.9 \times 10^{-10}\,\mathrm{s}$ and $\tau_{\mathrm{L}} = 0.5 \times 10^{-7}\,\mathrm{s}$. They are almost, but not quite, CP eigenstates:

$$\left|\mathrm{K_S}\right\rangle = \frac{1}{\sqrt{1+|\epsilon|^2}}\left(\left|\mathrm{K}_1\right\rangle + \epsilon\left|\mathrm{K}_2\right\rangle\right) \approx \left|\mathrm{K}_1\right\rangle \tag{5}$$

$$\left|\mathrm{K_L}\right\rangle = \frac{1}{\sqrt{1+|\epsilon|^2}}\left(\left|\mathrm{K}_2\right\rangle + \epsilon\left|\mathrm{K}_1\right\rangle\right) \approx \left|\mathrm{K}_2\right\rangle \tag{6}$$

[1] The K^0 and $\overline{\mathrm{K}}^0$ are the lightest hadrons which contain a strange quark or antiquark, and therefore cannot decay via the strong or electromagnetic interactions since these decays must conserve strangeness.

where ϵ (with $|\epsilon| \approx 2.3 \times 10^{-3}$) is a complex parameter quantifying the level of CP violation. The $\mathrm{K_S}$ meson decays overwhelmingly to two pions, while the $\mathrm{K_L}$ decays predominantly to three-pion or to semileptonic ($\pi \mathrm{e} \nu$ or $\pi \mu \nu$) final states:

$$\begin{aligned} \mathrm{K_S} &\to \pi^+\pi^- \qquad \mathrm{BR} = 68.6\% \\ &\to \pi^0\pi^0 \qquad \mathrm{BR} = 31.4\% \end{aligned}$$

$$\begin{aligned} \mathrm{K_L} &\to \pi^+\pi^-\pi^0 \qquad \mathrm{BR} = 12.6\% \\ &\to \pi^0\pi^0\pi^0 \qquad \mathrm{BR} = 21.1\% \\ &\to \pi^-\mathrm{e}^+\nu_\mathrm{e} \qquad \mathrm{BR} = 19.4\% \\ &\to \pi^+\mathrm{e}^-\overline{\nu}_\mathrm{e} \qquad \mathrm{BR} = 19.4\% \\ &\to \pi^-\mu^+\nu_\mu \qquad \mathrm{BR} = 13.6\% \\ &\to \pi^+\mu^-\overline{\nu}_\mu \qquad \mathrm{BR} = 13.6\% \end{aligned}$$

All other decay modes of the $\mathrm{K_S}$ or $\mathrm{K_L}$ have branching ratios below (and usually well below) 0.5%. Of particular importance are the $\mathrm{K_L}$ decays

$$\begin{aligned} \mathrm{K_L} &\to \pi^+\pi^- \qquad \mathrm{BR} = 2.1 \times 10^{-3} \\ &\to \pi^0\pi^0 \qquad \mathrm{BR} = 9.4 \times 10^{-4} \end{aligned}$$

whose observation in 1964 represented the original discovery of CP violation. Another important signal of CP violation is that the semileptonic $\mathrm{K_L}$ branching ratios listed above differ slightly for charge-conjugate final states. Specifically, the $\mathrm{K_L}$ decay rate to $\pi^-\mathrm{e}^+\nu_\mathrm{e}$ is slightly ($\sim 0.3\%$) larger than that to $\pi^+\mathrm{e}^-\overline{\nu}_\mathrm{e}$, and similarly the $\pi^-\mu^+\nu_\mu$ decay rate is slightly larger than that to $\pi^+\mu^-\overline{\nu}_\mu$.

The strangeness eigenstates K^0 and $\overline{\mathrm{K}}^0$ are orthogonal states:

$$\left\langle \mathrm{K}^0 | \overline{\mathrm{K}}^0 \right\rangle = 0 \ ,$$

and from Equations (3) and (4), it follows that the CP eigenstates K_1 and K_2 are also orthogonal states:

$$\langle \mathrm{K}_1 | \mathrm{K}_2 \rangle = 0 \ .$$

From Equations (5) and (6), the overlap $\langle \mathrm{K_S} | \mathrm{K_L} \rangle$ between the $\mathrm{K_S}$ and $\mathrm{K_L}$ states is

$$\langle \mathrm{K_S} | \mathrm{K_L} \rangle = \frac{1}{1+|\epsilon|^2} \langle \mathrm{K}_1 + \epsilon \mathrm{K}_2 | \mathrm{K}_2 + \epsilon \mathrm{K}_1 \rangle = \frac{1}{1+|\epsilon|^2} (\epsilon + \epsilon^*) = \frac{2\mathrm{Re}(\epsilon)}{1+|\epsilon|^2} \ ,$$

showing that the states $\mathrm{K_S}$ and $\mathrm{K_L}$ are orthogonal only if CP violation can be neglected ($\epsilon = 0$).

The states $\mathrm{K_L}$ and $\mathrm{K_S}$ have definite mass and lifetime and evolve with the proper time t through the multiplicative factors

$$\theta_\mathrm{S}(t) = e^{-im_\mathrm{S}t - \Gamma_\mathrm{S}t/2}, \qquad \theta_\mathrm{L}(t) = e^{-im_\mathrm{L}t - \Gamma_\mathrm{L}t/2} \tag{7}$$

where $\Gamma_\mathrm{L} = 1/\tau_\mathrm{L}$ and $\Gamma_\mathrm{S} = 1/\tau_\mathrm{S}$. Thus the $\mathrm{K_S}$ and $\mathrm{K_L}$ wavefunctions evolve as

$$\begin{aligned} |\mathrm{K_L}(t)\rangle &= |\mathrm{K_L}\rangle \, \theta_\mathrm{L}(t) = |\mathrm{K_L}\rangle \, e^{-im_\mathrm{L}t - \Gamma_\mathrm{L}t/2} \\ |\mathrm{K_S}(t)\rangle &= |\mathrm{K_S}\rangle \, \theta_\mathrm{S}(t) = |\mathrm{K_S}\rangle \, e^{-im_\mathrm{S}t - \Gamma_\mathrm{S}t/2} \ . \end{aligned}$$

The factors $\psi \sim \exp(-\Gamma t/2)$ give an exponentially decaying probability $|\psi|^2 \sim \exp(-\Gamma t) = \exp(-t/\tau)$, as required for an unstable particle with lifetime τ:

$$|\theta_\mathrm{S}(t)|^2 = e^{-\Gamma_\mathrm{S}t} = e^{-t/\tau_\mathrm{S}}; \qquad |\theta_\mathrm{L}(t)|^2 = e^{-\Gamma_\mathrm{L}t} = e^{-t/\tau_\mathrm{L}} \ .$$

A formal proof that the $\mathrm{K_S}$ and $\mathrm{K_L}$ eigenstates have the form given in Equations (5) and (6) and evolve with time as above is given in the Appendix (Section 8.12).

8.3 Strangeness Oscillations

If CP violation is neglected ($\epsilon = 0$), the states $\mathrm{K_S}$ and $\mathrm{K_L}$ become equivalent to the CP eigenstates $\mathrm{K_1}$ and $\mathrm{K_2}$:

$$|\mathrm{K_S}\rangle = |\mathrm{K_1}\rangle = \frac{1}{\sqrt{2}}\left(\left|\mathrm{K^0}\right\rangle - \left|\overline{\mathrm{K}}^0\right\rangle\right) \tag{8}$$

$$|\mathrm{K_L}\rangle = |\mathrm{K_2}\rangle = \frac{1}{\sqrt{2}}\left(\left|\mathrm{K^0}\right\rangle + \left|\overline{\mathrm{K}}^0\right\rangle\right) \ . \tag{9}$$

These equations can be inverted to give

$$\left|\mathrm{K^0}\right\rangle = \frac{1}{\sqrt{2}}\left(|\mathrm{K_L}\rangle + |\mathrm{K_S}\rangle\right), \qquad \left|\overline{\mathrm{K}}^0\right\rangle = \frac{1}{\sqrt{2}}\left(|\mathrm{K_L}\rangle - |\mathrm{K_S}\rangle\right) \ .$$

Consider a beam of neutral kaons which is in a pure $\left|\mathrm{K^0}\right\rangle$ state at time $t = 0$, produced via the strong interaction process $\pi^-\mathrm{p} \to \Lambda^0\mathrm{K^0}$, for example. The initial wavefunction is then

$$\left|\mathrm{K^0}(0)\right\rangle = \left|\mathrm{K^0}\right\rangle = \frac{1}{\sqrt{2}}\left(|\mathrm{K_L}\rangle + |\mathrm{K_S}\rangle\right) \ ,$$

and the time evolution of the system is given by

$$\left|\mathrm{K^0}(t)\right\rangle = \frac{1}{\sqrt{2}}\left(|\mathrm{K_L}(t)\rangle + |\mathrm{K_S}(t)\rangle\right) = \frac{1}{\sqrt{2}}\left(|\mathrm{K_L}\rangle\,\theta_\mathrm{L} + |\mathrm{K_S}\rangle\,\theta_\mathrm{S}\right) \ . \tag{10}$$

This can be expressed in terms of the basis states $\left|\mathrm{K^0}\right\rangle$ and $\left|\overline{\mathrm{K}}^0\right\rangle$ using Equations (8) and (9):

$$\begin{aligned}\left|\mathrm{K^0}(t)\right\rangle &= \frac{1}{\sqrt{2}}\left[\frac{1}{\sqrt{2}}\left(\left|\mathrm{K^0}\right\rangle + \left|\overline{\mathrm{K}}^0\right\rangle\right)\theta_\mathrm{L} + \frac{1}{\sqrt{2}}\left(\left|\mathrm{K^0}\right\rangle - \left|\overline{\mathrm{K}}^0\right\rangle\right)\theta_\mathrm{S}\right] \\ &= \frac{1}{2}(\theta_\mathrm{L} + \theta_\mathrm{S})\left|\mathrm{K^0}\right\rangle + \frac{1}{2}(\theta_\mathrm{L} - \theta_\mathrm{S})\left|\overline{\mathrm{K}}^0\right\rangle \ . \end{aligned} \tag{11}$$

Hence a beam which is initially pure $\mathrm{K^0}$ evolves in time to become a *mixture* of $\mathrm{K^0}$ and $\overline{\mathrm{K}}^0$, the relative $\mathrm{K^0}$ and $\overline{\mathrm{K}}^0$ intensities after time t being given by

$$\begin{aligned}\Gamma(\mathrm{K^0_{t=0}} \to \mathrm{K^0}) &\propto \left|\left\langle \mathrm{K^0}\middle|\mathrm{K^0}(t)\right\rangle\right|^2 = \frac{1}{4}\left|\theta_\mathrm{S} + \theta_\mathrm{L}\right|^2 \\ \Gamma(\mathrm{K^0_{t=0}} \to \overline{\mathrm{K}}^0) &\propto \left|\left\langle \overline{\mathrm{K}}^0\middle|\mathrm{K^0}(t)\right\rangle\right|^2 = \frac{1}{4}\left|\theta_\mathrm{S} - \theta_\mathrm{L}\right|^2 \ . \end{aligned}$$

From the definitions of θ_S and θ_L in Equation (7), and using the general complex number relation $|z_1 \pm z_2|^2 = |z_1|^2 + |z_2|^2 \pm 2\mathrm{Re}(z_1^* z_2)$, we obtain

$$\begin{aligned}|\theta_\mathrm{L} \pm \theta_\mathrm{S}|^2 &= \left|e^{-im_\mathrm{L}t - \Gamma_\mathrm{L}t/2} \pm e^{-im_\mathrm{S}t - \Gamma_\mathrm{S}t/2}\right|^2 \\ &= e^{-\Gamma_\mathrm{L}t} + e^{-\Gamma_\mathrm{S}t} \pm 2\mathrm{Re}\left(e^{im_\mathrm{L}t - \Gamma_\mathrm{L}t/2}e^{-im_\mathrm{S}t - \Gamma_\mathrm{S}t/2}\right) \\ &= e^{-\Gamma_\mathrm{L}t} + e^{-\Gamma_\mathrm{S}t} \pm 2e^{-(\Gamma_\mathrm{S}+\Gamma_\mathrm{L})t/2}\cos\Delta m t \end{aligned}$$

where Δm is the mass difference between the $\mathrm{K_L}$ and $\mathrm{K_S}$ states:

$$\Delta m \equiv m_\mathrm{L} - m_\mathrm{S} \ .$$

Therefore, finally

$$\Gamma(\mathrm{K}^0_{t=0} \to \mathrm{K}^0) \propto \tfrac{1}{4}\left[e^{-\Gamma_\mathrm{S} t} + e^{-\Gamma_\mathrm{L} t} + 2e^{-(\Gamma_\mathrm{S}+\Gamma_\mathrm{L})t/2}\cos\Delta m t\right] \tag{12}$$

$$\Gamma(\mathrm{K}^0_{t=0} \to \overline{\mathrm{K}}^0) \propto \tfrac{1}{4}\left[e^{-\Gamma_\mathrm{S} t} + e^{-\Gamma_\mathrm{L} t} - 2e^{-(\Gamma_\mathrm{S}+\Gamma_\mathrm{L})t/2}\cos\Delta m t\right] \ . \tag{13}$$

Thus, the K^0 and $\overline{\mathrm{K}}^0$ intensities oscillate with a frequency determined by $\Delta m = m_\mathrm{L} - m_\mathrm{S}$. This is illustrated in Figure 1 where the *strangeness oscillations* of Equations (12) and (13) are plotted versus proper time, using the measured values of Γ_S, Γ_L and Δm (see below) and with the initial K^0 intensity normalised arbitrarily to unity.

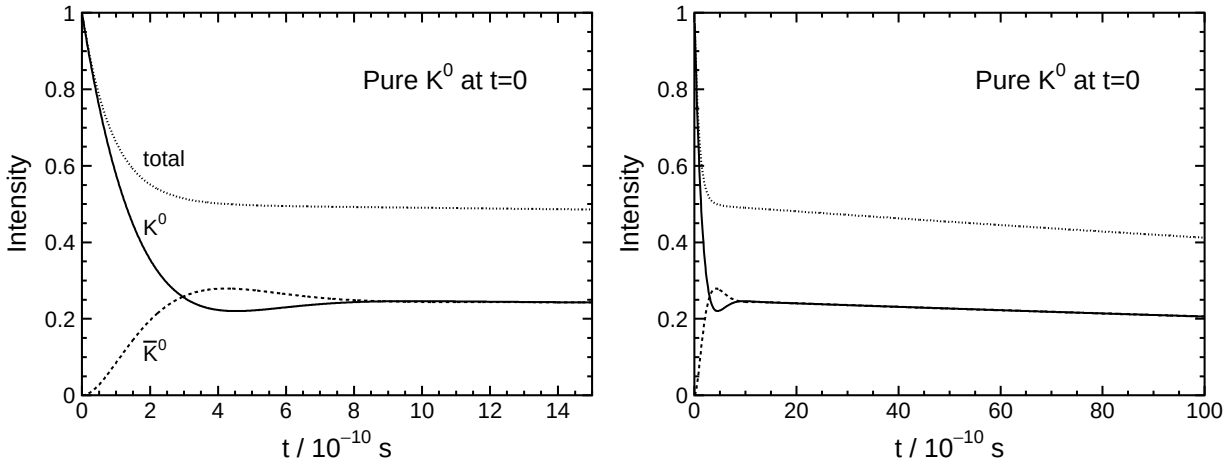

Figure 1: K^0 and $\overline{\mathrm{K}}^0$ intensities as a function of time for a beam which is initially pure K^0, showing the effects of strangeness oscillations. The two plots display the same information, but the right-hand plot covers a longer time scale to make the slow decay of the long-lifetime K_L component more visible.

If the system is initially in a pure $\overline{\mathrm{K}}^0$ state (rather than K^0), the wavefunction now evolves with time as

$$\begin{aligned}
\left|\overline{\mathrm{K}}^0(t)\right\rangle &= \frac{1}{\sqrt{2}}\left(\left|\mathrm{K}_\mathrm{L}(t)\right\rangle - \left|\mathrm{K}_\mathrm{S}(t)\right\rangle\right) \\
&= \frac{1}{\sqrt{2}}\left(\left|\mathrm{K}_\mathrm{L}\right\rangle\theta_\mathrm{L} - \left|\mathrm{K}_\mathrm{S}\right\rangle\theta_\mathrm{S}\right) \\
&= \frac{1}{\sqrt{2}}\left[\frac{1}{\sqrt{2}}\left(\left|\mathrm{K}^0\right\rangle + \left|\overline{\mathrm{K}}^0\right\rangle\right)\theta_\mathrm{L} - \frac{1}{\sqrt{2}}\left(\left|\mathrm{K}^0\right\rangle - \left|\overline{\mathrm{K}}^0\right\rangle\right)\theta_\mathrm{S}\right] \\
&= \frac{1}{2}(\theta_\mathrm{L} - \theta_\mathrm{S})\left|\mathrm{K}^0\right\rangle + \frac{1}{2}(\theta_\mathrm{L} + \theta_\mathrm{S})\left|\overline{\mathrm{K}}^0\right\rangle \ .
\end{aligned}$$

The coefficients in this expression are the same as those in Equation (11), giving oscillation probabilities for an initial $\overline{\mathrm{K}}^0$ which are the same as for an initial K^0:

$$\Gamma(\overline{\mathrm{K}}^0_{t=0} \to \mathrm{K}^0) = \Gamma(\mathrm{K}^0_{t=0} \to \overline{\mathrm{K}}^0) \tag{14}$$

$$\Gamma(\overline{\mathrm{K}}^0_{t=0} \to \overline{\mathrm{K}}^0) = \Gamma(\mathrm{K}^0_{t=0} \to \mathrm{K}^0) \tag{15}$$

8.3.1 Semileptonic decays

Strangeness oscillations can be studied experimentally by measuring semileptonic ($\pi e\nu$, $\pi\mu\nu$) decay rates as a function of proper time [2]. The final state $\pi^-e^+\nu_e$ can only come from the decay of the K^0 component in the beam, while $\pi^+e^-\overline{\nu}_e$ final states must come from the $\overline{K}^0$ component:

$$K^0 \longrightarrow \pi^-e^+\nu_e \qquad\qquad K^0 \not\longrightarrow \pi^+e^-\overline{\nu}_e \tag{16}$$

$$\overline{K}^0 \longrightarrow \pi^+e^-\overline{\nu}_e \qquad\qquad \overline{K}^0 \not\longrightarrow \pi^-e^+\nu_e \tag{17}$$

The sign (charge) of the $e^\pm$ or $\pi^\mp$ produced in such decays can therefore be used to determine the K^0 and $\overline{K}^0$ fractions at any point along a neutral kaon beam. From Equations (12), (13), (14), (15) we obtain directly

$$R_+ \equiv \Gamma(K^0_{t=0} \to \pi^-e^+\nu_e) = N_{\pi e\nu}\tfrac{1}{4}\left[e^{-\Gamma_S t} + e^{-\Gamma_L t} + 2e^{-(\Gamma_S+\Gamma_L)t/2}\cos\Delta m t\right] \tag{18}$$

$$R_- \equiv \Gamma(K^0_{t=0} \to \pi^+e^-\overline{\nu}_e) = N_{\pi e\nu}\tfrac{1}{4}\left[e^{-\Gamma_S t} + e^{-\Gamma_L t} - 2e^{-(\Gamma_S+\Gamma_L)t/2}\cos\Delta m t\right] \tag{19}$$

$$\bar{R}_- \equiv \Gamma(\overline{K}^0_{t=0} \to \pi^+e^-\overline{\nu}_e) = N_{\pi e\nu}\tfrac{1}{4}\left[e^{-\Gamma_S t} + e^{-\Gamma_L t} + 2e^{-(\Gamma_S+\Gamma_L)t/2}\cos\Delta m t\right] \tag{20}$$

$$\bar{R}_+ \equiv \Gamma(\overline{K}^0_{t=0} \to \pi^-e^+\nu_e) = N_{\pi e\nu}\tfrac{1}{4}\left[e^{-\Gamma_S t} + e^{-\Gamma_L t} - 2e^{-(\Gamma_S+\Gamma_L)t/2}\cos\Delta m t\right] \tag{21}$$

where $N_{\pi e\nu}$ is a common overall normalisation factor.

In general, a neutral kaon beam is formed by inclusively selecting long-lived neutral particles produced in proton-nucleus interactions when a proton beam is incident on a fixed target [3]. Since these proton-nucleus interactions produce complex final states consisting of a large number of hadrons, the initial mix of K^0 and $\overline{K}^0$ mesons in such a beam is not very well known. A notable exception was the CPLEAR experiment [2] at CERN where neutral kaons were instead produced in low energy proton-antiproton interactions, using a low energy antiproton beam incident on a hydrogen target. In this experiment, the flavour (K^0 or $\overline{K}^0$) of the initial kaon could be determined unambiguously by studying the reactions

$$p\overline{p} \to K^-\pi^+K^0 \qquad \text{and} \qquad p\overline{p} \to K^+\pi^-\overline{K}^0 \ .$$

In these processes, the charge of the $K^\mp$ (or $\pi^\pm$) determines unambiguously, for each neutral kaon, whether a K^0 or a $\overline{K}^0$ was initially produced.

The CPLEAR experiment was therefore able to measure separately the four decay rates R_+, R_-, $\bar{R}_-$ and $\bar{R}_+$. To extract the strangeness oscillations in a clean way, independent of the overall normalisation factor $N_{\pi e\nu}$, CPLEAR measured the following asymmetry [1]:

$$\boxed{A_{\Delta m} \equiv \frac{(R_+ + \bar{R}_-) - (R_- + \bar{R}_+)}{(R_+ + \bar{R}_-) + (R_- + \bar{R}_+)}}. \tag{22}$$

From Equations (18)−(21) we have

$$R_+ + \bar{R}_- = N_{\pi e\nu}\tfrac{1}{2}\left[e^{-\Gamma_S t} + e^{-\Gamma_L t} + 2e^{-(\Gamma_S+\Gamma_L)t/2}\cos\Delta m t\right]$$

$$R_- + \bar{R}_+ = N_{\pi e\nu}\tfrac{1}{2}\left[e^{-\Gamma_S t} + e^{-\Gamma_L t} - 2e^{-(\Gamma_S+\Gamma_L)t/2}\cos\Delta m t\right]$$

[2] In practice, this involves measuring decay rates as a function of *distance*. The distance travelled by a kaon of momentum p in proper time t is $L = v.\gamma t$ where $p = \gamma m_K v$, and hence the proper time can be determined as $t = m_K L/p$.

[3] A "neutral kaon beam" therefore consists in practice of an inclusive mixture of stable neutral particles, such as the photon and neutron, as well as unstable but relatively long-lived neutral particles such as neutral kaons and hyperons (baryons containing a strange quark).

and hence

$$\boxed{A_{\Delta m} = \frac{2e^{-(\Gamma_{\rm S}+\Gamma_{\rm L})t/2}\cos\Delta m t}{e^{-\Gamma_{\rm S}t}+e^{-\Gamma_{\rm L}t}}} \,. \tag{23}$$

The CPLEAR measurement of $A_{\Delta m}$ is shown in Figure 2, and a fit to the data gives the most precise single measurement of Δm to date:

$$\Delta m = (529.5 \pm 2.2) \times 10^7 \hbar/\,{\rm s} = (3.485 \pm 0.015) \times 10^{-12}\,{\rm MeV} \,.$$

The *sign* of Δm cannot be determined in this way, but other measurements show that Δm is positive, *i.e.* that the $\rm K_L$ is slightly heavier than $\rm K_S$. This value of Δm corresponds to strangeness oscillations with a period

$$\tau_{\rm osc} = \frac{2\pi}{\Delta m} = \frac{2\pi}{3.49 \times 10^{-12}\,{\rm MeV}} \times (6.582 \times 10^{-22}\,{\rm MeV\,s}) = 1.18\,{\rm ns} \,.$$

This oscillation period is $\tau_{\rm osc}/\tau_{\rm S} = 13.3$ times greater than the $\rm K_S$ lifetime, $\tau_{\rm S} = 0.9 \times 10^{-10}\,{\rm s}$. As is evident in Figures 1 and 2, the number of strangeness oscillations which can be observed in practice is therefore somewhat limited since a large fraction of the kaons decay even during the first oscillation cycle.

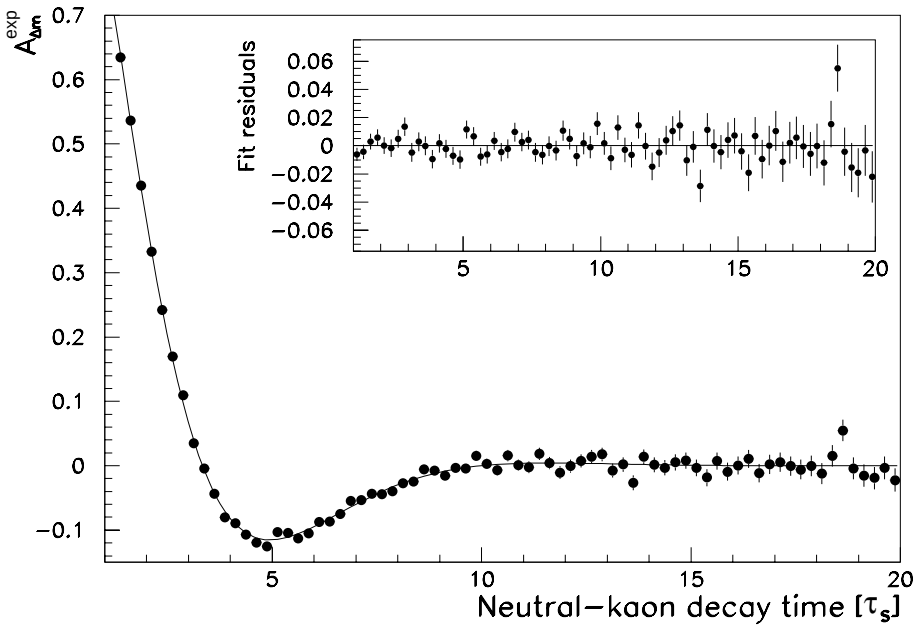

Figure 2: The asymmetry $A_{\Delta m}$ as a function of proper time, in units of the $\rm K_S$ lifetime $\tau_{\rm S}$, from the CPLEAR experiment.

It will be seen below in Section 8.6 that the above expression for the asymmetry $A_{\Delta m}$, Equation (23), remains unchanged when CP violation is taken into account.

8.3.2 $\pi\pi$ and $\pi\pi\pi$ decays

Besides the semileptonic decays to $\pi e\nu$ and $\pi\mu\nu$, we can also examine the time evolution of the decay rates to $\pi\pi$ and $\pi\pi\pi$ final states. Still neglecting CP violation, we have $|{\rm K_S}\rangle = |{\rm K_1}\rangle$ and $|{\rm K_L}\rangle = |{\rm K_2}\rangle$

so that the time evolution of the wavefunction $\mathrm{K}^0(t)$ in Equation (10) can equally well be written

$$\left|\mathrm{K}^0(t)\right\rangle = \frac{1}{\sqrt{2}}\left(\left|\mathrm{K}_2\right\rangle \theta_\mathrm{L} + \left|\mathrm{K}_1\right\rangle \theta_\mathrm{S}\right) \ .$$

The $\pi\pi$ final state is a CP eigenstate with $CP = +1$, and, if CP is conserved, it can only be produced from decays of the $CP = +1$ eigenstate K_1. Hence the decay rate to $\pi\pi$ is:

$$\Gamma(\mathrm{K}^0_{t=0} \to \pi\pi) = N_{\pi\pi}\left|\left\langle \mathrm{K}_1\middle|\mathrm{K}^0(t)\right\rangle\right|^2 = N_{\pi\pi}\frac{1}{2}\left|\theta_\mathrm{S}(t)\right|^2 = N_{\pi\pi}\frac{1}{2}e^{-\Gamma_\mathrm{S}t} \tag{24}$$

where $N_{\pi\pi}$ is an overall normalisation constant. Thus, in contrast to the strangeness oscillations evident in $\pi e\nu$ and $\pi\mu\nu$ decays, the proper decay time distribution for the $\pi\pi$ final state follows a simple exponential decay law with a single lifetime component, e^{-t/τ_S}. Similarly, the $\pi\pi\pi$ final state is a CP eigenstate with $CP = -1$ and must be produced from decays of the $CP = -1$ eigenstate K_2, giving a single lifetime component proportional to e^{-t/τ_L}:

$$\Gamma(\mathrm{K}^0_{t=0} \to \pi\pi\pi) = N_{\pi\pi\pi}\left|\left\langle \mathrm{K}_2\middle|\mathrm{K}^0(t)\right\rangle\right|^2 = N_{\pi\pi\pi}\frac{1}{2}\left|\theta_\mathrm{L}(t)\right|^2 = N_{\pi\pi\pi}\frac{1}{2}e^{-\Gamma_\mathrm{L}t} \ . \tag{25}$$

8.3.3 Summary, with CP conserved

In summary, neglecting CP violation, the principal decays seen in a beam which is initially pure K^0 are the semileptonic decays

$$\Gamma(\mathrm{K}^0_{t=0} \to \pi^-\mathrm{e}^+\nu_\mathrm{e}) = N_{\pi e\nu}\tfrac{1}{4}\left[e^{-\Gamma_\mathrm{S}t} + e^{-\Gamma_\mathrm{L}t} + 2e^{-(\Gamma_\mathrm{S}+\Gamma_\mathrm{L})t/2}\cos\Delta mt\right] \tag{18}'$$

$$\Gamma(\mathrm{K}^0_{t=0} \to \pi^+\mathrm{e}^-\overline{\nu}_\mathrm{e}) = N_{\pi e\nu}\tfrac{1}{4}\left[e^{-\Gamma_\mathrm{S}t} + e^{-\Gamma_\mathrm{L}t} - 2e^{-(\Gamma_\mathrm{S}+\Gamma_\mathrm{L})t/2}\cos\Delta mt\right] \tag{19}'$$

(with similar expressions for the muonic decays $\pi^-\mu^+\nu_\mu$ and $\pi^+\mu^-\overline{\nu}_\mu$) and the two-pion ($\pi^+\pi^-$, $\pi^0\pi^0$) and three-pion ($\pi^+\pi^-\pi^0$, $\pi^0\pi^0\pi^0$) decays

$$\Gamma(\mathrm{K}^0_{t=0} \to \pi\pi) = N_{\pi\pi}\frac{1}{2}e^{-\Gamma_\mathrm{S}t} \tag{24}'$$

$$\Gamma(\mathrm{K}^0_{t=0} \to \pi\pi\pi) = N_{\pi\pi\pi}\frac{1}{2}e^{-\Gamma_\mathrm{L}t} \ . \tag{25}'$$

The semileptonic decays arise from the K^0 and $\overline{\mathrm{K}}^0$ components of the beam and hence show directly the effects of strangeness oscillations. The $\pi\pi$ and $\pi\pi\pi$ decays arise from the K_S and K_L components of the beam, respectively, and hence are characterised by a single lifetime component τ_S or τ_L.

For an initially pure $\overline{\mathrm{K}}^0$ beam, the interference term in the semileptonic decay rates changes sign, but the $\pi\pi$ and $\pi\pi\pi$ decay rates are unchanged.

These features are summarised in Figure 3 where the principal decay rates are plotted together for an initially pure K^0 beam and for an initially pure $\overline{\mathrm{K}}^0$ beam, neglecting CP violation. The relative height of each curve in the plot (*i.e.* the relative size of the normalisation constants $N_{\pi e\nu}$, $N_{\pi\pi}$ and $N_{\pi\pi\pi}$) cannot be computed from first principles but must be determined experimentally using the measured branching ratios listed at the top of page 3.

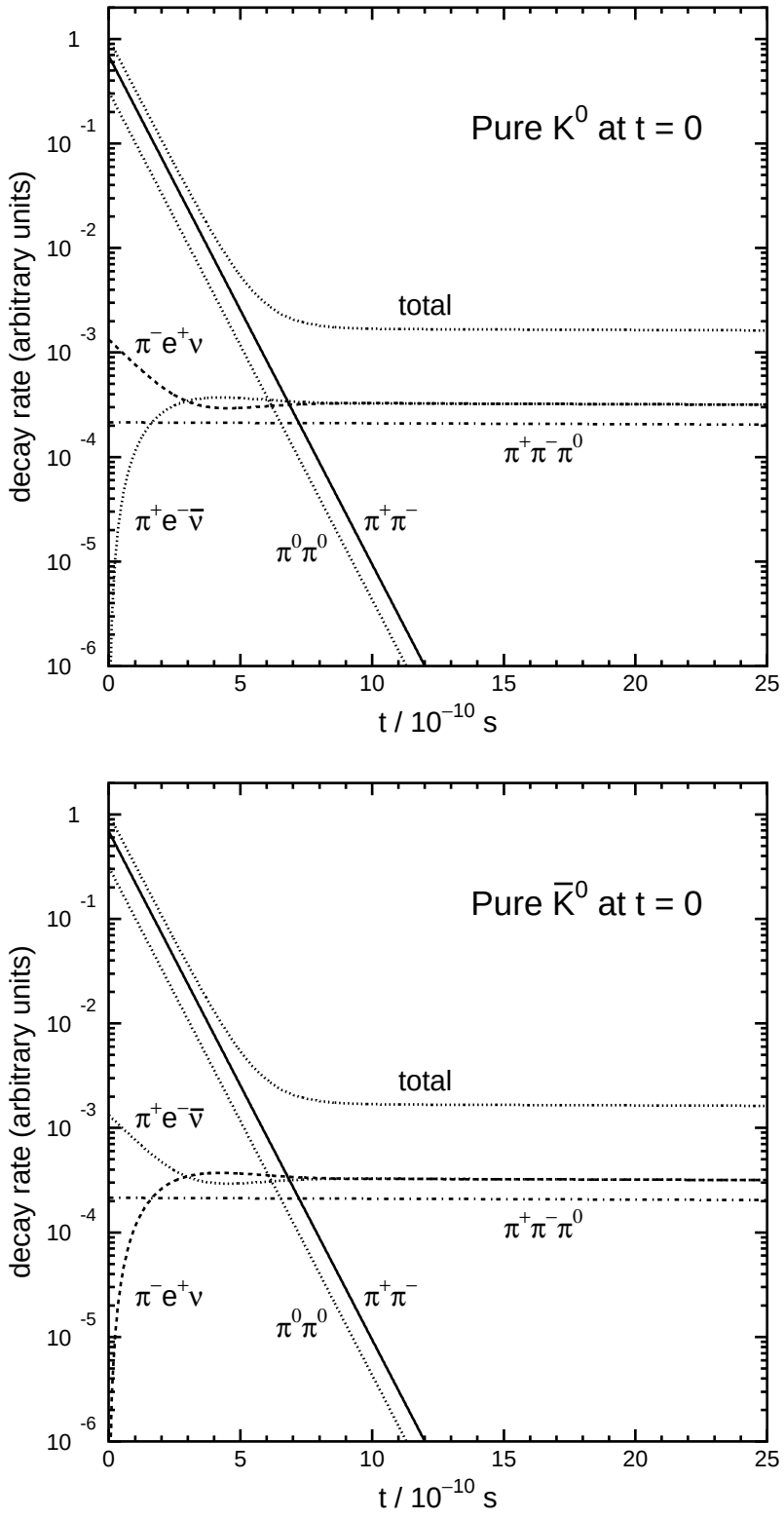

Figure 3: Summary of neutral kaon decay rates as a function of proper time for an initially pure K^0 beam (top plot) or $\overline{\mathrm{K}}^0$ beam (bottom plot), neglecting the effects of CP violation. For clarity, the decay rates to $\pi^-\mu^+\nu_\mu$ and $\pi^+\mu^-\overline{\nu}_\mu$ are not shown, but are very similar to those for $\pi^-\mathrm{e}^+\nu_\mathrm{e}$ and $\pi^+\mathrm{e}^-\overline{\nu}_\mathrm{e}$. Similarly, the $\pi^0\pi^0\pi^0$ decay rate (also not shown) is similar to the $\pi^+\pi^-\pi^0$ decay rate. Note the interchange of the $\pi^-\mathrm{e}^+\nu_\mathrm{e}$ and $\pi^+\mathrm{e}^-\overline{\nu}_\mathrm{e}$ curves between the top and bottom plots.

8.4 CP Violation: $\pi\pi$ decays

We now consider the time development of the $\mathrm{K}^0 - \overline{\mathrm{K}}^0$ system in the presence of CP violation ($\epsilon \neq 0$). As before, we have

$$|\mathrm{K_S}(t)\rangle = |\mathrm{K_S}\rangle\, \theta_\mathrm{S}(t) = |\mathrm{K_S}\rangle\, e^{-im_\mathrm{S}t - \Gamma_\mathrm{S}t/2}, \qquad |\mathrm{K_L}(t)\rangle = |\mathrm{K_L}\rangle\, \theta_\mathrm{L}(t) = |\mathrm{K_L}\rangle\, e^{-im_\mathrm{L}t - \Gamma_\mathrm{L}t/2}$$

but now

$$|\mathrm{K_S}\rangle = \frac{1}{\sqrt{1+|\epsilon|^2}}\left(|\mathrm{K}_1\rangle + \epsilon\,|\mathrm{K}_2\rangle\right), \qquad |\mathrm{K_L}\rangle = \frac{1}{\sqrt{1+|\epsilon|^2}}\left(|\mathrm{K}_2\rangle + \epsilon\,|\mathrm{K}_1\rangle\right)\ .$$

Using Equations (3) and (4), we can express the $\mathrm{K_L}$ and $\mathrm{K_S}$ eigenstates in terms of K^0 and $\overline{\mathrm{K}}^0$:

$$|\mathrm{K_L}\rangle = \frac{1}{\sqrt{2}}\frac{1}{\sqrt{1+|\epsilon|^2}}\left[(1+\epsilon)\left|\mathrm{K}^0\right\rangle + (1-\epsilon)\left|\overline{\mathrm{K}}^0\right\rangle\right] \tag{26}$$

$$|\mathrm{K_S}\rangle = \frac{1}{\sqrt{2}}\frac{1}{\sqrt{1+|\epsilon|^2}}\left[(1+\epsilon)\left|\mathrm{K}^0\right\rangle - (1-\epsilon)\left|\overline{\mathrm{K}}^0\right\rangle\right]\ . \tag{27}$$

These expressions can be inverted to obtain K^0 and $\overline{\mathrm{K}}^0$ in terms of $\mathrm{K_S}$ and $\mathrm{K_L}$:

$$\left|\mathrm{K}^0\right\rangle = \sqrt{\frac{1+|\epsilon|^2}{2}}\frac{1}{1+\epsilon}\left(|\mathrm{K_L}\rangle + |\mathrm{K_S}\rangle\right)$$

$$\left|\overline{\mathrm{K}}^0\right\rangle = \sqrt{\frac{1+|\epsilon|^2}{2}}\frac{1}{1-\epsilon}\left(|\mathrm{K_L}\rangle - |\mathrm{K_S}\rangle\right)\ .$$

A state which is initially pure K^0 therefore evolves with time as

$$\left|\mathrm{K}^0(t)\right\rangle = \sqrt{\frac{1+|\epsilon|^2}{2}}\frac{1}{1+\epsilon}\left(|\mathrm{K_L}\rangle\,\theta_\mathrm{L}(t) + |\mathrm{K_S}\rangle\,\theta_\mathrm{S}(t)\right)\ .$$

To study the decay rate to the $\pi\pi$ (and $\pi\pi\pi$) final states, we again express the time evolution in terms of the CP eigenstates K_1 and K_2, using Equations (26) and (27) :

$$\begin{aligned}\left|\mathrm{K}^0(t)\right\rangle &= \frac{1}{\sqrt{2}}\frac{1}{1+\epsilon}\left[\left(|\mathrm{K}_2\rangle + \epsilon\,|\mathrm{K}_1\rangle\right)\theta_\mathrm{L} + \left(|\mathrm{K}_1\rangle + \epsilon\,|\mathrm{K}_2\rangle\right)\theta_\mathrm{S}\right] \\ &= \frac{1}{\sqrt{2}}\frac{1}{1+\epsilon}\left[|\mathrm{K}_1\rangle\left(\theta_\mathrm{S} + \epsilon\theta_\mathrm{L}\right) + |\mathrm{K}_2\rangle\left(\theta_\mathrm{L} + \epsilon\theta_\mathrm{S}\right)\right]\ .\end{aligned} \tag{28}$$

Assuming that CP violation in the decay process itself can be neglected (which is known to be a good approximation), the $\pi\pi$ final state, with $CP = +1$, still arises entirely from the $CP = +1$ eigenstate K_1 (as in Section 8.3 above). Hence the decay rate to $\pi\pi$ is given by

$$\Gamma(\mathrm{K}^0_{t=0} \to \pi\pi) \propto \left|\left\langle \mathrm{K}_1 \middle| \mathrm{K}^0(t)\right\rangle\right|^2 = \frac{1}{2}\left|\frac{1}{1+\epsilon}\right|^2 |\theta_\mathrm{S} + \epsilon\theta_\mathrm{L}|^2\ . \tag{29}$$

Since $|\epsilon| \ll 1$, we have

$$\left|\frac{1}{1+\epsilon}\right|^2 = \frac{1}{(1+\epsilon^*)(1+\epsilon)} \approx \frac{1}{1+2\mathrm{Re}\epsilon} \approx 1 - 2\mathrm{Re}\epsilon\ .$$

We also have

$$|\theta_{\rm S} + \epsilon\theta_{\rm L}|^2 = \left|e^{-im_{\rm S}t-\Gamma_{\rm S}t/2} + \epsilon.e^{-im_{\rm L}t-\Gamma_{\rm L}t/2}\right|^2$$
$$= e^{-\Gamma_{\rm S}t} + |\epsilon|^2 e^{-\Gamma_{\rm L}t} + 2|\epsilon|e^{-(\Gamma_{\rm L}+\Gamma_{\rm S})t/2}\cos(\Delta m.t - \phi)$$

where $\Delta m \equiv m_{\rm L} - m_{\rm S}$, $\epsilon \equiv |\epsilon|e^{i\phi}$, and we have again used the complex number relation $|z_1 \pm z_2|^2 = |z_1|^2 + |z_2|^2 \pm 2{\rm Re}(z_1^* z_2)$. Hence, in the presence of CP violation and for a beam which is initially pure $\rm K^0$, the decay rate to $\pi\pi$ is

$$\boxed{\Gamma({\rm K}^0_{t=0} \to \pi\pi) = \frac{1}{2}(1 - 2{\rm Re}\epsilon)N_{\pi\pi}\left[e^{-\Gamma_{\rm S}t} + |\epsilon|^2 e^{-\Gamma_{\rm L}t} + 2|\epsilon|e^{-(\Gamma_{\rm L}+\Gamma_{\rm S})t/2}\cos(\Delta m.t - \phi)\right]} \quad (30)$$

In contrast to the CP conserving case of Equation (24), where the decay rate was a pure exponential of the form $e^{-\Gamma_{\rm S}t}$, the $\pi\pi$ decay rate now contains *two* lifetime components: a dominant $\tau_{\rm S}$ component and a small (since $|\epsilon|^2$ is small) $\tau_{\rm L}$ component [4]. At large proper times $t \gg \tau_{\rm S}$, the term proportional to $|\epsilon|^2 e^{-\Gamma_{\rm L}t}$ survives and dominates the decay rate. The observation of a small number of $\pi\pi$ decays at long lifetimes, after the $\rm K_S$ lifetime component had dropped away to a negligible level, formed the basis of the original discovery of CP violation by Fitch and Cronin in 1964.

As discussed below, Equation (30) also contains an *interference term* which allows the magnitude $|\epsilon|$ and phase ϕ of the CP violating parameter ϵ (as well as the mass difference Δm) to be determined.

For a beam which is initially in a pure $\overline{\rm K}^0$ state (rather than $\rm K^0$), the time evolution becomes

$$\left|\overline{\rm K}^0(t)\right\rangle = \sqrt{\frac{1+|\epsilon|^2}{2}}\frac{1}{1-\epsilon}\left[\,|{\rm K_L}\rangle\,\theta_{\rm L}(t) - |{\rm K_S}\rangle\,\theta_{\rm S}(t)\,\right]$$
$$= \frac{1}{\sqrt{2}}\frac{1}{1-\epsilon}\left[\left(|{\rm K_2}\rangle + \epsilon\,|{\rm K_1}\rangle\right)\theta_{\rm L} - \left(|{\rm K_1}\rangle + \epsilon\,|{\rm K_2}\rangle\right)\theta_{\rm S}\right]$$
$$= \frac{1}{\sqrt{2}}\frac{1}{1-\epsilon}\left[|{\rm K_1}\rangle\left(-\theta_{\rm S} + \epsilon\theta_{\rm L}\right) + |{\rm K_2}\rangle\left(\theta_{\rm L} - \epsilon\theta_{\rm S}\right)\right]\ .$$

The $\pi\pi$ decay rate is therefore

$$\Gamma(\overline{\rm K}^0_{t=0} \to \pi\pi) = \left|\left\langle {\rm K_1}\middle|\overline{\rm K}^0(t)\right\rangle\right|^2 = \frac{1}{2}\left|\frac{1}{1-\epsilon}\right|^2 |-\theta_{\rm S} + \epsilon\theta_{\rm L}|^2 \approx \frac{1}{2}(1 + 2{\rm Re}\epsilon)\,|\theta_{\rm S} - \epsilon\theta_{\rm L}|^2$$

But

$$|\theta_{\rm S} - \epsilon\theta_{\rm L}|^2 = e^{-\Gamma_{\rm S}t} + |\epsilon|^2 e^{-\Gamma_{\rm L}t} - 2|\epsilon|e^{-(\Gamma_{\rm L}+\Gamma_{\rm S})t/2}\cos(\Delta m.t - \phi)$$

so that, finally, the $\pi\pi$ decay rate for an initial $\overline{\rm K}^0$ is

$$\boxed{\Gamma(\overline{\rm K}^0_{t=0} \to \pi\pi) = \frac{1}{2}(1 + 2{\rm Re}\epsilon)N_{\pi\pi}\left[e^{-\Gamma_{\rm S}t} + |\epsilon|^2 e^{-\Gamma_{\rm L}t} - 2|\epsilon|e^{-(\Gamma_{\rm L}+\Gamma_{\rm S})t/2}\cos(\Delta m.t - \phi)\right]} \quad (31)$$

This is of the same form as Equation (30) for an initial $\rm K^0$ beam except that the overall normalisation factor is slightly different, $(1 + 2{\rm Re}\epsilon)$ instead of $(1 - 2{\rm Re}\epsilon)$, and, more importantly, the interference term has changed sign. The effect of this change in sign is seen clearly in the left-hand plot of Figure 4 where the decay rates for an initial $\rm K^0$ and an initial $\overline{\rm K}^0$ from Equations (30) and (31) are plotted together.

[4] In the limit $\epsilon = 0$ (*i.e.* no CP violation), Equation (30) reduces to Equation (24), as expected.

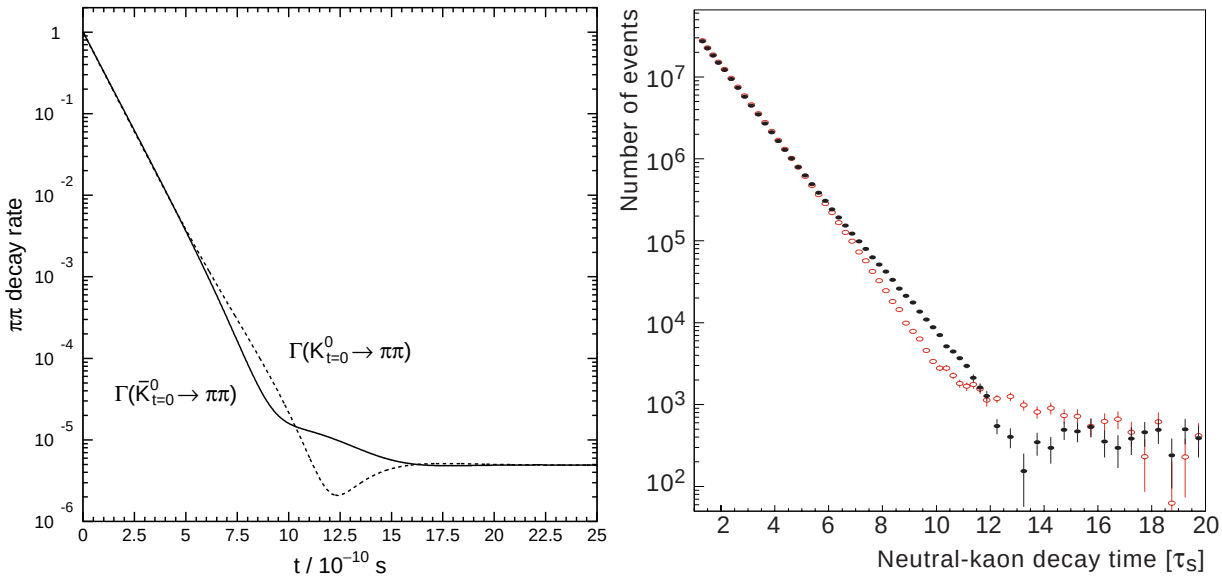

Figure 4: Comparison of the decay rates to $\pi\pi$ for an initial K^0 and an initial $\overline{\mathrm{K}}^0$. The left-hand plot is the theoretical prediction using the measured values of Δm, τ_{S}, τ_{L} and ϵ while the right-hand plot shows the CPLEAR data.

Measurements of $\Gamma(\mathrm{K}^0_{t=0} \to \pi\pi)$ and $\Gamma(\overline{\mathrm{K}}^0_{t=0} \to \pi\pi)$ from the CPLEAR experiment are shown in the right-hand plot of Figure 4. To isolate the CP violating effect due to the change in sign of the interference term, and hence measure $|\epsilon|$ and ϕ (and Δm), it is again helpful to define an appropriate asymmetry:

$$\boxed{A_{+-} \equiv \frac{\Gamma(\overline{\mathrm{K}}^0_{t=0} \to \pi\pi) - \Gamma(\mathrm{K}^0_{t=0} \to \pi\pi)}{\Gamma(\overline{\mathrm{K}}^0_{t=0} \to \pi\pi) + \Gamma(\mathrm{K}^0_{t=0} \to \pi\pi)}}.$$

From Equations (30) and (31), the numerator in this expression is proportional to

$$\Gamma(\overline{\mathrm{K}}^0_{t=0} \to \pi\pi) - \Gamma(\mathrm{K}^0_{t=0} \to \pi\pi) \propto 4\mathrm{Re}\epsilon \left[e^{-\Gamma_{\mathrm{S}}t} + |\epsilon|^2 e^{-\Gamma_{\mathrm{L}}t}\right] - 4|\epsilon| e^{-(\Gamma_{\mathrm{L}}+\Gamma_{\mathrm{S}})t/2} \cos(\Delta m.t - \phi)$$

while the denominator is proportional to

$$\Gamma(\overline{\mathrm{K}}^0_{t=0} \to \pi\pi) + \Gamma(\mathrm{K}^0_{t=0} \to \pi\pi) \propto 2\left[e^{-\Gamma_{\mathrm{S}}t} + |\epsilon|^2 e^{-\Gamma_{\mathrm{L}}t}\right] - 8(\mathrm{Re}\epsilon)|\epsilon| e^{-(\Gamma_{\mathrm{L}}+\Gamma_{\mathrm{S}})t/2} \cos(\Delta m.t - \phi)$$

The second term on the right-hand side of the above expression contains the product $(\mathrm{Re}\epsilon)|\epsilon|$ of two small quantities and can safely be neglected. We therefore obtain

$$\begin{aligned} A_{+-} &\approx \frac{4\mathrm{Re}\epsilon \left[e^{-\Gamma_{\mathrm{S}}t} + |\epsilon|^2 e^{-\Gamma_{\mathrm{L}}t}\right] - 4|\epsilon| e^{-(\Gamma_{\mathrm{L}}+\Gamma_{\mathrm{S}})t/2} \cos(\Delta m.t - \phi)}{2\left[e^{-\Gamma_{\mathrm{S}}t} + |\epsilon|^2 e^{-\Gamma_{\mathrm{L}}t}\right]} \\ &= 2\mathrm{Re}(\epsilon) - \frac{2|\epsilon| e^{-(\Gamma_{\mathrm{L}}+\Gamma_{\mathrm{S}})t/2} \cos(\Delta m.t - \phi)}{e^{-\Gamma_{\mathrm{S}}t} + |\epsilon|^2 e^{-\Gamma_{\mathrm{L}}t}}. \end{aligned}$$

After multiplying through top and bottom by $e^{\Gamma_{\mathrm{S}}t}$, this becomes

$$\boxed{A_{+-} = 2\mathrm{Re}(\epsilon) - \frac{2|\epsilon| e^{(\Gamma_{\mathrm{S}}-\Gamma_{\mathrm{L}})t/2} \cos(\Delta m.t - \phi)}{1 + |\epsilon|^2 e^{(\Gamma_{\mathrm{S}}-\Gamma_{\mathrm{L}})t}}}. \qquad (32)$$

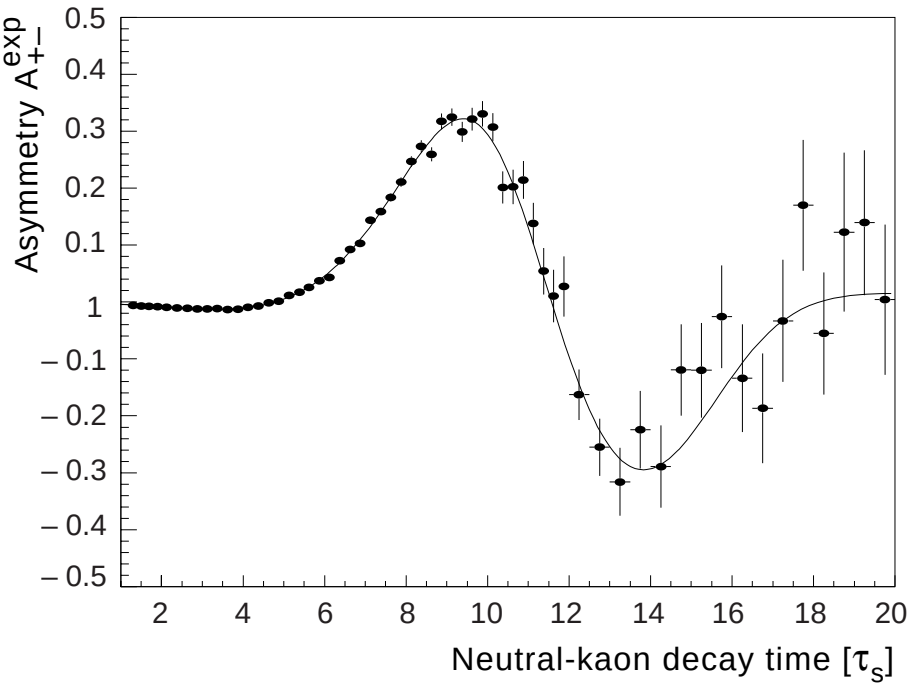

Figure 5: The asymmetry A_{+-} as a function of proper time measured by CPLEAR.

The measurement of the asymmetry A_{+-} by the CPLEAR experiment is shown in Figure 5. A fit of Equation (32) to this data gave the result

$$|\epsilon| = (2.264 \pm 0.035) \times 10^{-3} \qquad \phi = (43.19 \pm 0.73)^\circ \tag{33}$$

8.5 CP Violation: $\pi\pi\pi$ decays (non-examinable)

The $\pi\pi\pi$ final state can be analysed in similar fashion to the $\pi\pi$ case of the previous section. Since the $\pi\pi\pi$ final state has $CP = -1$, it must arise from the decay of the $CP = -1$ eigenstate K_2 rather than K_1. From Equation (28) we find

$$\Gamma(\mathrm{K}^0_{t=0} \to \pi\pi\pi) = \left|\left\langle \mathrm{K}_2 \middle| \mathrm{K}^0(t) \right\rangle\right|^2 = \frac{1}{2}\left|\frac{1}{1+\epsilon}\right|^2 \left|\theta_\mathrm{L} + \epsilon\theta_\mathrm{S}\right|^2$$

which is the same as Equation (29) but with the labels "L" and "S" interchanged. Therefore, from Equation (30), we obtain directly

$$\Gamma(\mathrm{K}^0_{t=0} \to \pi\pi\pi) = \frac{1}{2}(1 - 2\mathrm{Re}\epsilon)N_{\pi\pi\pi}\left[e^{-\Gamma_\mathrm{L}t} + |\epsilon|^2 e^{-\Gamma_\mathrm{S}t} + 2|\epsilon|e^{-(\Gamma_\mathrm{L}+\Gamma_\mathrm{S})t/2}\cos(\Delta m.t - \phi)\right] . \tag{34}$$

In the limit $\epsilon = 0$ (*i.e.* no CP violation), Equation (34) reduces to Equation (25), as expected. The effect of CP violation is to produce a small number of extra decays (represented by the $|\epsilon|^2 e^{-\Gamma_\mathrm{S}t}$ and interference terms) at small times t, on top of a large background from the CP conserving component $e^{-\Gamma_\mathrm{L}t}$. This is in contrast to the $\pi\pi$ case where, at large times, the decays observed ($\mathrm{K}_\mathrm{L} \to \pi\pi$) are due *entirely* to CP violation, with essentially no CP conserving background. The observation of CP violation in $\pi\pi\pi$ decays is therefore much more difficult than in the $\pi\pi$ case, and has not yet been demonstrated. The decay $\mathrm{K}_\mathrm{S} \to \pi^+\pi^-\pi^0$ has in fact been seen (albeit with large errors), but is consistent with being due entirely to the CP conserving $L = 1$ component of the decay.

8.6 CP Violation: $\pi e \nu$ decays

Besides the original observation of CP violation through the detection of a small fraction of $\mathrm{K_L} \to \pi\pi$ decays, CP violation has also been observed in the neutral kaon system as a small difference in the $\mathrm{K_L}$ decay rates to the $\pi^-\mathrm{e}^+\nu_\mathrm{e}$ and $\pi^+\mathrm{e}^-\overline{\nu}_\mathrm{e}$ final states. This difference is quantified via the *charge asymmetry* δ defined as

$$\delta \equiv \frac{\Gamma(\mathrm{K_L} \to \pi^-\mathrm{e}^+\nu_\mathrm{e}) - \Gamma(\mathrm{K_L} \to \pi^+\mathrm{e}^-\overline{\nu}_\mathrm{e})}{\Gamma(\mathrm{K_L} \to \pi^-\mathrm{e}^+\nu_\mathrm{e}) + \Gamma(\mathrm{K_L} \to \pi^+\mathrm{e}^-\overline{\nu}_\mathrm{e})} = (0.327 \pm 0.012)\,\% \,, \tag{35}$$

where the number quoted is the experimental measurement of δ.

As already noted in Equations (16) and (17), the final state $\pi^-\mathrm{e}^+\nu_\mathrm{e}$ can only come from the decay of the K^0 component in the beam, while $\pi^+\mathrm{e}^-\overline{\nu}_\mathrm{e}$ final states must come from $\overline{\mathrm{K}}^0$. From Equation (26), the $\mathrm{K_L}$ eigenstate can be expressed in terms of the K^0 and $\overline{\mathrm{K}}^0$ eigenstates as:

$$|\mathrm{K_L}\rangle = \frac{1}{\sqrt{1+|\epsilon|^2}} \cdot \frac{1}{\sqrt{2}} \left[(1+\epsilon) \left|\mathrm{K}^0\right\rangle + (1-\epsilon) \left|\overline{\mathrm{K}}^0\right\rangle \right] \,. \tag{26$'$}$$

Hence the decay rates to $\pi^-\mathrm{e}^+\nu_\mathrm{e}$ and $\pi^+\mathrm{e}^-\overline{\nu}_\mathrm{e}$ are

$$\Gamma(\mathrm{K_L} \to \pi^-\mathrm{e}^+\nu_\mathrm{e}) \propto \left|\left\langle \mathrm{K}^0 \middle| \mathrm{K_L} \right\rangle\right|^2 \propto |1+\epsilon|^2 \approx 1 + 2\mathrm{Re}(\epsilon)$$
$$\Gamma(\mathrm{K_L} \to \pi^+\mathrm{e}^-\overline{\nu}_\mathrm{e}) \propto \left|\left\langle \overline{\mathrm{K}}^0 \middle| \mathrm{K_L} \right\rangle\right|^2 \propto |1-\epsilon|^2 \approx 1 - 2\mathrm{Re}(\epsilon)$$

where, with $|\epsilon| \ll 1$, we have made the approximation

$$|1 \pm \epsilon|^2 = (1 \pm \epsilon)(1 \pm \epsilon^*) \approx 1 \pm 2\mathrm{Re}(\epsilon) \,.$$

The charge asymmetry is therefore

$$\delta \approx \frac{(1 + 2\mathrm{Re}(\epsilon)) - (1 - 2\mathrm{Re}(\epsilon))}{(1 + 2\mathrm{Re}(\epsilon)) + (1 - 2\mathrm{Re}(\epsilon))}$$

giving finally

$$\boxed{\delta \approx 2\mathrm{Re}(\epsilon) = 2|\epsilon| \cos\phi}$$

where $\epsilon \equiv |\epsilon| e^{i\phi}$. The measurements of $|\epsilon|$ and ϕ obtained from studies of $\pi\pi$ decays, given in Equation (33), can then be used to predict $\delta = 0.33$ %, in good agreement with Equation (35).

The charge asymmetry δ defined in Equation (35) is based on semileptonic decays at large times t such that the $\mathrm{K_S}$ component of the beam has died away to negligible levels, leaving an essentially pure $\mathrm{K_L}$ beam. It is also interesting to study semileptonic decay rate asymmetries at a general time t, allowing tests of T and CPT conservation to be made. The details of these calculations are deferred to the examples sheet; here we just summarise the results.

For an initially pure K^0 beam, and in the presence of CP violation, the CP-conserving strangeness oscillation expressions found above in Equations (12) and (13) become

$$\Gamma(\mathrm{K}^0_{t=0} \to \mathrm{K}^0) \propto \tfrac{1}{4}\left[e^{-\Gamma_\mathrm{S} t} + e^{-\Gamma_\mathrm{L} t} + 2e^{-(\Gamma_\mathrm{S}+\Gamma_\mathrm{L})t/2}\cos\Delta m t\right]$$
$$\Gamma(\mathrm{K}^0_{t=0} \to \overline{\mathrm{K}}^0) \propto \tfrac{1}{4}\left[1 - 4\mathrm{Re}\epsilon\right]\left[e^{-\Gamma_\mathrm{S} t} + e^{-\Gamma_\mathrm{L} t} - 2e^{-(\Gamma_\mathrm{S}+\Gamma_\mathrm{L})t/2}\cos\Delta m t\right] \,.$$

The effect of CP violation is simply to introduce an extra overall relative normalisation factor of $[1 - 4\mathrm{Re}\epsilon]$ between the two expressions. Similarly, for an initial $\overline{\mathrm{K}}^0$, the CP conserving expressions of Equations (14) and (15) become

$$\Gamma(\overline{\mathrm{K}}^0_{t=0} \to \mathrm{K}^0) \propto \tfrac{1}{4}\left[1 + 4\mathrm{Re}\epsilon\right]\left[e^{-\Gamma_\mathrm{S} t} + e^{-\Gamma_\mathrm{L} t} - 2e^{-(\Gamma_\mathrm{S}+\Gamma_\mathrm{L})t/2}\cos\Delta m t\right]$$
$$\Gamma(\overline{\mathrm{K}}^0_{t=0} \to \overline{\mathrm{K}}^0) \propto \tfrac{1}{4}\left[e^{-\Gamma_\mathrm{S} t} + e^{-\Gamma_\mathrm{L} t} + 2e^{-(\Gamma_\mathrm{S}+\Gamma_\mathrm{L})t/2}\cos\Delta m t\right] \ .$$

The extra relative normalisation factor is now $[1 + 4\mathrm{Re}\epsilon]$.

The decay rates to $\pi^-\mathrm{e}^+\nu_\mathrm{e}$ and $\pi^+\mathrm{e}^-\overline{\nu}_\mathrm{e}$ for an initial K^0 can be written down directly as

$$R_+ \equiv \Gamma(\mathrm{K}^0_{t=0} \to \pi^-\mathrm{e}^+\nu_\mathrm{e}) = N_{\pi e\nu}\tfrac{1}{4}\left[e^{-\Gamma_\mathrm{S} t} + e^{-\Gamma_\mathrm{L} t} + 2e^{-(\Gamma_\mathrm{S}+\Gamma_\mathrm{L})t/2}\cos\Delta m t\right] \quad (36)$$
$$R_- \equiv \Gamma(\mathrm{K}^0_{t=0} \to \pi^+\mathrm{e}^-\overline{\nu}_\mathrm{e}) = N_{\pi e\nu}\tfrac{1}{4}\left[1 - 4\mathrm{Re}\epsilon\right]\left[e^{-\Gamma_\mathrm{S} t} + e^{-\Gamma_\mathrm{L} t} - 2e^{-(\Gamma_\mathrm{S}+\Gamma_\mathrm{L})t/2}\cos\Delta m t\right] \ . \quad (37)$$

For an initial $\overline{\mathrm{K}}^0$, the corresponding expressions are

$$\bar{R}_+ \equiv \Gamma(\overline{\mathrm{K}}^0_{t=0} \to \pi^-\mathrm{e}^+\nu_\mathrm{e}) = N_{\pi e\nu}\tfrac{1}{4}\left[1 + 4\mathrm{Re}\epsilon\right]\left[e^{-\Gamma_\mathrm{S} t} + e^{-\Gamma_\mathrm{L} t} - 2e^{-(\Gamma_\mathrm{S}+\Gamma_\mathrm{L})t/2}\cos\Delta m t\right] \quad (38)$$
$$\bar{R}_- \equiv \Gamma(\overline{\mathrm{K}}^0_{t=0} \to \pi^+\mathrm{e}^-\overline{\nu}_\mathrm{e}) = N_{\pi e\nu}\tfrac{1}{4}\left[e^{-\Gamma_\mathrm{S} t} + e^{-\Gamma_\mathrm{L} t} + 2e^{-(\Gamma_\mathrm{S}+\Gamma_\mathrm{L})t/2}\cos\Delta m t\right] \ . \quad (39)$$

When CP violation is taken into account, the asymmetry $A_{\Delta m}$ defined earlier as

$$A_{\Delta m} = \frac{(R_+ + \bar{R}_-) - (R_- + \bar{R}_+)}{(R_+ + \bar{R}_-) + (R_- + \bar{R}_+)} \quad (22)'$$

therefore retains the same form as for the CP conserving case, Equation (23), namely

$$A_{\Delta m} = \frac{2e^{-(\Gamma_\mathrm{S}+\Gamma_\mathrm{L})t/2}\cos\Delta m t}{e^{-\Gamma_\mathrm{S} t} + e^{-\Gamma_\mathrm{L} t}} \ . \quad (23)'$$

From Equations (37) and (38), we see immediately that, because of the additional factors $1 \pm 4\mathrm{Re}\epsilon$, the rate for the transition $\mathrm{K}^0 \to \overline{\mathrm{K}}^0$ is no longer equal to the rate for the transition $\overline{\mathrm{K}}^0 \to \mathrm{K}^0$:

$$\Gamma(\mathrm{K}^0_{t=0} \to \overline{\mathrm{K}}^0) \neq \Gamma(\overline{\mathrm{K}}^0_{t=0} \to \mathrm{K}^0) \ .$$

Besides being an example of CP violation, this can equally well be viewed as a manifestation of T violation: the laws of physics are not invariant under the time reversal transformation $t \to -t$ at a microscopic level [5]. A fundamental result of Quantum Field Theory is that a Lorentz-invariant field theory must be invariant under the combined symmetry CPT. In this sense, T violation is an inevitable consequence of CP violation, and *vice-versa*.

The level of T violation can be quantified by defining the time-reversal asymmetry A_T:

$$\boxed{A_T \equiv \frac{\Gamma(\overline{\mathrm{K}}^0 \to \mathrm{K}^0) - \Gamma(\mathrm{K}^0 \to \overline{\mathrm{K}}^0)}{\Gamma(\overline{\mathrm{K}}^0 \to \mathrm{K}^0) + \Gamma(\mathrm{K}^0 \to \overline{\mathrm{K}}^0)}} \ .$$

[5] This is distinct from the asymmetry in the direction of time provided by the second law of thermodynamics, which can emerge even if the underlying physical laws are time-reversal invariant.

A non-zero value of A_T is then a signal for T violation (known as the Kabir test) [3]. In terms of measurable semi-leptonic decay rates, this is

$$A_T = \frac{\Gamma(\overline{\mathrm{K}}^0_{t=0} \to \pi^- \mathrm{e}^+ \nu_\mathrm{e}) - \Gamma(\mathrm{K}^0_{t=0} \to \pi^+ \mathrm{e}^- \overline{\nu}_\mathrm{e})}{\Gamma(\overline{\mathrm{K}}^0_{t=0} \to \pi^- \mathrm{e}^+ \nu_\mathrm{e}) + \Gamma(\mathrm{K}^0_{t=0} \to \pi^+ \mathrm{e}^- \overline{\nu}_\mathrm{e})}$$

From Equations (37) and (38), it follows that, to good approximation, A_T is a constant, independent of time:

$$\boxed{A_T \approx 4\mathrm{Re}(\epsilon) = 4|\epsilon| \cos\phi}\,.$$

This asymmetry has been measured by CPLEAR, with the results shown in Figure 6. A fit to the data gives

$$A_T = (6.2 \pm 1.7) \times 10^{-3}\,,$$

in good agreement with other measurements of the CP violation parameter $\epsilon \equiv |\epsilon| e^{i\phi}$.

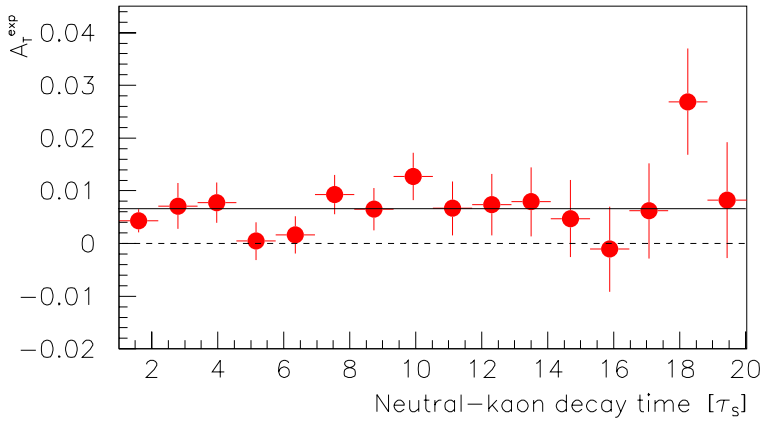

Figure 6: The asymmetry A_T as a function of proper time, in units of the $\mathrm{K_S}$ lifetime τ_S, from the CPLEAR experiment.

Finally, the semileptonic decays can be used to test that CPT is conserved, *i.e.* that the rates for the transitions $\mathrm{K}^0 \to \mathrm{K}^0$ and $\overline{\mathrm{K}}^0 \to \overline{\mathrm{K}}^0$ are equal. The appropriate asymmetry in this case is

$$\boxed{A_{CPT} \equiv \frac{\Gamma(\mathrm{K}^0 \to \mathrm{K}^0) - \Gamma(\overline{\mathrm{K}}^0 \to \overline{\mathrm{K}}^0)}{\Gamma(\mathrm{K}^0 \to \mathrm{K}^0) + \Gamma(\overline{\mathrm{K}}^0 \to \overline{\mathrm{K}}^0)}}$$

which can be determined experimentally by measuring

$$A_{CPT} = \frac{\Gamma(\mathrm{K}^0_{t=0} \to \pi^- \mathrm{e}^+ \nu_\mathrm{e}) - \Gamma(\overline{\mathrm{K}}^0_{t=0} \to \pi^+ \mathrm{e}^- \overline{\nu}_\mathrm{e})}{\Gamma(\mathrm{K}^0_{t=0} \to \pi^- \mathrm{e}^+ \nu_\mathrm{e}) + \Gamma(\overline{\mathrm{K}}^0_{t=0} \to \pi^+ \mathrm{e}^- \overline{\nu}_\mathrm{e})}\,.$$

From Equations (36) and (39), we expect $A_{CPT} = 0$ at all times t. The CPLEAR measurement of this asymmetry is shown in Figure 7 and is clearly consistent with conservation of CPT.

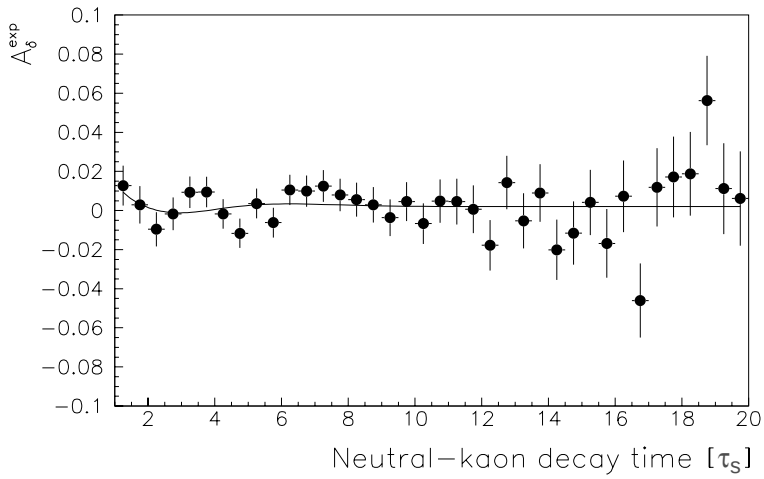

Figure 7: The asymmetry A_{CPT} as a function of proper time, in units of the $\mathrm{K_S}$ lifetime τ_S, from the CPLEAR experiment.

8.7 CP Violation in the Neutral Kaon System: Summary

In summary, with CP violation taken into account, the decay rates to $\pi\pi$ for an initially pure K^0 or $\overline{\mathrm{K}}^0$ beam are

$$\Gamma(\mathrm{K}^0_{t=0} \to \pi\pi) = \frac{1}{2}(1 - 2\mathrm{Re}\epsilon)N_{\pi\pi}\left[e^{-\Gamma_\mathrm{S}t} + |\epsilon|^2 e^{-\Gamma_\mathrm{L}t} + 2|\epsilon|e^{-(\Gamma_\mathrm{L}+\Gamma_\mathrm{S})t/2}\cos(\Delta m.t - \phi)\right] \quad (30)'$$

$$\Gamma(\overline{\mathrm{K}}^0_{t=0} \to \pi\pi) = \frac{1}{2}(1 + 2\mathrm{Re}\epsilon)N_{\pi\pi}\left[e^{-\Gamma_\mathrm{S}t} + |\epsilon|^2 e^{-\Gamma_\mathrm{L}t} - 2|\epsilon|e^{-(\Gamma_\mathrm{L}+\Gamma_\mathrm{S})t/2}\cos(\Delta m.t - \phi)\right] \quad (31)'$$

The corresponding decay rates for semileptonic final states are

$$\Gamma(\mathrm{K}^0_{t=0} \to \pi^-\mathrm{e}^+\nu_\mathrm{e}) = N_{\pi e\nu}\tfrac{1}{4}\left[e^{-\Gamma_\mathrm{S}t} + e^{-\Gamma_\mathrm{L}t} + 2e^{-(\Gamma_\mathrm{S}+\Gamma_\mathrm{L})t/2}\cos\Delta mt\right] \quad (36)'$$

$$\Gamma(\mathrm{K}^0_{t=0} \to \pi^+\mathrm{e}^-\overline{\nu}_\mathrm{e}) = N_{\pi e\nu}\tfrac{1}{4}\left[1 - 4\mathrm{Re}\epsilon\right]\left[e^{-\Gamma_\mathrm{S}t} + e^{-\Gamma_\mathrm{L}t} - 2e^{-(\Gamma_\mathrm{S}+\Gamma_\mathrm{L})t/2}\cos\Delta mt\right] \quad (37)'$$

$$\Gamma(\overline{\mathrm{K}}^0_{t=0} \to \pi^-\mathrm{e}^+\nu_\mathrm{e}) = N_{\pi e\nu}\tfrac{1}{4}\left[1 + 4\mathrm{Re}\epsilon\right]\left[e^{-\Gamma_\mathrm{S}t} + e^{-\Gamma_\mathrm{L}t} - 2e^{-(\Gamma_\mathrm{S}+\Gamma_\mathrm{L})t/2}\cos\Delta mt\right] \quad (38)'$$

$$\Gamma(\overline{\mathrm{K}}^0_{t=0} \to \pi^+\mathrm{e}^-\overline{\nu}_\mathrm{e}) = N_{\pi e\nu}\tfrac{1}{4}\left[e^{-\Gamma_\mathrm{S}t} + e^{-\Gamma_\mathrm{L}t} + 2e^{-(\Gamma_\mathrm{S}+\Gamma_\mathrm{L})t/2}\cos\Delta mt\right] \ . \quad (39)'$$

These decay rates are plotted in Figure 8.

A comparison with the CP conserving case shown earlier in Figure 3 shows immediately that the most visible consequence of CP violation is the existence of $\pi\pi$ decays at large decay times. Also present, but not visible in the plots because of the small relative size of the effect, is the fact that the $\pi^-\mathrm{e}^+\nu_\mathrm{e}$ decay rate is slightly greater than the $\pi^+\mathrm{e}^-\overline{\nu}_\mathrm{e}$ decay rate at large times, as quantified by the CP violating charge asymmetry δ. The small number of extra CP-violating $\mathrm{K_S} \to \pi\pi\pi$ decays at small times is also too small to be visible.

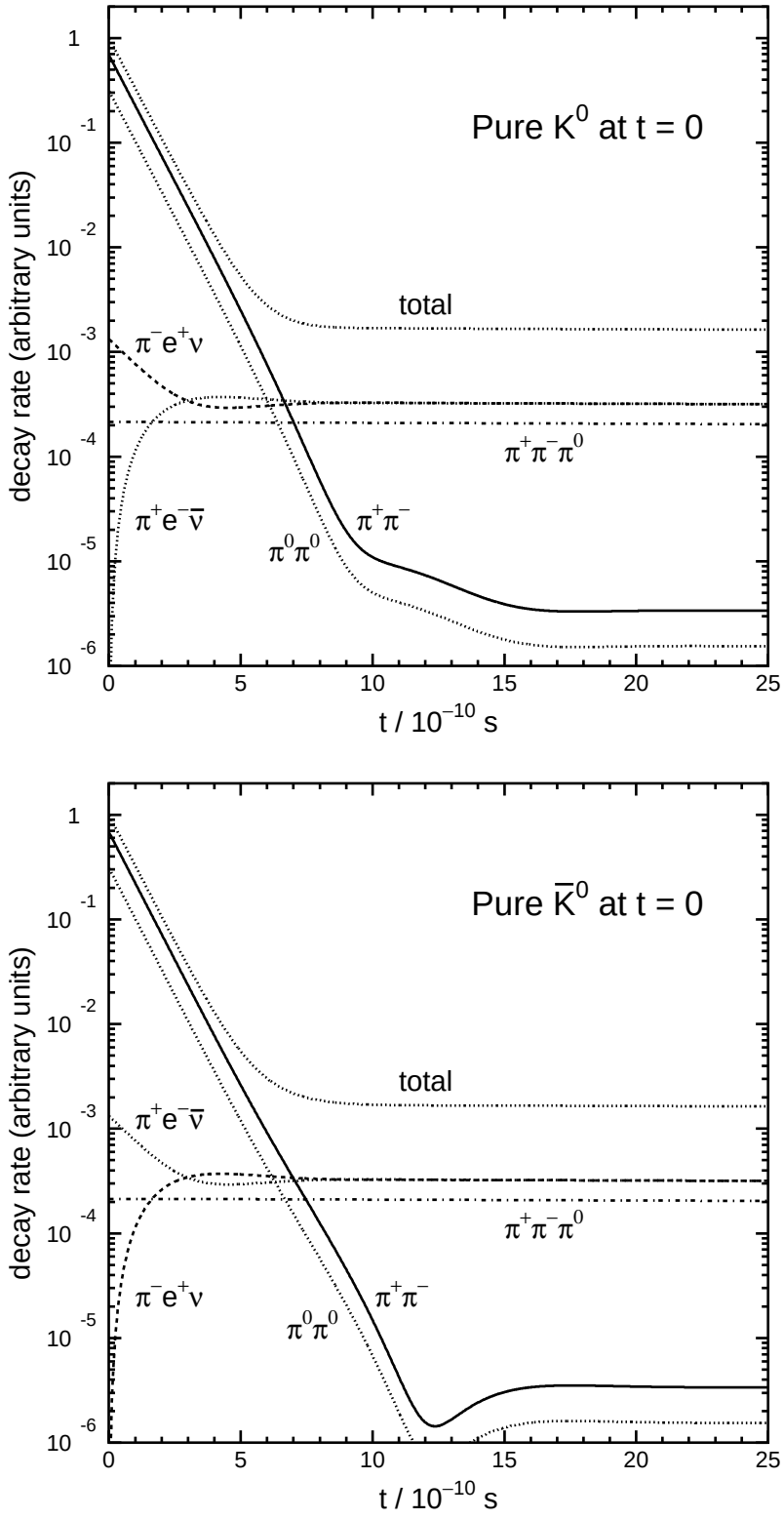

Figure 8: Summary of neutral kaon decay rates as a function of time for an initially pure K^0 beam (top plot) and for an initially pure $\overline{\mathrm{K}}^0$ beam (bottom plot), with CP violation taken into account. The $\pi^-\mu^+\nu_\mu$ and $\pi^+\mu^-\overline{\nu}_\mu$ final states (not shown, for clarity) are similar to $\pi^-\mathrm{e}^+\nu_\mathrm{e}$ and $\pi^+\mathrm{e}^-\overline{\nu}_\mathrm{e}$. The $\pi^0\pi^0\pi^0$ final state (also not shown) is similar to $\pi^+\pi^-\pi^0$. The small difference between the $\pi^-\mathrm{e}^+\nu_\mathrm{e}$ and $\pi^+\mathrm{e}^-\overline{\nu}_\mathrm{e}$ decay rates at large times (the semileptonic charge asymmetry δ) is too small an effect to be visible in the plot, as are the small number of extra CP-violating $\pi\pi\pi$ decays at small times.

8.8 The Neutral B Meson Systems

As well as the neutral kaons, there are heavier neutral meson systems where particle-antiparticle oscillations are possible, in particular the $\mathrm{B^0_d} - \overline{\mathrm{B}}{}^0_\mathrm{d}$ and $\mathrm{B^0_s} - \overline{\mathrm{B}}{}^0_\mathrm{s}$ systems:

$$\mathrm{B^0_d} = (\overline{\mathrm{b}}\mathrm{d}), \qquad \overline{\mathrm{B}}{}^0_\mathrm{d} = (\mathrm{b}\overline{\mathrm{d}}), \qquad \mathrm{B^0_s} = (\overline{\mathrm{b}}\mathrm{s}), \qquad \overline{\mathrm{B}}{}^0_\mathrm{s} = (\mathrm{b}\overline{\mathrm{s}})$$

As discussed in the Appendix, the equivalent of the neutral kaon states $\mathrm{K_S}$ and $\mathrm{K_L}$ for the $\mathrm{B^0_d} - \overline{\mathrm{B}}{}^0_\mathrm{d}$ system are the "heavy" (H) and "light" (L) eigenstates

$$|\mathrm{B_H}\rangle = \frac{1}{\sqrt{1+|\eta|^2}} \left(\left|\mathrm{B^0}\right\rangle + \eta \left|\overline{\mathrm{B}}{}^0\right\rangle \right) \tag{40}$$

$$|\mathrm{B_L}\rangle = \frac{1}{\sqrt{1+|\eta|^2}} \left(\left|\mathrm{B^0}\right\rangle - \eta \left|\overline{\mathrm{B}}{}^0\right\rangle \right) \ , \tag{41}$$

where the complex constant η (not to be confused with the parameter η appearing in the Wolfenstein parameterisation of the CKM matrix) is equivalent to $(1-\epsilon)/(1+\epsilon)$ in the kaon system. In contrast to the neutral kaon system, where the theoretical uncertainties on the prediction of the parameter ϵ are relatively large, the parameter η in the B system can be reliably predicted in the Standard Model:

$$\boxed{\eta = e^{-i2\beta}}$$

where β is one of the angles of the unitarity triangle. In the B system, the coefficients involved in the state mixing are therefore approximately pure phase factors ($e^{-i2\beta}$) rather than numbers close to unity, so that η is a more convenient parameter than ϵ.

Equations (40) and (41) can be inverted to give

$$\left|\mathrm{B^0}\right\rangle = \frac{1}{2}\sqrt{1+|\eta|^2}\,(|\mathrm{B_H}\rangle + |\mathrm{B_L}\rangle) \tag{42}$$

$$\left|\overline{\mathrm{B}}{}^0\right\rangle = \frac{1}{2\eta}\sqrt{1+|\eta|^2}\,(|\mathrm{B_H}\rangle - |\mathrm{B_L}\rangle) \ . \tag{43}$$

The $\mathrm{B_H}$ and $\mathrm{B_L}$ eigenstates have well-defined masses m_H, m_L and lifetimes $1/\Gamma_\mathrm{H}$, $1/\Gamma_\mathrm{L}$, and evolve with time according to

$$|\mathrm{B_H}(t)\rangle = |\mathrm{B_H}\rangle\,\theta_\mathrm{H}(t) = |\mathrm{B_H}\rangle\,e^{-im_\mathrm{H}t-\Gamma_\mathrm{H}t/2}$$
$$|\mathrm{B_L}(t)\rangle = |\mathrm{B_L}\rangle\,\theta_\mathrm{L}(t) = |\mathrm{B_L}\rangle\,e^{-im_\mathrm{L}t-\Gamma_\mathrm{L}t/2}$$

where we have introduced the functions

$$\theta_\mathrm{H}(t) \equiv e^{-im_\mathrm{H}t-\Gamma_\mathrm{H}t/2}, \qquad \theta_\mathrm{L}(t) \equiv e^{-im_\mathrm{L}t-\Gamma_\mathrm{L}t/2} \ . \tag{44}$$

As also discussed in the Appendix, a feature of the B meson systems is that, in contrast to the kaon system where $\tau_\mathrm{L} \gg \tau_\mathrm{S}$ ($\Gamma_\mathrm{L} \ll \Gamma_\mathrm{S}$), the two B eigenstates have very similar lifetimes:

$$\Gamma_\mathrm{H} \approx \Gamma_\mathrm{L} = \Gamma$$

As in the kaon system, the mass difference between the $\mathrm{B_H}$ and $\mathrm{B_L}$ eigenstates is very small:

$$m_\mathrm{H} \approx m_\mathrm{L} = M; \qquad \Delta m \equiv m_\mathrm{H} - m_\mathrm{L} > 0; \qquad \Delta m \ll M \ .$$

8.9 B Meson Oscillations

From Equation (42), a system which is initially in a pure B^0 state evolves with time as

$$\begin{aligned}
\left|\mathrm{B}^0(t)\right\rangle &= \frac{1}{2}\sqrt{1+|\eta|^2}\left[\theta_{\mathrm{H}}\left|\mathrm{B_H}\right\rangle + \theta_{\mathrm{L}}\left|\mathrm{B_L}\right\rangle\right] \\
&= \frac{1}{2}\left[\theta_{\mathrm{H}}\left(\left|\mathrm{B}^0\right\rangle + \eta\left|\overline{\mathrm{B}}^0\right\rangle\right) + \theta_{\mathrm{L}}\left(\left|\mathrm{B}^0\right\rangle - \eta\left|\overline{\mathrm{B}}^0\right\rangle\right)\right] \\
&= \frac{1}{2}(\theta_{\mathrm{H}}+\theta_{\mathrm{L}})\left|\mathrm{B}^0\right\rangle + \frac{\eta}{2}(\theta_{\mathrm{H}}-\theta_{\mathrm{L}})\left|\overline{\mathrm{B}}^0\right\rangle \\
&= f_+(t)\left|\mathrm{B}^0\right\rangle + \eta f_-(t)\left|\overline{\mathrm{B}}^0\right\rangle
\end{aligned} \tag{45}$$

where we have introduced the functions

$$f_\pm(t) \equiv \frac{1}{2}\left[\theta_{\mathrm{H}}(t) \pm \theta_{\mathrm{L}}(t)\right] = \frac{1}{2}e^{-i(m_{\mathrm{H}}-\frac{1}{2}i\Gamma_{\mathrm{H}})t} \pm \frac{1}{2}e^{-i(m_{\mathrm{L}}-\frac{1}{2}i\Gamma_{\mathrm{L}})t} .$$

Since the $\mathrm{B_H}$ and $\mathrm{B_L}$ lifetimes are very similar ($\Gamma_{\mathrm{L}} \approx \Gamma_{\mathrm{H}} \approx \Gamma$), these functions simplify to

$$\begin{aligned}
f_\pm(t) &\approx \tfrac{1}{2}e^{-\frac{1}{2}\Gamma t}\left(e^{-im_{\mathrm{H}}t} \pm e^{-im_{\mathrm{L}}t}\right) \\
&= \tfrac{1}{2}e^{-\frac{1}{2}\Gamma t}e^{-i\frac{1}{2}(m_{\mathrm{H}}+m_{\mathrm{L}})t}\left[e^{-i\frac{1}{2}(m_{\mathrm{H}}-m_{\mathrm{L}})t} \pm e^{i\frac{1}{2}(m_{\mathrm{H}}-m_{\mathrm{L}})t}\right] \\
&= \tfrac{1}{2}e^{-\frac{1}{2}\Gamma t}e^{-iMt}\left[e^{-i\frac{1}{2}\Delta m t} \pm e^{i\frac{1}{2}\Delta m t}\right]
\end{aligned}$$

where $\Delta m \equiv m_{\mathrm{H}} - m_{\mathrm{L}} > 0$. Hence we have

$$\begin{aligned}
f_+(t) &= e^{-iMt}e^{-\frac{1}{2}\Gamma t}\cos(\tfrac{1}{2}\Delta m t) \\
f_-(t) &= -ie^{-iMt}e^{-\frac{1}{2}\Gamma t}\sin(\tfrac{1}{2}\Delta m t)
\end{aligned}$$

and the time evolution of a system which is initially pure B^0 can be written

$$\left|\mathrm{B}^0(t)\right\rangle = e^{-iMt}e^{-\frac{1}{2}\Gamma t}\left[\cos(\tfrac{1}{2}\Delta m t)\left|\mathrm{B}^0\right\rangle - i\eta\sin(\tfrac{1}{2}\Delta m t)\left|\overline{\mathrm{B}}^0\right\rangle\right] . \tag{46}$$

For a system which is initially in a pure $\overline{\mathrm{B}}^0$ state, we have

$$\begin{aligned}
\left|\overline{\mathrm{B}}^0(t)\right\rangle &= \frac{1}{2\eta}\sqrt{1+|\eta|^2}\left[\theta_{\mathrm{H}}\left|\mathrm{B_H}\right\rangle - \theta_{\mathrm{L}}\left|\mathrm{B_L}\right\rangle\right] \\
&= \frac{1}{2\eta}\left[\theta_{\mathrm{H}}(\left|\mathrm{B}^0\right\rangle + \eta\left|\overline{\mathrm{B}}^0\right\rangle) - \theta_{\mathrm{L}}(\left|\mathrm{B}^0\right\rangle - \eta\left|\overline{\mathrm{B}}^0\right\rangle)\right] \\
&= \frac{1}{2\eta}(\theta_{\mathrm{H}}-\theta_{\mathrm{L}})\left|\mathrm{B}^0\right\rangle + \frac{1}{2}(\theta_{\mathrm{H}}+\theta_{\mathrm{L}})\left|\overline{\mathrm{B}}^0\right\rangle \\
&= \frac{1}{\eta}f_-(t)\left|\mathrm{B}^0\right\rangle + f_+(t)\left|\overline{\mathrm{B}}^0\right\rangle
\end{aligned}$$

and hence

$$\left|\overline{\mathrm{B}}^0(t)\right\rangle = e^{-iMt}e^{-\frac{1}{2}\Gamma t}\left[-\frac{i}{\eta}\sin(\tfrac{1}{2}\Delta m t)\left|\mathrm{B}^0\right\rangle + \cos(\tfrac{1}{2}\Delta m t)\left|\overline{\mathrm{B}}^0\right\rangle\right] \tag{47}$$

We therefore expect $\mathrm{B}^0 \leftrightarrow \overline{\mathrm{B}}^0$ flavour oscillations in the B system analagous to $\mathrm{K}^0 \leftrightarrow \overline{\mathrm{K}}^0$ strangeness oscillations in the neutral kaon system. The oscillation probabilities for an initial B^0 can be read off directly from Equation (46):

$$\Gamma(\mathrm{B}^0_{t=0} \to \mathrm{B}^0) = e^{-\Gamma t}\cos^2(\tfrac{1}{2}\Delta m t) \tag{48}$$

$$\Gamma(\mathrm{B}^0_{t=0} \to \overline{\mathrm{B}}^0) = |\eta|^2\, e^{-\Gamma t}\sin^2(\tfrac{1}{2}\Delta m t) \tag{49}$$

while those for an initial $\overline{\mathrm{B}}^0$ are given by Equation (47):

$$\Gamma(\overline{\mathrm{B}}^0_{t=0} \to \overline{\mathrm{B}}^0) = e^{-\Gamma t}\cos^2(\tfrac{1}{2}\Delta m t) \tag{50}$$

$$\Gamma(\overline{\mathrm{B}}^0_{t=0} \to \mathrm{B}^0) = \left|\frac{1}{\eta}\right|^2 e^{-\Gamma t}\sin^2(\tfrac{1}{2}\Delta m t)\ . \tag{51}$$

The effect of B oscillations is shown in Figure 9 for a beam which is initially pure B^0. The measured value of the $\mathrm{B_H} - \mathrm{B_L}$ mass difference is $\Delta m \approx 3.2 \times 10^{-10}\,\mathrm{MeV}$, corresponding to an oscillation period $\tau_{\mathrm{osc}} = 2\pi/\Delta m \approx 12.8\,\mathrm{ps}$. This is to be compared with the measured B^0 lifetime $\tau_{\mathrm{B}} \approx 1.5\,\mathrm{ps}$. Thus, as seen in the figure, only a limited oscillation is visible in practice because the number of B mesons remaining decays rapidly.

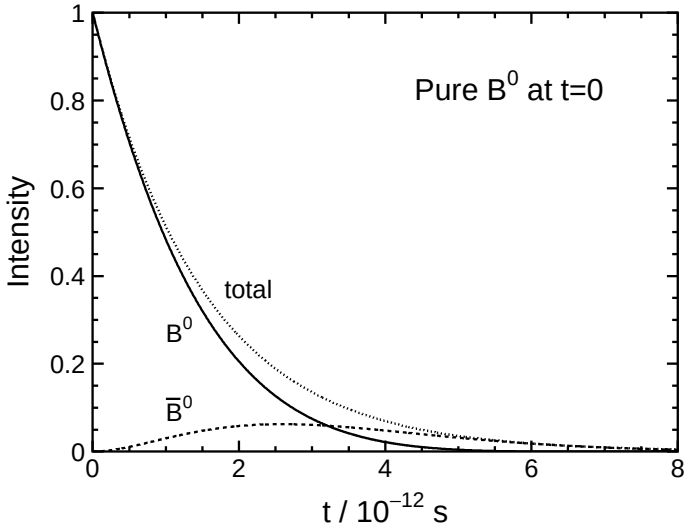

Figure 9: B^0 and $\overline{\mathrm{B}}^0$ intensities as a function of time for a beam which is initially pure B^0, showing the effects of B oscillations.

A comparison of Equations (48) and (50) shows that CPT is always conserved:

$$\Gamma(\mathrm{B}^0_{t=0} \to \mathrm{B}^0) = \Gamma(\overline{\mathrm{B}}^0_{t=0} \to \overline{\mathrm{B}}^0)\ ,$$

while a comparison of Equations (49) and (51) shows that CP violation:

$$\Gamma(\mathrm{B}^0_{t=0} \to \overline{\mathrm{B}}^0) \neq \Gamma(\overline{\mathrm{B}}^0_{t=0} \to \mathrm{B}^0)$$

requires $|\eta| \neq 1$. Since $\eta = e^{-2i\beta}$ in the Standard Model, we expect $|\eta| = 1$ to very good approximation, and it will therefore be very difficult to detect CP violation purely through the mixing of the B^0 and $\overline{\mathrm{B}}^0$ states (the dominant source of CP violation in the $\mathrm{K}^0 - \overline{\mathrm{K}}^0$ system).

Fortunately, as shown in the next section, large CP violating asymmetries are expected in other aspects of the $\mathrm{B}^0 - \overline{\mathrm{B}}^0$ system. Within the last few years, CP violation has in fact finally been observed outside the neutral kaon system, through study of the decay $\mathrm{B}^0_{\mathrm{d}}(\overline{\mathrm{B}}^0_{\mathrm{d}}) \to \mathrm{J}/\psi\mathrm{K_S}$.

8.10 CP Violation in the B System

The J/ψ (which we shall henceforth abbreviate just to ψ) is a charmonium $\mathrm{c\overline{c}}$ state with $J^{PC} = 1^{--}$ and hence is a CP eigenstate with eigenvalue $CP = +1$. To very good approximation (*i.e.* neglecting CP violation effects in the mixing of neutral kaons) the $\mathrm{K_S}$ is a CP eigenstate with $CP = +1$. Since the $\mathrm{B}^0(\overline{\mathrm{B}}^0)$ has zero spin, the $\psi\mathrm{K_S}$ final state must have orbital angular momentum $L = 1$. Overall therefore, in the decay $\mathrm{B}^0(\overline{\mathrm{B}}^0) \to \psi\mathrm{K_S}$, the final state must be an eigenstate of CP with eigenvalue $CP = -1$:

$$CP(\psi\mathrm{K_S}) = CP(\psi).CP(\mathrm{K_S}).(-1)^L = +1.+1.-1 = -1\ .$$

For the final state $\mathrm{J}/\psi\mathrm{K_L}$, the overall CP eigenvalue becomes $CP = +1$ since now the $\mathrm{K_L}$ has $CP = -1$:

$$CP(\psi\mathrm{K_L}) = CP(\psi).CP(\mathrm{K_L}).(-1)^L = +1.-1.-1 = +1\ .$$

For a system which is initially in a pure B^0 state, Equation (45) gives the amplitude (matrix element) for a decay to $\psi\mathrm{K_S}$ to be

$$\begin{aligned} A(\mathrm{B}^0 \to \psi\mathrm{K_S}) &= \left\langle \psi\mathrm{K_S}|H|\mathrm{B}^0(t)\right\rangle \\ &= f_+(t)\left\langle \psi\mathrm{K_S}|H|\mathrm{B}^0\right\rangle + \eta f_-(t)\left\langle \psi\mathrm{K_S}|H|\overline{\mathrm{B}}^0\right\rangle \\ &= \left\langle \psi\mathrm{K_S}|H|\mathrm{B}^0\right\rangle \left[f_+(t) + \eta f_-(t)\frac{\left\langle \psi\mathrm{K_S}|H|\overline{\mathrm{B}}^0\right\rangle}{\left\langle \psi\mathrm{K_S}|H|\mathrm{B}^0\right\rangle}\right]\ . \end{aligned}$$

The decay of a B^0 or $\overline{\mathrm{B}}^0$ to $\psi\mathrm{K_S}$ occurs in two steps, as a decay to $\psi\mathrm{K}^0$ or $\psi\overline{\mathrm{K}}^0$ followed by kaon mixing to give a $\mathrm{K_S}$:

$$\mathrm{B}^0 \to \psi\mathrm{K}^0 \to \psi\mathrm{K_S}; \qquad \overline{\mathrm{B}}^0 \to \psi\overline{\mathrm{K}}^0 \to \psi\mathrm{K_S}$$

But $\mathrm{B}^0 \to \psi\mathrm{K}^0$ involves $\mathrm{\overline{b}} \to \mathrm{\overline{c}c\overline{s}}$ while $\overline{\mathrm{B}}^0 \to \psi\overline{\mathrm{K}}^0$ involves $\mathrm{b} \to \mathrm{c\overline{c}s}$, so

$$A(\mathrm{B}^0 \to \psi\mathrm{K}^0) \propto V^*_{\mathrm{cb}}V_{\mathrm{cs}}, \qquad A(\overline{\mathrm{B}}^0 \to \psi\overline{\mathrm{K}}^0) \propto V_{\mathrm{cb}}V^*_{\mathrm{cs}}$$

which, in the Wolfenstein parameterisation, are purely real and equal to each other. It can be shown that the kaon mixing has no further effect on the ratio of B^0 and $\overline{\mathrm{B}}^0$ amplitudes, giving overall

$$\frac{\left\langle \psi\mathrm{K_S}|H|\overline{\mathrm{B}}^0\right\rangle}{\left\langle \psi\mathrm{K_S}|H|\mathrm{B}^0\right\rangle} = +1\ .$$

Hence, up to the overall normalisation factor of $|\left\langle \psi\mathrm{K_S}|H|\mathrm{B}^0\right\rangle|^2$, we have

$$\begin{aligned} \Gamma(\mathrm{B}^0_{t=0} \to \psi\mathrm{K_S}) &\propto |f_+(t) + \eta f_-(t)|^2 \\ &= e^{-\Gamma t}\left|\cos(\tfrac{1}{2}\Delta m t) - ie^{-i2\beta}\sin(\tfrac{1}{2}\Delta m t)\right|^2 \\ &= e^{-\Gamma t}\left(1 - \sin(\Delta m t)\sin 2\beta\right) \end{aligned} \tag{52}$$

where we have used the complex relation $|z_1 \pm z_2|^2 = |z_1|^2 + |z_2|^2 \pm 2\mathrm{Re}(z_1^* z_2)$. Similarly, for an initial $\overline{\mathrm{B}}^0$ we have

$$\begin{aligned} \Gamma(\overline{\mathrm{B}}^0_{t=0} \to \psi\mathrm{K_S}) &\propto \left| f_+(t) + \frac{1}{\eta}f_-(t)\right|^2 \\ &= e^{-\Gamma t}\left|\cos(\tfrac{1}{2}\Delta m t) - ie^{i2\beta}\sin(\tfrac{1}{2}\Delta m t)\right|^2 \\ &= e^{-\Gamma t}\left(1 + \sin(\Delta m t)\sin 2\beta\right)\ . \end{aligned} \tag{53}$$

As usual, we can define an asymmetry $A(t)$ which is independent of the unknown overall normalisation factor:

$$\boxed{A_{\psi \mathrm{K_S}}(t) \equiv \frac{\Gamma(\overline{\mathrm{B}}^0_{t=0} \to \psi \mathrm{K_S}) - \Gamma(\mathrm{B}^0_{t=0} \to \psi \mathrm{K_S})}{\Gamma(\overline{\mathrm{B}}^0_{t=0} \to \psi \mathrm{K_S}) + \Gamma(\mathrm{B}^0_{t=0} \to \psi \mathrm{K_S})}} .$$

From Equations (52) and (53) we obtain the clean Standard Model prediction

$$\boxed{A_{\psi \mathrm{K_S}}(t) = \sin(\Delta m t) \sin 2\beta}$$

This analysis applies also to the final state $\psi \mathrm{K_L}$, except that now the $\psi \mathrm{K_L}$ system has $CP = +1$ instead of $CP = -1$. It can be shown that this induces a change in sign of the B^0 and $\overline{\mathrm{B}}^0$ amplitude ratio:

$$\frac{\langle \psi \mathrm{K_L} | H | \overline{\mathrm{B}}^0 \rangle}{\langle \psi \mathrm{K_L} | H | \mathrm{B}^0 \rangle} = -1 .$$

This in turn gives a change in sign of the asymmetry:

$$\boxed{A_{\psi \mathrm{K_L}}(t) = -\sin(\Delta m t) \sin 2\beta}$$

8.11 Appendix: The CKM Matrix

8.11.1 The Wolfenstein Parameterisation

The CKM matrix is a unitary matrix which relates the weak interaction eigenstates d', s', b' to the strong interaction eigenstates $\mathrm{d}, \mathrm{s}, \mathrm{b}$:

$$\begin{pmatrix} d' \\ s' \\ b' \end{pmatrix} = \begin{pmatrix} V_{\mathrm{ud}} & V_{\mathrm{us}} & V_{\mathrm{ub}} \\ V_{\mathrm{cd}} & V_{\mathrm{cs}} & V_{\mathrm{cb}} \\ V_{\mathrm{td}} & V_{\mathrm{ts}} & V_{\mathrm{tb}} \end{pmatrix} \begin{pmatrix} d \\ s \\ b \end{pmatrix} .$$

We state without proof that if any of the elements of the CKM matrix are complex rather than real, then the Standard Model can accommodate CP violation. We also assert that a complex CKM matrix requires at least three generations of quarks (*i.e.* CP violation is not possible with only two generations), and that a 3×3 CKM matrix can always be parameterised in terms of three observable mixing angles and one observable phase angle, for example as the product of three rotation matrices:

$$V_{\mathrm{CKM}} = R_{23}(\theta_{23}, 0) \times R_{13}(\theta_{13}, -\delta) \times R_{12}(\theta_{12}, 0) \tag{54}$$

$$= \begin{pmatrix} 1 & 0 & 0 \\ 0 & c_{23} & s_{23} \\ 0 & -s_{23} & c_{23} \end{pmatrix} \times \begin{pmatrix} c_{13} & 0 & s_{13}e^{-i\delta} \\ 0 & 1 & 0 \\ -s_{13}e^{i\delta} & 0 & c_{13} \end{pmatrix} \times \begin{pmatrix} c_{12} & s_{12} & 0 \\ -s_{12} & c_{12} & 0 \\ 0 & 0 & 1 \end{pmatrix} \tag{55}$$

$$= \begin{pmatrix} c_{12}c_{13} & s_{12}c_{13} & s_{13}e^{-i\delta} \\ -s_{12}c_{23} - c_{12}s_{23}s_{13}e^{i\delta} & c_{12}c_{23} - s_{12}s_{23}s_{13}e^{i\delta} & s_{23}c_{13} \\ s_{12}s_{23} - c_{12}c_{23}s_{13}e^{i\delta} & -c_{12}s_{23} - s_{12}c_{23}s_{13}e^{i\delta} & c_{23}c_{13} \end{pmatrix} \tag{56}$$

where $s_{ij} \equiv \sin\theta_{ij}$ and $c_{ij} \equiv \cos\theta_{ij}$. This is an exact parameterisation based on three mixing angles θ_{12}, θ_{23}, θ_{13} and a phase angle δ which enters through the phase factor $e^{i\delta}$.

The Wolfenstein parameterisation [4] is obtained by defining

$$s_{12} \equiv \lambda, \qquad s_{23} \equiv A\lambda^2, \qquad s_{13}e^{-i\delta} \equiv A\lambda^3(\rho - i\eta)$$

and is particularly useful because it reflects the observed hierarchy of the measured values of the CKM matrix elements. Here, A is a real parameter of order unity ($A \approx 0.83$) while λ is approximately the sine of the Cabbibo angle:

$$\lambda \approx \sin\theta_C \approx 0.22 \; .$$

The remaining parameters, ρ and η, enter as $e^{i\delta} = (\rho + i\eta)/\sqrt{\rho^2 + \eta^2}$ and fix the complex (CP violating) component of the CKM matrix.

The Wolfenstein parameterisation can be obtained to any desired order of accuracy by Taylor expanding the c_{ij} and s_{ij} in powers of the parameter λ:

$$\begin{aligned}
c_{12} &= \sqrt{1-\lambda^2} && = 1 - \tfrac{1}{2}\lambda^2 - \tfrac{1}{8}\lambda^4 + \mathcal{O}(\lambda^6) \\
c_{23} &= \sqrt{1-A^2\lambda^4} && = 1 - \tfrac{1}{2}A^2\lambda^4 - \tfrac{1}{8}A^4\lambda^8 + \mathcal{O}(\lambda^{12}) \\
c_{13} &= \sqrt{1-A^2\lambda^6(\rho^2+\eta^2)} && = 1 - \tfrac{1}{2}A^2\lambda^6(\rho^2+\eta^2) + \mathcal{O}(\lambda^{12}) \\
s_{13} &= A\lambda^3\sqrt{\rho^2+\eta^2}
\end{aligned}$$

Keeping only terms up to $\mathcal{O}(\lambda^3)$, which is sufficient given the precision of current measurements, the CKM matrix is

$$V_{\rm CKM} = \begin{pmatrix} V_{\rm ud} & V_{\rm us} & V_{\rm ub} \\ V_{\rm cd} & V_{\rm cs} & V_{\rm cb} \\ V_{\rm td} & V_{\rm ts} & V_{\rm tb} \end{pmatrix} = \begin{pmatrix} 1 - \frac{1}{2}\lambda^2 & \lambda & A\lambda^3(\rho - i\eta) \\ -\lambda & 1 - \frac{1}{2}\lambda^2 & A\lambda^2 \\ A\lambda^3(1 - \rho - i\eta) & -A\lambda^2 & 1 \end{pmatrix} + \mathcal{O}(\lambda^4) \qquad (57)$$

At this order, only $V_{\rm ub} = A\lambda^3(\rho - i\eta)$ and $V_{\rm td} = A\lambda^3(1 - \rho - i\eta)$ are complex; the remaining seven elements are real. In the Wolfenstein parameterisation, CP violation arises if the constant η is non-zero.

8.11.2 The Unitarity Triangle

The diagonal elements of the unitarity equation $V_{\rm CKM}V_{\rm CKM}^\dagger = I$ show that the moduli squared in any row of the CKM matrix sum to unity:

$$|V_{\rm ud}|^2 + |V_{\rm us}|^2 + |V_{\rm ub}|^2 = 1 \qquad (58)$$
$$|V_{\rm cd}|^2 + |V_{\rm cs}|^2 + |V_{\rm cb}|^2 = 1 \qquad (59)$$
$$|V_{\rm td}|^2 + |V_{\rm ts}|^2 + |V_{\rm tb}|^2 = 1 \; . \qquad (60)$$

Similarly, writing the unitarity relation in the form $V_{\rm CKM}^\dagger V_{\rm CKM} = I$, the sum within any *column* of the CKM matrix is also unity:

$$\begin{aligned}
|V_{\rm ud}|^2 + |V_{\rm cd}|^2 + |V_{\rm td}|^2 &= 1 \\
|V_{\rm us}|^2 + |V_{\rm cs}|^2 + |V_{\rm ts}|^2 &= 1 \\
|V_{\rm ub}|^2 + |V_{\rm cb}|^2 + |V_{\rm tb}|^2 &= 1 \; .
\end{aligned}$$

The off-diagonal elements of the unitarity relation $V_{\rm CKM}V_{\rm CKM}^\dagger = I$ provide six further equations:

$$(uc) \qquad V_{\rm cd}V_{\rm ud}^* + V_{\rm cs}V_{\rm us}^* + V_{\rm cb}V_{\rm ub}^* = 0 \tag{61}$$

$$(ct) \qquad V_{\rm td}V_{\rm cd}^* + V_{\rm ts}V_{\rm cs}^* + V_{\rm tb}V_{\rm cb}^* = 0 \tag{62}$$

$$(ut) \qquad V_{\rm td}V_{\rm ud}^* + V_{\rm ts}V_{\rm us}^* + V_{\rm tb}V_{\rm ub}^* = 0 \tag{63}$$

$$(ds) \qquad V_{\rm ud}V_{\rm us}^* + V_{\rm cd}V_{\rm cs}^* + V_{\rm td}V_{\rm ts}^* = 0 \tag{64}$$

$$(sb) \qquad V_{\rm us}V_{\rm ub}^* + V_{\rm cs}V_{\rm cb}^* + V_{\rm ts}V_{\rm tb}^* = 0 \tag{65}$$

$$(db) \qquad V_{\rm ud}V_{\rm ub}^* + V_{\rm cd}V_{\rm cb}^* + V_{\rm td}V_{\rm tb}^* = 0 \tag{66}$$

These equations correspond to six triangles in the complex (ρ, η) plane. Particularly useful as a means of representing current measurements connected with CP violation is the triangle represented by Equation (66):

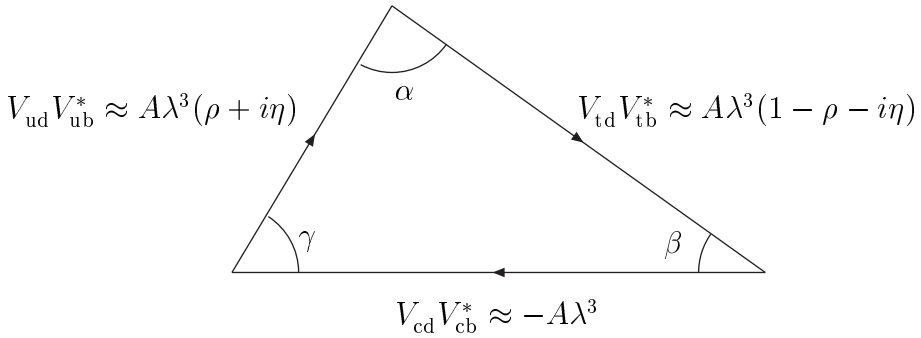

Scaling this triangle by dividing all sides by a factor $|V_{\rm cd}V_{\rm cb}^*| \approx A\lambda^3$ then gives the *unitarity triangle*, with base of length unity along the real axis and apex at the point $\rho + i\eta$:

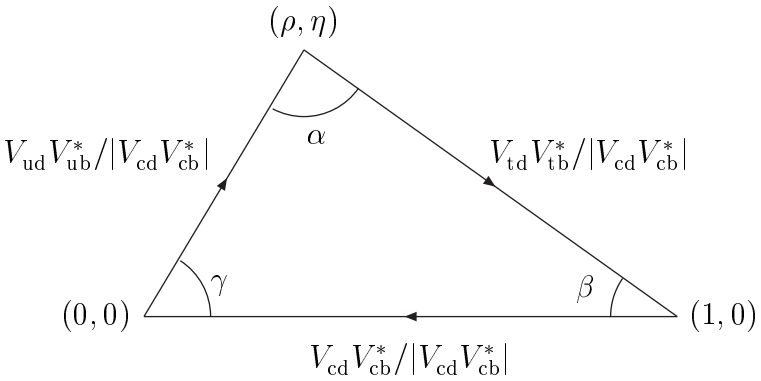

In the Wolfenstein parameterisation, two of the CKM matrix elements are complex: $V_{\rm td}$ and $V_{\rm ub}$. These elements can be expressed in terms of the angles β and γ of the unitarity triangle as

$$V_{\rm td} = A\lambda^3(1 - \rho - i\eta) = |V_{\rm td}|e^{-i\beta}$$

$$V_{\rm ub} = A\lambda^3(\rho - i\eta) = |V_{\rm ub}|e^{-i\gamma}$$

8.12 Appendix: Particle-Antiparticle Mixing (non-examinable)

The wavefunction of a single particle of mass M and lifetime $\tau = 1/\Gamma$ at rest evolves with time as

$$\psi(t) = Ae^{-\Gamma t/2}e^{-iMt} ,$$

giving a probability $|\psi|^2 \propto e^{-\Gamma t} = e^{-t/\tau}$ appropriate to exponential decay. This wavefunction satisfies the time-dependent Schrodinger equation

$$(M - \tfrac{1}{2}i\Gamma)\psi(t) = i\frac{\partial}{\partial t}\,|\psi(t)\rangle \ .$$

For the $\mathrm{K}^0 - \overline{\mathrm{K}}^0$ system, the wavefunction becomes a linear combination of the K^0 and $\overline{\mathrm{K}}^0$ states:

$$|\psi(t)\rangle = a(t)\left|\mathrm{K}^0\right\rangle + b(t)\left|\overline{\mathrm{K}}^0\right\rangle \tag{67}$$

and the time-dependent Schrodinger becomes a two-dimensional matrix equation for the functions $a(t)$ and $b(t)$:

$$(\boldsymbol{M} - \tfrac{1}{2}i\boldsymbol{\Gamma})\begin{pmatrix} a \\ b \end{pmatrix} = i\frac{\partial}{\partial t}\begin{pmatrix} a \\ b \end{pmatrix}$$

with Hamiltonian

$$\boldsymbol{H} = \boldsymbol{M} - \tfrac{1}{2}i\boldsymbol{\Gamma} = \begin{pmatrix} M_{11} & M_{12} \\ M_{21} & M_{22} \end{pmatrix} - \tfrac{1}{2}i\begin{pmatrix} \Gamma_{11} & \Gamma_{12} \\ \Gamma_{21} & \Gamma_{22} \end{pmatrix} \ .$$

For the Hamiltonian to be hermitian, we must have

$$\begin{array}{lll} M_{11} = M_{11}^*, & M_{22} = M_{22}^*, & M_{12} = M_{21}^*; \\ \Gamma_{11} = \Gamma_{11}^*, & \Gamma_{22} = \Gamma_{22}^*, & \Gamma_{12} = \Gamma_{21}^* \ . \end{array}$$

If CPT is conserved, it can be shown further that the diagonal elements of each matrix must be real and equal to each other:

$$M_{11} = M_{22} \equiv M \qquad \text{and} \qquad \Gamma_{11} = \Gamma_{22} \equiv \Gamma$$

where M and Γ are real constants. Overall, therefore, the Schrodinger equation must take the form

$$\boxed{\begin{pmatrix} M - \frac{1}{2}i\Gamma & M_{12} - \frac{1}{2}i\Gamma_{12} \\ M_{12}^* - \frac{1}{2}i\Gamma_{12}^* & M - \frac{1}{2}i\Gamma \end{pmatrix}\begin{pmatrix} a \\ b \end{pmatrix} = i\frac{\partial}{\partial t}\begin{pmatrix} a \\ b \end{pmatrix}} \ . \tag{68}$$

The coupled differential equations for $a(t)$ and $b(t)$ in Equation (68) can be solved by first finding the eigenstates (which we shall call $\mathrm{K_L}$ and $\mathrm{K_S}$) of the Hamiltonian $\boldsymbol{H}$ and then transforming Equation (68) into the $\mathrm{K_L}$, $\mathrm{K_S}$ basis. The eigenvalues and eigenvectors of $\boldsymbol{H}$ can be found by solving the equation

$$\begin{pmatrix} M - \frac{1}{2}i\Gamma & M_{12} - \frac{1}{2}i\Gamma_{12} \\ M_{12}^* - \frac{1}{2}i\Gamma_{12}^* & M - \frac{1}{2}i\Gamma \end{pmatrix}\begin{pmatrix} p \\ q \end{pmatrix} = \lambda\begin{pmatrix} p \\ q \end{pmatrix} \ . \tag{69}$$

This equation has non-trivial solutions only if the determinant $|H - \lambda I| = 0$ vanishes:

$$(M - \tfrac{1}{2}i\Gamma - \lambda)^2 - (M_{12}^* - \tfrac{1}{2}i\Gamma_{12}^*)(M_{12} - \tfrac{1}{2}i\Gamma_{12}) = 0 \ .$$

This gives

$$\lambda = M - \tfrac{1}{2}i\Gamma \pm \sqrt{(M_{12}^* - \tfrac{1}{2}i\Gamma_{12}^*)(M_{12} - \tfrac{1}{2}i\Gamma_{12})}\,. \tag{70}$$

Writing the two possible solutions as $\lambda_i \equiv m_i - \frac{1}{2}i\Gamma_i$ with $i = 1, 2$, or equivalently i =S,L, the eigenvalues are

$$\lambda_L = m_{\rm L} - \tfrac{1}{2}i\Gamma_{\rm L} = M - \tfrac{1}{2}i\Gamma + \sqrt{(M_{12}^* - \tfrac{1}{2}i\Gamma_{12}^*)(M_{12} - \tfrac{1}{2}i\Gamma_{12})} \tag{71}$$

$$\lambda_S = m_{\rm S} - \tfrac{1}{2}i\Gamma_{\rm S} = M - \tfrac{1}{2}i\Gamma - \sqrt{(M_{12}^* - \tfrac{1}{2}i\Gamma_{12}^*)(M_{12} - \tfrac{1}{2}i\Gamma_{12})} \tag{72}$$

where $m_{\rm L}$, $m_{\rm S}$, $\Gamma_{\rm L}$ and $\Gamma_{\rm S}$ are real constants which we shall see below are the masses and inverse lifetimes of the $\rm K_L$ and $\rm K_S$ states.

The eigenstates corresponding to the eigenvalues λ_L and λ_S can be found by substituting Equation (70) into Equation (69):

$$(M - \tfrac{1}{2}i\Gamma)p + (M_{12} - \tfrac{1}{2}i\Gamma_{12})q = \left[M - \tfrac{1}{2}i\Gamma \pm \sqrt{(M_{12}^* - \tfrac{1}{2}i\Gamma_{12}^*)(M_{12} - \tfrac{1}{2}i\Gamma_{12})}\right] p$$

which gives

$$\left(\frac{q}{p}\right)_L = +\sqrt{\frac{M_{12}^* - \frac{1}{2}i\Gamma_{12}^*}{M_{12} - \frac{1}{2}i\Gamma_{12}}}, \qquad \left(\frac{q}{p}\right)_S = -\sqrt{\frac{M_{12}^* - \frac{1}{2}i\Gamma_{12}^*}{M_{12} - \frac{1}{2}i\Gamma_{12}}}$$

Thus, denoting the eigenstates corresponding to the eigenvalues λ_L and λ_S by $|\rm K_L\rangle$ and $|\rm K_S\rangle$, we have

$$H\,|\mathrm{K_L}\rangle = (m_{\rm L} - \tfrac{1}{2}i\Gamma_{\rm L})\,|\mathrm{K_L}\rangle$$
$$H\,|\mathrm{K_S}\rangle = (m_{\rm S} - \tfrac{1}{2}i\Gamma_{\rm S})\,|\mathrm{K_S}\rangle$$

with normalised eigenstates

$$|\mathrm{K_L}\rangle = \frac{1}{\sqrt{1+|\eta|^2}}\begin{pmatrix}1\\ \eta\end{pmatrix} = \frac{1}{\sqrt{1+|\eta|^2}}\left(\left|\mathrm{K^0}\right\rangle + \eta\left|\overline{\mathrm{K}}^0\right\rangle\right) \tag{73}$$

$$|\mathrm{K_S}\rangle = \frac{1}{\sqrt{1+|\eta|^2}}\begin{pmatrix}1\\ -\eta\end{pmatrix} = \frac{1}{\sqrt{1+|\eta|^2}}\left(\left|\mathrm{K^0}\right\rangle - \eta\left|\overline{\mathrm{K}}^0\right\rangle\right) \tag{74}$$

where we have defined

$$\eta \equiv \sqrt{\frac{M_{12}^* - \frac{1}{2}i\Gamma_{12}^*}{M_{12} - \frac{1}{2}i\Gamma_{12}}}\,. \tag{75}$$

Inverting Equations (73) and (74), in the $\rm K_L$, $\rm K_S$ basis the wavefunction $\psi(t)$ of Equation (67) becomes

$$\begin{aligned}|\psi(t)\rangle &= a(t)\left|\mathrm{K^0}\right\rangle + b(t)\left|\overline{\mathrm{K}}^0\right\rangle \\ &= \sqrt{1+|\eta|^2}\left[\frac{a(t)}{2}(\mathrm{K_L}+\mathrm{K_S}) + \frac{b(t)}{2\eta}(\mathrm{K_L}-\mathrm{K_S})\right] \\ &= \frac{\sqrt{1+|\eta|^2}}{2}\left[a_{\rm L}(t)\,|\mathrm{K_L}\rangle + a_{\rm S}(t)\,|\mathrm{K_S}\rangle\right]\end{aligned}$$

where the functions $a_{\rm L}(t)$ and $a_{\rm S}(t)$ are defined as

$$a_{\rm L}(t) \equiv a(t) + \frac{b(t)}{\eta}; \qquad a_{\rm S}(t) \equiv a(t) - \frac{b(t)}{\eta}\ . \tag{76}$$

The Schrodinger equation, Equation (68), can be used to obtain differential equations for the functions $a_{\rm L}(t)$ and $a_{\rm S}(t)$. For $a_{\rm L}(t)$ for example, we obtain

$$\begin{aligned}
i\frac{\partial a_{\rm L}}{\partial t} &= i\frac{\partial a}{\partial t} + \frac{i}{\eta}\frac{\partial b}{\partial t} \\
&= \left[(M - \tfrac{1}{2}i\Gamma)a + (M_{12} - \tfrac{1}{2}i\Gamma_{12})b\right] + \frac{1}{\eta}\left[(M^*_{12} - \tfrac{1}{2}i\Gamma^*_{12})a + (M - \tfrac{1}{2}i\Gamma)b\right] \\
&= (M - \tfrac{1}{2}i\Gamma)\left(a + \frac{b}{\eta}\right) + (M_{12} - \tfrac{1}{2}i\Gamma_{12})b + \frac{1}{\eta}(M^*_{12} - \tfrac{1}{2}i\Gamma^*_{12})a \\
&= (M - \tfrac{1}{2}i\Gamma)\left(a + \frac{b}{\eta}\right) + (M_{12} - \tfrac{1}{2}i\Gamma_{12})b + \sqrt{(M^*_{12} - \tfrac{1}{2}i\Gamma^*_{12})(M^*_{12} - \tfrac{1}{2}i\Gamma^*_{12})}a \\
&= (M - \tfrac{1}{2}i\Gamma)\left(a + \frac{b}{\eta}\right) + \sqrt{(M^*_{12} - \tfrac{1}{2}i\Gamma^*_{12})(M^*_{12} - \tfrac{1}{2}i\Gamma^*_{12})}\left(a + \frac{b}{\eta}\right) \\
&= (m_{\rm L} - \tfrac{1}{2}i\Gamma_{\rm L})a_{\rm L}
\end{aligned}$$

where we have made use of Equations (75), (71) and (76). A similar argument works for the function $a_{\rm S}(t)$, giving altogether

$$i\frac{\partial a_{\rm L}}{\partial t} = (m_{\rm L} - \tfrac{1}{2}i\Gamma_{\rm L})a_{\rm L}\,; \qquad i\frac{\partial a_{\rm S}}{\partial t} = (m_{\rm S} - \tfrac{1}{2}i\Gamma_{\rm S})a_{\rm S}\ .$$

In matrix notation this is

$$\begin{pmatrix} m_{\rm L} - \frac{1}{2}i\Gamma_{\rm L} & 0 \\ 0 & m_{\rm S} - \frac{1}{2}i\Gamma_{\rm S} \end{pmatrix} \begin{pmatrix} a_{\rm L} \\ a_{\rm S} \end{pmatrix} = i\frac{\partial}{\partial t}\begin{pmatrix} a_{\rm L} \\ a_{\rm S} \end{pmatrix}\ ,$$

which is just the time-dependent Schrodinger equation in the $\rm K_L$, $\rm K_S$ basis.

The differential equations for $a_{\rm L}(t)$ and $a_{\rm S}(t)$ are easily solved to give

$$\begin{aligned}
a_{\rm L}(t) &\propto e^{-im_{\rm L}t - \Gamma_{\rm L}t/2} \\
a_{\rm S}(t) &\propto e^{-im_{\rm S}t - \Gamma_{\rm S}t/2}
\end{aligned}$$

and the general solution to the time-dependent Schrodinger equation is therefore

$$\boxed{\psi(t) = A_L e^{-im_{\rm L}t - \Gamma_{\rm L}t/2}\,|{\rm K_L}\rangle + A_S e^{-im_{\rm S}t - \Gamma_{\rm S}t/2}\,|{\rm K_S}\rangle}$$

where A_L and A_S are complex constants which are determined by the initial conditions. This form of the solution demonstrates explicitly that the eigenstates $\rm K_L$ and $\rm K_S$ are indeed the neutral kaon states with definite mass ($m_{\rm S}$, $m_{\rm L}$) and lifetime ($1/\Gamma_{\rm L}$, $1/\Gamma_{\rm S}$).

The case $\eta = 1$ corresponds to CP conservation with eigenstates

$$|{\rm K_L}\rangle = \frac{1}{\sqrt{2}}\left(\left|{\rm K^0}\right\rangle + \left|\overline{\rm K}^0\right\rangle\right), \qquad |{\rm K_S}\rangle = \frac{1}{\sqrt{2}}\left(\left|{\rm K^0}\right\rangle - \left|\overline{\rm K}^0\right\rangle\right)\ .$$

In the kaon system, it is found that $\eta \simeq 1$ and it is convenient to introduce the small parameter ϵ to quantify the amount of CP violation present:

$$\epsilon \equiv \frac{1-\eta}{1+\eta} \, .$$

This can be inverted to give

$$\eta = \frac{1-\epsilon}{1+\epsilon}$$

and, in terms of ϵ, the neutral kaon eigenstates become

$$\begin{aligned} |\mathrm{K_L}\rangle &= \frac{1}{\sqrt{2(1+|\epsilon|^2)}} \left[(1+\epsilon) \left|\mathrm{K}^0\right\rangle + (1-\epsilon) \left|\overline{\mathrm{K}}^0\right\rangle \right] \\ |\mathrm{K_S}\rangle &= \frac{1}{\sqrt{2(1+|\epsilon|^2)}} \left[(1+\epsilon) \left|\mathrm{K}^0\right\rangle - (1-\epsilon) \left|\overline{\mathrm{K}}^0\right\rangle \right] \, . \end{aligned}$$

The analysis above applies also to the neutral B meson systems $\mathrm{B}^0_\mathrm{d} - \overline{\mathrm{B}}^0_\mathrm{d}$ and $\mathrm{B}^0_\mathrm{s} - \overline{\mathrm{B}}^0_\mathrm{s}$. For the B mesons, some simplification is possible because the off-diagonal decay matrix element is very small:

$$|\Gamma_{12}| \ll |M_{12}| \, .$$

This condition arises because the B mesons have a very large number of possible decay modes available to them, which are charge conjugates of each other (*e.g.* $\mathrm{B}^0 \to \mathrm{K}^+\pi^-$ and $\overline{\mathrm{B}}^0 \to \mathrm{K}^-\pi^+$), but only a small fraction of the decay final states are common to both the B^0 and the $\overline{\mathrm{B}}^0$ (*e.g.* $\mathrm{B}^0 \to \pi^+\pi^-$ and $\overline{\mathrm{B}}^0 \to \pi^+\pi^-$). With $|\Gamma_{12}|$ small, the eigenvalues of Equations (72) and (71) become

$$\begin{aligned} \lambda_L &= m_\mathrm{L} - \tfrac{1}{2} i \Gamma_\mathrm{L} \approx M - \tfrac{1}{2} i \Gamma + |M_{12}| \\ \lambda_S &= m_\mathrm{S} - \tfrac{1}{2} i \Gamma_\mathrm{S} \approx M - \tfrac{1}{2} i \Gamma - |M_{12}| \end{aligned}$$

Hence, the eigenstate $\mathrm{B_L}$ is heavier than the eigenstate $\mathrm{B_S}$:

$$m_\mathrm{L} \approx M + |M_{12}|, \qquad m_\mathrm{S} \approx M - |M_{12}|$$

and the two eigenstates have approximately the same lifetime:

$$\Gamma_\mathrm{L} \approx \Gamma_\mathrm{S} \approx \Gamma \, .$$

This is in contrast to the neutral kaon system where the two eigenstates decay into very different final states ($\mathrm{K_S} \to \pi\pi, \mathrm{K_L} \to \pi\pi\pi, \pi\ell\nu$) and therefore have very different lifetimes.

Given these features of the B meson systems, it is standard to refer to the B eigenstates as "heavy" (H) and "light" (L) rather than "short" (S) and "long" (L), so that Equations (74) and (73) become

$$\begin{aligned} |\mathrm{B_H}\rangle &= \frac{1}{\sqrt{1+|\eta|^2}} \left(\left|\mathrm{B}^0\right\rangle + \eta \left|\overline{\mathrm{B}}^0\right\rangle \right) \\ |\mathrm{B_L}\rangle &= \frac{1}{\sqrt{1+|\eta|^2}} \left(\left|\mathrm{B}^0\right\rangle - \eta \left|\overline{\mathrm{B}}^0\right\rangle \right) \, . \end{aligned}$$

We then have

$$\Delta m \equiv m_\mathrm{H} - m_\mathrm{L} \approx 2|M_{12}| \, .$$

For the B systems, Equation (75) simplifies to

$$\eta = \sqrt{\frac{M_{12}^* - \frac{1}{2}i\Gamma_{12}^*}{M_{12} - \frac{1}{2}i\Gamma_{12}}} \approx \sqrt{\frac{M_{12}^*}{M_{12}}} = \frac{M_{12}^*}{|M_{12}|}$$

Unlike the kaon system, where virtual u, c and t quarks all contribute, mixing in the B systems is completely dominated by the Feynman box diagrams with two virtual top quarks. For the B_d^0 meson, for example, the dominant diagrams are

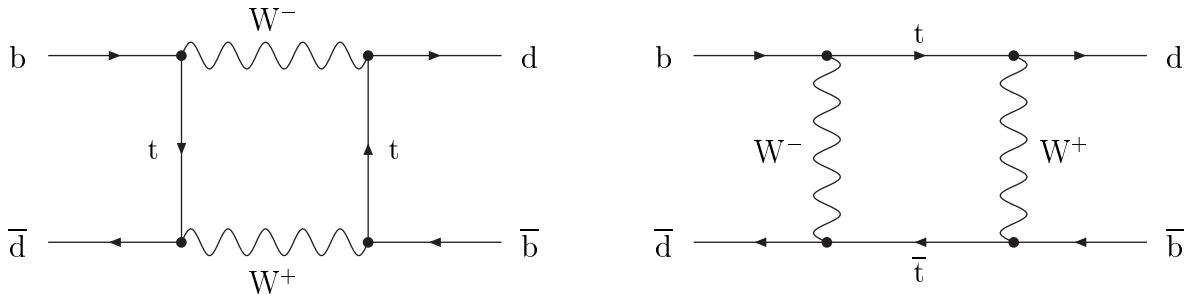

The dependence of the matrix element M_{12} on the CKM matrix elements can therefore be reliably predicted:

$$M_{12}^* \propto (V_{\mathrm{td}}V_{\mathrm{tb}}^*)^2 \ .$$

In the standard Wolfenstein parameterisation of the CKM matrix, the elements V_{td} and V_{tb} are given by $V_{\mathrm{td}} = |V_{\mathrm{td}}|e^{-i\beta}$ and $V_{\mathrm{tb}} \approx 1$. Therefore, to very good approximation,

$$\boxed{\eta = e^{-i2\beta}} \ .$$

Also, the mass difference is

$$\boxed{\Delta m \approx 2|M_{12}| \propto |V_{\mathrm{td}}V_{\mathrm{tb}}|^2} \ .$$

Measurements of the flavour oscillation frequency determine Δm, which in turn determines the product $|V_{\mathrm{td}}V_{\mathrm{tb}}|$.

References

[1] CPLEAR Collab., A. Angelopoulos *et al.*, E. Phys. J. **C22** (2001) 55.

[2] CPLEAR Collab., A. Apostolakis *et al.*, E. Phys. J. **C18** (2000) 41.

[3] P. K. Kabir, Phys. Rev. **D2** (1970) 540.

[4] L. Wolfenstein, Phys. Rev. Lett. **51** (1983) 1945.

9 Spin 1 Particles and Gauge Invariance

(Non-examinable)

9.1 Relativistic Electromagnetism

In units where $\epsilon_0 = \mu_0 = c = 1$ ('Heaviside-Lorentz' units) Maxwell's equations in vacuo, in the presence of charge density $\rho(\boldsymbol{x}, t)$ and current density $\boldsymbol{J}(\boldsymbol{x}, t)$, are

$$\boldsymbol{\nabla} \cdot \boldsymbol{E} = \rho \qquad \boldsymbol{\nabla} \wedge \boldsymbol{E} = -\frac{\partial \boldsymbol{B}}{\partial t}$$
$$\boldsymbol{\nabla} \cdot \boldsymbol{B} = 0 \qquad \boldsymbol{\nabla} \wedge \boldsymbol{B} = \boldsymbol{J} + \frac{\partial \boldsymbol{E}}{\partial t}$$

The electric and magnetic fields $\boldsymbol{E}$ and $\boldsymbol{B}$ are given in terms of the scalar and vector potentials ϕ, $\boldsymbol{A}$ by

$$\boldsymbol{E} = -\frac{\partial \boldsymbol{A}}{\partial t} - \boldsymbol{\nabla}\phi, \qquad \boldsymbol{B} = \boldsymbol{\nabla} \wedge \boldsymbol{A} \tag{1}$$

Introducing the 4-vector potential $A^\mu = (\phi, \boldsymbol{A})$ and the 4-vector current $j^\mu = (\rho, \boldsymbol{J})$ allows Maxwell's equations to be expressed in the compact covariant form

$$\partial_\mu F^{\mu\nu} = j^\nu \tag{2}$$

where $F^{\mu\nu}$ is the antisymmetric field strength tensor

$$F^{\mu\nu} \equiv \partial^\mu A^\nu - \partial^\nu A^\mu = \begin{pmatrix} 0 & -E_x & -E_y & -E_z \\ E_x & 0 & -B_z & B_y \\ E_y & B_z & 0 & -B_x \\ E_z & -B_y & B_x & 0 \end{pmatrix}. \tag{3}$$

Combining Equations (2) and (3) gives the following covariant equation for A^μ:

$$\partial_\mu \left(\partial^\mu A^\nu - \partial^\nu A^\mu\right) = j^\nu$$

or equivalently

$$\Box^2 A^\mu - \partial^\mu(\partial_\nu A^\nu) = j^\mu \tag{4}$$

where

$$\Box^2 \equiv \partial_\nu \partial^\nu = \left(\frac{\partial}{\partial t}, \boldsymbol{\nabla}\right) \cdot \left(\frac{\partial}{\partial t}, \boldsymbol{\nabla}\right) = \frac{\partial^2}{\partial t^2} - \boldsymbol{\nabla}^2$$

is the d'Alembertian operator.

Operating on Equation (2) with ∂_ν gives immediately the continuity equation

$$\partial_\nu j^\nu = 0$$

which, in terms of ρ and $\boldsymbol{J}$, is

$$\frac{\partial \rho}{\partial t} + \boldsymbol{\nabla} \cdot \boldsymbol{J} = 0$$

expressing conservation of electric charge. The symmetry underlying this conservation law is *gauge invariance*.

9.2 Gauge Invariance

The electric and magnetic fields $\boldsymbol{E}$ and $\boldsymbol{B}$ in Equation (1) are unchanged by the application of a *gauge transformation*

$$\boldsymbol{A} \to \boldsymbol{A}' = \boldsymbol{A} + \boldsymbol{\nabla}\chi$$
$$\phi \to \phi' = \phi - \frac{\partial \chi}{\partial t}$$

where $\chi = \chi(x) = \chi(t, \boldsymbol{x})$ is any function of position and time. In 4-vector notation, a gauge transformation can be written compactly as

$$A_\mu \to A'_\mu = A_\mu + \partial_\mu \chi$$

Choosing $\chi(x)$ to be a solution of the equation

$$\Box^2 \chi = -\partial_\mu A^\mu$$

gives

$$\partial^\mu A'_\mu = \partial^\mu \left(A_\mu + \partial_\mu \chi\right) = -\Box^2 \chi + \Box^2 \chi = 0$$

Thus, dropping the prime, gauge invariance can be used to impose the *Lorentz condition*

$$\partial_\mu A^\mu = 0$$

in which case Equation (4) becomes

$$\Box^2 A^\mu = j^\mu \ . \tag{5}$$

Even after imposing the Lorentz condition, there is still some freedom in the choice of the potential A^μ; we can still make a gauge transformation of the form

$$A_\mu \to A'_\mu = A_\mu + \partial_\mu \Lambda \tag{6}$$

where $\Lambda(t, \boldsymbol{x})$ is any function which satisfies

$$\Box^2 \Lambda = 0 \ . \tag{7}$$

Under this transformation we have

$$\partial^\mu A'_\mu = \partial^\mu \left(A_\mu + \partial_\mu \Lambda\right) = \partial^\mu A_\mu + \Box^2 \Lambda = \partial^\mu A_\mu$$

so that the Lorentz condition $\partial^\mu A_\mu = 0$ is indeed preserved (as are Maxwell's equations).

9.3 Photon Polarisation

For a free photon (*i.e.* $\rho = 0, \boldsymbol{J} = \mathbf{0}$: *i.e.* $j^\mu = 0$), Equation (5) for the potential A^μ becomes

$$\Box^2 A^\mu = 0 \ . \tag{8}$$

This admits plane wave solutions of the form

$$A^\mu = \epsilon^\mu e^{-iq.x} \tag{9}$$

where the 4-vector ϵ^μ is the *polarisation vector* of the photon and q^μ is its 4-momentum. Substituting Equation (9) into Equation (8) gives

$$\begin{aligned} 0 = \Box^2 A^\mu = \partial^\nu \partial_\nu \left(\epsilon^\mu e^{-iq.x}\right) &= \epsilon^\mu \frac{\partial}{\partial x_\nu}\frac{\partial}{\partial x^\nu} e^{-iq_\lambda x^\lambda} \\ &= \epsilon^\mu \frac{\partial}{\partial x_\nu} \cdot -iq_\nu e^{-iq_\lambda x^\lambda} = \epsilon^\mu \cdot -iq^\nu \cdot -iq_\nu e^{-iq_\lambda x^\lambda} = -q^2 \epsilon^\mu e^{-iq.x} \end{aligned}$$

and hence

$$q^2 = 0$$

reflecting the fact that a free (real) photon is massless.

The Lorentz condition, $\partial_\mu A^\mu = 0$, gives

$$0 = \partial_\mu A^\mu = \partial_\mu \left(\epsilon^\mu e^{-iq.x}\right) = \epsilon^\mu \partial_\mu \left(e^{-iq.x}\right) = \epsilon^\mu \cdot -iq_\mu e^{-iq.x}$$

and hence

$$q_\mu \epsilon^\mu = 0 \tag{10}$$

which reduces the number of independent components of ϵ^μ from four to three. Further, the additional gauge freedom represented by Equation (6) can be exploited by choosing a gauge function

$$\Lambda = iae^{-iq.x}$$

where a is a constant. It is straightforward to verify that this expression for Λ does indeed satisfy Equation (7). Under this gauge transformation, the 4-vector potential becomes

$$A'_\mu = A_\mu + \partial_\mu \Lambda = \epsilon_\mu e^{-iq.x} + \partial_\mu \left(iae^{-iq.x}\right) = \epsilon_\mu e^{-iq.x} - iq_\mu \left(iae^{-iq.x}\right) = \left(\epsilon_\mu + aq_\mu\right) e^{-iq.x} \ .$$

The electromagnetic potential is therefore left unchanged by the replacement

$$\epsilon_\mu \to \epsilon'_\mu = \epsilon_\mu + aq_\mu,$$

which in turn means that two polarisation vectors ϵ_μ and ϵ'_μ differing by a multiple of q_μ describe the same photon. In the *Coulomb gauge*, this freedom is used to set the time component of the polarisation vector to zero:

$$\epsilon^\mu = (0, \boldsymbol{\epsilon})$$

and Equation (10) then gives

$$\epsilon.q = \epsilon^0 q^0 - \boldsymbol{\epsilon}.\boldsymbol{q} = 0 \qquad \Rightarrow \qquad \boldsymbol{\epsilon}.\boldsymbol{q} = 0$$

Thus a real photon has only *two* independent polarisation vectors, both of which must be transverse to the photon direction. For example, for a photon travelling along the z axis, possible choices are the *plane polarisation* states

$$\epsilon_1^\mu = (0,1,0,0); \qquad \epsilon_2^\mu = (0,0,1,0)$$

or the *circular polarisation* states

$$\epsilon_-^\mu = \frac{1}{\sqrt{2}}(0,1,-i,0); \qquad \epsilon_+^\mu = -\frac{1}{\sqrt{2}}(0,1,i,0)\ . \tag{11}$$

It can be shown that ϵ_- corresponds to a polarisation state in which the photon spin is directed in the $-z$ direction (*i.e.* $S_z = -1$) while ϵ_+ corresponds to $S_z = +1$. In particular, for a photon travelling in the $+z$ direction, ϵ_- (ϵ_+) corresponds to a left-handed (right-handed) photon with helicity $h = -1$ ($h = +1$), while for a photon travelling in the $-z$ direction the helicities are reversed.

9.4 Relativistic Electrodynamics

In classical electrodynamics, the equation of motion of a particle of charge e in an electromagnetic field can be obtained by applying the *minimal substitution*

$$\boldsymbol{p} \to \boldsymbol{p} - e\boldsymbol{A}; \qquad E \to E - e\phi$$

For a non-relativistic free particle obeying

$$E = \frac{|\boldsymbol{p}|^2}{2m}\ ,$$

minimal substitution gives

$$E - e\phi = \frac{(\boldsymbol{p} - e\boldsymbol{A})^2}{2m}$$

and so leads to the Hamiltonian

$$H = \frac{(\boldsymbol{p} - e\boldsymbol{A})^2}{2m} + e\phi\ .$$

In the Part II Quantum Mechanics II course, this Hamiltonian was shown to lead to the Lorentz force equation

$$\boldsymbol{F} = e\boldsymbol{E} + e\boldsymbol{v} \wedge \boldsymbol{B}\ .$$

Minimal substitution works equally well in relativistic quantum mechanics where it can be written compactly as

$$p^\mu \to p^\mu - eA^\mu$$

or, since $p^\mu = i\partial^\mu$, as

$$\partial^\mu \to \partial^\mu + ieA^\mu\ .$$

The equation of motion for a spin $\frac{1}{2}$ Dirac particle in an electromagnetic field can be obtained by applying minimal substitution to the free particle Dirac equation

$$(i\gamma^\mu\partial_\mu - m)\,\psi = 0$$

giving

$$\boxed{\gamma^\mu \left(i\partial_\mu - eA_\mu\right)\psi - m\psi = 0} \tag{12}$$

(a result which already appeared in Section 2.20). The term $-e\gamma^\mu A_\mu \psi$ represents the interaction between the electromagnetic potential A_μ and the fermion spinor ψ and ultimately gives rise to the vertex factor $-ie\gamma^\mu$ in the Feynman rules for QED.

9.5 Local Phase Transformations

Applying a gauge transformation

$$A_\mu \to A'_\mu = A_\mu + \partial_\mu \chi$$

to Equation (12) gives

$$\begin{aligned} & \gamma^\mu \left(i\partial_\mu - eA'_\mu\right)\psi - m\psi = 0 \\ \Rightarrow \qquad & \gamma^\mu \left(i\partial_\mu - eA_\mu - e\partial_\mu\chi\right)\psi - m\psi = 0 \end{aligned}$$

This is *not* of the same form as the original equation (Equation (12)) because of the term containing $\partial_\mu \chi$; *i.e.* gauge invariance has (for the moment) been lost.

Invariance can be restored if, as well as applying a gauge transformation to the electromagnetic potential A_μ, we simultaneously apply a *local phase transformation*

$$\psi \to \psi' = e^{-ie\chi(x)}\psi \tag{13}$$

to the spin $\frac{1}{2}$ field ψ. Under such a transformation, the phase of ψ is transformed by an amount which varies with position and time. Applying a gauge transformation *and* a local phase transformation together, Equation (12) becomes

$$\gamma^\mu \left[i\partial_\mu - eA'_\mu\right]\psi' - m\psi' = 0 \ . \tag{14}$$

Equation (14) contains the factor

$$\begin{aligned} (i\partial_\mu - eA'_\mu)\psi' &= \left[i\partial_\mu - e(A_\mu + \partial_\mu\chi)\right](e^{-ie\chi}\psi) \\ &= (i\partial_\mu - eA_\mu)(e^{-ie\chi}\psi) - e(\partial_\mu\chi)(e^{-ie\chi}\psi) \ . \end{aligned} \tag{15}$$

The first term on the right-hand side is

$$\begin{aligned} (i\partial_\mu - eA_\mu)(e^{-ie\chi}\psi) &= e^{-ie\chi}i\partial_\mu\psi + e(\partial_\mu\chi)e^{-ie\chi}\psi - eA_\mu e^{-ie\chi}\psi \\ &= e^{-ie\chi}\left[i\partial_\mu - eA_\mu + e(\partial_\mu\chi)\right]\psi \end{aligned}$$

so that Equation (15) is

$$\begin{aligned} (i\partial_\mu - eA'_\mu)\psi' &= e^{-ie\chi}\left[i\partial_\mu - eA_\mu + e\partial_\mu\chi\right]\psi - e(\partial_\mu\chi)e^{-ie\chi}\psi \\ &= e^{-ie\chi}\left[i\partial_\mu - eA_\mu\right]\psi \ . \end{aligned}$$

Thus, the combined effect of a gauge transformation and a local phase transformation is simply to multiply the quantity $(i\partial_\mu - eA_\mu)\psi$ by the phase factor $e^{-ie\chi}$. Applying this result, and Equation (13), to Equation (14) then gives

$$e^{-ie\chi}\gamma^\mu \left[i\partial_\mu - eA_\mu\right]\psi - me^{-ie\chi}\psi = 0 \ .$$

After cancelling the factor of $e^{-ie\chi}$, we recover the original Dirac equation, Equation (12).

In summary, the form of the equation of motion is preserved under the simultaneous application of a local phase transformation and a gauge transformation:

$$\psi \rightarrow \psi' = e^{-ie\chi(x)}\psi$$
$$A_\mu \rightarrow A'_\mu = A_\mu + \partial_\mu \chi(x)$$

The above argument can also be completely reversed: if we demand that the free particle Dirac equation

$$(i\gamma^\mu \partial_\mu - m)\psi = 0$$

be invariant under a *local* phase transformation

$$\psi \rightarrow \psi' = e^{-ie\chi(x)}\psi \ ,$$

then we *must* introduce a massless gauge boson A_μ which transforms as

$$A_\mu \rightarrow A'_\mu = A_\mu + \partial_\mu \chi(x)$$

and satisfies Equation (12). The form of the interaction between the spin $\frac{1}{2}$ particle ψ and the gauge boson A_μ is then completely specified. The principle of local phase invariance underpins the quantum field theories not only of the electromagnetic interaction (QED) but also of the strong (QCD) and electroweak interactions.

9.6 Massive Spin 1 Particles

Returning to Equation (4), the 4-vector potential A^μ for a free photon $(j^\mu = 0)$ satisfies the equation

$$\Box^2 A^\mu - \partial^\mu(\partial_\nu A^\nu) = 0 \ . \tag{16}$$

Equation (16) is the general equation satisfied by A^μ, without imposing any particular choice of gauge such as the Lorentz condition $\partial_\mu A^\mu = 0$.

The Klein-Gordon equation for a spin 0 boson of mass m is

$$(\Box^2 + m^2)\phi = 0$$

This suggests that the equation describing a *massive* particle can be obtained from that describing a *massless* particle via the replacement $\Box^2 \rightarrow \Box^2 + m^2$. Applying this procedure to Equation (16) gives the following equation for the field B^μ of a spin 1 particle of mass m:

$$(\Box^2 + m^2)B^\mu - \partial^\mu(\partial_\nu B^\nu) = 0 \tag{17}$$

Operating with ∂_μ then gives

$$\begin{aligned} & (\Box^2 + m^2)\partial_\mu B^\mu - \partial_\mu \partial^\mu (\partial_\nu B^\nu) = 0 \\ \Rightarrow \quad & (\Box^2 + m^2)\partial_\mu B^\mu - \Box^2 (\partial_\nu B^\nu) = 0 \\ \Rightarrow \quad & m^2 \partial_\mu B^\mu = 0 \end{aligned}$$

and hence

$$\partial_\mu B^\mu = 0 \ . \tag{18}$$

Thus, for a massive spin 1 particle, we *unavoidably* have $\partial_\mu B^\mu = 0$; this is *not* a gauge condition reflecting a particular choice of gauge. Using this result, Equation (17) becomes

$$\boxed{(\Box^2 + m^2) B_\mu = 0} \, . \tag{19}$$

For a free particle with 4-momentum p^μ, Equation (19) admits plane wave solutions of the form

$$B_\mu = \epsilon_\mu e^{-ip.x}$$

Substituting this into Equation (18) gives

$$p_\mu \epsilon^\mu = 0 \ , \tag{20}$$

which reduces the number of independent components of ϵ^μ from four to three. Unlike the case of a massless photon however, Equation (19) for a *massive* particle does *not* allow a gauge symmetry, and the number of independent spin components cannot be reduced further.

For a particle of mass m, energy E and momentum $\boldsymbol{p}$ travelling along the z axis, with four-momentum $p^\mu = (E, 0, 0, p_z)$, the three independent polarisation 4-vectors ϵ^μ satisfying Equation (20) can be taken to be

			$p_z > 0$	$p_z < 0$
$\epsilon_+^\mu = -\frac{1}{\sqrt{2}}(0, 1, i, 0)$		$S_z = +1$	$h = +1$	$h = -1$
$\epsilon_-^\mu = \frac{1}{\sqrt{2}}(0, 1, -i, 0)$		$S_z = -1$	$h = -1$	$h = +1$
$\epsilon_L^\mu = \frac{1}{m}(p_z, 0, 0, E)$		$S_z = 0$	$h = 0$	$h = 0$

The 4-vectors ϵ_- and ϵ_+ are the same as those already introduced in Equation (11) for the photon and are known as *transverse* polarisation states, reflecting the fact that the electric and magnetic fields in an electromagnetic wave are transverse to the direction of motion. The new *longitudinal* spin state ϵ_L is present only for a *massive* particle (and in fact also for a *virtual* photon).

For a spin 1 particle at rest, the longitudinal (helicity 0) polarisation 4-vector becomes simply

$$\epsilon_L^\mu = (0, 0, 0, 1) \, .$$

10 W Decay

10.1 Matrix Element for $\mathrm{W}^- \to \mathrm{e}^-\overline{\nu}_\mathrm{e}$ Decays

The leading-order Feynman diagram for the decay $\mathrm{W}^- \to \mathrm{e}^-\overline{\nu}_\mathrm{e}$ is

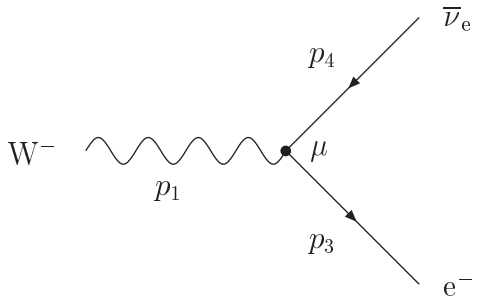

The Feynman rules determine the invariant matrix element to be

$$-iM_{\mathrm{fi}} = \epsilon_\mu(p_1) \cdot \overline{u}(p_3) \cdot -i\frac{g_\mathrm{W}}{\sqrt{2}}\gamma^\mu \tfrac{1}{2}(1-\gamma^5) \cdot v(p_4)$$

where $\epsilon_\mu(p_1)$ is the polarisation four-vector of the W^- (with four-momentum p_1), and p_3 and p_4 are the four-momenta of the e^- and $\overline{\nu}_\mathrm{e}$, respectively. Hence

$$\boxed{M_{\mathrm{fi}} = \frac{g_\mathrm{W}}{\sqrt{2}}\epsilon_\mu(p_1)\overline{u}(p_3)\gamma^\mu \tfrac{1}{2}(1-\gamma^5)v(p_4)}\,.$$

This involves the scalar product of the polarisation four-vector $\epsilon_\mu(p_1)$ with a weak charged-current four-vector j^μ which is $(V-A)$ in form:

$$M_{\mathrm{fi}} = \frac{g_\mathrm{W}}{\sqrt{2}}\epsilon_\mu j^\mu, \qquad j^\mu = \overline{u}(p_3)\gamma^\mu \tfrac{1}{2}(1-\gamma^5)v(p_4)\,. \tag{1}$$

The current j^μ and matrix element M_{fi} will be evaluated in the rest frame of the W^-, neglecting the mass of the electron (and antineutrino):

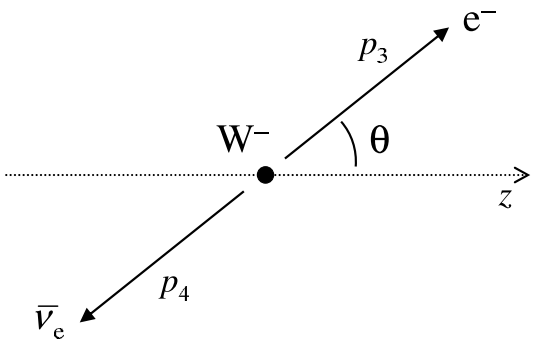

Without loss of generality, the four-momenta of the W^-, e^- and $\overline{\nu}_\mathrm{e}$ can be taken to be

$$p_1 = (m_\mathrm{W}, 0, 0, 0), \qquad p_3 = (E, E\sin\theta, 0, E\cos\theta), \qquad p_4 = (E, -E\sin\theta, 0, -E\cos\theta) \tag{2}$$

with $E = m_\mathrm{W}/2$.

10.2 The Lepton Current

In the massless limit, only left-handed ($h = -1$) particles and right-handed ($h = +1$) antiparticles participate in a $(V-A)$ interaction. Hence, for the lepton current j^μ to be non-zero, the electron must be left-handed and the antineutrino right-handed, *i.e.* we must choose [1]

$$u(p_3) = u_\downarrow(p_3), \qquad\qquad v(p_4) = v_\uparrow(p_4)\ .$$

The current j^μ then becomes

$$j^\mu = \overline{u}_\downarrow(p_3)\gamma^\mu \tfrac{1}{2}(1-\gamma^5)v_\uparrow(p_4) = \overline{u}_\downarrow(p_3)\gamma^\mu v_\uparrow(p_4)\ , \tag{3}$$

where we have used the fact that $\gamma^5 v_\uparrow = -v_\uparrow$ in the massless limit, and hence $\frac{1}{2}(1-\gamma^5)v_\uparrow(p_4) = v_\uparrow(p_4)$.

The lepton current $j^\mu = \overline{u}_\downarrow(p_3)\gamma^\mu v_\uparrow(p_4)$ in Equation (3), and the final state four-momenta p_3 and p_4 in Equation (2), are identical to the muon current and muon four-momenta already considered in Section 4.2 in connection with the QED scattering process $\mathrm{e}^+\mathrm{e}^- \to \mu^+\mu^-$. There, it was found that [2]

$$\overline{u}_\downarrow(p_3)\gamma^\mu v_\uparrow(p_4) = 2E\,(0, -\cos\theta, -i, \sin\theta)\ ,$$

a result which can be carried over directly to $\mathrm{W}^- \to \mathrm{e}^-\overline{\nu}_\mathrm{e}$ decay.

In summary, for $\mathrm{W}^- \to \mathrm{e}^-\overline{\nu}_\mathrm{e}$ decay, only one of the four possible final state spin configurations gives a non-zero contribution to the matrix element:

$$\boxed{j^\mu = \overline{u}_\downarrow(p_3)\gamma^\mu \tfrac{1}{2}(1-\gamma^5)v_\uparrow(p_4) = 2E\,(0, -\cos\theta, -i, \sin\theta)}\ ,$$

namely the configuration with a left-handed (negative helicity) electron and a right-handed (positive helicity) antineutrino:

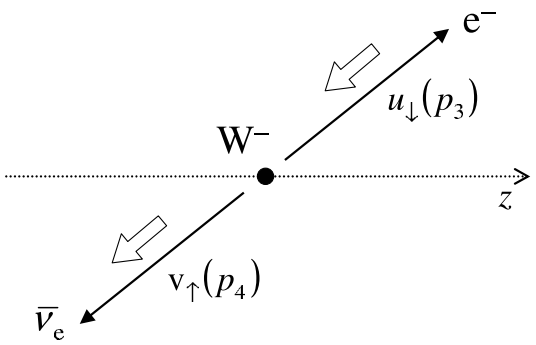

[1] This can be shown formally using the same arguments as in Section 7.1.1 for neutrino scattering, or the results of Question 17 on the examples sheet.

[2] See Equation (11) in Handout 4.

10.3 $\mathrm{W}^- \to \mathrm{e}^-\overline{\nu}_\mathrm{e}$ Decay Rate

For a spin-one particle of mass m, energy E and momentum $\boldsymbol{p}$ travelling along the z axis, with four-momentum $p^\mu = (E, 0, 0, p_z)$, the polarisation four-vectors ϵ^μ_+, ϵ^μ_- and ϵ^μ_L corresponding to the spin eigenstates with $S_z = +1$, $S_z = -1$ and $S_z = 0$ are

$$\epsilon^\mu_+ = -\frac{1}{\sqrt{2}}(0, 1, i, 0), \qquad \epsilon^\mu_- = \frac{1}{\sqrt{2}}(0, 1, -i, 0), \qquad \epsilon^\mu_\mathrm{L} = \frac{1}{m}(p_z, 0, 0, E)\ .$$

Hence, for the parent W boson (at rest with $p_z = 0$, $E = m_\mathrm{W}$), the polarisation 4-vectors $\epsilon^\mu(p_1)$ are

$$\epsilon^\mu_+ = -\frac{1}{\sqrt{2}}(0, 1, i, 0), \qquad \epsilon^\mu_- = \frac{1}{\sqrt{2}}(0, 1, -i, 0), \qquad \epsilon^\mu_\mathrm{L} = (0, 0, 0, 1)\ .$$

The scalar product $\epsilon.j$ for each of these spin eigenstates is

$$\begin{aligned}
\epsilon^\mu_+ :&\quad -\frac{1}{\sqrt{2}}(0, 1, i, 0)\cdot 2E\,(0, -\cos\theta, -i, \sin\theta) = \sqrt{2}E(1-\cos\theta)\\
\epsilon^\mu_- :&\quad \frac{1}{\sqrt{2}}(0, 1, -i, 0)\cdot 2E\,(0, -\cos\theta, -i, \sin\theta) = \sqrt{2}E(1+\cos\theta)\\
\epsilon^\mu_\mathrm{L} :&\quad (0, 0, 0, 1)\cdot 2E\,(0, -\cos\theta, -i, \sin\theta) = -2E\sin\theta\ .
\end{aligned}$$

From Equation (1), the corresponding values $|M_+|^2$, $|M_-|^2$, $|M_\mathrm{L}|^2$ of the matrix element squared $|M_\mathrm{fi}|^2 = \frac{1}{2}g_\mathrm{W}^2(\epsilon.j)^2$ are then given by [3]

$$|M_+|^2 = \tfrac{1}{2}g_\mathrm{W}^2\left[\sqrt{2}E(1-\cos\theta)\right]^2 = g_\mathrm{W}^2 m_\mathrm{W}^2\cdot\tfrac{1}{4}(1-\cos\theta)^2 \tag{4}$$

$$|M_-|^2 = \tfrac{1}{2}g_\mathrm{W}^2\left[\sqrt{2}E(1+\cos\theta)\right]^2 = g_\mathrm{W}^2 m_\mathrm{W}^2\cdot\tfrac{1}{4}(1+\cos\theta)^2 \tag{5}$$

$$|M_\mathrm{L}|^2 = \tfrac{1}{2}g_\mathrm{W}^2\left[-2E\sin\theta\right]^2 = g_\mathrm{W}^2 m_\mathrm{W}^2\cdot\tfrac{1}{2}\sin^2\theta \tag{6}$$

The differential decay rate $\mathrm{d}\Gamma/\mathrm{d}\Omega$ is obtained from the matrix element squared as [4]

$$\frac{\mathrm{d}\Gamma}{\mathrm{d}\Omega} = \frac{p^*}{32\pi^2 m_\mathrm{W}^2}|M_\mathrm{fi}|^2\ ,$$

where $p^* = m_\mathrm{W}/2$ for W decay. Hence we obtain, for each of the three possible W^- spin eigenstates,

$$\frac{\mathrm{d}\Gamma_+}{\mathrm{d}\Omega} = \frac{g_\mathrm{W}^2 m_\mathrm{W}}{256\pi^2}(1-\cos\theta)^2\ , \qquad \frac{\mathrm{d}\Gamma_-}{\mathrm{d}\Omega} = \frac{g_\mathrm{W}^2 m_\mathrm{W}}{256\pi^2}(1+\cos\theta)^2\ , \qquad \frac{\mathrm{d}\Gamma_\mathrm{L}}{\mathrm{d}\Omega} = \frac{g_\mathrm{W}^2 m_\mathrm{W}}{128\pi^2}\sin^2\theta\ .$$

Using

$$\int \tfrac{1}{4}(1\pm\cos\theta)^2\,\mathrm{d}\cos\theta\,\mathrm{d}\phi = \int \tfrac{1}{2}\sin^2\theta\,\mathrm{d}\cos\theta\,\mathrm{d}\phi = \frac{4\pi}{3}$$

to integrate over all possible decay angles, the total decay rate is found to be the same for each W^- spin eigenstate:

$$\boxed{\Gamma_- = \Gamma_+ = \Gamma_\mathrm{L} = \frac{g_\mathrm{W}^2 m_\mathrm{W}}{48\pi}}\ .$$

[3] Note that the factors of $\frac{1}{4}(1\pm\cos\theta)^2$ and $\frac{1}{2}\sin^2\theta$ are precisely those that emerged in Section 4.8 from a calculation of the overlap probabilities of the spin eigenstates $|1,-1\rangle$, $|1,0\rangle$, $|1,+1\rangle$ using standard "Part 1B" quantum mechanics.

[4] See Equation 14 of Handout 3.

10.4 Unpolarised $\mathrm{W}^- \to \mathrm{e}^-\overline{\nu}_\mathrm{e}$ Decay

For a sample of *unpolarised* W bosons, where the spin of each W boson is randomly oriented in space, the W bosons are effectively an equal mix of the three polarisation states ϵ_+, ϵ_- and ϵ_L. The corresponding matrix element squared is obtained by averaging over the three possible initial spin states of the W^-:

$$\begin{aligned}\langle|M_\mathrm{fi}|^2\rangle &= \frac{1}{3}\left(|M_+|^2 + |M_-|^2 + |M_\mathrm{L}|^2\right) \\ &= \frac{1}{3}g_\mathrm{W}^2 m_\mathrm{W}^2\left[\tfrac{1}{4}(1-\cos\theta)^2 + \tfrac{1}{4}(1+\cos\theta)^2 + \tfrac{1}{2}\sin^2\theta\right] \\ &= \frac{1}{3}g_\mathrm{W}^2 m_\mathrm{W}^2 \ . \end{aligned} \tag{7}$$

The spin-averaged matrix element is therefore a constant, independent of θ, implying that the decay of unpolarised W bosons is isotropic. This is to be expected since, for a W boson at rest with randomly oriented spin direction, there is no preferred spatial direction associated with the decay process.

For an isotropic two-body decay, the total decay rate is given by

$$\Gamma = \frac{p^*}{8\pi m_\mathrm{W}^2}\langle|M_\mathrm{fi}|^2\rangle = \frac{m_\mathrm{W}/2}{8\pi m_\mathrm{W}^2}\cdot\frac{1}{3}g_\mathrm{W}^2 m_\mathrm{W}^2$$

so that, for unpolarised W decay,

$$\boxed{\Gamma(\mathrm{W}\to\mathrm{e}\nu) = \frac{g_\mathrm{W}^2 m_\mathrm{W}}{48\pi}} \ . \tag{8}$$

This result could equally well be obtained by averaging the total decay rates for each individual spin state:

$$\Gamma(\mathrm{W}\to\mathrm{e}\nu) = \frac{1}{3}\left[\Gamma_- + \Gamma_+ + \Gamma_\mathrm{L}\right] \ .$$

Finally, once it is appreciated that the decay of an unpolarised particle must be isotropic, the calculation of the total decay rate can be simplified by noting that it is only necessary to calculate the matrix element for one particular spatial orientation of the final state. For example, choosing the electron to be emitted in the $+z$ direction, the spin states of all the particles involved can be written down immediately as

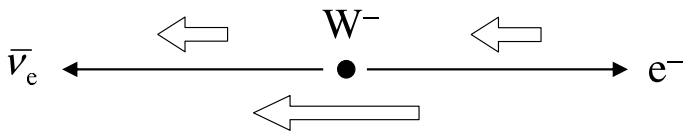

The total spin of the $\mathrm{e}^-\overline{\nu}_\mathrm{e}$ final state is $S_z = -1$, and the matrix element M_fi will therefore be non-zero only if the initial W^- is in the spin eigenstate ϵ_-. The matrix element for the above configuration is therefore given by M_-, with $\theta = 0$. From Equation (5), the matrix element squared is therefore

$$|M_-|^2_{(\theta=0)} = g_\mathrm{W}^2 m_\mathrm{W}^2 \ .$$

Since the decay of unpolarised particles is isotropic, this result must apply equally for *all* angles θ:

$$|M_\mathrm{fi}|^2 = g_\mathrm{W}^2 m_\mathrm{W}^2 \ .$$

Including a factor $1/3$ to average over the three possible initial spins of the W^- then immediately gives Equation (7) again.

11 The Z Resonance

11.1 e^+e^- Annihilation in QED

We begin by reviewing the results obtained in Handout 4 for the QED process $e^+e^- \to \gamma^* \to \mu^+\mu^-$:

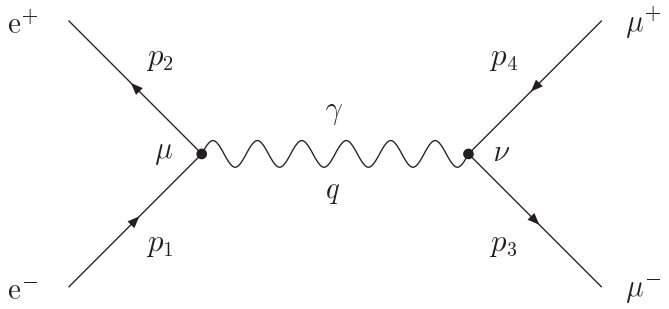

The Feynman rules determine the invariant matrix element to be

$$M_{fi} = -\frac{e^2}{s} g_{\mu\nu} \left[\overline{v}(p_2)\gamma^\mu u(p_1)\right] \left[\overline{u}(p_3)\gamma^\nu v(p_4)\right] \tag{1}$$

where p_1 and p_2 are the 4-momenta of the incoming e^- and e^+, p_3 and p_4 are the 4-momenta of the outgoing μ^- and μ^+, and $s = (p_1 + p_2)^2 = (p_3 + p_4)^2$ is the centre of mass energy squared. At high energy, as a consequence of helicity conservation, the matrix element was found to be non-zero for only four out of the sixteen possible spin configurations in the scattering:

$$e^-_R e^+_L \to \mu^-_R \mu^+_L \ : \quad M_{RR} = -(e^2/s) g_{\mu\nu} \left[\overline{v}_\downarrow(p_2)\gamma^\mu u_\uparrow(p_1)\right] \left[\overline{u}_\uparrow(p_3)\gamma^\nu v_\downarrow(p_4)\right] = e^2(1+\cos\theta) \tag{2}$$

$$e^-_R e^+_L \to \mu^-_L \mu^+_R \ : \quad M_{RL} = -(e^2/s) g_{\mu\nu} \left[\overline{v}_\downarrow(p_2)\gamma^\mu u_\uparrow(p_1)\right] \left[\overline{u}_\downarrow(p_3)\gamma^\nu v_\uparrow(p_4)\right] = e^2(1-\cos\theta) \tag{3}$$

$$e^-_L e^+_R \to \mu^-_R \mu^+_L \ : \quad M_{LR} = -(e^2/s) g_{\mu\nu} \left[\overline{v}_\uparrow(p_2)\gamma^\mu u_\downarrow(p_1)\right] \left[\overline{u}_\uparrow(p_3)\gamma^\nu v_\downarrow(p_4)\right] = e^2(1-\cos\theta) \tag{4}$$

$$e^-_L e^+_R \to \mu^-_L \mu^+_R \ : \quad M_{LL} = -(e^2/s) g_{\mu\nu} \left[\overline{v}_\uparrow(p_2)\gamma^\mu u_\downarrow(p_1)\right] \left[\overline{u}_\downarrow(p_3)\gamma^\nu v_\uparrow(p_4)\right] = e^2(1+\cos\theta) \tag{5}$$

where θ is the angle of the outgoing μ^- with respect to the incoming electron direction in the centre of mass frame:

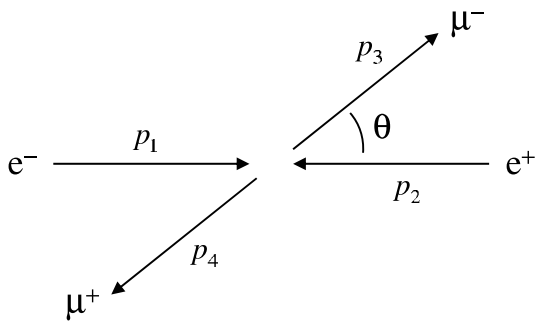

Using

$$\frac{\mathrm{d}\sigma}{\mathrm{d}\Omega} = \frac{1}{64\pi^2 s}\,|M_{\mathrm{fi}}|^2 \tag{6}$$

and $e^2 = 4\pi\alpha$ then gives the following differential cross sections:

$$\frac{\mathrm{d}\sigma_{\mathrm{RR}}}{\mathrm{d}\Omega} = \frac{\mathrm{d}\sigma_{\mathrm{LL}}}{\mathrm{d}\Omega} = \frac{\alpha^2}{4s}(1+\cos\theta)^2$$
$$\frac{\mathrm{d}\sigma_{\mathrm{RL}}}{\mathrm{d}\Omega} = \frac{\mathrm{d}\sigma_{\mathrm{LR}}}{\mathrm{d}\Omega} = \frac{\alpha^2}{4s}(1-\cos\theta)^2\ .$$

Since $\int_{-1}^{+1}(1\pm\cos\theta)^2\mathrm{d}\cos\theta = 8/3$ and $d\Omega = 2\pi\mathrm{d}\cos\theta$, we obtain the following total cross sections:

$$\sigma_{\mathrm{RR}} = \sigma_{\mathrm{RL}} = \sigma_{\mathrm{LR}} = \sigma_{\mathrm{LL}} = \frac{4\pi\alpha^2}{3s}\ .$$

Thus, in QED, the total cross sections for left-handed and right-handed particles are identical, reflecting the fact that parity is conserved.

The *unpolarised* differential and total cross sections are obtained by summing over the final state μ^+ and μ^- spins and averaging over the initial state e^+ and e^- spins:

$$\langle|M_{\mathrm{fi}}|^2\rangle = \tfrac{1}{2}\cdot\tfrac{1}{2}\cdot e^4\left[2(1+\cos\theta)^2 + 2(1-\cos\theta)^2\right] = e^4(1+\cos^2\theta) \tag{7}$$

which gives

$$\frac{\mathrm{d}\sigma}{\mathrm{d}\Omega} = \tfrac{1}{2}\cdot\tfrac{1}{2}\cdot\left[\frac{\mathrm{d}\sigma_{\mathrm{RR}}}{\mathrm{d}\Omega} + \frac{\mathrm{d}\sigma_{\mathrm{RL}}}{\mathrm{d}\Omega} + \frac{\mathrm{d}\sigma_{\mathrm{LR}}}{\mathrm{d}\Omega} + \frac{\mathrm{d}\sigma_{\mathrm{LL}}}{\mathrm{d}\Omega}\right] = \frac{\alpha^2}{4s}(1+\cos^2\theta)$$

and

$$\sigma = \tfrac{1}{2}\cdot\tfrac{1}{2}\cdot[\sigma_{\mathrm{RR}} + \sigma_{\mathrm{RL}} + \sigma_{\mathrm{LR}} + \sigma_{\mathrm{LL}}] = \frac{4\pi\alpha^2}{3s}\ .$$

The matrix element of Equation (1) can be reformulated in a way which makes more evident the allowed spin configurations and allows for a direct comparison with the equivalent weak interaction process $\mathrm{e}^+\mathrm{e}^- \to \mathrm{Z}^0 \to \mu^+\mu^-$ discussed below. Inserting trivial factors of

$$1 = \tfrac{1}{2}(1+\gamma^5) + \tfrac{1}{2}(1-\gamma^5)$$

into each of the currents in Equation (1), allows the QED matrix element to be expressed as

$$M_{\mathrm{fi}} = M_{\mathrm{RR}} + M_{\mathrm{RL}} + M_{\mathrm{LR}} + M_{\mathrm{LL}} \tag{8}$$

where

$$M_{\mathrm{RR}} = -(e^2/s)g_{\mu\nu}\left[\overline{v}(p_2)\gamma^\mu\tfrac{1}{2}(1+\gamma^5)u(p_1)\right]\left[\overline{u}(p_3)\gamma^\nu\tfrac{1}{2}(1+\gamma^5)v(p_4)\right] \tag{9}$$
$$M_{\mathrm{RL}} = -(e^2/s)g_{\mu\nu}\left[\overline{v}(p_2)\gamma^\mu\tfrac{1}{2}(1+\gamma^5)u(p_1)\right]\left[\overline{u}(p_3)\gamma^\nu\tfrac{1}{2}(1-\gamma^5)v(p_4)\right] \tag{10}$$
$$M_{\mathrm{LR}} = -(e^2/s)g_{\mu\nu}\left[\overline{v}(p_2)\gamma^\mu\tfrac{1}{2}(1-\gamma^5)u(p_1)\right]\left[\overline{u}(p_3)\gamma^\nu\tfrac{1}{2}(1+\gamma^5)v(p_4)\right] \tag{11}$$
$$M_{\mathrm{LL}} = -(e^2/s)g_{\mu\nu}\left[\overline{v}(p_2)\gamma^\mu\tfrac{1}{2}(1-\gamma^5)u(p_1)\right]\left[\overline{u}(p_3)\gamma^\nu\tfrac{1}{2}(1-\gamma^5)v(p_4)\right]\ . \tag{12}$$

For the matrix element M_{RR} of Equation (9), for example, the electron and muon currents each have a $V+A$ structure. In the relativistic limit, these currents are non-zero only for right-handed particles and

left-handed antiparticles, *i.e.* only for the choices $u(p_1) = u_\uparrow(p_1)$, $v(p_2) = v_\downarrow(p_2)$, $u(p_3) = u_\uparrow(p_3)$, $v(p_4) = v_\downarrow(p_4)$:

$$M_{\rm RR} = -\frac{e^2}{s} g_{\mu\nu} \left[\overline{v}_\downarrow(p_2)\gamma^\mu \tfrac{1}{2}(1+\gamma^5) u_\uparrow(p_1)\right] \left[\overline{u}_\uparrow(p_3)\gamma^\nu \tfrac{1}{2}(1+\gamma^5) v_\downarrow(p_4)\right] \ .$$

Since $\frac{1}{2}(1+\gamma^5)u_\uparrow(p_1) = u_\uparrow(p_1)$ and $\frac{1}{2}(1+\gamma^5)v_\downarrow(p_4) = v_\downarrow(p_4)$, we have

$$M_{\rm RR} = -\frac{e^2}{s} g_{\mu\nu} \left[\overline{v}_\downarrow(p_2)\gamma^\mu u_\uparrow(p_1)\right] \left[\overline{u}_\uparrow(p_3)\gamma^\nu v_\downarrow(p_4)\right] \ ,$$

which is identical to the expression for $M_{\rm RR}$ in Equation (2). Similar arguments hold also for $M_{\rm RL}$, $M_{\rm LR}$ and $M_{\rm LL}$.

In the formulation of Equations (8)-(12), the QED matrix element $M_{\rm fi}$ has been broken down into four contributions of equal strength, determined by the value of $e^2 = 4\pi\alpha$. We shall see in the next section that the matrix element for the process $\rm e^+e^- \to Z^0 \to \mu^+\mu^-$ resolves into four contributions similar in structure to those of QED but each of *different* strength, reflecting parity violation in the weak interactions.

11.2 $\rm e^+e^-$ Annihilation on the $\rm Z^0$ Resonance

11.2.1 The matrix element $M_{\rm fi}$

For the weak interaction process $\rm e^+e^- \to Z^0 \to \mu^+\mu^-$, the virtual photon is replaced by a (real or virtual) $\rm Z^0$ boson:

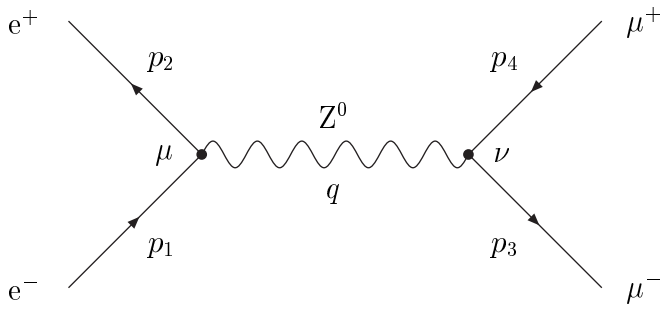

The Feynman rules give

$$-iM_{\rm fi} = \left[\overline{v}(p_2)\cdot -ig_{\rm Z}\gamma^\mu \tfrac{1}{2}(c_{\rm V}^{\rm e} - c_{\rm A}^{\rm e}\gamma^5)\cdot u(p_1)\right] \cdot \frac{-ig_{\mu\nu}}{q^2 - m_{\rm Z}^2} \cdot \left[\overline{u}(p_3)\cdot -ig_{\rm Z}\gamma^\nu \tfrac{1}{2}(c_{\rm V}^{\mu} - c_{\rm A}^{\mu}\gamma^5)\cdot v(p_4)\right]$$

where $c_{\rm V}^{\rm e}$ and $c_{\rm A}^{\rm e}$ are the vector and axial vector coupling constants for the electron, and $c_{\rm V}^{\mu}$ and $c_{\rm A}^{\mu}$ are the vector and axial vector coupling constants for the muon [1]. Hence

$$M_{\rm fi} = -\frac{g_{\rm Z}^2}{q^2 - m_{\rm Z}^2} g_{\mu\nu} \left[\overline{v}(p_2)\gamma^\mu \tfrac{1}{2}(c_{\rm V}^{\rm e} - c_{\rm A}^{\rm e}\gamma^5) u(p_1)\right] \left[\overline{u}(p_3)\gamma^\nu \tfrac{1}{2}(c_{\rm V}^{\mu} - c_{\rm A}^{\mu}\gamma^5) v(p_4)\right] \ .$$

[1] In the Standard Model, the coupling constants are $c_{\rm V}^{\rm e} = c_{\rm V}^{\mu} = -\frac{1}{2} + 2\sin^2\theta_{\rm W}$ and $c_{\rm A}^{\rm e} = c_{\rm A}^{\mu} = -\frac{1}{2}$, where $\theta_{\rm W}$ is the Weinberg angle.

Defining the left-handed and right-handed coupling constants $c_{\rm L}$ and $c_{\rm R}$ by

$$\tfrac{1}{2}(c_{\rm V} - c_{\rm A}\gamma^5) = c_{\rm L}.\tfrac{1}{2}(1-\gamma^5) + c_{\rm R}.\tfrac{1}{2}(1+\gamma^5)$$

we have

$$c_{\rm L} = \tfrac{1}{2}(c_{\rm V} + c_{\rm A}), \qquad c_{\rm R} = \tfrac{1}{2}(c_{\rm V} - c_{\rm A})$$

or equivalently

$$c_{\rm V} = c_{\rm L} + c_{\rm R}, \qquad c_{\rm A} = c_{\rm L} - c_{\rm R}\ .$$

In terms of $c_{\rm L}$ and $c_{\rm R}$, the matrix element becomes

$$\begin{aligned} M_{\rm fi} = -\frac{g_{\rm Z}^2}{s-m_{\rm Z}^2} g_{\mu\nu} &\left[c_{\rm L}^{\rm e}\,\overline{v}(p_2)\gamma^\mu \tfrac{1}{2}(1-\gamma^5)u(p_1) + c_{\rm R}^{\rm e}\,\overline{v}(p_2)\gamma^\mu\tfrac{1}{2}(1+\gamma^5)u(p_1)\right] \\ &\times \left[c_{\rm L}^{\mu}\,\overline{u}(p_3)\gamma^\nu \tfrac{1}{2}(1-\gamma^5)v(p_4) + c_{\rm R}^{\mu}\,\overline{u}(p_3)\gamma^\nu\tfrac{1}{2}(1+\gamma^5)v(p_4)\right]\ . \end{aligned}$$

Multiplying out, the matrix element is seen to be the sum of four similar contributions,

$$M_{\rm fi} = M_{\rm RR} + M_{\rm RL} + M_{\rm LR} + M_{\rm LL}\ ,$$

where

$$\begin{aligned} M_{\rm RR} &= -\frac{g_{\rm Z}^2}{s-m_{\rm Z}^2} c_{\rm R}^{\rm e} c_{\rm R}^{\mu}\, g_{\mu\nu} \left[\overline{v}(p_2)\gamma^\mu\tfrac{1}{2}(1+\gamma^5)u(p_1)\right]\left[\overline{u}(p_3)\gamma^\nu\tfrac{1}{2}(1+\gamma^5)v(p_4)\right] \\ M_{\rm RL} &= -\frac{g_{\rm Z}^2}{s-m_{\rm Z}^2} c_{\rm R}^{\rm e} c_{\rm L}^{\mu}\, g_{\mu\nu} \left[\overline{v}(p_2)\gamma^\mu\tfrac{1}{2}(1+\gamma^5)u(p_1)\right]\left[\overline{u}(p_3)\gamma^\nu\tfrac{1}{2}(1-\gamma^5)v(p_4)\right] \\ M_{\rm LR} &= -\frac{g_{\rm Z}^2}{s-m_{\rm Z}^2} c_{\rm L}^{\rm e} c_{\rm R}^{\mu}\, g_{\mu\nu} \left[\overline{v}(p_2)\gamma^\mu\tfrac{1}{2}(1-\gamma^5)u(p_1)\right]\left[\overline{u}(p_3)\gamma^\nu\tfrac{1}{2}(1+\gamma^5)v(p_4)\right] \\ M_{\rm LL} &= -\frac{g_{\rm Z}^2}{s-m_{\rm Z}^2} c_{\rm L}^{\rm e} c_{\rm L}^{\mu}\, g_{\mu\nu} \left[\overline{v}(p_2)\gamma^\mu\tfrac{1}{2}(1-\gamma^5)u(p_1)\right]\left[\overline{u}(p_3)\gamma^\nu\tfrac{1}{2}(1-\gamma^5)v(p_4)\right]\ . \end{aligned}$$

These expressions are identical to those already considered for the QED process, Equations (9)-(12), except for the replacement

$$\frac{e^2}{s} \quad \longrightarrow \quad \frac{g_{\rm Z}^2}{s-m_{\rm Z}^2} \tag{13}$$

and for the additional overall factors of $c_{\rm R}^{\rm e}c_{\rm R}^{\mu}$, $c_{\rm R}^{\rm e}c_{\rm L}^{\mu}$, $c_{\rm L}^{\rm e}c_{\rm R}^{\mu}$ and $c_{\rm L}^{\rm e}c_{\rm L}^{\mu}$, giving different overall strengths to each contribution.

11.2.2 Evaluation of the cross section

Applying the transformation of Equation (13) to the results of the QED calculation in Equations (2)-(5), and including the extra coupling constant factors $c_{\rm R}$ and $c_{\rm L}$, we obtain immediately the matrix

elements squared for the weak interaction process $\mathrm{e^+e^-} \to \mathrm{Z^0} \to \mu^+\mu^-$:

$$|M_{\mathrm{RR}}|^2 = \left(\frac{g_{\mathrm{Z}}^2}{s - m_{\mathrm{Z}}^2}\right)^2 (c_{\mathrm{R}}^{\mathrm{e}})^2 (c_{\mathrm{R}}^{\mu})^2 s^2 (1 + \cos\theta)^2 \tag{14}$$

$$|M_{\mathrm{LL}}|^2 = \left(\frac{g_{\mathrm{Z}}^2}{s - m_{\mathrm{Z}}^2}\right)^2 (c_{\mathrm{L}}^{\mathrm{e}})^2 (c_{\mathrm{L}}^{\mu})^2 s^2 (1 + \cos\theta)^2 \tag{15}$$

$$|M_{\mathrm{LR}}|^2 = \left(\frac{g_{\mathrm{Z}}^2}{s - m_{\mathrm{Z}}^2}\right)^2 (c_{\mathrm{L}}^{\mathrm{e}})^2 (c_{\mathrm{R}}^{\mu})^2 s^2 (1 - \cos\theta)^2 \tag{16}$$

$$|M_{\mathrm{RL}}|^2 = \left(\frac{g_{\mathrm{Z}}^2}{s - m_{\mathrm{Z}}^2}\right)^2 (c_{\mathrm{R}}^{\mathrm{e}})^2 (c_{\mathrm{L}}^{\mu})^2 s^2 (1 - \cos\theta)^2 \,. \tag{17}$$

Because of the contribution $1/(s - m_{\mathrm{Z}}^2)$ from the $\mathrm{Z^0}$ propagator, these expressions become divergent when $\sqrt{s} = m_{\mathrm{Z}}$. (In the centre of mass frame, for example, this occurs when the incoming beam energies are both equal to $E = m_{\mathrm{Z}}/2$). This problem is resolved by taking into account the fact that, unlike the photon, the $\mathrm{Z^0}$ is an unstable particle with a finite decay width. This is accomplished by making the replacement

$$m_{\mathrm{Z}} \quad \longrightarrow \quad m_{\mathrm{Z}} - i\Gamma_Z/2 \,. \tag{18}$$

Under this transformation, a wavefunction $\psi \sim e^{-imt}$ becomes $\psi \sim e^{-imt}e^{-\Gamma t/2}$. This gives a probability density which varies as $|\psi^2| \sim e^{-\Gamma t} = e^{-t/\tau}$, as required for a particle with lifetime $\tau = 1/\Gamma$.

Applying the transformation of Equation (18) to the factor $s - m_{\mathrm{Z}}^2$ gives

$$s - m_{\mathrm{Z}}^2 \quad \longrightarrow \quad s - m_{\mathrm{Z}}^2 + im_{\mathrm{Z}}\Gamma_Z + \tfrac{1}{4}\Gamma_Z^2 \;\approx\; s - m_{\mathrm{Z}}^2 + im_{\mathrm{Z}}\Gamma_Z$$

where the approximation $\Gamma_Z \ll m_{\mathrm{Z}}$ has been used in the last step. Hence

$$\left(\frac{1}{s - m_{\mathrm{Z}}^2}\right)^2 \quad \longrightarrow \quad \left|\frac{1}{s - m_{\mathrm{Z}}^2 + im_{\mathrm{Z}}\Gamma_Z}\right|^2 = \frac{1}{(s - m_{\mathrm{Z}}^2)^2 + m_{\mathrm{Z}}^2\Gamma_Z^2} \,. \tag{19}$$

It will be shown below that this results in a total cross section which has a Breit-Wigner resonance shape as a function of energy, centred around a resonant peak at $\sqrt{s} = m_{\mathrm{Z}}$ and of width Γ_Z.

Making the replacement of Equation (19), and using Equation (6), gives the following differential cross sections:

$$\frac{\mathrm{d}\sigma_{\mathrm{RR}}}{\mathrm{d}\Omega} = \frac{1}{64\pi^2}\frac{g_{\mathrm{Z}}^4 s}{(s - m_{\mathrm{Z}}^2)^2 + m_{\mathrm{Z}}^2\Gamma_Z^2}(c_{\mathrm{R}}^{\mathrm{e}})^2(c_{\mathrm{R}}^{\mu})^2(1 + \cos\theta)^2$$

$$\frac{\mathrm{d}\sigma_{\mathrm{LL}}}{\mathrm{d}\Omega} = \frac{1}{64\pi^2}\frac{g_{\mathrm{Z}}^4 s}{(s - m_{\mathrm{Z}}^2)^2 + m_{\mathrm{Z}}^2\Gamma_Z^2}(c_{\mathrm{L}}^{\mathrm{e}})^2(c_{\mathrm{L}}^{\mu})^2(1 + \cos\theta)^2$$

$$\frac{\mathrm{d}\sigma_{\mathrm{LR}}}{\mathrm{d}\Omega} = \frac{1}{64\pi^2}\frac{g_{\mathrm{Z}}^4 s}{(s - m_{\mathrm{Z}}^2)^2 + m_{\mathrm{Z}}^2\Gamma_Z^2}(c_{\mathrm{L}}^{\mathrm{e}})^2(c_{\mathrm{R}}^{\mu})^2(1 - \cos\theta)^2$$

$$\frac{\mathrm{d}\sigma_{\mathrm{RL}}}{\mathrm{d}\Omega} = \frac{1}{64\pi^2}\frac{g_{\mathrm{Z}}^4 s}{(s - m_{\mathrm{Z}}^2)^2 + m_{\mathrm{Z}}^2\Gamma_Z^2}(c_{\mathrm{R}}^{\mathrm{e}})^2(c_{\mathrm{L}}^{\mu})^2(1 - \cos\theta)^2 \,.$$

The corresponding total cross sections are

$$\sigma_{\rm RR} = \frac{1}{12\pi}\frac{g_{\rm Z}^4 s}{(s-m_{\rm Z}^2)^2+m_{\rm Z}^2\Gamma_Z^2}(c_{\rm R}^{\rm e})^2(c_{\rm R}^{\mu})^2$$
$$\sigma_{\rm LL} = \frac{1}{12\pi}\frac{g_{\rm Z}^4 s}{(s-m_{\rm Z}^2)^2+m_{\rm Z}^2\Gamma_Z^2}(c_{\rm L}^{\rm e})^2(c_{\rm L}^{\mu})^2$$
$$\sigma_{\rm LR} = \frac{1}{12\pi}\frac{g_{\rm Z}^4 s}{(s-m_{\rm Z}^2)^2+m_{\rm Z}^2\Gamma_Z^2}(c_{\rm L}^{\rm e})^2(c_{\rm R}^{\mu})^2$$
$$\sigma_{\rm RL} = \frac{1}{12\pi}\frac{g_{\rm Z}^4 s}{(s-m_{\rm Z}^2)^2+m_{\rm Z}^2\Gamma_Z^2}(c_{\rm R}^{\rm e})^2(c_{\rm L}^{\mu})^2 \ .$$

Thus, for the weak interactions, the cross sections for the various allowed spin configurations are no longer all equal, but depend on the values of the left-handed and right-handed couplings to the $\rm Z^0$:

$$\boxed{\sigma_{\rm RR} \propto (c_{\rm R}^{\rm e})^2(c_{\rm R}^{\mu})^2, \quad \sigma_{\rm RL} \propto (c_{\rm R}^{\rm e})^2(c_{\rm L}^{\mu})^2, \quad \sigma_{\rm LR} \propto (c_{\rm L}^{\rm e})^2(c_{\rm R}^{\mu})^2, \quad \sigma_{\rm LL} \propto (c_{\rm L}^{\rm e})^2(c_{\rm L}^{\mu})^2} \ . \qquad (20)$$

The differences in magnitude of each of these cross sections is a reflection of parity violation in the weak interactions.

11.2.3 The cross section with unpolarised beams

For unpolarised electron and positron beams, the matrix elements squared of Equations (14)-(17) must be summed over the final state μ^+ and μ^- spins (helicities) and averaged over the initial $\rm e^-$ and $\rm e^+$ spins. This gives

$$\begin{aligned}\langle|M_{\rm fi}|^2\rangle &= \tfrac{1}{2}\cdot\tfrac{1}{2}\cdot\left[|M_{\rm RR}|^2+|M_{\rm LL}|^2+|M_{\rm LR}|^2+|M_{\rm RL}|^2\right] \\ &= \tfrac{1}{2}\cdot\tfrac{1}{2}\cdot\left(\frac{g_{\rm Z}^2}{s-m_{\rm Z}^2}\right)^2 s^2 \\ &\quad\times\left(\left[(c_{\rm R}^{\rm e})^2(c_{\rm R}^{\mu})^2+(c_{\rm L}^{\rm e})^2(c_{\rm L}^{\mu})^2\right](1+\cos\theta)^2+\left[(c_{\rm R}^{\rm e})^2(c_{\rm L}^{\mu})^2+(c_{\rm L}^{\rm e})^2(c_{\rm R}^{\mu})^2\right](1-\cos\theta)^2\right) \ .\end{aligned}$$

The last line in the above equation can be rearranged as

$$\begin{aligned}(...) = &\quad \left[(c_{\rm R}^{\rm e})^2+(c_{\rm L}^{\rm e})^2\right]\left[(c_{\rm R}^{\mu})^2+(c_{\rm L}^{\mu})^2\right](1+\cos^2\theta)+2\left[(c_{\rm R}^{\rm e})^2-(c_{\rm L}^{\rm e})^2\right]\left[(c_{\rm R}^{\mu})^2-(c_{\rm L}^{\mu})^2\right]\cos\theta \\ = &\ \frac{1}{4}\left[(c_{\rm V}^{\rm e})^2+(c_{\rm A}^{\rm e})^2\right]\left[(c_{\rm V}^{\mu})^2+(c_{\rm A}^{\mu})^2\right](1+\cos^2\theta)+2c_{\rm V}^{\rm e}c_{\rm A}^{\rm e}c_{\rm V}^{\mu}c_{\rm A}^{\mu}\cos\theta\end{aligned}$$

where we have used

$$c_{\rm V}^2+c_{\rm A}^2 = 2\left(c_{\rm L}^2+c_{\rm R}^2\right), \qquad c_{\rm V}c_{\rm A} = c_{\rm L}^2-c_{\rm R}^2 \ .$$

Hence the unpolarised differential cross section is

$$\begin{aligned}\frac{{\rm d}\sigma}{{\rm d}\Omega} &= \frac{1}{64\pi^2 s}\langle|M_{\rm fi}|^2\rangle \\ &= \frac{1}{64\pi^2}\cdot\frac{1}{4}\cdot\frac{g_{\rm Z}^4 s}{(s-m_{\rm Z}^2)^2+m_{\rm Z}^2\Gamma_Z^2} \\ &\quad\times\left(\frac{1}{4}\left[(c_{\rm V}^{\rm e})^2+(c_{\rm A}^{\rm e})^2\right]\left[(c_{\rm V}^{\mu})^2+(c_{\rm A}^{\mu})^2\right](1+\cos^2\theta)+2c_{\rm V}^{\rm e}c_{\rm A}^{\rm e}c_{\rm V}^{\mu}c_{\rm A}^{\mu}\cos\theta\right) \ . \qquad (21)\end{aligned}$$

Integrating over the full solid angle using $\mathrm{d}\Omega = 2\pi \mathrm{d}\cos\theta$, $\int_{-1}^{+1}(1+\cos^2\theta)\,\mathrm{d}\cos\theta = 8/3$, and $\int_{-1}^{+1}\cos\theta\,\mathrm{d}\cos\theta = 0$, gives the total cross section

$$\boxed{\sigma = \frac{1}{192\pi}\,\frac{g_{\mathrm{Z}}^4 s}{(s-m_{\mathrm{Z}}^2)^2 + m_{\mathrm{Z}}^2\Gamma_Z^2}\,\left[(c_{\mathrm{V}}^{\mathrm{e}})^2+(c_{\mathrm{A}}^{\mathrm{e}})^2\right]\left[(c_{\mathrm{V}}^{\mu})^2+(c_{\mathrm{A}}^{\mu})^2\right]}\,. \tag{22}$$

11.2.4 The Breit-Wigner resonance formula

In Question 26 on the examples sheet, the decay rates (partial widths) for the decays $\mathrm{Z}^0 \to \mathrm{e}^+\mathrm{e}^-$ and $\mathrm{Z}^0 \to \mu^+\mu^-$ are shown to be

$$\Gamma(\mathrm{Z}^0 \to \mathrm{e}^+\mathrm{e}^-) = \frac{g_{\mathrm{Z}}^2 m_{\mathrm{Z}}}{24\pi}\left[(c_{\mathrm{L}}^{\mathrm{e}})^2+(c_{\mathrm{R}}^{\mathrm{e}})^2\right] = \frac{g_{\mathrm{Z}}^2 m_{\mathrm{Z}}}{48\pi}\left[(c_{\mathrm{V}}^{\mathrm{e}})^2+(c_{\mathrm{A}}^{\mathrm{e}})^2\right]$$
$$\Gamma(\mathrm{Z}^0 \to \mu^+\mu^-) = \frac{g_{\mathrm{Z}}^2 m_{\mathrm{Z}}}{24\pi}\left[(c_{\mathrm{L}}^{\mu})^2+(c_{\mathrm{R}}^{\mu})^2\right] = \frac{g_{\mathrm{Z}}^2 m_{\mathrm{Z}}}{48\pi}\left[(c_{\mathrm{V}}^{\mu})^2+(c_{\mathrm{A}}^{\mu})^2\right]$$

Hence the total cross section for the process $\mathrm{e}^+\mathrm{e}^- \to \mathrm{Z}^0 \to \mu^+\mu^-$ in Equation (22) can be written as

$$\begin{aligned}\sigma &= \frac{1}{192\pi}\,\frac{g_{\mathrm{Z}}^4 s}{(s-m_{\mathrm{Z}}^2)^2 + m_{\mathrm{Z}}^2\Gamma_Z^2}\,\left(\frac{48\pi}{g_{\mathrm{Z}}^2 m_{\mathrm{Z}}}\right)^2 \Gamma(\mathrm{Z}^0 \to \mathrm{e}^+\mathrm{e}^-)\Gamma(\mathrm{Z}^0 \to \mu^+\mu^-) \\ &= \frac{12\pi}{m_{\mathrm{Z}}^2}\,\frac{s}{(s-m_{\mathrm{Z}}^2)^2 + m_{\mathrm{Z}}^2\Gamma_Z^2}\,\Gamma(\mathrm{Z}^0 \to \mathrm{e}^+\mathrm{e}^-)\Gamma(\mathrm{Z}^0 \to \mu^+\mu^-)\,.\end{aligned}$$

This result applies equally if the $\mu^+\mu^-$ pair is replaced by any other kinematically-allowed fermion-antifermion final state. Therefore, in general, for the process $\mathrm{e}^+\mathrm{e}^- \to \mathrm{Z}^0 \to \mathrm{f}\bar{\mathrm{f}}$ using unpolarised beams, we have

$$\boxed{\sigma(\mathrm{e}^+\mathrm{e}^- \to \mathrm{Z}^0 \to \mathrm{f}\bar{\mathrm{f}}) = \frac{12\pi}{m_{\mathrm{Z}}^2}\,\frac{s}{(s-m_{\mathrm{Z}}^2)^2 + m_{\mathrm{Z}}^2\Gamma_Z^2}\,\Gamma_i\Gamma_f}\tag{23}$$

where $\Gamma_i = \Gamma(\mathrm{Z}^0 \to \mathrm{e}^+\mathrm{e}^-)$ and $\Gamma_f = \Gamma(\mathrm{Z}^0 \to \mathrm{f}\bar{\mathrm{f}})$. Note that although Equation (23) has been derived working in the centre of mass frame, all quantities appearing in the equation are Lorentz invariant, so that Equation (23) in fact applies in any reference frame.

For energies near the peak of the resonance, we can write $\sqrt{s} = m_{\mathrm{Z}} + \Delta$ say, with Δ small. Then $s \approx m_{\mathrm{Z}}^2 + 2m_{\mathrm{Z}}\Delta$ and

$$(s-m_{\mathrm{Z}}^2)^2 + m_{\mathrm{Z}}^2\Gamma^2 \approx (2m_{\mathrm{Z}}\Delta)^2 + m_{\mathrm{Z}}^2\Gamma^2 = 4m_{\mathrm{Z}}^2\left[\Delta^2 + \tfrac{1}{4}\Gamma^2\right] = 4m_{\mathrm{Z}}^2\left[(\sqrt{s}-m_{\mathrm{Z}})^2 + \tfrac{1}{4}\Gamma^2\right]\,.$$

Near the resonance peak, the $\mathrm{e}^+\mathrm{e}^- \to \mathrm{Z}^0 \to \mathrm{f}\bar{\mathrm{f}}$ cross section is then

$$\sigma(\mathrm{e}^+\mathrm{e}^- \to \mathrm{Z}^0 \to \mathrm{f}\bar{\mathrm{f}}) \approx \frac{12\pi}{4m_{\mathrm{Z}}^4}\,\frac{s}{(\sqrt{s}-m_{\mathrm{Z}})^2 + \frac{1}{4}\Gamma^2}\cdot\Gamma_i\Gamma_f$$

Changing notation to $E = \sqrt{s}$ and $E_0 = m_{\mathrm{Z}}$, we then recover the Breit-Wigner resonance formula in the form in which it appeared in the Part II Particles and Nuclear Physics course :

$$\sigma(E) = \frac{g\lambda^2}{4\pi}\cdot\frac{\Gamma_i\Gamma_f}{(E-E_0)^2 + \frac{1}{4}\Gamma^2}$$

where $g = (2J+1)/(2s_1+1)(2s_2+1) = 3/4$ is the spin counting factor and

$$\lambda = \frac{2\pi}{E} \approx \frac{4\pi}{m_{\mathrm{Z}}}$$

is the de Broglie wavelength of either of the incoming particles in the centre of mass frame (in natural units).

11.3 The Forward-Backward Asymmetry

For the QED process $\mathrm{e^+e^-} \to \gamma^* \to \mu^+\mu^-$, the unpolarised differential cross section of Equation (7), $\mathrm{d}\sigma/\mathrm{d}\cos\theta \propto (1+\cos^2\theta)$, is symmetric about $\theta = 90^\circ$ ($\cos\theta = 0$). For the weak interaction process $\mathrm{e^+e^-} \to \mathrm{Z}^0 \to \mu^+\mu^-$ on the other hand, the appearance of the term proportional to $\cos\theta$ in Equation (21) leads to a cross section which is *asymmetric* about $\cos\theta = 0$ [2]. The level of this asymmetry can be quantified by introducing the *forward* and *backward* cross sections σ_{F} and σ_{B} defined as

$$\sigma_{\mathrm{F}} \equiv \int_0^1 \frac{\mathrm{d}\sigma}{\mathrm{d}\cos\theta}\,\mathrm{d}\cos\theta, \qquad \sigma_{\mathrm{B}} \equiv \int_{-1}^0 \frac{\mathrm{d}\sigma}{\mathrm{d}\cos\theta}\,\mathrm{d}\cos\theta\ .$$

These cross sections correspond to the outgoing μ^- being emitted in the forward or backward hemisphere, respectively, as defined by the direction of motion of the incoming electron:

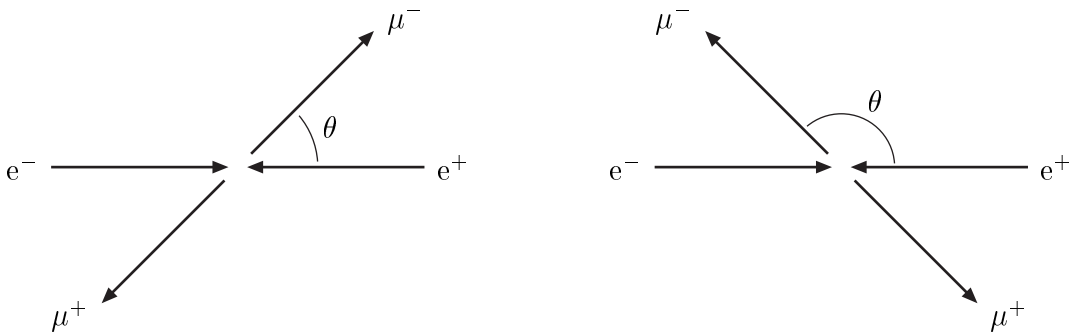

The *forward-backward asymmetry* A_{FB} is then defined as

$$\boxed{A_{\mathrm{FB}} \equiv \frac{\sigma_{\mathrm{F}} - \sigma_{\mathrm{B}}}{\sigma_{\mathrm{F}} + \sigma_{\mathrm{B}}}}\ .$$

The differential cross section of Equation (21) is of the form

$$\frac{\mathrm{d}\sigma}{\mathrm{d}\cos\theta} \propto A(1+\cos^2\theta) + B\cos\theta$$

where A and B are constants:

$$A = \left[(c_{\mathrm{L}}^{\mathrm{e}})^2 + (c_{\mathrm{R}}^{\mathrm{e}})^2\right]\left[(c_{\mathrm{L}}^{\mu})^2 + (c_{\mathrm{R}}^{\mu})^2\right]$$
$$B = 2\left[(c_{\mathrm{L}}^{\mathrm{e}})^2 - (c_{\mathrm{R}}^{\mathrm{e}})^2\right]\left[(c_{\mathrm{L}}^{\mu})^2 - (c_{\mathrm{R}}^{\mu})^2\right]\ .$$

[2] unless, by chance, one of the coupling constants $c_{\mathrm{V}}^{\mathrm{e}}$, $c_{\mathrm{A}}^{\mathrm{e}}$, c_{V}^{μ}, c_{A}^{μ} happens to be zero, which in the Standard Model, would require $\sin^2\theta_{\mathrm{W}} = 1/4$.

The forward and backward cross sections $\sigma_{\rm F}$ and $\sigma_{\rm B}$ are therefore given by

$$\sigma_{\rm F} \propto \int_0^1 \left[A(1+\cos^2\theta) + B\cos\theta\right]\,{\rm d}\cos\theta = \frac{4}{3}A + \frac{1}{2}B$$
$$\sigma_{\rm B} \propto \int_{-1}^0 \left[A(1+\cos^2\theta) + B\cos\theta\right]\,{\rm d}\cos\theta = \frac{4}{3}A - \frac{1}{2}B\ ,$$

which results in a forward-backward asymmetry

$$A_{\rm FB} = \frac{\sigma_{\rm F}-\sigma_{\rm B}}{\sigma_{\rm F}+\sigma_{\rm B}} = \frac{B}{(8/3)A} = \frac{3}{4}\cdot\frac{[(c_{\rm L}^{\rm e})^2-(c_{\rm R}^{\rm e})^2]}{[(c_{\rm L}^{\rm e})^2+(c_{\rm R}^{\rm e})^2]}\cdot\frac{[(c_{\rm L}^{\mu})^2-(c_{\rm R}^{\mu})^2]}{[(c_{\rm L}^{\mu})^2+(c_{\rm R}^{\mu})^2]}\ .$$

This can be written more compactly as

$$\boxed{A_{\rm FB} = \frac{3}{4}A_e A_\mu} \qquad \text{where} \qquad \boxed{A_f \equiv \frac{(c_{\rm L}^{\rm f})^2-(c_{\rm R}^{\rm f})^2}{(c_{\rm L}^{\rm f})^2+(c_{\rm R}^{\rm f})^2} = \frac{2c_{\rm V}^{\rm f}c_{\rm A}^{\rm f}}{(c_{\rm V}^{\rm f})^2+(c_{\rm A}^{\rm f})^2}}\ . \tag{24}$$

For the weak interactions therefore, a non-zero forward-backward asymmetry is expected due to the different coupling strengths of left-handed and right-handed particles to the $\rm Z^0$ ($c_{\rm R} \neq c_{\rm L}$). For the corresponding QED process, the coupling strengths for left-handed and right-handed particles are equal, and we expect $A_{\rm FB} = 0$ (at leading order).

11.4 The Left-Right Asymmetry

If *polarised* electron beams are available (as at the SLC linear $\rm e^+e^-$ collider at SLAC for example), it is also possible to measure the *left-right asymmetry*

$$\boxed{A_{\rm LR} \equiv \frac{\sigma_{\rm L}-\sigma_{\rm R}}{\sigma_{\rm L}+\sigma_{\rm R}}}$$

between the cross sections $\sigma_{\rm L}$ and $\sigma_{\rm R}$ for left-handed (negatively polarised) and right-handed (positively polarised) electron beams.

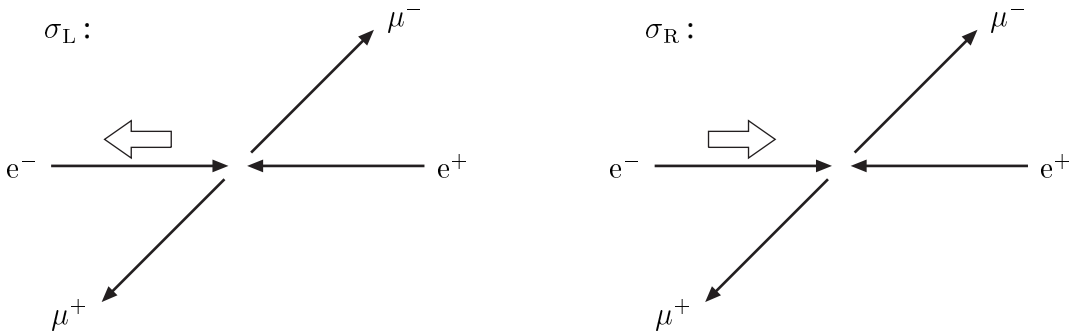

Only the electron beam at SLAC can be polarised; the positron beam is still an unpolarised mix of the two possible spin states.

The cross sections $\sigma_{\rm L}$, $\sigma_{\rm R}$ are obtained by summing over the final state (μ^+, μ^-) helicities, and averaging over the $\rm e^+$ spins in the unpolarised $\rm e^+$ beam:

$$\begin{aligned}\sigma_{\rm L} &= \tfrac{1}{2}\left(\sigma_{\rm LL} + \sigma_{\rm LR}\right) \\ \sigma_{\rm R} &= \tfrac{1}{2}\left(\sigma_{\rm RL} + \sigma_{\rm RR}\right) \ .\end{aligned}$$

From Equation (20), we have $\sigma_{\rm LL} \propto (c_{\rm L}^{\rm e})^2(c_{\rm L}^{\mu})^2$, $\sigma_{\rm LR} \propto (c_{\rm L}^{\rm e})^2(c_{\rm R}^{\mu})^2$ *etc.*. Hence the cross sections $\sigma_{\rm L}$ and $\sigma_{\rm R}$ are in the ratio

$$\begin{aligned}\sigma_{\rm L} &\propto (c_{\rm L}^{\rm e})^2(c_{\rm L}^{\mu})^2 + (c_{\rm L}^{\rm e})^2(c_{\rm R}^{\mu})^2 \propto (c_{\rm L}^{\rm e})^2 \\ \sigma_{\rm R} &\propto (c_{\rm R}^{\rm e})^2(c_{\rm L}^{\mu})^2 + (c_{\rm R}^{\rm e})^2(c_{\rm R}^{\mu})^2 \propto (c_{\rm R}^{\rm e})^2 \ .\end{aligned}$$

The left-right asymmetry is therefore

$$\boxed{A_{\rm LR} = \frac{(c_{\rm L}^{\rm e})^2 - (c_{\rm R}^{\rm e})^2}{(c_{\rm L}^{\rm e})^2 + (c_{\rm R}^{\rm e})^2} = A_e} \ . \tag{25}$$

A comparison of Equations (24) and (25) shows that while the forward-backward asymmetry $A_{\rm FB}$ measures the combination $A_e A_\mu$ of initial and final state couplings, the left-right asymmetry $A_{\rm LR}$ is sensitive to the initial state (electron) couplings alone. A combination of measurements of $A_{\rm FB}$ and $A_{\rm LR}$ therefore allows A_e and A_μ to be extracted separately.

12 Neutrino Oscillations

In the Standard Model, the three neutrino flavours $\nu_{\rm e}$, ν_μ and ν_τ are all assumed to be exactly massless. In addition, the three generations of leptons are completely decoupled from each other, as exemplified by the fact that the lepton numbers $L_{\rm e}$, L_μ and L_τ are separately conserved. In interactions involving a $\rm Z^0$, for example, transitions such as $\nu_{\rm e} \rightarrow \nu_{\rm e}$ or $\overline{\nu}_\mu \rightarrow \overline{\nu}_\mu$ are allowed, while transitions such as $\nu_\mu \rightarrow \nu_\tau$ or $\overline{\nu}_{\rm e} \rightarrow \overline{\nu}_\mu$ are forbidden. Similarly, in interactions involving a $\rm W^\pm$ boson, transitions such as $\nu_{\rm e} \rightarrow {\rm e}^-$ and $\overline{\nu}_{\rm e} \rightarrow {\rm e}^+$ are allowed, while transitions such as $\nu_{\rm e} \rightarrow \mu^-$ or $\overline{\nu}_\mu \rightarrow \tau^+$ are forbidden.

In general, beyond the Standard Model, neutrinos are expected to have a small but finite mass. In this case, the flavour (or weak) eigenstates $\nu_{\rm e}$, ν_μ, ν_τ will in general be different from the mass eigenstates ν_1, ν_2, ν_3 (with masses m_1, m_2, m_3). The connection between the flavour and mass eigenstates is described by a unitary 3×3 matrix, the PMNS matrix, analogous to the CKM matrix of the quark sector. One consequence of the mismatch between the flavour and mass eigenstates is that neutrinos produced as one flavour (a ν_μ produced in $\pi^+ \rightarrow \mu^+\nu_\mu$ decay, for example) can be detected subsequently as a *different* flavour ($\nu_{\rm e}$, for example, which gives an electron in a charged-current interaction: $\nu_{\rm e}{\rm p} \rightarrow {\rm e}^-{\rm X}$). Neutrino flavour conversion can be studied by searching for *neutrino oscillations* in a beam of neutrinos.

In this handout, expressions for the neutrino conversion probabilities $P(\nu_\alpha \rightarrow \nu_\beta)$ are derived, first for the simple case of two neutrino flavours alone and then for the more general case of three neutrino flavours. The formalism will bear many similarities to that developed in Handout 8 to describe strangeness oscillations in the neutral kaon system. The main differences are that we will now be dealing with a general three-way mixing between three different types of particle, rather than an oscillation between a single particle and its antiparticle, and that neutrinos are stable particles, in contrast to the weakly-decaying neutral kaons. In addition, neutrino oscillations are "cleaner" in the sense that the difficulties inherent in dealing with hadronic bound states are avoided.

12.1 Oscillations of two neutrino flavours

We consider first the case where there exists only two flavours of neutrino, $\nu_{\rm e}$ and ν_μ say. The flavour eigenstates (or weak eigenstates) can be expressed in terms of the mass eigenstates ν_1 and ν_2 via a 2×2 rotation matrix:

$$\begin{pmatrix} \nu_{\rm e} \\ \nu_\mu \end{pmatrix} = \begin{pmatrix} \cos\theta & \sin\theta \\ -\sin\theta & \cos\theta \end{pmatrix} \begin{pmatrix} \nu_1 \\ \nu_2 \end{pmatrix} \tag{1}$$

where θ is a constant rotation angle. Equation (1) can be inverted to give the mass eigenstates in terms of the flavour eigenstates:

$$\begin{pmatrix}\nu_1\\ \nu_2\end{pmatrix} = \begin{pmatrix}\cos\theta & -\sin\theta\\ \sin\theta & \cos\theta\end{pmatrix}\begin{pmatrix}\nu_{\rm e}\\ \nu_\mu\end{pmatrix} \ . \tag{2}$$

Consider a neutrino which is produced in a pure $\nu_{\rm e}$ state at time $t = 0$ (from a $\pi^+ \to {\rm e}^+\nu_{\rm e}$ decay for example). The initial wavefunction is then

$$|\nu_{\rm e}(0)\rangle = |\nu_{\rm e}\rangle = |\nu_1\rangle\cos\theta + |\nu_2\rangle\sin\theta \ . \tag{3}$$

Choosing the $+x$ axis to lie along the direction of travel of the neutrino, the mass eigenstates can be taken to evolve as the plane waves

$$|\nu_1(t)\rangle = |\nu_1\rangle\, e^{ip_1x - iE_1t} \ , \qquad |\nu_2(t)\rangle = |\nu_2\rangle\, e^{ip_2x - iE_2t}$$

where $p_1 = |\boldsymbol{p}_1|$ and $p_2 = |\boldsymbol{p}_2|$ are the three-momenta associated with each mass eigenstate, and $E_1 = \sqrt{p_1^2 + m_1^2}$ and $E_2 = \sqrt{p_2^2 + m_2^2}$ are the corresponding energies. At later times $t > 0$ therefore, the neutrino wavefunction of Equation (3) becomes

$$|\nu_{\rm e}(t)\rangle = |\nu_1\rangle\, e^{ip_1x - iE_1t}\cos\theta + |\nu_2\rangle\, e^{ip_2x - iE_2t}\sin\theta \ .$$

Using Equation (2), this can be expressed in terms of the flavour eigenstates $\nu_{\rm e}$ and ν_μ as

$$\begin{aligned}|\nu_{\rm e}(t)\rangle &= \left[\cos\theta\,|\nu_{\rm e}\rangle - \sin\theta\,|\nu_\mu\rangle\right] e^{ip_1x - iE_1t}\cos\theta + \left[\sin\theta\,|\nu_{\rm e}\rangle + \cos\theta\,|\nu_\mu\rangle\right] e^{ip_2x - iE_2t}\sin\theta\\ &= |\nu_{\rm e}\rangle\left(\cos^2\theta e^{ip_1x - iE_1t} + \sin^2\theta e^{ip_2x - iE_2t}\right) + |\nu_\mu\rangle\sin\theta\cos\theta\left(-e^{ip_1x - iE_1t} + e^{ip_2x - iE_2t}\right) \ .\end{aligned}$$

Thus, the wavefunction develops a ν_μ component, giving rise to the possibility that the original $\nu_{\rm e}$ is detected as a ν_μ. The probability that this occurs is

$$\begin{aligned}P(\nu_{\rm e} \to \nu_\mu) &= |\langle\nu_\mu|\nu_{\rm e}(t)\rangle|^2\\ &= \sin^2\theta\cos^2\theta\left|-e^{ip_1x - iE_1t} + e^{ip_2x - iE_2t}\right|^2\\ &= \tfrac{1}{2}\sin^2 2\theta\left(1 - \cos\left[(p_1x - E_1t) - (p_2x - E_2t)\right]\right) \ ,\end{aligned} \tag{4}$$

where the complex number relation $|z_1 \pm z_2|^2 = |z_1|^2 + |z_2|^2 \pm 2{\rm Re}(z_1z_2^*)$ has been used in the last step. Neutrino masses are known to be very small, $m_i \ll p_i$, so that for each mass eigenstate, we have

$$E_i = \sqrt{p_i^2 + m_i^2} \approx p_i + \frac{m_i^2}{2p_i} \ . \tag{5}$$

Further, since neutrinos are extremely relativistic ($v_i \approx c$), we can also make the approximation $x \approx t$. Hence

$$p_ix - E_it \approx (p_i - E_i)x \approx -\frac{m_i^2}{2p_i}x \approx -\frac{m_i^2}{2E_i}x \ . \tag{6}$$

With these approximations, the $\nu_{\rm e} \to \nu_\mu$ conversion probability of Equation (4) becomes

$$\boxed{P(\nu_{\rm e} \to \nu_\mu) = \tfrac{1}{2}\sin^2 2\theta\left[1 - \cos\left(\frac{\Delta m_{12}^2 L}{2E}\right)\right]} \tag{7}$$

where we have defined

$$\Delta m_{12}^2 \equiv m_1^2 - m_2^2 \ .$$

We have also set $E \approx E_1 \approx E_2$, and replaced x by L to conform with standard notation.

Equation (7) corresponds to *neutrino oscillations* with wavelength

$$\lambda = \frac{4\pi E}{\Delta m^2_{12}} \, .$$

Neutrino oscillations can occur only if there is a non-zero mass difference between the two mass eigenstates, and therefore at least one of the two masses must be non-zero. Note however that, because of the cosine in Equation (7), neutrino oscillations are sensitive only to the absolute mass-squared difference $|m_1^2 - m_2^2|$; they cannot provide information on the *absolute values* of the masses m_1 and m_2, nor can they distinguish between the two possibilities $m_1 > m_2$ and $m_1 < m_2$.

Using the identity $1 - \cos\theta = 2\sin^2\theta/2$, we can also write Equation (7) in the form

$$\boxed{P(\nu_{\rm e} \to \nu_\mu) = \sin^2 2\theta \sin^2\left(\frac{\Delta m^2_{12} L}{4E}\right)} \, . \tag{8}$$

The probability that the neutrino flavour remains unchanged, the *survival probability*, is clearly

$$\boxed{P(\nu_{\rm e} \to \nu_{\rm e}) = 1 - \sin^2 2\theta \sin^2\left(\frac{\Delta m^2_{12} L}{4E}\right)} \, . \tag{9}$$

12.2 Oscillations of three neutrino flavours

12.2.1 General Expressions for the Oscillation Probabilities

In the case of three neutrino flavours, $\nu_{\rm e}$, ν_μ and ν_τ, Equation (1) generalises to

$$\begin{pmatrix} \nu_{\rm e} \\ \nu_\mu \\ \nu_\tau \end{pmatrix} = \begin{pmatrix} U_{e1} & U_{e2} & U_{e3} \\ U_{\mu 1} & U_{\mu 2} & U_{\mu 3} \\ U_{\tau 1} & U_{\tau 2} & U_{\tau 3} \end{pmatrix} \begin{pmatrix} \nu_1 \\ \nu_2 \\ \nu_3 \end{pmatrix}$$

where U is a unitary matrix, $U^\dagger U = I$, known as the PMNS matrix (analogous to the CKM matrix in the quark sector). Since $U^{-1} = U^\dagger = (U^*)^T$, this equation can be inverted to give

$$\begin{pmatrix} \nu_1 \\ \nu_2 \\ \nu_3 \end{pmatrix} = \begin{pmatrix} U^*_{e1} & U^*_{\mu 1} & U^*_{\tau 1} \\ U^*_{e2} & U^*_{\mu 2} & U^*_{\tau 2} \\ U^*_{e3} & U^*_{\mu 3} & U^*_{\tau 3} \end{pmatrix} \begin{pmatrix} \nu_{\rm e} \\ \nu_\mu \\ \nu_\tau \end{pmatrix} \, . \tag{10}$$

For a system which is initially in a pure $\nu_{\rm e}$ state, for example, the wavefunction at time $t = 0$ is

$$|\nu_{\rm e}(0)\rangle = U_{e1} \, |\nu_1\rangle + U_{e2} \, |\nu_2\rangle + U_{e3} \, |\nu_3\rangle \ ,$$

and evolves as

$$|\nu_{\rm e}(t)\rangle = U_{e1} \, |\nu_1\rangle \, e^{-iE_1 t} + U_{e2} \, |\nu_2\rangle \, e^{-iE_2 t} + U_{e3} \, |\nu_3\rangle \, e^{-iE_3 t} \ ,$$

where here and in the following it is to be understood that $e^{-iE_i t}$ is being used as a shorthand for $e^{ip_i x - iE_i t}$. Using Equation (10), the wavefunction $\nu_{\rm e}(t)$ can be expressed in terms of the flavour eigenstates as

$$\begin{aligned}|\nu_{\rm e}(t)\rangle = U_{e1}\left(U^*_{e1}\,|\nu_{\rm e}\rangle + U^*_{\mu 1}\,|\nu_\mu\rangle + U^*_{\tau 1}\,|\nu_\tau\rangle\right)e^{-iE_1 t} \\ + U_{e2}\left(U^*_{e2}\,|\nu_{\rm e}\rangle + U^*_{\mu 2}\,|\nu_\mu\rangle + U^*_{\tau 2}\,|\nu_\tau\rangle\right)e^{-iE_2 t} \\ + U_{e3}\left(U^*_{e3}\,|\nu_{\rm e}\rangle + U^*_{\mu 3}\,|\nu_\mu\rangle + U^*_{\tau 3}\,|\nu_\tau\rangle\right)e^{-iE_3 t}\end{aligned}$$

giving

$$\begin{aligned}|\nu_{\rm e}(t)\rangle = \left(U_{e1}U^*_{e1}e^{-iE_1 t} + U_{e2}U^*_{e2}e^{-iE_2 t} + U_{e3}U^*_{e3}e^{-iE_3 t}\right)|\nu_{\rm e}\rangle \\ + \left(U_{e1}U^*_{\mu 1}e^{-iE_1 t} + U_{e2}U^*_{\mu 2}e^{-iE_2 t} + U_{e3}U^*_{\mu 3}e^{-iE_3 t}\right)|\nu_\mu\rangle \\ + \left(U_{e1}U^*_{\tau 1}e^{-iE_1 t} + U_{e2}U^*_{\tau 2}e^{-iE_2 t} + U_{e3}U^*_{\tau 3}e^{-iE_3 t}\right)|\nu_\tau\rangle\ .\end{aligned} \tag{11}$$

The probability for neutrino flavour conversion, such as $\nu_{\rm e} \to \nu_\mu$, can be read off directly as

$$P(\nu_{\rm e} \to \nu_\mu) = \left|U_{e1}U^*_{\mu 1}e^{-iE_1 t} + U_{e2}U^*_{\mu 2}e^{-iE_2 t} + U_{e3}U^*_{\mu 3}e^{-iE_3 t}\right|^2\ .$$

In terms of Feynman diagrams, the first term on the right-hand side of the above equation can be represented as:

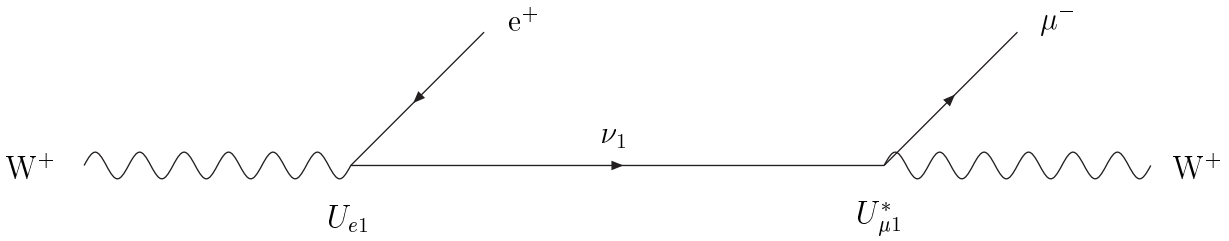

and similarly for the remaining terms with ν_1 replaced by ν_2 and ν_3. In this picture, the initial W^+ could be a virtual W^+ in a $\pi^+ \to \mathrm{e}^+\nu_{\rm e}$ decay for example, while the final W^+ is a virtual W^+ produced in a neutrino interaction of the form $\nu_\mu \to \mu^- + \mathrm{X}$.

Using the relation

$$|z_1 + z_2 + z_3|^2 = |z_1|^2 + |z_2|^2 + |z_3|^2 + 2\mathrm{Re}(z_1 z_2^* + z_1 z_3^* + z_2 z_3^*) \tag{12}$$

where z_1, z_2, z_3 are any three complex numbers, we can write the oscillation probability as

$$\begin{aligned}P(\nu_{\rm e} \to \nu_\mu) = |U_{e1}U_{\mu 1}|^2 + |U_{e2}U_{\mu 2}|^2 + |U_{e3}U_{\mu 3}|^2 \\ + 2\mathrm{Re}\left[U_{e1}U^*_{\mu 1}U^*_{e2}U_{\mu 2}e^{-i(E_1-E_2)t} + U_{e1}U^*_{\mu 1}U^*_{e3}U_{\mu 3}e^{-i(E_1-E_3)t} + U_{e2}U^*_{\mu 2}U^*_{e3}U_{\mu 3}e^{-i(E_2-E_3)t}\right]\ .\end{aligned} \tag{13}$$

Unitarity of the PMNS matrix gives (amongst others) the relation

$$U_{e1}U^*_{\mu 1} + U_{e2}U^*_{\mu 2} + U_{e3}U^*_{\mu 3} = 0\ .$$

Taking the modulus-squared of this equation, using Equation (12), then gives

$$|U_{e1}U_{\mu 1}|^2 + |U_{e2}U_{\mu 2}|^2 + |U_{e3}U_{\mu 3}|^2 + 2\mathrm{Re}(U_{e1}U^*_{\mu 1}U^*_{e2}U_{\mu 2} + U_{e1}U^*_{\mu 1}U^*_{e3}U_{\mu 3} + U_{e2}U^*_{\mu 2}U^*_{e3}U_{\mu 3}) = 0\ .$$

Using this relation to eliminate the sum $|U_{e1}U_{\mu 1}|^2 + |U_{e2}U_{\mu 2}|^2 + |U_{e3}U_{\mu 3}|^2$ in Equation (13) allows the conversion probability to be written as

$$\boxed{\begin{aligned} P(\nu_{\rm e} \to \nu_\mu) = {} & 2{\rm Re}\left(U_{e1}U^*_{\mu 1}U^*_{e2}U_{\mu 2}\left[e^{-i(E_1-E_2)t}-1\right]\right) \\ & + 2{\rm Re}\left(U_{e1}U^*_{\mu 1}U^*_{e3}U_{\mu 3}\left[e^{-i(E_1-E_3)t}-1\right]\right) \\ & + 2{\rm Re}\left(U_{e2}U^*_{\mu 2}U^*_{e3}U_{\mu 3}\left[e^{-i(E_2-E_3)t}-1\right]\right) \ . \end{aligned}} \tag{14}$$

Similar expressions can be written down directly for the other conversion probabilities $P(\nu_{\rm e} \to \nu_\tau)$, $P(\nu_\tau \to \nu_\mu)$, *etc.*.

The survival probability $P(\nu_{\rm e} \to \nu_{\rm e})$ can be obtained from the coefficient of $|\nu_{\rm e}\rangle$ in Equation (11) as

$$P(\nu_{\rm e} \to \nu_{\rm e}) = \left|U_{e1}U^*_{e1}e^{-iE_1 t} + U_{e2}U^*_{e2}e^{-iE_2 t} + U_{e3}U^*_{e3}e^{-iE_3 t}\right|^2 \ .$$

In this case, the relevant unitarity relation is

$$U_{e1}U^*_{e1} + U_{e2}U^*_{e2} + U_{e3}U^*_{e3} = 1 \ ,$$

and the expression equivalent to Equation (14) is

$$\begin{aligned} P(\nu_{\rm e} \to \nu_{\rm e}) = 1 & + 2|U_{e1}|^2|U_{e2}|^2{\rm Re}\left(\left[e^{-i(E_1-E_2)t}-1\right]\right) \\ & + 2|U_{e1}|^2|U_{e3}|^2{\rm Re}\left(\left[e^{-i(E_1-E_3)t}-1\right]\right) \\ & + 2|U_{e2}|^2|U_{e3}|^2{\rm Re}\left(\left[e^{-i(E_2-E_3)t}-1\right]\right) \ . \end{aligned}$$

Remembering that $-iE_it$ is being used as a shorthand for $ip_ix - iE_it$, and using again the approximation of Equation (6), the time-dependent factors can be written as

$$\begin{aligned} {\rm Re}\left[e^{-i(E_1-E_2)t}-1\right] & = \cos\left[(p_1x - E_1t) - (p_2x - E_2t)\right] - 1 \\ & = -2\sin^2\frac{(m_2^2-m_1^2)L}{4E} = -2\sin^2\Delta_{12} \end{aligned} \tag{15}$$

(and similarly for the other terms) where, for convenience, we have introduced

$$\Delta_{12} \equiv \frac{(m_1^2-m_2^2)L}{4E} = \frac{\Delta m^2_{12}L}{4E} \ .$$

Hence, finally,

$$\boxed{P(\nu_{\rm e} \to \nu_{\rm e}) = 1 - 4|U_{e1}|^2|U_{e2}|^2\sin^2\Delta_{12} - 4|U_{e1}|^2|U_{e3}|^2\sin^2\Delta_{13} - 4|U_{e2}|^2|U_{e3}|^2\sin^2\Delta_{23}} \ . \tag{16}$$

Similar expressions can be written down directly for the other survival probabilities $P(\nu_\mu \to \nu_\mu)$ and $P(\nu_\tau \to \nu_\tau)$. Note that, due to the constraint

$$\Delta_{12} + \Delta_{23} = \Delta_{13} \ ,$$

only two of the three Δ_{ij} appearing in Equation (16) are independent.

12.2.2 CP and T violation

Interchanging the labels "e" and "μ" in Equation (14) gives

$$\begin{aligned} P(\nu_\mu \to \nu_\mathrm{e}) = & \; 2\mathrm{Re}\left(U_{\mu 1}U_{e1}^*U_{\mu 2}^*U_{e2}\left[e^{-i(E_1-E_2)t}-1\right]\right) \\ & + 2\mathrm{Re}\left(U_{\mu 1}U_{e1}^*U_{\mu 3}^*U_{e3}\left[e^{-i(E_1-E_3)t}-1\right]\right) \\ & + 2\mathrm{Re}\left(U_{\mu 2}U_{e2}^*U_{\mu 3}^*U_{e3}\left[e^{-i(E_2-E_3)t}-1\right]\right) \; . \end{aligned} \tag{17}$$

Comparing this expression with Equation (14), it follows immediately that, unless the PMNS matrix is purely real, we have

$$P(\nu_\mu \to \nu_\mathrm{e}) \neq P(\nu_\mathrm{e} \to \nu_\mu) \; . \tag{18}$$

In other words, if any of the PMNS matrix elements are complex, neutrino oscillations are not invariant under time reversal, $t \to -t$, and we obtain T violation.

Under a combination of C and P operations, left-handed neutrinos are transformed into right-handed antineutrinos, and vice-versa. Thus, under CP, the transition $\nu_\mathrm{e} \to \nu_\mu$ becomes the transition $\overline{\nu}_\mathrm{e} \to \overline{\nu}_\mu$, for example. Under a combination of C, P *and* T (*i.e.* under a combined CPT operation), the transition $\nu_\mathrm{e} \to \nu_\mu$ becomes the transition $\overline{\nu}_\mu \to \overline{\nu}_\mathrm{e}$. If the weak interactions are invariant under CPT, we therefore have

$$P(\overline{\nu}_\mathrm{e} \to \overline{\nu}_\mu) = P(\nu_\mu \to \nu_\mathrm{e}) \; . \tag{19}$$

Comparing Equations (18) and (19), we see immediately that, unless the PMNS matrix is real, the antineutrino and neutrino conversion probabilities are different:

$$P(\overline{\nu}_\mathrm{e} \to \overline{\nu}_\mu) \neq P(\nu_\mathrm{e} \to \nu_\mu) \; .$$

In other words, if any of the PMNS matrix elements are complex, we expect to observe *CP violation* in neutrino oscillations. This is analogous to the quark sector where a complex CKM matrix gives rise to CP violation in hadronic systems.

Combining Equations (17) and (19), and reordering the factors of U_{ij} and U_{ij}^*, gives

$$\begin{aligned} P(\overline{\nu}_\mathrm{e} \to \overline{\nu}_\mu) = & \; 2\mathrm{Re}\left(U_{e1}^*U_{\mu 1}U_{e2}U_{\mu 2}^*\left[e^{-i(E_1-E_2)t}-1\right]\right) \\ & + 2\mathrm{Re}\left(U_{e1}^*U_{\mu 1}U_{e3}U_{\mu 3}^*\left[e^{-i(E_1-E_3)t}-1\right]\right) \\ & + 2\mathrm{Re}\left(U_{e2}^*U_{\mu 2}U_{e3}U_{\mu 3}^*\left[e^{-i(E_2-E_3)t}-1\right]\right) \; . \end{aligned}$$

Comparing with Equation (14), we see that the conversion probabilities for *antineutrinos* are obtained from those for neutrinos by replacing each PMNS matrix element U_{ij} by its complex conjugate U_{ij}^*.

The possibility of observing CP violation in neutrino oscillations is explored further in the examples sheet. A search for CP violation will be the subject of an intense experimental effort over the next decade or so, but as yet there is no evidence for such effects. For the remainder of this handout therefore, we shall neglect the possibility of CP violation and consider a PMNS matrix which is purely real.

12.2.3 Oscillation Probabilities Neglecting CP Violation

If the possibility of CP violation in the neutrino sector is neglected, the PMNS matrix can be taken to be purely real, and Equation (14) becomes

$$\begin{aligned} P(\nu_{\rm e} \to \nu_\mu) = {} & 2U_{e1}U_{\mu 1}U_{e2}U_{\mu 2}{\rm Re}\left[e^{-i(E_1-E_2)t}-1\right] \\ & + 2U_{e1}U_{\mu 1}U_{e3}U_{\mu 3}{\rm Re}\left[e^{-i(E_1-E_3)t}-1\right] \\ & + 2U_{e2}U_{\mu 2}U_{e3}U_{\mu 3}{\rm Re}\left[e^{-i(E_2-E_3)t}-1\right] \ . \end{aligned}$$

Hence, using Equation (15), we obtain

$$\boxed{P(\nu_{\rm e} \to \nu_\mu) = -4U_{e1}U_{\mu 1}U_{e2}U_{\mu 2}\sin^2\Delta_{12} - 4U_{e1}U_{\mu 1}U_{e3}U_{\mu 3}\sin^2\Delta_{13} - 4U_{e2}U_{\mu 2}U_{e3}U_{\mu 3}\sin^2\Delta_{23}} \tag{20}$$

plus similar equations for $P(\nu_{\rm e} \to \nu_\tau)$, $P(\nu_\mu \to \nu_\tau)$ *etc.*.

Similarly, neglecting CP violation, the survival probability $P(\nu_{\rm e} \to \nu_{\rm e})$ of Equation (16) becomes

$$\boxed{P(\nu_{\rm e} \to \nu_{\rm e}) = 1 - 4U_{e1}^2U_{e2}^2\sin^2\Delta_{12} - 4U_{e1}^2U_{e3}^2\sin^2\Delta_{13} - 4U_{e2}^2U_{e3}^2\sin^2\Delta_{23}}\ , \tag{21}$$

plus similar equations for $P(\nu_\mu \to \nu_\mu)$ and $P(\nu_\tau \to \nu_\tau)$.

It is easily seen from Equations (20) and (21) that, with U real, CP and T are now both conserved: $P(\nu_\mu \to \nu_{\rm e}) = P(\nu_{\rm e} \to \nu_\mu) = P(\overline{\nu}_{\rm e} \to \overline{\nu}_\mu)$, and so on.

12.2.4 Oscillation Probabilities with a Hierarchy of Masses

As will be explained in the next section, the data from a variety of neutrino experiments reveal evidence for neutrino oscillations with two very different scales for the mass-squared difference Δm^2. Specifically, the value of Δm^2 relevant to experiments using solar neutrinos and reactor antineutrinos, $|\Delta m^2| \approx 7 \times 10^{-5}\,{\rm eV}^2$, is determined experimentally to be much smaller than that appropriate to atmospheric neutrino oscillations, $|\Delta m^2| \approx 2 \times 10^{-3}\,{\rm eV}^2$:

$$|\Delta m^2|_{\rm solar} \ll |\Delta m^2|_{\rm atmo}\ .$$

This hierarchical structure of the mass eigenstates allows the expressions for the conversion and survival probabilities derived in the previous section to be greatly simplified, as we see below.

Since the *sign* of the mass-squared differences $\Delta m^2_{\rm solar}$ and $\Delta m^2_{\rm atmo}$ cannot be determined from observations of neutrino oscillations, two distinct ordering schemes are possible for the mass eigenstates:

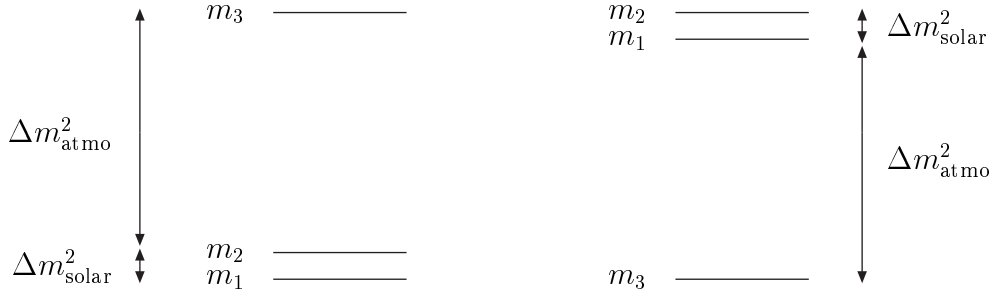

Normal hierarchy Inverted hierarchy

The labelling of the mass eigenstates in each scheme is completely arbitrary. The convention adopted is that, in either scheme, the labels "1" and "2" are assigned to the solar/reactor mass splitting, with the ordering $m_2 > m_1$. In either scheme, with this convention, we have

$$|\Delta m^2_{12}| \ll |\Delta m^2_{23}| \approx |\Delta m^2_{13}| \; .$$

For a *normal hierarchy* of masses (left-hand side), we have

$$m_1 < m_2 \ll m_3 \qquad\qquad 0 < \Delta_{21} \ll \Delta_{32} \approx \Delta_{31}$$

while for an *inverted hierarchy* of masses (right-hand side) we have [1]

$$m_3 \ll m_1 < m_2 \qquad\qquad 0 < \Delta_{21} \ll \Delta_{23} \approx \Delta_{13}$$

For both the normal and inverted mass hierarchies, we have $|\Delta_{13}| \approx |\Delta_{23}|$, so that the conversion probability of Equation (20) becomes

$$P(\nu_{\rm e} \to \nu_\mu) \approx -4U_{e1}U_{\mu 1}U_{e2}U_{\mu 2}\sin^2\Delta_{12} - 4(U_{e1}U_{\mu 1} + U_{e2}U_{\mu 2})U_{e3}U_{\mu 3}\sin^2\Delta_{23} \; .$$

Using the unitarity relation

$$U_{e1}U_{\mu 1} + U_{e2}U_{\mu 2} + U_{e3}U_{\mu 3} = 0$$

this can be written

$$\boxed{P(\nu_{\rm e} \to \nu_\mu) \approx -4U_{e1}U_{\mu 1}U_{e2}U_{\mu 2}\sin^2\Delta_{12} + 4U^2_{e3}U^2_{\mu 3}\sin^2\Delta_{23}} \tag{22}$$

The same form holds for other conversion processes such as $\nu_{\rm e} \to \nu_\tau$ and $\nu_\mu \to \nu_\tau$:

$$\boxed{P(\nu_{\rm e} \to \nu_\tau) \approx -4U_{e1}U_{\tau 1}U_{e2}U_{\tau 2}\sin^2\Delta_{12} + 4U^2_{e3}U^2_{\tau 3}\sin^2\Delta_{23}} \tag{23}$$

$$\boxed{P(\nu_\mu \to \nu_\tau) \approx -4U_{\mu 1}U_{\tau 1}U_{\mu 2}U_{\tau 2}\sin^2\Delta_{12} + 4U^2_{\mu 3}U^2_{\tau 3}\sin^2\Delta_{23}} \; . \tag{24}$$

The remaining conversion probabilities are given directly by

$$P(\nu_\mu \to \nu_{\rm e}) = P(\nu_{\rm e} \to \nu_\mu), \qquad P(\nu_\tau \to \nu_{\rm e}) = P(\nu_{\rm e} \to \nu_\tau), \qquad P(\nu_\tau \to \nu_\mu) = P(\nu_\mu \to \nu_\tau) \; .$$

For either mass hierarchy, the survival probability of Equation (21) can be written

$$P(\nu_{\rm e} \to \nu_{\rm e}) \approx 1 - 4U^2_{e1}U^2_{e2}\sin^2\Delta_{12} - 4\left(U^2_{e1} + U^2_{e2}\right)U^2_{e3}\sin^2\Delta_{23} \; .$$

Unitarity of the PMNS matrix gives the relation

$$U^2_{e1} + U^2_{e2} + U^2_{e3} = 1$$

and hence the survival probability is

$$\boxed{P(\nu_{\rm e} \to \nu_{\rm e}) \approx 1 - 4U^2_{e1}U^2_{e2}\sin^2\Delta_{12} - 4\left(1 - U^2_{e3}\right)U^2_{e3}\sin^2\Delta_{23}}, \tag{25}$$

[1] Since the *absolute* values of the masses m_i cannot be determined from observations of neutrino oscillations, it is also possible that, even though the mass-squared splittings $|\Delta m^2_{12}|$ and $|\Delta m^2_{23}|$ are very different, the neutrino masses themselves could all be approximately equal: $m_1 \approx m_2 \approx m_3$. This latter possibility is, however, theoretically disfavoured in most models.

with similar equations for $P(\nu_\mu \to \nu_\mu)$ and $P(\nu_\tau \to \nu_\tau)$.

In summary, neglecting CP violation and assuming a hierarchical mass structure based on one large and one small mass-squared splitting ($|\Delta m^2_{12}| \ll |\Delta m^2_{23}| \approx |\Delta m^2_{13}|$), the conversion and survival probabilities are given by Equations (22)-(25) :

$$P(\nu_{\rm e} \to \nu_\mu) = P(\nu_\mu \to \nu_{\rm e}) \approx -4U_{e1}U_{\mu 1}U_{e2}U_{\mu 2}\sin^2\Delta_{12} + 4U^2_{e3}U^2_{\mu 3}\sin^2\Delta_{23} \qquad (22)'$$

$$P(\nu_{\rm e} \to \nu_\tau) = P(\nu_\tau \to \nu_{\rm e}) \approx -4U_{e1}U_{\tau 1}U_{e2}U_{\tau 2}\sin^2\Delta_{12} + 4U^2_{e3}U^2_{\tau 3}\sin^2\Delta_{23} \qquad (23)'$$

$$P(\nu_\mu \to \nu_\tau) = P(\nu_\tau \to \nu_\mu) \approx -4U_{\mu 1}U_{\tau 1}U_{\mu 2}U_{\tau 2}\sin^2\Delta_{12} + 4U^2_{\mu 3}U^2_{\tau 3}\sin^2\Delta_{23} \qquad (24)'$$

$$\begin{aligned} P(\nu_{\rm e} \to \nu_{\rm e}) &\approx 1 - 4U^2_{e1}U^2_{e2}\sin^2\Delta_{12} - 4\left(1-U^2_{e3}\right)U^2_{e3}\sin^2\Delta_{23} \qquad (25)' \\ P(\nu_\mu \to \nu_\mu) &\approx 1 - 4U^2_{\mu 1}U^2_{\mu 2}\sin^2\Delta_{12} - 4\left(1-U^2_{\mu 3}\right)U^2_{\mu 3}\sin^2\Delta_{23} \\ P(\nu_\tau \to \nu_\tau) &\approx 1 - 4U^2_{\tau 1}U^2_{\tau 2}\sin^2\Delta_{12} - 4\left(1-U^2_{\tau 3}\right)U^2_{\tau 3}\sin^2\Delta_{23} \end{aligned}$$

In the next section, a subset of these equations will be used to interpret the experimental results on neutrino oscaillations.

The wavelengths λ_{12} and λ_{23} associated with the terms containing $\sin^2\Delta_{12}$ and $\sin^2\Delta_{23}$ are

$$\lambda_{12} = \frac{4\pi E}{\Delta m^2_{12}}, \qquad \lambda_{23} = \frac{4\pi E}{\Delta m^2_{23}}\,.$$

Since $|\Delta m^2_{12}| \ll |\Delta m^2_{23}|$, the oscillation probabilities of Equations (22)-(25) are a combination of a *long*-wavelength component due to the solar mass splitting $|\Delta m^2_{12}| \approx 7\times 10^{-5}\,{\rm eV}^2$, and a *short*-wavelength component due to the atmospheric mass splitting $|\Delta m^2_{23}| \approx 2\times 10^{-3}\,{\rm eV}^2$.

12.3 Comparison with Experiment

12.3.1 Standard Representation of the PMNS Matrix

To interpret the data from neutrino oscillation experiments, it is useful to employ a particular, specific representation of the PMNS matrix U. The standard representation universally used is obtained by expressing U as a product of three rotation matrices based on angles θ_{12}, θ_{23} and θ_{13}, together with a complex phase factor $e^{i\delta}$:

$$\begin{aligned} \begin{pmatrix} U_{e1} & U_{e2} & U_{e3} \\ U_{\mu 1} & U_{\mu 2} & U_{\mu 3} \\ U_{\tau 1} & U_{\tau 2} & U_{\tau 3} \end{pmatrix} &= \begin{pmatrix} 1 & 0 & 0 \\ 0 & c_{23} & s_{23} \\ 0 & -s_{23} & c_{23} \end{pmatrix} \times \begin{pmatrix} c_{13} & 0 & s_{13}e^{-i\delta} \\ 0 & 1 & 0 \\ -s_{13}e^{i\delta} & 0 & c_{13} \end{pmatrix} \times \begin{pmatrix} c_{12} & s_{12} & 0 \\ -s_{12} & c_{12} & 0 \\ 0 & 0 & 1 \end{pmatrix} \\ &= \begin{pmatrix} c_{12}c_{13} & s_{12}c_{13} & s_{13}e^{-i\delta} \\ -s_{12}c_{23} - c_{12}s_{23}s_{13}e^{i\delta} & c_{12}c_{23} - s_{12}s_{23}s_{13}e^{i\delta} & s_{23}c_{13} \\ s_{12}s_{23} - c_{12}c_{23}s_{13}e^{i\delta} & -c_{12}s_{23} - s_{12}c_{23}s_{13}e^{i\delta} & c_{23}c_{13} \end{pmatrix} \end{aligned} \qquad (26)$$

where $s_{ij} \equiv \sin\theta_{ij}$, $c_{ij} \equiv \cos\theta_{ij}$. This is the same form as that considered earlier for the CKM matrix. All physical observables are independent of the particular representation of the PMNS (or CKM) matrix.

In terms of the standard representation of Equation (26), with $U_{e1} = c_{12}c_{13}$, $U_{e2} = s_{12}c_{13}$ and $U_{e3} = s_{13}$, the $\nu_{\rm e} \to \nu_{\rm e}$ survival probability of Equation (25) becomes

$$\begin{aligned} P(\nu_{\rm e} \to \nu_{\rm e}) &\approx 1 - 4U_{e1}^2 U_{e2}^2 \sin^2\Delta_{12} - 4\left(1 - U_{e3}^2\right) U_{e3}^2 \sin^2\Delta_{23} \\ &= 1 - 4(c_{12}c_{13})^2 (s_{12}c_{13})^2 \sin^2\Delta_{12} - 4\left(1 - s_{13}^2\right) s_{13}^2 \sin^2\Delta_{23} \\ &= 1 - \cos^4\theta_{13} \sin^2 2\theta_{12} \sin^2\Delta_{12} - \sin^2 2\theta_{13} \sin^2\Delta_{23} \; . \end{aligned} \tag{27}$$

This expression will be used below to discuss the evidence for neutrino oscillations obtained in experiments studying solar neutrinos, and using antineutrinos from commercial nuclear power reactors. Similar expressions can be written down for the conversion probabilities $P(\nu_{\rm e} \to \nu_\mu)$ *etc.*, and will be used below to discuss the results obtained by experiments studying neutrinos produced in cosmic ray interactions in the Earth's atmosphere. When considered together, we shall see that the experimental results now constrain reasonably well the overall structure of the PMNS matrix.

12.3.2 Solar Neutrinos

For a typical solar neutrino energy of $1\,{\rm MeV}$, the wavelength λ_{23} associated with the "large" (atmospheric neutrino) mass-squared difference $\Delta m^2_{23} \approx 2.5 \times 10^{-3}\,{\rm eV}^2$ is

$$\lambda_{23} = \frac{4\pi E}{\Delta m^2_{23}} \sim \frac{4\pi \times 1\,{\rm MeV}}{2.5 \times 10^{-3}\,{\rm eV}^2} \times (0.197\,{\rm GeV\,fm}) = 1.0\,{\rm km} \; .$$

This wavelength is negligible in comparison with the size of the neutrino production region in the core of the Sun, and solar neutrino experiments therefore detect only an *average* of many such oscillations. The factor $\sin^2\Delta_{23}$ in Equation (27) should therefore be replaced by its average value of one-half, giving

$$P(\nu_{\rm e} \to \nu_{\rm e}) \approx (1 - \tfrac{1}{2}\sin^2 2\theta_{13}) - \cos^4\theta_{13} \sin^2 2\theta_{12} \sin^2\Delta_{12} \; .$$

As explained below, results from the CHOOZ reactor experiment show that the matrix element $U_{e3} = s_{13}$ is small, so that $s_{13} \approx 0$, $c_{13} \approx 1$. The survival probability for solar neutrinos then becomes

$$\boxed{P(\nu_{\rm e} \to \nu_{\rm e}) \approx 1 - \sin^2 2\theta_{12} \sin^2\Delta_{12}} \, , \tag{28}$$

which has the same form as the simple two-flavour survival probability expression of Equation (9). Solar neutrino experiments therefore primarily determine the angle θ_{12} and the mass-squared splitting Δm^2_{12}.

As explained in the lectures, the survival probability for solar neutrinos is strongly affected by *matter effects*, namely the *coherent* effect of scattering on solar material during the propagation of a neutrino from the core to the surface of the Sun. Because solar material contains only *electrons* (not muons or tau leptons), the propagation of electron-neutrinos is affected differently to that of muon- and tau-neutrinos. It can be shown that, when matter effects are taken into account, the form of Equation (28) remains valid but θ_{12} and Δm_{12} have to be replaced by *effective* values θ^m_{12} and Δm^m_{12} which are calculable functions of θ_{12} and Δm_{12}. A combined analysis of all available data favours the so-called LMA solution:

$$\boxed{|\Delta m^2_{12}| \approx 7 \times 10^{-5}\,{\rm eV}^2, \quad \sin^2 2\theta_{12} \approx 0.8 \qquad (c_{12} \approx 0.85, \;\; s_{12} \approx 0.53)} \, . \tag{29}$$

This interpretation of the data has recently received support from the KamLAND reactor experiment (see below).

12.3.3 Atmospheric Neutrinos

The energy of atmospheric neutrinos is of order $1\,\mathrm{GeV}$. At this energy, the wavelength λ_{12} associated with the solar term containing $\Delta m^2_{12} \approx 7 \times 10^{-5}\,\mathrm{eV}^2$ is

$$\lambda_{12} = \frac{4\pi E}{\Delta m^2_{12}} = \frac{4\pi \times 1\,\mathrm{GeV}}{7 \times 10^{-5}\,\mathrm{eV}^2} \times (0.197\,\mathrm{GeV\,fm}) = 35,000\,\mathrm{km}\,.$$

Since this wavelength is several times the diameter of the Earth, oscillations due to terms containing Δm^2_{12} barely have time to develop between production of the neutrino in the Earth's atmosphere and its arrival at the detector; such terms can therefore safely be neglected.

Atmospheric neutrino experiments observe only about one-half the expected number (assuming no neutrino oscillations) of upward-going muon neutrinos. The number of downward-going muon neutrinos, and the number of electron neutrinos from all directions, are approximately as expected. This suggests that the dominant conversion process is $\nu_\mu \to \nu_\tau$ oscillations, and we consider this process first. Neglecting the term containing Δm^2_{12}, the oscillation probability for $\nu_\mu \to \nu_\tau$ oscillations in Equation (24) takes the form

$$P(\nu_\mu \to \nu_\tau) \approx 4U^2_{\mu 3}U^2_{\tau 3}\sin^2\Delta_{23}\,.$$

Since $U_{\mu 3} = s_{23}c_{13}$ and $U_{\tau 3} = c_{23}c_{13}$ we have

$$P(\nu_\mu \to \nu_\tau) \approx 4s^2_{23}c^2_{13}c^2_{23}c^2_{13}\sin^2\Delta_{23} = 4s^2_{23}c^2_{23}(1-s^2_{13})^2\sin^2\Delta_{23}$$

which can be written

$$\boxed{P(\nu_\mu \to \nu_\tau) \approx (1-s^2_{13})^2\sin^2 2\theta_{23}\sin^2\Delta_{23}}\,. \tag{30}$$

This is of the same form as the standard two-neutrino oscillation formula, Equation (8). Since the results from the CHOOZ reactor experiment show that the matrix element $U_{e3} = s_{13}$ is small, atmospheric neutrino oscillations primarily depend on the parameters Δm^2_{23} and θ_{23}. The results from the SuperKamiokande experiment determine that

$$\boxed{\Delta m^2_{23} \approx 2 \times 10^{-3}\,\mathrm{eV}^2, \qquad \sin^2 2\theta_{23} \approx 1.0, \qquad \left(c_{23} \approx s_{23} \approx 1/\sqrt{2}\right)}\,.$$

Neglecting the Δ_{12} term in Equations (22) and (23), the remaining conversion probabilities are given approximately by

$$P(\nu_\mathrm{e} \to \nu_\mu) = P(\nu_\mu \to \nu_\mathrm{e}) \approx 4U^2_{e3}U^2_{\mu 3}\sin^2\Delta_{23} = 4s^2_{13}s^2_{23}c^2_{13}\sin^2\Delta_{23}$$

and

$$P(\nu_\mathrm{e} \to \nu_\tau) \approx 4U^2_{e3}U^2_{\tau 3}\sin^2\Delta_{23} = 4s^2_{13}c^2_{23}c^2_{13}\sin^2\Delta_{23}$$

where we have used $U_{e3} = s_{13}$, $U_{\mu 3} = s_{23}c_{13}$ and $U_{\tau 3} = c_{23}c_{13}$. These conversion probabilities are all proportional to $\sin^2 2\theta_{13}$, and are therefore small.

The results above are summarised in Figure 1, where the various conversion and survival probabilities are shown as a function of distance for a neutrino energy of $1\ \mathrm{GeV}$, typical of atmospheric neutrinos. The angle θ_{13} has been arbitrarily set to a value of $11.5°$, a little below the constraint $\theta_{13} < 14.8°$

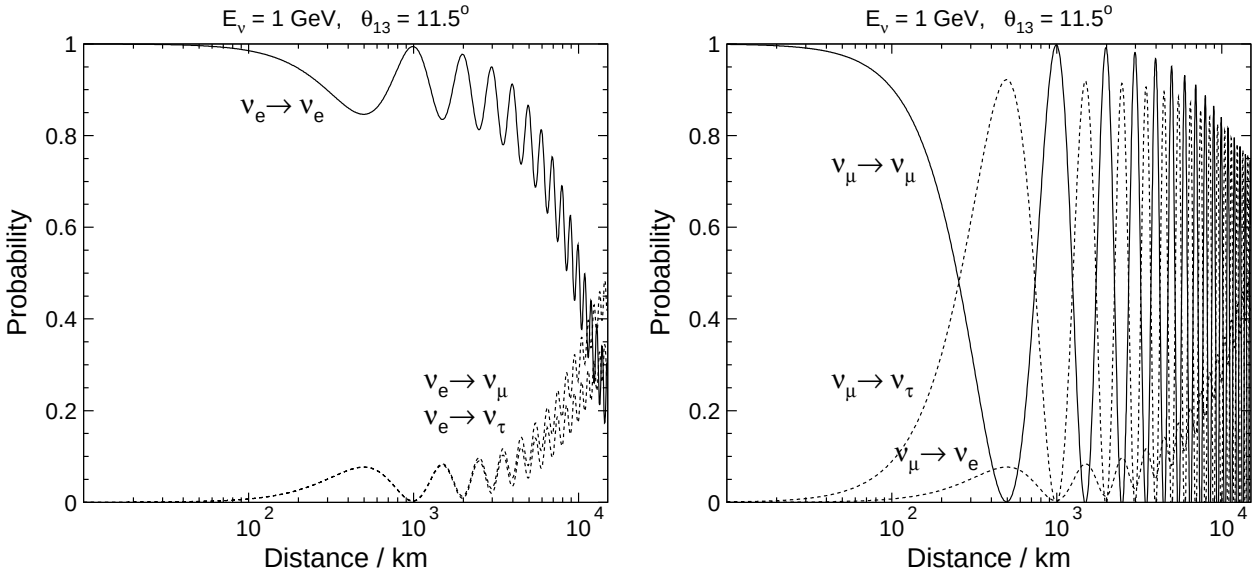

Figure 1: Oscillation probabilities for an initial $\nu_{\rm e}$ (left-hand plot) or initial ν_μ (right-hand plot) for a typical atmospheric neutrino energy of $1\ \mathrm{GeV}$.

from the CHOOZ experiment. The oscillations are dominated by the transition $\nu_\mu \to \nu_\tau$, except for neutrinos which traverse essentially a complete Earth diameter, where $\nu_\mu \to \nu_{\rm e}$ and $\nu_{\rm e} \to \nu_\mu, \nu_\tau$ oscillations become significant.

Atmospheric neutrinos are initially produced in cosmic ray interactions as a mixture of ν_μ and $\nu_{\rm e}$ neutrinos (and antineutrinos), with approximately twice as many ν_μ as $\nu_{\rm e}$. If the initial flavour fractions in a beam of neutrinos are specified by $f_e(0)$, $f_\mu(0)$, $f_\tau(0)$, with $f_e(0) + f_\mu(0) + f_\tau(0) = 1$, then the fractions $f_e(t)$, $f_\mu(t)$, $f_\tau(t)$ of each type of neutrino in the beam at a later time t is given by

$$\begin{aligned} f_e(t) &= f_e(0)P(\nu_{\rm e} \to \nu_{\rm e}) + f_\mu(0)P(\nu_\mu \to \nu_{\rm e}) + f_\tau(0)P(\nu_\tau \to \nu_{\rm e}) \\ f_\mu(t) &= f_e(0)P(\nu_{\rm e} \to \nu_\mu) + f_\mu(0)P(\nu_\mu \to \nu_\mu) + f_\tau(0)P(\nu_\tau \to \nu_\mu) \\ f_\tau(t) &= f_e(0)P(\nu_{\rm e} \to \nu_\tau) + f_\mu(0)P(\nu_\mu \to \nu_\tau) + f_\tau(0)P(\nu_\tau \to \nu_\tau)\ . \end{aligned}$$

Figure 2 shows the composition of a "beam" of atmospheric neutrinos as a function of distance, assuming an initial composition of one-third $\nu_{\rm e}$ and two-thirds ν_μ (and no ν_τ). The $\nu_{\rm e}$ fraction remains approximately constant, even at large distances, because the transitions $\nu_{\rm e} \to \nu_x$ and $\nu_x \to \nu_{\rm e}$ partially compensate each other.

12.3.4 Reactor Experiments

Reactor experiments involve (anti)neutrino energies of order $1\,\mathrm{MeV}$. At this energy, the wavelength associated with the solar mass difference term in Equation (22) containing Δm^2_{12} is

$$\lambda_{12} = \frac{4\pi E}{\Delta m^2_{12}} = \frac{4\pi \times 1\,\mathrm{MeV}}{7 \times 10^{-5}\,\mathrm{eV}^2} \times (0.197\,\mathrm{GeV\,fm}) = 35\,\mathrm{km}\ ,$$

while the wavelength associated with the atmospheric mass difference Δm^2_{23} is

$$\lambda_{23} = \frac{4\pi E}{\Delta m^2_{23}} = \frac{4\pi \times 1\,\mathrm{MeV}}{2 \times 10^{-3}\,\mathrm{eV}^2} \times (0.197\,\mathrm{GeV\,fm}) = 1.2\,\mathrm{km}\ .$$

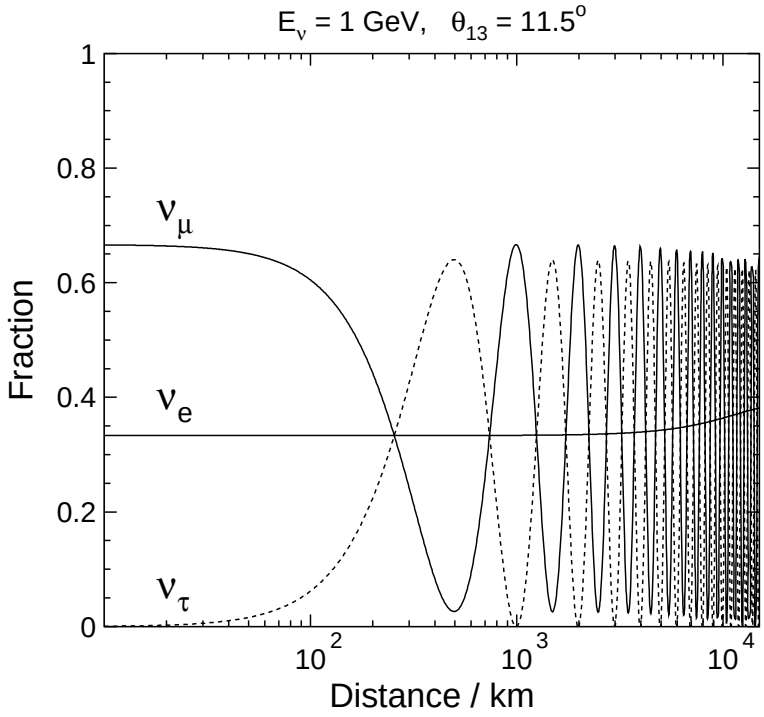

Figure 2: Neutrino fractions in a "beam" of atmospheric neutrinos which initially contains twice as many ν_μ as $\nu_{\rm e}$, and no ν_τ.

For the CHOOZ experiment, located about $1\,\mathrm{km}$ from the reactor core, oscillations due to Δm^2_{12} do not have time to develop appreciably, and the term involving Δm^2_{12} in Equation (27) can safely be neglected:

$$P(\nu_{\rm e} \to \nu_{\rm e}) \approx 1 - 4\left(1 - s^2_{13}\right) s^2_{13} \sin^2 \Delta_{23} \ . \tag{31}$$

This is again of the same form as the simple two-neutrino survival probability expression of Equation (9). The null result from CHOOZ, *i.e.* $P(\nu_{\rm e} \to \nu_{\rm e}) \approx 1$, therefore requires either $s_{13} \approx 0$ or $s_{13} \approx 1$. The latter possibility can be ruled out since then the atmospheric neutrino oscillation probability $P(\nu_\mu \to \nu_\tau)$ of Equation (30) would be very small; the CHOOZ result therefore determines that the angle θ_{13} is small. A detailed analysis of the data (considered also in the examples sheet) gives

$$\boxed{\sin^2 \theta_{13} < 0.065 \qquad (\theta_{13} < 14.8^\circ, \quad s_{13} < 0.26, \quad c_{13} > 0.97)} \ .$$

In the KamLAND experiment, the detector is located at a typical distance $\sim 150\,\mathrm{km}$ from a variety of nuclear reactors, so that the solar term involving Δm^2_{12} in Equation (27) can no longer be neglected:

$$\begin{aligned} P(\nu_{\rm e} \to \nu_{\rm e}) &= 1 - \cos^4 \theta_{13} \sin^2 2\theta_{12} \sin^2 \Delta_{12} - \sin^2 2\theta_{13} \sin^2 \Delta_{23} \\ &\approx 1 - \sin^2 2\theta_{12} \sin^2 \Delta_{12} \end{aligned}$$

where the last line follows because θ_{13} is small. This expression is the same as Equation (28) for the survival probability in solar neutrino experiments. The measurement of a value of $P(\nu_{\rm e} \to \nu_{\rm e})$ (actually $P(\overline{\nu}_{\rm e} \to \overline{\nu}_{\rm e})$) significantly below unity by the KamLAND experiment strongly favours the LMA solution from the solar neutrino experiments, Equation (29).

Figure 3 illustrates the neutrino oscillation probabilities relevant to the CHOOZ and KamLAND reactor experiments, plotted for a neutrino energy of $1\ \mathrm{MeV}$ using the complete expressions in Equations (22)-(25). For the KamLAND experiment (well off the right-hand edge of the plot) the long wavelength (λ_{12}) oscillations are well developed while the small wavelength (λ_{23}) oscillations are only a minor perturbation. The KamLAND experiment is therefore primarily sensitive to the same parameters, θ_{12} and Δm^2_{12}, as the solar neutrino experiments. On the other hand, the CHOOZ experiment, at a distance of about $1\ \mathrm{km}$, is only sensitive to the short wavelength λ_{23} oscillations, and places an upper limit on the amplitude ($\sin^2 2\theta_{13}$) of these oscillations.

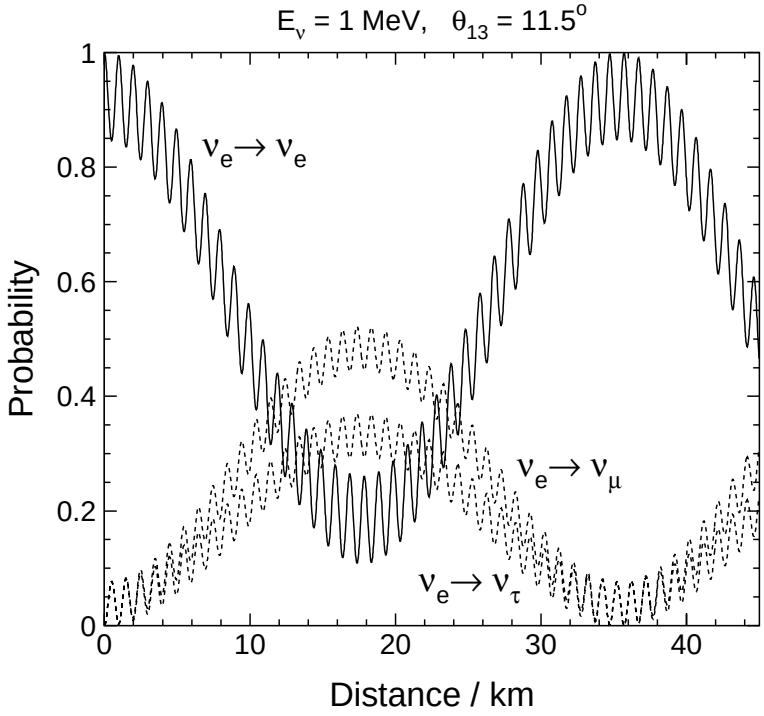

Figure 3: Oscillation probabilities as a function of distance for an initial ν_{e} (actually $\overline{\nu}_{\mathrm{e}}$) of energy $1\ \mathrm{MeV}$, typical of reactor antineutrinos. The CHOOZ experiment is situated at a distance of about $1\ \mathrm{km}$ from a reactor, while the typical distance of the KamLAND experiment from various reactors is about $150\ \mathrm{km}$. The high amplitude, long wavelength oscillations are driven by the mass-squared difference $\Delta m^{\,2}_{12} \approx 7 \times 10^{-5}\,\mathrm{eV}^2$. The small amplitude, short wavelength oscillations are driven by the mass-squared difference $\Delta m^2_{23} \approx 2 \times 10^{-3}\,\mathrm{eV}^2$.

12.3.5 Putting it all Together

The experimental results on neutrino oscillations, and their impact on the parameters in the PMNS matrix, can be summarised as follows:

1) Solar neutrino experiments (a mixture of $\nu_{\mathrm{e}} \to \nu_\mu$ and $\nu_{\mathrm{e}} \to \nu_\tau$ oscillations) favour the so-called LMA solution

$$|\Delta m^2_{12}| \approx 7 \times 10^{-5}\,\mathrm{eV}^2, \quad \sin^2 2\theta_{12} \approx 0.8, \quad c_{12} \approx 0.85, \quad s_{12} \approx 0.53\ ;$$

2) Atmospheric neutrino experiments are dominated by $\nu_\mu \to \nu_\tau$ oscillations with

$$\Delta m^2_{23} \approx 2 \times 10^{-3}\,\mathrm{eV}^2, \quad \sin^2 2\theta_{23} \approx 1.0, \quad c_{23} \approx s_{23} \approx 1/\sqrt{2}\ ;$$

3) The KamLAND reactor experiment observes a deficit of $\overline{\nu}_{\rm e}$ antineutrinos which confirms the solar LMA solution, while the CHOOZ experiment shows that the angle θ_{13} is small:

$$\sin^2\theta_{13} < 0.065\ .$$

In the limit $\theta_{13} = 0$ (and hence $c_{13} = 1$, $s_{13} = 0$), the PMNS matrix, Equation (26), takes the form

$$\begin{pmatrix} U_{e1} & U_{e2} & U_{e3} \\ U_{\mu 1} & U_{\mu 2} & U_{\mu 3} \\ U_{\tau 1} & U_{\tau 2} & U_{\tau 3} \end{pmatrix} = \begin{pmatrix} c_{12} & s_{12} & 0 \\ -s_{12}c_{23} & c_{12}c_{23} & s_{23} \\ s_{12}s_{23} & -c_{12}s_{23} & c_{23} \end{pmatrix}\ .$$

The structure of the PMNS matrix is therefore approximately

$$\begin{pmatrix} U_{e1} & U_{e2} & U_{e3} \\ U_{\mu 1} & U_{\mu 2} & U_{\mu 3} \\ U_{\tau 1} & U_{\tau 2} & U_{\tau 3} \end{pmatrix} \approx \begin{pmatrix} c_{12} & s_{12} & 0 \\ -s_{12}/\sqrt{2} & c_{12}/\sqrt{2} & 1/\sqrt{2} \\ s_{12}/\sqrt{2} & -c_{12}/\sqrt{2} & 1/\sqrt{2} \end{pmatrix} \approx \begin{pmatrix} 0.85 & 0.53 & 0 \\ -0.37 & 0.60 & 0.71 \\ 0.37 & -0.60 & 0.71 \end{pmatrix}$$

The presence of two large mixing angles θ_{12} and θ_{23}, and the corresponding large mixing between the neutrino flavour eigenstates, means that the PMNS matrix is very different in form to the approximately diagonal CKM matrix in the quark sector.

From Equation (10), the PMNS matrix determined above corresponds to neutrino mass eigenstates with the approximate form

$$\begin{aligned} \nu_1 &\approx c_{12}\nu_{\rm e} - \frac{s_{12}}{\sqrt{2}}(\nu_\mu - \nu_\tau) &&\approx (0.85)\nu_{\rm e} - (0.37)(\nu_\mu - \nu_\tau) \\ \nu_2 &\approx s_{12}\nu_{\rm e} + \frac{c_{12}}{\sqrt{2}}(\nu_\mu - \nu_\tau) &&\approx (0.53)\nu_{\rm e} + (0.60)(\nu_\mu - \nu_\tau) \\ \nu_3 &\approx \frac{1}{\sqrt{2}}(\nu_\mu + \nu_\tau) &&\approx (0.71)(\nu_\mu + \nu_\tau)\ . \end{aligned}$$

There is as yet no experimental information on the phase angle δ in the PMNS matrix. Obtaining such information will require high sensitivity searches for CP violation in neutrino oscillations.

12.4 Appendix: Particle Oscillations (non-examinable)

The neutrino oscillation probabilities in this handout were derived assuming that each neutrino mass eigenstate propagated as a plane wave with definite energy E_i and three-momentum p_i. A more correct treatment of neutrino oscillations takes into account the uncertainties in the positions and momenta of the neutrino using a wave packet (or field theoretic) description. This is illustrated schematically in Figure 4 for the case of two neutrino mass eigenstates ν_1 and ν_2.

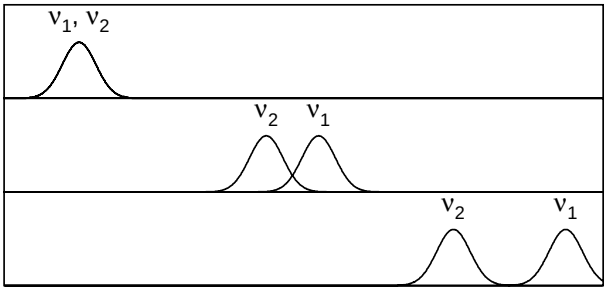

Figure 4: Schematic illustration of neutrino wave packet propagation.

After propagating a sufficiently large distance, the individual wave packets no longer overlap and neutrino oscillations no longer occur. The velocity v_i associated with each mass eigenstate is given by

$$v_i = \frac{p_i}{E_i} \, .$$

From Equation (5), we have

$$\frac{E_i}{p_i} \approx 1 + \frac{m_i^2}{2p_i^2} \, ,$$

and hence

$$v_i \approx 1 - \frac{m_i^2}{2p_i^2} \, .$$

After a time t, the spatial separation between the two mass eigenstates is

$$\Delta x = (v_1 - v_2)t \approx \frac{\Delta m^2 L}{2p^2}$$

where $L \approx t$ is the distance travelled and $p \approx p_1 \approx p_2$.

As a concrete example, consider a neutrino of momentum $1 \ \mathrm{MeV}$ which propagates over a distance $L = 100 \ \mathrm{km}$, with a mass splitting $\Delta m^2 = 2 \times 10^{-3} \, \mathrm{eV}^2$. Then

$$\Delta x \approx \frac{2 \times 10^{-3} \, \mathrm{eV}^2 \times 100 \ \mathrm{km}}{2 \ \mathrm{MeV}^2} \approx 10^{-10} \ \mathrm{m} \, .$$

This example serves to illustrate that, in all practical circumstances, the separation of the individual mass eigenstates is a negligibly small effect, and that an approximate treatment using plane waves is perfectly acceptable.

Similar remarks apply also to strangeness oscillations in the neutral kaon system.